ScienceInnovation
INTERNATIONAL SCIENTIFIC JOURNAL

ISSN:
2181-3337

INTERNATIONAL SCIENTIFIC JOURNAL

SCIENCE AND INNOVATION

VOLUME 5 / ISSUE 5

D:
BIOLOGY
AGRICULTURE
MEDICINE
PHARMACETICS
VETERINARY

MAY 2026

International Scientific Journal
SCIENCE AND INNOVATION
Series D
Volume 5 Issue 5
May 2026

Tashkent 2026

ISSN: 2181-3337

International Scientific Journal SCIENCE AND INNOVATION. Series D volume 5 issue 5 – 152 p.

The collection contains scientific articles accepted for issue 5 for 2026 of the international scientific journal "Science and Innovation".

In this scientific journal, in the form of scientific articles, the results of scientific research conducted by professors and teachers of the Republic of Uzbekistan and international higher educational institutions, independent researchers, doctoral students, undergraduates were published. In addition to higher educational institutions, the journal also includes scientific articles by employees working in other research institutes, production organizations and enterprises of our region and republic.

The materials of the journal can be used by professors, teachers, independent researchers, doctoral students, undergraduates, students, teachers of lyceums and schools, scientists and everyone who is interested in science.

This issue of the journal is indexed in the international scientific databases Index Copernicus, eLibrary.ru, OpenAire, EuroPub, ZENODO and Google Scholar.

All articles were placed in the electronic scientific database of the journal (scientists.uz).

© Science and Innovation

© Authors

Editorial team			
Baxtiyor Rustamov	Chief Editor	**Gulirano Raxmatullayeva**	Deputy Chief Editor
Mahliyo Sotivoldiyeva	Reception Manager	**Feruza Ollomurodova**	Reception Manager
Farangiz Sagdullayeva	Technical Editor	**Dilnoza Narzullayeva**	Manager
Zulayxo Xakimova	Editor	**Sevara O'rinboyeva**	Manager
Kozim Ergashov	Editor	**Humoyun Qodirov**	Technical Editor
Feruzabonu Mannonova	Translator	**Mansur Suyunqulov**	Technical Editor
Jahongir Bekmuradov	Translator	**Samandar Rasulov**	Motion Designer
Asila Xaydaralieva	Editor	**Zafarbek Madaminov**	Motion Designer

Scientific editorial board	
Khashim Yakhyayev	Doctor of Agricultural Sciences, professor, Leading scientific researcher of the laboratory for pest control of landscape and forest trees at Scientific research institute for plant quarantine and protection.
Azimjon Anorbaev	Doctor of Agricultural Sciences, professor, Director a.i. of the Scientific Research Institute of Plant Quarantine and Protection.
Ajimurat Jumamuratov	Doctor of agricultural sciences, Professor of Nukus State Pedagogical Institute named after Ajiniyaz.
Murodjon Isagaliyev	Doctor of Biological sciences, Associate Professor, Dean of the Faculty of Animal Husbandry of Fergana State University.
Avazbek Turdaliyev	Doctor of Biological sciences, Associate Professor, Head of the Department of Zootechnics and Agronomy pf Fergana State University.
Zafarjon Jabbarov	Doctor of Biological Sciences, Head of the Department of Soil Science of the National University of Uzbekistan named after Mirzo Ulugbek, Professor.
Gulnora Djalilova	Doctor of Biological Sciences, Associate Professor a.i. of the Department of Soil Science of National University of Uzbekistan named after Mirzo Ulugbek.
Mokhidil Yusupova	Philosofy Doctor on Biological sciences, Head a.i. of the Department of "Effective Use of Residential Estates" of Fergana State University.
Dilmurod Darmonov	Philosofy Doctor on Biological sciences, Dean of the Faculty of Viticulture, Fruit Growing and Vegetable Growing of Fergana State University.
Ulugbek Mirzayev	Candidate of Biological Sciences, Associate Professor, Head of the Department of Soil Science of Fergana State University.
Bakhtiyor Ruziyev	Candidate of Biological Sciences, Associate Professor of the Department of Zoology of Karshi State University.
Akmal Yuldashev	Philosofy Doctor on Biological Sciences, Dean of the Faculty of Teaching Methodology of Exact and Natural Sciences of Pedagogical Institute of Andijan State University.
Khusanjon Idrisov	Philosofy Doctor on Agricultural Sciences, Head of the Department of Fruit and Vegetable Growing of Fergana State University.
Sherzod Teshabayev	Philosofy Doctor on agricultural sciences, Head of the Department of Agriculture and Forest Reclamation of Andijan Institute of Agriculture and Agrotechnologies.
Shavkat Eshpulatov	Candidate of agricultural sciences, Head of the Department of EIAT of Ferghana State University.
Madinakhon Rakhmonova	Philosofy Doctor on Agricultural sciences, Head of the Department "Quarantine of plants and agricultural products" of the Andijan Institute of Agriculture and Agrotechnologies.
Bobomurod Kuldashov	Philosofy Doctor on Agricultural sciences, Head of the department "Agrotechnology, automation and management of production " of Samarkand State University of Veterinary Medicine, Animal Husbandry and Biotechnology.
Khasanboy Askarov	Philosofy Doctor on Agricultural sciences, Head of the Department "Technology of production, storage and preliminary processing of agricultural products" of Fergana Polytechnic Institute.
Sevara Nazarova	Philosofy Doctor on Agricultural sciences, Associate Professor of the Department of Soil Science of Bukhara State University.
Gayratbek Rakhmatullayev	Philosofy Doctor on Agricultural sciences, Head of the Department "Genetics, selection and seed production of agricultural crops" of Andijan Institute of Agriculture and Agrotechnologies, Associate professor a.i..
Dilfuza Jalolova	Candidate of Medical Sciences, Associate Professor of Samarkand State Medical University.
Shakhnoza Abzalova	Candidate of medical sciences, Head of the Department of Scientific Research, Innovation and Scientific Pedagogical Personnel Training of the Tashkent State Medical University, Associate Professor
Khusnidakhon Abdukhakimova	Philosofy Doctor on Biological sciences, Assistant professor of the Department of Soil Science of Fergana State University

BIODIVERSITY AND SIGNIFICANCE OF INVERTEBRATE ANIMALS OF THE KYZYLKUM STATE NATURE RESERVE

N.R. Rahmonov[1], G.A. Goziyeva[2]
Bukhara State University[1,2]
https://doi.org/10.5281/zenodo.20302825

Abstract. *This article analyzes the biodiversity, taxonomic composition, and ecological significance of invertebrate animals found in Kyzylkum State Nature Reserve. During the research, 16 species of invertebrates were identified, belonging to the phyla Arthropoda and Mollusca, 3 classes, 6 orders, and 8 families. The results showed that representatives of the class Insecta, particularly the order Lepidoptera, dominate the faunal complex of the region. In addition, certain species such as Hipermniestra helios, Laothoe philerema, and several others were found to possess significant scientific importance as relict and bioindicator organisms. Bivalve mollusks and copepods inhabiting aquatic ecosystems were evaluated as important hydrobionts that ensure the ecological stability of water bodies. The findings confirm the important ecological role of invertebrates in desert and riparian ecosystems, including nutrient cycling, pollination, biological control, and maintenance of trophic system stability.*

Keywords: *invertebrates, biodiversity, Kyzylkum State Nature Reserve, Arthropoda, Mollusca, Lepidoptera, bioindicator species, desert ecosystem, riparian ecosystem, ecological stability, taxonomic composition, hydrobionts.*

Introduction

The conservation of biological diversity is considered one of the most pressing issues of modern ecology [1,2]. In particular, the study of invertebrate animals, which play an important role in maintaining the stability of natural ecosystems, is regarded as one of the priority directions of modern zoology and ecology. Invertebrates constitute the major part of the animal world on Earth and perform important ecological functions in matter and energy exchange, maintenance of trophic chain stability, decomposition of organic residues, soil formation, and pollination of plants [2,3]. Therefore, they possess particular scientific significance as bioindicators of ecosystems.

The Kyzylkum Desert, one of the largest desert regions of Central Asia, represents a complex and unique natural-geographical ecosystem. Located within this region, Kyzylkum State Nature Reserve occupies a special place not only in the biodiversity of Uzbekistan but also throughout Central Asia as an important natural area preserving desert and riparian landscapes [1,7]. The sharply continental climate of the reserve, sandy and saline soils, hydrological conditions, and riparian vegetation complex have created favorable conditions for the formation and distribution of invertebrate animals belonging to various ecological groups.

Among the invertebrates occurring in the Kyzylkum State Nature Reserve, insects belonging to the orders Lepidoptera, Coleoptera, and Hymenoptera, as well as mollusks and microscopic crustaceans inhabiting aquatic ecosystems, occupy a special place [4,6]. In particular, certain species such as *Catocala remissa*, *Laothoe philerema*, and *Hipermniestra helios* are of important ecological significance as relict and bioindicator organisms of the region [4,6,8]. In addition, bivalve mollusks and copepods found in water bodies constitute important components of the trophic system of aquatic ecosystems.

In recent years, due to climate change, reduction of water resources, and degradation of riparian ecosystems, a sharp decline has been observed in the natural populations of many invertebrate species. This situation poses a serious threat, especially to ecologically specialized and narrow-range species. Therefore, determining the taxonomic composition of invertebrate animals occurring within the reserve, studying their ecological characteristics, and evaluating their role in biodiversity are of significant scientific and practical importance.

The main purpose of this study is to analyze the taxonomic composition of invertebrate animals occurring in the Kyzylkum State Nature Reserve and to elucidate their role in biodiversity and ecological significance.

Research Object and Methods

The research was conducted during 2024–2026 within the territory of the Kyzylkum State Nature Reserve. This area represents an integrated natural complex of desert and riparian ecosystems and is distinguished by its ecological conditions and biological diversity. Determining the species composition of invertebrate animals occurring within the reserve, evaluating their taxonomic status, and studying their ecological significance constituted the main focus of the research.

During the study, zoological observation, route survey, morphological comparison, and taxonomic analysis methods were used to determine the species composition of invertebrate animals [3]. Modern zoological classifications, identification literature, and scientific sources related to the fauna of Central Asia were used for species identification [4,5,8,9,10,11,12].

Research Results and Discussion

As a result of the study, 16 species of invertebrate animals belonging to different systematic groups were identified within the reserve territory. Among the identified species, insects, mollusks, and aquatic organisms were observed to occupy a special place. The table below presents the taxonomic composition of the invertebrate animals recorded during the research.

Table 1

No.	Species Name	Phylum	Class	Order	Family
1	*Catocala remissa*	Arthropoda	Insecta	Lepidoptera	Erebidae
2	*Catocala optima*	Arthropoda	Insecta	Lepidoptera	Erebidae
3	*Laothoe philerema*	Arthropoda	Insecta	Lepidoptera	Sphingidae
4	*Laothoe philerema sioxiana*	Arthropoda	Insecta	Lepidoptera	Sphingidae
5	*Streblote fainae*	Arthropoda	Insecta	Lepidoptera	Lasiocampidae
6	*Glaucopsyche charibdis*	Arthropoda	Insecta	Lepidoptera	Lycaenidae
7	*Hipermniestra helios*	Arthropoda	Insecta	Lepidoptera	Zygaenidae
8	*Prionyx macula*	Arthropoda	Insecta	Hymenoptera	Sphecidae
9	Tugai Buprestid	Arthropoda	Insecta	Coleoptera	Buprestidae
10	Solomon’s Bug	Arthropoda	Insecta	Coleoptera	Buprestidae

11	Lemman’s Bug	Arthropoda	Insecta	Hemiptera	—
12	*Eremochares mirabilis*	Arthropoda	Insecta	Hymenoptera	Sphecidae
13	Purple Freshwater Clam	Mollusca	Bivalvia	Unionida	Unionidae
14	Sogd Freshwater Clam	Mollusca	Bivalvia	Unionida	Unionidae
15	Cordate Freshwater Clam	Mollusca	Bivalvia	Unionida	Unionidae
16	Lower Copepod	Arthropoda	Crustacea	Copepoda	—

The taxonomic composition of invertebrate animals identified in the Kyzylkum State Nature Reserve demonstrated a high level of ecological and systematic diversity within the faunal complex of the region. According to the research results, the recorded 16 species were found to belong to two phyla, Arthropoda and Mollusca. Representatives of the phylum Arthropoda were observed to be absolutely dominant among the species. This condition can be explained by the ecological adaptability of insects and their important role in the trophic system of desert and riparian ecosystems.

From a taxonomic point of view, the largest proportion was represented by the class Insecta. Within this class, representatives of the order Lepidoptera were recorded as the dominant group in terms of species number. During the research, 7 species belonging to this order were identified, and they were found to belong to the families Erebidae, Sphingidae, Lasiocampidae, Lycaenidae, and Zygaenidae. The abundance of Lepidoptera representatives indicates the complex development of vegetation cover and trophic relationships within the region. Ecologically, representatives of this order play an important role in pollination processes, maintenance of food chain stability, and functioning as bioindicators.

The species Catocala remissa and Catocala optima, belonging to the family Erebidae, are nocturnal butterflies characteristic of riparian ecosystems. Species of this family possess scientific importance as ecological indicator organisms used in assessing the condition of vegetation cover. Representatives of the family Sphingidae — Laothoe philerema and Laothoe philerema sioxiana — are distinguished by their high ecological specialization. These species actively participate in plant pollination and play an important role in maintaining the trophic stability of riparian ecosystems.

The species Streblote fainae, belonging to the family Lasiocampidae, is characterized by its adaptation to desert conditions. Representatives of this family perform important ecological functions in organic matter cycling and biomass formation. The representative of the family Lycaenidae, Glaucopsyche charibdis, is considered one of the ecologically sensitive species of entomofauna. This species is distinguished by forming complex trophic relationships with plants.

Hipermniestra helios, belonging to the family Zygaenidae, possesses particular scientific significance as a relict and narrow-range species. The presence of this species serves as an important bioindicator reflecting the natural preservation of the regional ecosystem. Therefore,

this species is regarded as one of the priority objects in ecological monitoring and conservation measures.

The representative of the family Sphecidae belonging to the order Hymenoptera, Prionyx macula, performs the function of biological control in the ecosystem as a predatory wasp. The trophic activity of this species is of great importance in the natural regulation of populations of other small insects and contributes to maintaining ecological balance.

Representatives of the family Buprestidae belonging to the order Coleoptera were recorded as bioindicator organisms ecologically associated with riparian forests. This group of beetles plays an important role in the decomposition of organic residues and matter cycling processes. Solomon's Bug is also considered one of the ecologically important representatives of the order Coleoptera, participating in soil formation and detritus decomposition processes.

The species Lemman's Bug, belonging to the order Hemiptera, is regarded as an important ecological component participating in trophic relationships between plants and insects. The species Eremochares mirabilis was recorded as a rare representative of entomofauna highly adapted to desert regions. Although the ecology of this species has not been sufficiently studied, its presence reflects the biological diversity of desert ecosystems.

Representatives of the class Bivalvia belonging to the phylum Mollusca — Purple Freshwater Clam, Sogd Freshwater Clam, and Cordate Freshwater Clam — were identified as belonging to the family Unionidae. These mollusks are of significant importance in maintaining the ecological stability of water bodies as natural water-filtering organisms. Their presence is also of great scientific importance as bioindicators of water quality.

Representatives of the Lower Copepod belonging to the class Crustacea are considered one of the main components of the trophic system of aquatic ecosystems. Organisms belonging to the group Copepoda serve as a food base for fish and other hydrobionts, ensuring the biological productivity of water bodies.

In general, the conducted taxonomic analysis demonstrated that the Qizilqum State Nature Reserve is a region rich in the biodiversity of invertebrate animals. The presence of relict, endemic, and bioindicator species confirms the high ecological value of these ecosystems. Therefore, the conservation of the identified species and regular monitoring of their population status are considered important factors in maintaining ecological stability.

In conclusion, the studies conducted in the Qizilqum State Nature Reserve demonstrated that the invertebrate fauna of the region is taxonomically and ecologically rich and diverse. During the research, a total of 16 species were identified, belonging to 2 phyla, 3 classes, 6 orders, and 8 families. Among the identified species, representatives of the phylum Arthropoda, particularly the class Insecta, were found to dominate. The abundance of representatives of the order Lepidoptera indicates the complex development of trophic relationships and plant–insect interactions within the region.

As a result of the taxonomic analyses, certain species such as Hipermniestra helios, Laothoe philerema, and Tugai Buprestid were identified as possessing particular scientific significance as relict, ecologically sensitive, and bioindicator organisms. Bivalve mollusks and copepods inhabiting aquatic ecosystems were also recorded as important hydrobionts ensuring the ecological stability of water bodies.

The research results demonstrated that invertebrate animals perform important ecological functions in desert and riparian ecosystems, including matter cycling, decomposition of organic residues, pollination, biological control, and maintenance of food chain stability. At the same time,

a decline in the populations of certain species was observed to be associated with climate change, reduction of water resources, and soil degradation.

Conclusion

The conducted studies confirm that the Qizilqum State Nature Reserve is an important natural area for the conservation of invertebrate biodiversity. Therefore, the protection of rare and bioindicator species occurring in the region, regular monitoring of their population status, and preservation of their natural habitats are considered important factors in ensuring ecological stability.

REFERENCES

1. Red Data Book of the Republic of Uzbekistan. (2019). Tashkent: Chinor ENK.
2. Odum, E. P. (1971). *Fundamentals of ecology*. Philadelphia: Saunders.
3. Ruppert, E. E., Fox, R. S., & Barnes, R. D. (2004). *Invertebrate zoology*. Brooks/Cole.
4. Kryzhanovsky, O. L. (1965). *Composition and origin of the terrestrial fauna of Middle Asia*. Moscow: Nauka.
5. Mordukhay-Boltovskoy, F. D. (1972). *Freshwater invertebrates of Central Asia*. Moscow.
6. Dubatolov, V. V. *Lepidoptera of Central Asia and related scientific articles*.
7. Qizilqum State Nature Reserve. (2024–2026). *Scientific observation materials*.
8. Global Biodiversity Information Facility. (n.d.). *GBIF database*.
9. Catalogue of Life. (n.d.). *Catalogue of Life database*.
10. BioLib.cz. (n.d.). *Biological library database*.
11. National Center for Biotechnology Information. (n.d.). *NCBI Taxonomy Browser*.

THE INFLUENCE OF SOWING DATES, SEEDING RATES AND STIMULANTS ON THE DEVELOPMENT OF MUNG BEAN VARIETIES

G.B. Khalimova
Independent Applicant of the Research Institute of Paperwork, Lecturer at the Department of Energy and Environmental Protection of the Yangiyer branch of the Tashkent Institute of Chemical Technology
https://doi.org/10.5281/zenodo.20080592

Abstract. *With an increase in plant density, differences were observed: at the first true leaf stage +7.20%, budding +3.38%, flowering +3.54%, pod formation +2.12%, and maturation +0.71%. At the seeding rate in the 8th variant (400 thousand seeds/ha, Potex 2.5/5.0 L/ha), under the highest density, the indicator at the first true leaf stage did not change, while it increased at budding by +3.15%, flowering by +2.28%, pod formation by +4.63%, and maturation by +1.28%. It was determined that when sowing on July 15, the effect of the biostimulator was most pronounced during the leaf formation and budding stages. An increase in plant density led to a rise in accumulated temperature during the budding and flowering periods.*

Keywords: *population, stress, protein, iron, mung bean, leguminous crops, sowing time, seeding rate, growth dynamics, plant, temperature, yield, photosynthesis, nodules, bacteria.*

Introduction. In the world, the area under mung bean is approximately 7.3 million hectares, and the total production reaches about 5.3 million tons. The main share is accounted for by India and Myanmar - about 30%, China provides 16%, Indonesia - 5%. Mung bean has significant potential for providing nutrition to the population in the future, as it is resistant to heat and dry stress, and its grain is a good source of protein and iron for human nutrition.

According to Kh.N. Ataboeva, mung bean belongs to the genus *Phaseolus* and makes up the bulk of Asian legumes. Some legumes originate from South America - these include common beans, multiflorum, lima and tepari. The other part is typical for Asia, which includes mung beans (*Phaseolus aureus L.*), adzuki (*Phaseolus angularis Wilch*) and rice beans (*Phaseolus calcaratus Piper*). According to historical data, mung bean has been cultivated in agriculture for 5-6 thousand years and is considered a valuable food crop [1; p. 134-137].

According to D. Yormatova, the homeland of mung bean is considered to be Southwest Asia. At present, this crop is widely cultivated in many countries of the world - in India, Afghanistan, Iran, Pakistan, Burma, Japan, China, Vietnam, Uzbekistan, Turkmenistan, Tajikistan, as well as in the CIS countries [3; pp. 100-102].

According to D. Yormatova, there are different views on the origin of mung bean: some researchers believe that it, like other leguminous crops, originated from plants of the mimosa family [2; pp. 138-242].

Mung bean is an annual plant of the legume family, geographically and morphologically divided into three subspecies: s. sp. indicus - thin-handed, bean length 7 cm, weight of 1000 grains 15-30 g; medium- and late-ripening, mainly distributed in India, the stem is erect, suitable for harvesting with a combine, s. sp. chinensis - large-legged, bean length 9-17 cm, seeds are large; early-ripening, mainly distributed in China and the Far East, valuable form, s. sp. Iranicus - length

of beans 7-8 cm, weight of 1000 grains 35-38 g; medium-ripening, widespread in Central Asia, Afghanistan and Iran, the stem is creeping [4; p. 35].

Materials and Methods

The experiment was conducted in 2022–2024 to study the influence of sowing dates, seeding rates, and the Potex biostimulant on the development of mung bean varieties. The research objects were the Mahsuldor and Durdona mung bean varieties. The experiment included two sowing dates: June 30 and July 15. Seeding rates were 230, 300, and 400 thousand seeds per hectare. The Potex biostimulant was applied at the rates of 1.5/3.5, 2.0/4.0, and 2.5/5.0 L/ha. The main phenological phases studied were first true leaf formation, budding, flowering, bean formation, and ripening. The duration of interphase periods and the sum of effective temperatures during the growing season were analyzed.

Results

In 2022, the Mahsuldor and Durdona mung bean varieties were studied in the dynamics of the development phases. According to the data obtained, in the Mahsuldor variety, with a sowing date of June 30 and a seeding rate of 230 thousand / ha (1st version), the first true leaf appeared on July 13, the budding phase began on July 24, flowering - on August 17, bean formation - on August 25, ripening - on September 25. In the 2nd variant (230 thousand hectares), the first true leaf appeared on July 12, budding on July 23, flowering on August 16, bean formation on August 24, ripening on September 22. In the 3rd option, at a rate of 300 thousand per hectare, the first true leaf was observed on July 12, budding - on July 24, flowering - on August 15, bean formation - on August 23, ripening - on September 19. In the 4th variant, at a rate of 400 thousand per hectare, the first true leaf appeared on July 12, budding on July 25, flowering on August 14, bean formation on August 22, ripening on September 18.

Table 1

Timing of the development phases of the Mung Mahsuldor variety in 2022.

T/r	Sowing date	Seeding rate, thousand pieces/ha	Developmental phase				
			1 sheet	Butoni Promotion	Color In this case, the	Bobo Obrazo The First Edition of the	Mature The First Edition of the
1	30 Jun	**230**	13.VII	24.VII	17.VIII	25.VIII	25.IX
2		**230**	12.VII	23.VII	16.VIII	24.VIII	22.IX
3		**300**	12.VII	24.VII	15.VIII	23.VIII	19.IX
4		**400**	12.VII	25.VII	14.VIII	22.VIII	18.IX
5	15 Jul	**230**	24.VII	05.VIII	28.VIII	07.IX	14.X
6		**230**	24.VII	05.VIII	26.VIII	05.IX	11.X
7		**300**	25.VII	06.VIII	25.VIII	04.IX	09.X
8		**400**	26.VII	07.VIII	24.VIII	03.IX	06.X

With a sowing date of July 15, in variant 5 with a seeding rate of 230 thousand/ha, the first true leaf appeared on July 24, the budding phase began on August 5, flowering on August 28, bean formation on September 7, ripening on October 14. In variant 6 (230 thousand/ha), the first true leaf also appeared on July 24, budding on August 5, flowering on August 26, bean formation on

September 5, ripening - October 11. In variant 7, at a rate of 300 thousand per hectare, the first true leaf was observed on July 25, budding on August 6, flowering on August 25, bean formation on September 4, ripening on October 9. In variant 8, at a rate of 400 thousand per hectare, the first true leaf appeared on July 26, budding - on August 7, flowering - on August 24, bean formation - on September 3, ripening - on October 6. At a later sowing date, there was a slowdown in the onset of developmental phases, including leaf formation and other growth stages. For example, when sowing on July 15 in the variant with a norm of 230 thousand / ha, the first true leaf appeared on July 24, while when sowing on June 30 - already on July 12-13. An increase in the seeding rate slightly accelerated the onset of the phases of leaf formation and flowering, but the total difference did not exceed 1-2 days. The ripening period significantly depended on the sowing date: with later sowing, the vegetation period increased by 7-9 days. The results obtained show that the development of the Mahsuldor variety is closely related to local climatic conditions and sowing dates.

Based on the results of the analysis of the timing of the development phases of the Durdona variety in 2022, the following was established. With a sowing date of June 30 and a seeding rate of 230 thousand per hectare (1st version), the first true leaf appeared on July 14, the budding phase began on July 25, flowering on August 21, bean formation on August 30, ripening on September 29. In the 2nd variant (230 thousand hectares), the first true leaf appeared on July 13, budding on July 24, flowering on August 21, bean formation on August 29, ripening on September 27. In the 3rd variant, at a rate of 300 thousand per hectare, the first true leaf was observed on July 13, budding - on July 24, flowering - on August 20, bean formation - on August 28, ripening - on September 24. In the 4th variant, at a rate of 400 thousand per hectare, the first true leaf appeared on July 14, budding - on July 25, flowering - on August 19, bean formation - on August 27, ripening - on September 23.

When sowing on July 15, the phases of development of the Durdona variety, depending on the seeding rate, lagged behind somewhat. 230 thousand hectares/ha, 5th option: 1st true leaf - July 26, budding - August 6, flowering - September 1, beaver formation - September 11, ripening - October 20. 230 thousand hectares/ha, 6th option: 1st true leaf - July 27, budding - August 5, flowering - August 31, beaver formation - September 10, ripening - October 18. 300 thousand hectares/ha, 7th option: 1st true leaf - July 27, budding - August 6, flowering - August 30, beaver formation - September 9, ripening - October 16. 400 thousand hectares/ha, 8th option: 1st true leaf - July 27, budding - August 8, flowering - August 28, beaver formation - September 8, ripening - October 14. When sown on June 30, leaf formation and flowering were observed from July 13-14 to August 19-21. When sown on July 15, leaf formation was observed on July 26-27, flowering and bean formation were delayed by 1-2 days, and ripening was completed in mid-October. These data show that at later sowing dates, the growth phases are somewhat delayed, but the sequence of development remains stable.

The duration of the interphase periods of the Durdona variety in 2022 was analyzed depending on the sowing dates, seeding rate and the use of the Potex biostimulant. 1st variant (control, 230 thousand per hectare): 1st true leaf - 13 days, budding - 24 days, flowering - 48 days, bean formation - 56 days, ripening - 87 days. The growing season remained longer. 2nd option (230 thsd/ha + Potex 1.5+3.5 l/ha): ripening - 84 days, 3 days earlier compared to the control. The biostimulant accelerated the passage of the phases. 3rd option (300 thousand/ha + Potex 2.0+4.0 l/ha): ripening - 81 days, 6 days earlier than the control. Increased density and the use of a stimulant accelerated development. 4th option (400 thousand/ha + Potex 2.5+5.0 l/ha): ripening - 80 days, 7

days earlier than the control. The high density accelerated the passage of phases, but the physiological load on the plants increased.

Table 1

Timing of the development phases of the mung bean variety "Durdona", days (2022).

№	Sowing dates	Seeding rate, thousand pieces/ha	Phases of development				
			First page	Butoni Promotion	Flowering	First page	Ripening
1	June 30	**230**	14,VII	25,VII	21,VIII	30,VIII	29,IX
2		**230**	13,VII	24,VII	21,VIII	29,VIII	27,IX
3		**300**	13,VII	24,VII	20,VIII	28,VIII	24,IX
4		**400**	14,VII	25,VII	19,VIII	27,VIII	23,IX
5	July 15	**230**	26,VII	06,VIII	01,IX	11,IX	20,X
6		**230**	27,VII	05,VIII	31,VIII	10,IX	18,X
7		**300**	27,VII	06,VIII	30,VIII	09,IX	16,X
8		**400**	27,VII	08,VIII	28,VIII	08,IX	14,X

According to the experiments (June 30), with an increase in the rate of "Potex" and the sowing density, the development phases decreased, and ripening occurred 3-7 days earlier. At the sowing date of July 15, the 5th option (control, 230 thousand / ha): ripening - 91 days. In conditions of late sowing, due to changes in temperature and day length, the growing season was longer. 6th option (230 thousand/ha + Potex 1.5+3.5 l/ha): ripening - 88 days, 3 days earlier than the control. 7th option (300 thousand/ha + Potex 2.0+4.0 l/ha): ripening - 86 days, 5 days before the control. Option 8 (400 thsd/ha + Potex 2.5+5.0 l/ha): ripening - 83 days, 8 days before the control. Thus, (July 15), with an increase in the rate of biostimulant and sowing density, the phases of development were more intensive, and ripening occurred 3-8 days earlier.

The use of the biostimulant "Potex" activated the metabolism in plants, which led to a faster passage of phenological phases. With the increase in the seeding rate, competition between plants intensified, as a result of which the development processes were reduced. The ripening phase at the sowing date of June 30 varied within 80-87 days, and at sowing on July 15 - 83-91 days. The earliest ripening was observed when sowing on June 30 in the variant with a density of 400 thousand plants/ha and the use of "Potex" at a dose of 2.5 + 5.0 l/ha (80 days), and when sowing on July 15 - in the same variant (83 days).

According to the scientific analysis of the interphase duration of the mung bean variety "Durdona" (2022), with a sowing date of June 30 in the 1st option (control, 230 thousand plants/ha), the following was noted: 1st true leaf - 14 days, budding - 25 days, flowering - 52 days, beaver formation - 61 days, ripening - 91 days. In the control variant, the phenological phases proceeded naturally, and the vegetation period remained relatively longer. 2nd option (230 thousand/ha + Potex 1.5 + 3.5 l/ha): ripening - 89 days, 2 days earlier compared to the control.

Table 3

Interphase duration of the productive mung bean variety, 2022, days.

№	Sowing dates	Elevation rate, thousand pieces/ha	Phases of development				
			First page	Budding	Flowering	Bean formation	Ripening

1	June 30	230	13	24	48	56	87
2		230	12	23	47	55	84
3		300	12	24	46	54	81
4		400	12	25	45	53	80
5	July 15	230	9	21	44	54	91
6		230	9	21	42	52	88
7		300	10	22	41	51	86
8		400	11	23	40	50	83

According to the scientific analysis of the interphase duration of the mung bean variety "Durdona" (2022), with a sowing date of June 30 in the 1st option (control, 230 thousand plants/ha), the following was noted: 1st true leaf - 14 days, budding - 25 days, flowering - 52 days, beaver formation - 61 days, ripening - 91 days. In the control variant, the phenological phases proceeded naturally, and the vegetation period remained relatively longer. 2nd option (230 thousand/ha + Potex 1.5 + 3.5 l/ha): ripening - 89 days, 2 days earlier compared to the control. The use of a biostimulant activated physiological processes and led to a reduction in phases. 3rd option (300 thousand/ha + Potex 2.0+4.0 l/ha): ripening - 86 days, 5 days before the control. The combined effect of seeding density and the stimulant contributed to the acceleration of the rate of development. 4th option (400 thousand / ha + Potex 2.5 + 5.0 l / ha): ripening - 85 days, 6 days before the control. In conditions of increased density, plants under the influence of competition completed their development faster. In general, at the sowing date of June 30, with an increase in the Potex rate and sowing density, the development phases were more intensive, and ripening occurred 2-6 days earlier.

With the sowing date of July 15 in the 5th variant (control, 230 thousand plants/ha), the following was noted: 1st true leaf - 11 days, budding - 22 days, flowering - 48 days, beaver formation - 58 days, ripening - 97 days. With late sowing, under the influence of environmental factors (temperature, day length), the growing season was lengthened. 6th option (230 thousand/ha + Potex 1.5+3.5 l/ha): ripening - 95 days, 2 days earlier than the control. 7th option (300 thousand/ha + Potex 2.0+4.0 l/ha): ripening - 93 days, 4 days earlier than the control. 8th option (400 thsd/ha + Potex 2.5+5.0 l/ha): ripening - 91 days, 6 days before the control. In general, at the sowing date of July 15, with an increase in the rate of biostimulant and sowing density, phenological phases accelerated, and mung bean ripening decreased by 2-6 days.

Table 4

Interphase duration of mung bean variety "Durdona", 2022, days

№	**Sowing dates**	**Seeding rate, thousand pieces/ha**	**Phases of development**				
			First page	**Butoni Promotion**	**Flowering**	**Bobo Education**	**Ripening**
1	June 30	**230**	14	25	52	61	91
2		**230**	13	24	52	60	89
3		**300**	13	24	51	59	86
4		**400**	14	25	50	58	85
5	July 15	**230**	11	22	48	58	97

6		**230**	12	21	47	57	95
7		**300**	12	22	46	56	93
8		**400**	12	24	44	55	91

Discussion

The Potex biostimulant activated enzymatic and physiological processes in plants, contributing to the accelerated passage of phenological phases. With an increase in the seeding rate from 230 thousand to 400 thousand plants/ha, competition between plants intensified, which led to an acceleration of the rate of development. The ripening period for sowing on June 30 varied within 85-91 days, and for sowing on July 15 - 91-97 days. The earliest ripening was observed when sowing on June 30 in the variant of 400 thousand plants/ha + Potex 2.5 + 5.0 l/ha (85 days), and when sowing on July 15 - in the same variant (91 days).

According to the results of experiments conducted in 2022 on the Durdona mung bean variety, seeding rates and the use of the Potex biostimulant had a significant impact on the passage of development phases. With an increase in the dose of the biostimulant and the sowing density, the phenological phases were more intensive, and the ripening period at the sowing dates of June 30 and July 15 came 2-6 days earlier. This effect is explained by the activation of physiological processes in plants and the improvement of their adaptation to environmental factors.

The duration of the reduction phases in the varieties "Mahsuldor" and "Durdona" depends on factors such as temperature, sowing density, application of a biostimulant, humidity and plant nutrition conditions. For the "Mahsuldor" variety at the sowing date of June 30 (2022-2024 data), the total temperatures by phases were as follows:1st variant (230 thousand/ha, without stimulant): first true leaf - 255°C, budding - 430°C, flowering - 1115°C, beaver formation - 1185°C, ripening - 1350°C. 2nd variant (230 thousand/ha + Potex 1.5/3.5 l/ha): compared to the control, there was an increase of +0.42-2.33% in all phases, which indicates the effect of the biostimulant. 3rd option (300 thsd/ha + Potex 2.0/4.0 l/ha): the increase was +3.11% in the first leaf phase, +4.55% in budding, +1.34% in flowering, +1.68% in beaver formation and +1.84% in ripening; The greatest effect is noted in the phases of budding and ripening. 4th variant (400 thsd/ha + Potex 2.5/5.0 l/ha): at the maximum density and dose of the stimulant, the total temperatures increased in all phases: +5.28% (first leaf), +4.35% (budding), +3.54% (flowering), +2.07% (beaver formation), +5.42% (ripening); The maximum effect is also noted in budding and ripening. Thus, when sowing on June 30, the biostimulant and high seeding density increased the total temperatures in all phases, especially during the budding and ripening stages. At the sowing date of July 15 for the "Mahsuldor" variety, the temperature sums and the influence of the biostimulant and sowing density were distributed as follows. 5th variant (230 ths./ha, without stimulant): first true leaf - 260°C, budding - 495°C, flowering - 1105°C, beaver formation - 1155°C, ripening - 1310°C; This option is the base for the July sowing period.

Option 6 (230 thsd/ha + Potex 1.5/3.5 l/ha): increased by +0.43-3.46% by phase; The effect was weaker than in June sowing due to less favorable climatic conditions. 7th option (300 thsd/ha + Potex 2.0/4.0 l/ha): the increase was +7.43% (first leaf), +3.0% (budding), +2.23% (flowering), +2.16% (beaver formation), +0.76% (ripening); The sowing density had a noticeable effect on the temperature amounts. 8th variant (400 thsd/ha + Potex 2.5/5.0 l/ha): no changes were observed at the stage of the first leaf, then +2.91% (budding), +2.18% (flowering), +2.11% (beaver formation), +0.75% (ripening); High density in combination with a biostimulant provided a moderate increase in temperature amounts.

5-Grim

Sum of effective temperatures (average for 2022-2024) during the growing season of mung bean variety "Mahsuldor", °C.

№	Sowing dates	Seeding rate, thousand pieces/ha	Phases of development				
			First page	Butoni Promotion	Flowering	First page	Ripening
1	June 30	230	255,0	430,0	1115,0	1185,0	1350,0
2		230	257,0	440,0	1120,0	1190,0	1360,0
3		300	265,0	460,0	1135,0	1210,0	1385,0
4		400	279,0	480,0	1175,0	1235,0	1460,0
5	July 15	230	260,0	495,0	1105,0	1155,0	1310,0
6		230	269,0	500,0	1120,0	1160,0	1320,0
7		300	289,0	515,0	1145,0	1185,0	1330,0
8		400	289,0	530,0	1170,0	1210,0	1340,0

Since the sowing date was in July, even with a high sowing density, the total temperature did not increase significantly. When sowing on July 15, the effect of the biostimulant manifested itself mainly in the ripening phase, where the effect was minimal (+0.7%). An increase in sowing density increased the total temperature at the stages of budding and flowering, but due to the climatic conditions of July, the maximum values were lower compared to the June sowing date.

When studying the sum of effective temperatures in the growing season of the mung bean variety "Durdona" (in the context of 2022-2024), it was found that at the sowing date of June 30 in variant 1 (230 thousand seeds/ha, without the use of a stimulant), the total temperatures were: at the phase of the first true leaf - 255.7°C, budding - 433.2°C, flowering - 1148.1°C, beaver formation - 1238.6°C, ripening - 1421.3°C.

With a seeding rate of 230 thousand seeds/ha in the 2nd variant (Potex 1.5/3.5 l/ha), the use of a biostimulant led to an increase in the sum of effective temperatures compared to the control: at the phase of the first true leaf by +0.66%, budding by +2.68%, flowering by +0.15%, beaver formation by +0.44%, ripening by +0.88%. This impact contributed to the acceleration of growth and development processes in all phases. With an increase in the seeding rate to 300 thousand plants/ha in the 3rd option (Potex 2.0/4.0 l/ha), a further increase in the sum of temperatures was observed due to the thickening of crops: at the phase of the first true leaf +3.20%, budding +4.18%, flowering +1.24%, beaver formation +2.13%, ripening +1.88%. The greatest increase was noted at the stages of budding and ripening. In the 4th variant (400 thousand plants/ha + Potex 2.5/5.0 l/ha), at the maximum density and the use of a biostimulant, the largest increase in the sum of effective temperatures was observed: at the phase of the first true leaf +5.17%, budding +4.11%, flowering +3.50%, beaver formation +4.53%, ripening +4.83%. Thus, the combined effect of seed thickening and the biostimulant "Potex" provided the most pronounced increase in total temperatures and contributed to more intensive growth and development of plants.

At the sowing date of July 15, the accumulation of effective temperatures for the control variant (5th option, 230 thousand seeds/ha, without the use of a stimulant) was: the first true leaf - 260.1°C, budding - 500.8°C, flowering - 1132.4°C, beaver formation - 1194.0°C, ripening - 1367.7°C. In the 6th variant (230 thousand/ha + Potex 1.5/3.5 l/ha), the use of a biostimulant

provided an increase in total temperatures compared to the control: at the phase of the first true leaf by +3.55%, budding +0.78%, flowering +1.40%, bean formation +0.42%, ripening +0.76%. The most pronounced effect was observed in the early phases (leaf formation and budding), while at the ripening stage the effect was less significant. In the 7th variant (300 thousand/ha + Potex 2.0/4.0 l/ha), the increase in sowing density had a noticeable effect on the sum of temperatures: the first true leaf +7.20%, budding +3.38%, flowering +3.54%, beaver formation +2.12%, ripening +0.71%. In the 8th variant (400 thousand/ha + Potex 2.5/5.0 l/ha) at the maximum density and dose of the biostimulant, the following increase was observed: at the stage of the first true leaf, no changes were noted, budding +3.15%, flowering +2.28%, beaver formation +4.63%, ripening +1.28%.

Table 6

Sum of effective temperatures during the growing season of mung bean variety "Durdona" (average for 2022-2024), °C.

№	Sowing dates	Seeding rate, thousand pieces/ha	Phases of development				
			First page	Budding	Flowering	First page	Ripening
1	June 30	**230**	255,7	433,2	1148,1	1238,6	1421,3
2		**230**	257,4	445,0	1149,8	1244,1	1433,7
3		**300**	265,3	463,9	1163,8	1270,8	1460,7
4		**400**	278,8	483,1	1204,0	1295,2	1531,8
5	July 15	**230**	260,1	500,8	1132,4	1194,0	1367,7
6		**230**	269,4	504,7	1148,1	1199,1	1378,2
7		**300**	289,0	521,7	1173,1	1224,8	1387,4
8		**400**	289,0	538,4	1199,1	1251,0	1393,4

Conclusion

Thus, when sowing on July 15, it was found that the effect of the biostimulant is most pronounced in the early phases of development (leaf formation and budding), and an increase in sowing density enhances heat accumulation mainly in the phases of budding and flowering.

REFERENCES.

1. Bakhromov S., Bakhromov Sh. Influence of repeated (intermediate) crops on cotton yield. In: Proceedings of the Scientific and Practical Conference "Sources and Water-Saving Technologies for Obtaining High Yields in the Farming System". Tashkent, 2010. Pp. 125-127.
2. Yormatova D. Plant Production. Textbook. - Tashkent. East. 2002. Pp. 138-242.
3. Yormatova D. Technology of Plant Products Production. Textbook. - Tashkent: Ilm-Ziyo, 2010. Pp. 100-102.
4. Bitocchi E., Nani L., Bellucci E., Rossi M., Giardini A., Spagnoletti Zeuli P., Logozzo G., Stougaard J., McClean P., Attene G., and Papa R. 2012. Mesoamerican pp-35.

ANTIDIABETIC AND HYPOGLYCEMIC ACTIVITY OF PROTEIN ISOLATE FROM *BERBERIS VULGARIS* FRUITS

D.A. Amanlikova[1,2], M.J. Oripova[1], D.G. Abdugafurova[1], G.G. Rakhmonova[1]
Institute of Bioorganic Chemistry named A.S. Sadykov of the Science Academy of Uzbekistan[1]
Gulistan State University[2]
https://doi.org/10.5281/zenodo.20303041

Abstract. *This study investigates the antidiabetic and hypoglycemic activity of a protein isolate obtained from* Berberis vulgaris *fruits (BPI). The isolate was prepared using acid extraction followed by isoelectric precipitation, yielding 3.84% with a protein content of 44.1% as determined by the Lowry method. SDS-PAGE analysis revealed a heterogeneous distribution of proteins with molecular weights ranging from 15 to 70 kDa, indicating the presence of both low- and high-molecular-weight fractions, including potential bioactive peptides. The biological activity of BPI was evaluated in an alloxan-induced diabetes model in rats. Oral administration of BPI at a dose of 25 mg/kg for 14 days resulted in a significant reduction in blood glucose levels compared to the control group, along with stabilization of body weight. By day 14, glucose levels decreased to 5.9 ± 0.3 mmol/L versus 11.2 ± 0.43 mmol/L in untreated diabetic animals. The observed hypoglycemic effect may be associated with the presence of bioactive peptides capable of inhibiting carbohydrate-digesting enzymes, improving insulin sensitivity, and reducing oxidative stress. Overall, the findings demonstrate that BPI exhibits pronounced antidiabetic potential and may serve as a promising natural source for the development of functional foods and nutraceuticals aimed at diabetes management.*

Keywords*: berberis vulgaris*; *barberry protein isolate; antidiabetic activity; hypoglycemic effect; alloxan-induced diabetes; bioactive peptides; blood glucose regulation.*

Introduction

Diabetes mellitus is a chronic metabolic disorder characterized by persistent hyperglycemia resulting from defects in insulin secretion, insulin action, or both. The global prevalence of diabetes continues to rise, posing a significant burden on healthcare systems and increasing the risk of severe complications such as cardiovascular diseases, neuropathy, nephropathy, and retinopathy. Although synthetic antidiabetic drugs are widely used, their long-term administration is often associated with adverse effects, high costs, and limited accessibility in some regions. Therefore, the search for safer, more effective, and naturally derived therapeutic agents remains an important area of research.

Medicinal plants have long been recognized as valuable sources of bioactive compounds with diverse pharmacological properties, including antidiabetic and hypoglycemic effects. Among them, *Berberis vulgaris* (barberry) has attracted considerable attention due to its rich phytochemical composition and traditional use in managing metabolic disorders. The fruits of this plant are known to contain alkaloids, phenolic compounds, organic acids, vitamins, and other biologically active substances that contribute to its therapeutic potential [1-3].

While most studies have focused on low-molecular-weight compounds such as berberine, recent attention has shifted toward macromolecules, particularly proteins and bioactive peptides, which may exhibit significant biological activities. Protein isolates derived from plant sources are

increasingly recognized for their potential health benefits, including antioxidant, anti-inflammatory, and glucose-regulating effects. However, the antidiabetic potential of protein isolates obtained from *Berberis vulgaris* fruits remains insufficiently explored. Protein isolates may exert hypoglycemic effects through various mechanisms, such as inhibition of carbohydrate-digesting enzymes, enhancement of insulin sensitivity, modulation of glucose uptake, and protection of pancreatic β-cells from oxidative stress [4,5]. Investigating these mechanisms could provide new insights into the development of functional foods or nutraceuticals aimed at diabetes management.

The aim of study is to investigate the antidiabetic and hypoglycemic activity of a protein isolate obtained from the fruits of *Berberis vulgaris*. The study seeks to evaluate its potential effects on glucose regulation and to explore its possible mechanisms of action, including its influence on carbohydrate metabolism and insulin-related pathways. Furthermore, this research aims to assess the feasibility of using this plant-derived protein isolate as a natural therapeutic agent for the management of diabetes mellitus.

Materials and methods

Preparation of Barberry Protein Isolate (BPI). Protein isolates were prepared from freeze-dried barberry fruits using acid extraction according to a modified method of Acosta et al. [6]. Briefly, 100 g of freeze-dried fruit powder was mixed with 1 L of 10% (v/v) acetic acid solution (pH ~2.3) in a glass beaker and stirred continuously using a magnetic stirrer at room temperature (22 ± 2°C) for 3 hours to facilitate protein solubilization. The mixture was then centrifuged at 6000 rpm (5000 × g) for 20 minutes at 4°C using a refrigerated centrifuge (Eppendorf 5810 R, Germany), and the supernatant was collected. The pellet was re-extracted with 500 mL of 10% acetic acid for 1 hour, centrifuged, and the supernatants were combined. Protein precipitation was achieved by adjusting the pH of the combined supernatant to 4.5 (the isoelectric point of most plant proteins) using 1 M NaOH solution with continuous stirring. The precipitate was allowed to settle overnight at 4°C, then collected by centrifugation at 6000 rpm for 20 minutes. The protein precipitate was washed three times with distilled water (pH adjusted to 4.5) to remove residual salts and acetic acid, then freeze-dried at −55°C and 0.05 mbar for 48 hours. The dried BPI was ground to a fine powder, stored in airtight containers at −20°C, and protected from light until analysis. The yield of protein isolate was calculated as:

Yield (%) = (Weight of BPI / Weight of freeze-dried fruit powder) × 100

Protein Content Determination. The protein content of BPI was determined using the Lowry method [7] with bovine serum albumin (BSA, Sigma-Aldrich, USA) as the standard. Briefly, BPI samples (1 mg) were dissolved in 1 mL of 0.1 M NaOH, and 0.1 mL of the solution was mixed with 1 mL of alkaline copper reagent (prepared by mixing 50 mL of 2% Na_2CO_3 in 0.1 M NaOH with 0.5 mL of 1% $CuSO_4 \cdot 5H_2O$ and 0.5 mL of 2% sodium potassium tartrate). After 10 minutes of incubation at room temperature, 0.1 mL of Folin-Ciocalteu reagent (diluted 1:1 with distilled water) was added, and the mixture was vortexed immediately. After 30 minutes of incubation in the dark, absorbance was measured at 750 nm using a UV-Vis spectrophotometer (METASH UV-5100, China). A calibration curve was prepared using BSA solutions (0–1000 µg/mL), and results were expressed as µg protein per mg of BPI.

SDS-PAGE Analysis. SDS–PAGE was performed according to the Laemmli method to determine the molecular weight distribution of BPI proteins. Samples (2 mg/mL) were mixed with sample buffer (62.5 mM Tris–HCl, pH 6.8; 2% SDS; 10% glycerol; 5% β-mercaptoethanol; 0.01% bromophenol blue), heated at 95°C for 5 min, and cooled on ice. Electrophoresis was carried out

using a Dual Mini Vertical Electrophoresis Unit (Sigma-Aldrich, USA) with 12% resolving and 4% stacking gels at 120 V for ~90 min in Tris–glycine–SDS buffer. A pre-stained protein marker (10–180 kDa) was used as a reference. Gels were stained with Coomassie Brilliant Blue R-250 and destained until clear bands appeared. Protein molecular weights were estimated using standard markers (10–130 kDa).

Determination of antidiabetic and hypoglycemic activity. The experiments were conducted on 18 adult white rats weighing 220–250 g, maintained on a standard diet. The animals were divided into three groups, each consisting of 6 rats. In the first group, the studied parameters were evaluated under conditions of diabetes mellitus: pathological control (PC) — animals with experimentally induced diabetes receiving physiological saline with alloxan hydrate. The second group consisted of diabetic animals treated with the reference drug AlaDiabet (capsules, manufacturer: "AS-SUNNA PHARMACEUTICAL", Uzbekistan) at a dose of 106 mg/kg. The third group (PC) included diabetic animals treated with *Berberis vulgaris* protein isolate at a dose of 25 mg/kg. In this study, diabetes mellitus was induced by intraperitoneal injection of Alloxan at a dose of 120 mg/kg. The development of diabetes was monitored by an increase in blood glucose levels to no less than 17–20 mmol/L, as well as by increased water intake and body weight loss. *Berberis vulgaris* protein isolate was administered orally to animals with alloxan-induced diabetes once daily for 14 days at a dose of 25 mg/kg. The selected dose and duration of treatment were based on previously observed efficacy at this dosage. Animals were monitored for general condition over a two-week period under vivarium conditions. On the second day after diabetes induction, the *Berberis vulgaris* protein isolate substance was administered intragastrically at a dose of 25 mg/kg for 14 days. Blood samples were collected on day 7 to determine glucose levels. Blood glucose levels were measured using test strips and the Contour Plus glucometer.

Animal Ethics. All preoperative and experimental protocols have been thoroughly reviewed and approved by the Institutional Committee for the Use and Care of Animals. The animals were kept in the rooms of the vivarium under controlled conditions, with a relative humidity of 55-65%, an ambient temperature of 22±2 ° C and had free access to water and regular laboratory feed. All procedures for the treatment and care of animals strictly comply with the European Directive 2010/63/EU on the protection of animals used for scientific purposes. The ethical approval of this study was received by the Institute of Bioorganic Chemistry of the Academy of Sciences of the Republic of Uzbekistan, the Committee on Animal Ethics (Protocol No. 133/1a/h dated August 4, 2014).

Results

The yield of barberry protein isolate (BPI) obtained using 10% acetic acid extraction was 3.84% of the initial freeze-dried fruit powder mass. This yield is comparable to protein isolates obtained from other fruit sources using similar acid extraction methods. For example, Acosta et al. [6] reported protein isolate yields of 4.2% from *B. microphylla* fruits using alkaline extraction followed by isoelectric precipitation. The relatively modest yield reflects the low total protein content of barberry fruits (10.7% DW) and the selectivity of the acid extraction method, which preferentially solubilizes certain protein fractions while leaving others in the insoluble residue [6, 8]. The protein content of BPI, determined by the Lowry method, was 441 µg/mg (44.1% w/w), indicating a high degree of protein enrichment in the isolate compared to the whole fruit (10.7% DW). The SDS-PAGE analysis of BPI (Figure) revealed protein bands at 15, 25, 35, 50, and 70 kDa, indicating a heterogeneous mixture of low-, medium-, and high-molecular-weight proteins obtained via acid extraction. The presence of low-molecular-weight fractions may reflect bioactive

peptides or partial protein hydrolysis. This compositional diversity may be linked to the antidiabetic potential of BPI, as such peptides are known to inhibit α-amylase and α-glucosidase, improve insulin sensitivity, and exert antioxidant effects [9-11] Additionally, higher-molecular-weight proteins may contribute synergistically or serve as precursors of bioactive peptides [12].

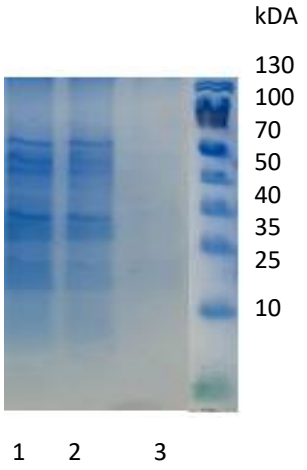


Figure. The electrophoretic profiles of Berberis vulgaris fruit protein isolate on SDS-PAGE; 1, 2: BPI, 2: Marker.

Table 1. Blood glucose levels in rats with alloxan-induced diabetes on days 7 and 14 after the administration of Berberis vulgaris, (M±m, n=6)

Experimental groups and doses	Initial values	Values on day 7 of the experiment		Values on day 14 of the experiment	
		Animal weight	Glucose, mmol/L	Animal weight	Glucose, mmol/L
Control, water 2 ml	301,6±9,3	269±2,3	9,6±2,1	251,3±6,0	11,2±0,43
AlaDiabet 106 mg/kg	276,3±8,6	287,3±8,6	8,6±2,7	297,2±4,0** p=0.0001	8,9±3,3
BPI, 25 mg/kg	299,1±8,6	315,3±13,7* p=0.008	7,3±1,5	318,6±7,3** p=0.00005	5,9±0,3** p=0.000003

*p<0,01; **p<0,005 - significant differences versus the control group

The results showed a positive effect of BPI on metabolic parameters in experimental animals (Table 1). In the BPI-treated group, a stable increase in body weight was observed over 7 and 14 days, accompanied by a significant reduction in blood glucose levels. In particular, by day 7, the dynamics of body weight were significantly higher compared with the control group ($p<0.01$). After 14 days of treatment, body weight showed a statistically significant increase in both the *AlaDiabet* and BPI groups compared with the control group ($p<0.005$ for both groups). During the same period, a statistically significant decrease in blood glucose levels was observed in the BPI-treated group compared with the control group ($p<0.005$).

Although the reference drug *AlaDiabet* also demonstrated a certain degree of activity, the BPI-treated group exhibited more stable and pronounced antidiabetic effects. These findings suggest that the bioactive protein fractions and peptides present in BPI may play an important role in regulating glucose metabolism. Overall, these data indicate the potential of *Berberis vulgaris* proteins as a promising component of functional foods and nutraceuticals for the prevention and correction of metabolic disorders.

Conclusions. The results of this study demonstrate that the protein isolate obtained from *Berberis vulgaris* fruits possesses significant antidiabetic and hypoglycemic activity in an alloxan-

induced diabetes model. Oral administration of BPI at a dose of 25 mg/kg for 14 days led to a pronounced reduction in blood glucose levels and stabilization of body weight in experimental animals, indicating an improvement in metabolic status. SDS-PAGE analysis revealed a heterogeneous composition of proteins with molecular weights ranging from 15 to 70 kDa, suggesting the presence of both high-molecular-weight proteins and low-molecular-weight peptides. These bioactive fractions may play a key role in the observed biological effects, potentially through mechanisms such as modulation of carbohydrate metabolism, enhancement of insulin sensitivity, and reduction of oxidative stress.

Overall, the findings indicate that BPI represents a promising natural source of biologically active compounds with antidiabetic potential. The study supports the feasibility of using *Berberis vulgaris*-derived protein isolates as functional ingredients in the development of nutraceuticals or therapeutic agents for the management of diabetes mellitus.

REFERENCES

1. Imenshahidi M., Hosseinzadeh H. *Berberis vulgaris* and berberine: A review of pharmacological effects. Phytotherapy Research, 2016, 30(11): 1745–1764.
2. Tillhon M., Guamán Ortiz L.M., Lombardi P., Scovassi A.I. Berberine: New perspectives for old remedies. Biochemical Pharmacology, 2012, 84(10): 1260–1267.
3. Gokhale A.B., Damre A.S., Saraf M.N. Investigations into the immunomodulatory activity of *Berberis aristata*. Journal of Ethnopharmacology, 2003, 84(1): 49–55.
4. Lacroix I.M.E., Li-Chan E.C.Y. Dipeptidyl peptidase-IV inhibitory activity of dairy protein hydrolysates. *International Dairy Journal*, 2016, 54: 1–7.
5. Maritim A.C., Sanders R.A., Watkins J.B. Diabetes, oxidative stress, and antioxidants: A review. *Journal of Biochemical and Molecular Toxicology*, 2003, 17(1): 24–38.
6. Acosta C, Carpio C, Vilcacundo R, Carrillo W. Argentine Patagonia barberry (*Berberis microphylla*): proximate composition including proteins and phenolic compounds, antioxidant capacity, and protein isolate profile. *Food Chemistry*. 2020;330:127209. doi: 10.1016/j.foodchem.2020.127209
7. Lowry OH, Rosebrough NJ, Farr AL, Randall RJ. Protein measurement with the Folin phenol reagent. *Journal of Biological Chemistry*. 1951;193:265–275.
8. Boeri P, Piñuel L, Dalzotto D, Monasterio R, Fontanella B, Campanella O, Sabbag N. Argentine Patagonia barberry chemical composition and evaluation of its antioxidant capacity. *Journal of Food Biochemistry*. 2020;44:e13254. doi: 10.1111/jfbc.13254
9. Nongonierma A.B., FitzGerald R.J. Bioactive properties of milk proteins in humans: A review. *Peptides*, 2015, 73: 20–34.
10. Udenigwe C.C., Aluko R.E. Food protein-derived bioactive peptides: Production, processing, and potential health benefits. *Journal of Food Science*, 2012, 77(1): R11–R24.
11. Patil P., Mandal S., Tomar S.K., Anand S. Food protein-derived bioactive peptides in management of type 2 diabetes. *European Journal of Nutrition*, 2015, 54: 863–880.
12. Maritim A.C., Sanders R.A., Watkins J.B. Diabetes, oxidative stress, and antioxidants: A review. *Journal of Biochemical and Molecular Toxicology*, 2003, 17(1): 24–38.

ANTICOAGULANT AND ANTI-INFLAMMATORY ACTIVITIES OF METABOLITES PRODUCED BY THE ENDOPHYTIC FUNGUS *ASPERGILLUS CHEVALIERI* PM4S ISOLATED FROM *PLANTAGO MAJOR*

N. Kuzieva[1], L. Abdulmyanova[2], M. Sheripbayeva[3]
Junior Researcher, Laboratory of Biochemistry and Biotechnology of Bioactive Compounds, Institute of Microbiology of Uzbekistan[1]
Leading Researcher, Doctor of Biological Sciences, Institute of Microbiology of Uzbekistan[2]
Master's Student, Department of Microbiology, National University of Uzbekistan named after Mirzo Ulugbek[3]
https://doi.org/10.5281/zenodo.20303449

Abstract. *The present study aimed to evaluate the anticoagulant and anti-inflammatory activities of secondary metabolites produced by the endophytic fungus Aspergillus chevalieri PM4S isolated from Plantago major. Anticoagulant activity was investigated using plasma recalcification time (PRT), prothrombin time (PT), activated partial thromboplastin time (APTT), thrombin time (TT), and fibrinogen (FIB) assays. Anti-inflammatory activity was assessed in vitro by inhibition of ovalbumin denaturation. The obtained results demonstrated pronounced anticoagulant activity of the fungal extract. Treatment with the 96% ethanol extract of A. chevalieri PM4S completely suppressed clot formation for more than 120 min in the PRT assay. In coagulation tests, the extract significantly prolonged APTT from 27.9 ± 0.42 sec to 117.2 ± 1.76 sec and TT from 20.4 ± 0.01 sec to 223.5 ± 0.11 sec, while fibrinogen concentration decreased from 3.4 ± 0.07 g/L to 2.04 ± 0.03 g/L. These findings indicate strong inhibition of intrinsic and common coagulation pathways. In the anti-inflammatory assay, the extract exhibited concentration-dependent inhibition of ovalbumin denaturation. The maximum inhibitory activity was observed at 75 µg/ml, reaching 64.7 ± 0.32%, which exceeded the activity of aspirin at the same concentration (62.2 ± 0.31%). The IC_{50} value of the fungal extract was 122.899 µg/ml, compared with 113.7489 µg/ml for aspirin. The observed biological activities may be associated with polyphenolic, flavonoid, and antioxidant metabolites synthesized by the fungus. The obtained results demonstrate the potential of A. chevalieri PM4S as a promising source of multifunctional natural compounds with anticoagulant and anti-inflammatory properties and support further investigation of its bioactive metabolites for pharmaceutical applications.*

Keywords: *endophytic fungi, Aspergillus chevalieri, Plantago major, anticoagulant activity, plasma recalcification time (PRT),prothrombin time (PT), partially activated thromboplastin time (aPTT), thrombin time (TT), fibrinogen, anti-inflammatory activity, biologically active metabolites.*

Introduction

Thrombotic disorders and inflammatory diseases remain among the major causes of mortality and morbidity worldwide. Excessive activation of coagulation pathways and inflammatory mediators contributes significantly to the development of cardiovascular diseases, venous thrombosis, stroke, and chronic inflammatory conditions (Hirsh et al., 2001, p. 2994).

Although anticoagulant drugs such as heparin and warfarin are widely used in clinical practice, their prolonged administration is frequently associated with hemorrhagic complications, bleeding risks, and other adverse side effects (Hirsh et al., 2001, p. 2994). Therefore, the discovery of novel natural compounds with anticoagulant and anti-inflammatory activities has become an important direction in modern pharmacology and biotechnology.

Medicinal plants are considered valuable natural sources of biologically active metabolites. Among them, *Plantago major* has been traditionally used for centuries as a wound-healing, analgesic, antioxidant, antimicrobial, and anti-inflammatory remedy (Samuelsen, 2000, p. 1). Previous studies demonstrated that the leaves of *P. major* contain numerous bioactive compounds including flavonoids, caffeic acid derivatives, iridoid glycosides, polysaccharides, terpenoids, and other phenolic substances responsible for its pharmacological properties properties (Samuelsen, 2000, p. 1; Chiang et al., 2002, p. 53). In particular, baicalein and aucubin have been identified as major active constituents exhibiting strong antioxidant and anti-inflammatory effects effects (Zubair et al., 2012, p. 825).

Several pharmacological investigations confirmed the anti-inflammatory potential of *Plantago major* extracts. The aqueous extract of the plant significantly reduced carrageenan-induced edema, pleurisy, and exudative inflammatory reactions in experimental animals (Olennikov et al., 2015, p. 118). Moreover, *P. major* extracts and their active metabolites were reported to suppress reactive oxygen species (ROS) production in human neutrophils (Zubair et al., 2012, p. 825). Reduction of ROS generation decreases oxidative stress and inflammatory mediator activity, which are closely associated with platelet activation and coagulation abnormalities. Therefore, metabolites derived from *P. major* may also possess potential anticoagulant properties.

In recent years, endophytic microorganisms, particularly fungal endophytes, have attracted increasing scientific attention as promising producers of pharmacologically important secondary metabolites (Strobel & Daisy, 2003, p. 491).. Endophytes inhabit internal plant tissues without causing damage to their host plants and are capable of synthesizing diverse biologically active compounds. Species belonging to the genus *Aspergillus* are especially recognized for producing metabolites with antioxidant, antimicrobial, anti-inflammatory, fibrinolytic, and anticoagulant activities (Frisvad & Larsen, 2015, p. 45). In addition, fungal metabolites offer several advantages over plant-derived compounds, including rapid growth, high productivity, and easier biotechnological manipulation.

Earlier, the Laboratory of Biochemistry and Biotechnology of Bioactive Compounds at the Institute of Microbiology of the Academy of Sciences of the Republic of Uzbekistan conducted a screening study of preserved and newly isolated endophytic fungal strains to evaluate their anticoagulant activity (Kuzieva et al., 2024,p. 16-22). As a result of this screening, the strain *Aspergillus chevalieri* PM4S isolated from *Plantago major* was selected as a promising producer of biologically active metabolites. Despite extensive studies on the pharmacological properties of *Plantago major*, limited information is available regarding the bioactivity of its associated endophytic fungi.

Materials and Methods

Cultivation and Extraction of Fungal Secondary Metabolites. To isolate metabolites from the biomass of endophytic fungi, the method of Hazalin and co-workers was used with minor modifications (Hazalin, N. A. et al., 2009, p 46). The fungi were grown in a liquid culture medium with potato dextrose broth on a shaker at 180 rpm and 28 °C for 7-10 days. The culture liquid and

biomass were separated by centrifugation at 6000 rpm, and the samples were stored in a freezer at -20 °C. The grown biomass was ground in a porcelain mortar with quartz sand. After obtaining the homogenate, it was placed in a flask, 50 ml of ethyl ester of acetic acid was added and left for 24 hours at room temperature on a rocking table for extraction. Then the mass was filtered through paper (watman No. 1), 40 mkg/ml of sodium sulfate was added to remove the water layer, and the obtained extract was evaporated on a rotary evaporator. To the dry mass, 1.5 ml of 96% solution of ethyl alcohol was added to obtain the extract, which was stored at +4 °C.

Plasma Recalcification Time (PRT) Assay. Extractions were tested for plasma recalcification time (PRT) by the following method. A 0.2 ml citrated blood sample was transferred to a 12 x 75 mm tube. The glass tube was incubated in a water bath at 37 °C for 2 min. To this was added 0.2 ml 0.025 M calcium chloride and a timer was started simultaneously. The ingredients were mixed and the tube was slowly tilted back and forth with a gentle rotating motion for approximately 20 s to observe the appearance of fibrin strands. The time between the addition of calcium chloride and the formation of the first observed fibrin strands was recorded as the blood recalcification time(Sinyuk, I. V., & Dudarev, V. A.,2015, p.78-80).

Coagulation Assays. Coagulation tests — prothrombin time (PT), partially activated thromboplastin time (aPTT), thrombin time (TT), and fibrinogen test — were performed on the HumaClot Junior apparatus(Human GmbH, Wiesbaden, Germany). To do this, 3 ml of blood was taken from the subject,placed in a tube with 3.8% sodium citrate, and centrifuged at 3000 rpm for 3 minutes to separate the plasma. Plasma and extracts were mixed in a 1:5 ratio, and the corresponding reagents (Human GmbH, Wiesbaden, Germany) were added to a clean cuvette. The mixture was incubated for 15seconds and tested on a device at 37 °C.

Inhibition of denaturation of ovalbumin. A 4 ml reaction mixture was prepared containing 0.2 ml of ovalbumin, 2.8 ml of phosphate buffer (pH 6.4), and 1 ml of extracts of different concentrations. A distilled water of the same volume was used as a control. Then the sample was incubated at 37°C for 15 min using water bath and after heated at 65°C for 5 min. After cooling, the absorbance of the reaction mixtures was measured spectrophotometrically at 660 nm. As a standard was assessed acetylsalicylic acid from which a control was prepared at a concentration analogue to the experimental extract. Protein denaturation inhibition (X) by the extract and standard was expressed as a percentage and calculated according to the formula: $X = \frac{A0 - At}{A0} \times 100$, where A_0 is the optical density of the control; At is the optical density of the test sample(Sree Kumari, C. et al., 2015, p. 482–485).

Results and Discussion

The anticoagulant activity of secondary metabolites produced by the endophytic fungus *Aspergillus chevalieri* PM4S was evaluated using plasma recalcification time (PRT) and standard coagulation parameters, including prothrombin time (PT), activated partial thromboplastin time (APTT), thrombin time (TT), and fibrinogen concentration (FIB). The obtained results demonstrated a pronounced anticoagulant effect of the fungal extract on both intrinsic and common coagulation pathways (Table 1).

Table 1. Effect of extracts of the endophytic fungus Aspergillus chevalieri – PM4S on PRT and coagulation tests(n=3, p <0.05).

Indicators		Normal	Heparin (+)	Warfarin (+)	Ethanol (-)	*A.chevalieri* PM4S
PRT	Time,min	1.43±0,04	+	+	1.48±0,06	>120

PT	Time,sec	12,4±0,19	+	+	10,8±0,22	9,7±0,15
	PTI,%	131±0,07	+	+	166±2,49	199,4±3,99
	INR	0,85±0,02	+	+	0,73±0,02	0,66±0,01
APTT	Time,sec	27,9±0,42	+	+	36,8±0,74	117,2±1,76
	Ratio	0,83±0,01	+	+	1,24±0,02	3,91±0,06
TT	Time,sec	20,4±0,01	+	+	19,8±0,29	223,5±0,11
	Ratio	1,25±0,02	+	+	1,21±0,02	13,7±0,27
FIB	g/l	3,4±0,07	>0.70	>0.70	2,35±0,03	2,04±0,03

Under normal conditions, plasma recalcification occurred within 1.43±0,04 min, whereas treatment with the 96% ethanol extract of *A. chevalieri* PM4S resulted in complete suppression of clot formation for more than 120 min. Such a significant prolongation of PRT indicates strong inhibition of coagulation cascade activation and suggests the presence of biologically active metabolites capable of interfering with fibrin clot formation. In contrast, the negative ethanol control demonstrated only minor changes in coagulation parameters, confirming that the observed activity was associated with fungal metabolites rather than solvent effects.

The extract also markedly influenced individual coagulation indicators. APTT increased from 27.9 ± 0.42 sec in the control to 117.2 ± 1.76 sec after treatment with the fungal extract, corresponding to a ratio increase from 0.83 ± 0.01 to 3.91 ± 0.06. This pronounced prolongation indicates substantial inhibition of the intrinsic coagulation pathway. Similarly, TT increased from 20.4 ± 0.01 sec to 223.5 ± 0.11 sec, with the TT ratio rising to 13.7 ± 0.27, demonstrating a strong inhibitory effect on thrombin-mediated fibrin formation. The fibrinogen concentration simultaneously decreased from 3.4 ± 0.07 g/L in normal plasma to 2.04 ± 0.03 g/L following treatment with the extract, further supporting disruption of fibrin polymerization processes. Similar anticoagulant effects of endophytic fungal metabolites rich in phenolic and flavonoid compounds have previously been reported in representatives of *Aspergillus* and *Penicillium* species (Ha et al., 2020, p. 247).

In contrast to the substantial effects observed for APTT and TT, PT values showed only moderate variation. The PT decreased from 12.4 ± 0.19 sec to 9.7 ± 0.15 sec, while the INR value declined from 0.85 ± 0.02 to 0.66 ± 0.01. These findings suggest that the metabolites of *A. chevalieri* PM4S may predominantly target components of the intrinsic and thrombin-dependent stages of coagulation rather than the extrinsic pathway. Similar observations have been described for fungal metabolites possessing antioxidant and enzyme-modulating properties capable of suppressing fibrin clot formation (Toghueo and Boyom, 2019, p. 43).

The obtained results are consistent with previous studies demonstrating anticoagulant properties of secondary metabolites produced by species of the genera *Aspergillus* and *Penicillium*. Several fungal metabolites, including phenolic derivatives, quinones, and flavonoids, have been reported to prolong coagulation time by suppressing thrombin activity, reducing fibrin formation, or modulating calcium-dependent coagulation reactions (Khan et al., 2020, p. 20738). The exceptionally prolonged TT observed in this study may indicate direct inhibition of thrombin activity or interference with fibrinogen conversion into fibrin.

The anti-inflammatory activity of the ethyl acetate extract of *A. chevalieri* PM4S was investigated using an in vitro ovalbumin denaturation inhibition model. Protein denaturation assays are widely used for evaluation of anti-inflammatory potential because denatured proteins can induce inflammatory and autoimmune responses. Prevention of thermal protein denaturation

therefore reflects the capacity of biologically active compounds to stabilize protein structures under inflammatory conditions (Chi et al., 2019, p. 1).

The fungal extract demonstrated concentration-dependent anti-inflammatory activity comparable to aspirin at several tested concentrations (Table 2). At 25 μg/ml, the extract inhibited ovalbumin denaturation by 44.8 ± 0.45%, while aspirin demonstrated 49.7 ± 0.25% inhibition. Increasing the concentration to 50 μg/ml enhanced the inhibitory activity of the extract to 49.8 ± 0.75%. The maximum anti-inflammatory effect of the fungal extract was observed at 75 μg/ml, where inhibition reached 64.7 ± 0.32%, exceeding the activity of aspirin at the same concentration (62.2 ± 0.31%).

Table 2. Anti-inflammatory activity of Aspergillus chevalieri – PM4S determined by inhibition of ovalbumin denaturation (n = 3, p <0.05).

№	Concentration μg/ml	Aspirin, %	*A.chevalieri* – PM4S, %
1	25	49,7±0,25	44,8±0,45
2	50	68,1±0,27	49,8±0,75
3	75	62,2±0,31	64,7±0.32
4	100	58,4±0,18	58,4±0,23
5	125	52,2±0,52	44,3±0,44
6	150	50,2±1,00	38,8±0,58
	IC_{50} (μg/ml)	113,7489	122,899

At higher concentrations (100–150 μg/ml), a gradual decline in inhibitory activity was observed for both aspirin and the fungal extract. Nevertheless, the extract retained substantial anti-inflammatory potential throughout the tested concentration range. The IC_{50} value of *A. chevalieri* PM4S extract was calculated as 122.899 μg/ml, which was relatively close to that of aspirin (113.7489 μg/ml). These findings indicate that the metabolites produced by the studied endophytic fungus possess pronounced protein-stabilizing activity and may serve as promising natural anti-inflammatory agents.

The observed anti-inflammatory activity may be associated with the presence of polyphenolic metabolites, flavonoids, terpenoids, and related antioxidant compounds previously reported in endophytic fungi (Zhao et al., 2020, p. 20738). Such metabolites are known to suppress inflammatory processes through inhibition of protein denaturation, reduction of oxidative stress, stabilization of biomembranes, and modulation of inflammatory mediators. Phenolic compounds, in particular, can inhibit reactive oxygen species formation and reduce oxidative modification of proteins, thereby limiting inflammatory damage Prospective Leads from Endophytic Fungi for Anti-Inflammatory Drug Discovery.

Overall, the obtained results demonstrate that metabolites produced by *A. chevalieri* PM4S possess both anticoagulant and anti-inflammatory activities. The pronounced prolongation of coagulation parameters together with significant inhibition of protein denaturation suggests the multifunctional biological potential of metabolites synthesized by this endophytic fungus. These findings support the possibility of using endophytic fungal metabolites as promising sources of novel bioactive compounds for development of natural anticoagulant and anti-inflammatory agents.

Conclusion

This study demonstrated that secondary metabolites produced by the endophytic fungus *Aspergillus chevalieri* PM4S exhibit pronounced anticoagulant and anti-inflammatory activities in vitro. The ethanol extract of the fungus significantly prolonged plasma recalcification time (PRT), activated partial thromboplastin time (APTT), and thrombin time (TT), indicating strong inhibition of the intrinsic and common coagulation pathways. In addition, the reduction in fibrinogen concentration suggests suppression of fibrin formation and polymerization processes.

The anti-inflammatory potential of the fungal extract was confirmed using the ovalbumin denaturation inhibition model. The extract demonstrated concentration-dependent protein-stabilizing activity, with the maximum inhibitory effect observed at 75 μg/ml, where the activity exceeded that of aspirin. Furthermore, the IC_{50} value of the extract was comparable to the standard anti-inflammatory drug, indicating substantial anti-inflammatory potential.

The scientific novelty of this study lies in the first comprehensive evaluation of both anticoagulant and anti-inflammatory properties of metabolites produced by *A. chevalieri* PM4S isolated from *Plantago major*. The obtained results expand current knowledge regarding the pharmacological potential of endophytic fungi and demonstrate that metabolites synthesized by this strain are capable of modulating coagulation processes while simultaneously stabilizing protein structures under inflammatory conditions.

The observed biological activities are likely associated with the presence of polyphenolic, flavonoid, and other antioxidant metabolites capable of suppressing thrombin-mediated fibrin formation, reducing oxidative stress, and inhibiting protein denaturation. Overall, the findings confirm the potential of endophytic fungi as promising sources of multifunctional natural bioactive compounds and support the need for further purification, structural characterization, and mechanistic investigation of individual active metabolites for potential biomedical and pharmaceutical applications.

REFERENCES

1. Chi, W. C., Pang, K. L., Chen, W. L., Wang, G. J., & Lee, T. H. (2019). Antimicrobial and iNOS inhibitory activities of endophytic fungi isolated from *Acanthus ilicifolius* var. *xiamenensis*. *Botanical Studies, 60*(4), 1–9.
2. Chiang, L. C., Chiang, W., Chang, M. Y., Ng, L. T., & Lin, C. C. (2002). Antiviral activity of *Plantago major* extracts and related compounds in vitro. *Antiviral Research, 55*(1), 53–62.
3. Frisvad, J. C., & Larsen, T. O. (2015). Extrolites of *Aspergillus* species. *Chemical Fungal Taxonomy, 45*, 45–56.
4. Ha, T. M., Kim, D. C., Sohn, J. H., Yim, J. H., & Oh, H. (2020). Anti-inflammatory and protein tyrosine phosphatase 1B inhibitory metabolites from the Antarctic marine-derived fungal strain *Penicillium glabrum* SF-7123. *Marine Drugs, 18*(5), 247. https://doi.org/10.3390/md18050247
5. Hazalin, N. A., Ramasamy, K., Lim, S. M., Wahab, I. A., Cole, A. L. J., & Majeed, A. A. (2009). Cytotoxic and antibacterial activities of endophytic fungi isolated from plants at the National Park, Pahang, Malaysia. *BMC Complementary and Alternative Medicine, 9*, 46. https://doi.org/10.1186/1472-6882-9-46
6. Hirsh, J., Anand, S. S., Halperin, J. L., & Fuster, V. (2001). Guide to anticoagulant therapy. *Circulation, 103*(24), 2994–3018. https://doi.org/10.1161/01.CIR.103.24.2994
7. Khan, I., Zhang, H., Liu, W., Zhang, L., Peng, F., Chen, Y., et al. (2020). Identification and bioactivity evaluation of secondary metabolites from Antarctic-derived *Penicillium*

chrysogenum CCTCC M 2020019. *RSC Advances, 10*, 20738–20744. https://doi.org/10.1039/D0RA03144A

8. Kuzieva N. H., Abdulmyanova L. I., & Gulyamova T. G. (2024). Skrining antikoagulyantnykh svoystv etanol'nykh ekstraktov endofitnykh gribov. *Universum: Khimiya i biologiya, 9*(123).16-22. https://doi.org/10.32743/UniChem.2024.123.9.18172
9. Olennikov, D. N., Kashchenko, N. I., & Chirikova, N. K. (2015). Anti-inflammatory and antioxidant activity of *Plantago major* extracts. *Pharmaceutical Chemistry Journal, 49*, 118–122.
10. Samuelsen, A. B. (2000). The traditional uses, chemical constituents and biological activities of *Plantago major* L. *Journal of Ethnopharmacology, 71*(1–2), 1–21.https://doi.org/10.1016/S0378-8741(00)00212-9
11. Sinyuk, I. V., & Dudarev, V. A. (2015). Svertyvayushchey sistemy krovi i krovosnabzheniya golovki tazobedrennogo sustava v patogeneze bolezni Pertesa. *Mezhdunarodnyy zhurnal eksperimental'nogo obrazovaniya, 11*(1), 78–80.
12. Sree Kumari, C., Reddy, B. S., & Kumar, B. A. (2015). In vitro anti-inflammatory and anti-arthritic activity of *Rhizophora mucronata* leaves. *International Journal of Pharma Sciences and Research, 6*(3), 482–485.
13. Strobel, G., & Daisy, B. (2003). Bioprospecting for microbial endophytes and their natural products. *Microbiology and Molecular Biology Reviews, 67*(4), 491–502. https://doi.org/10.1128/MMBR.67.4.491-502.2003
14. Toghueo, R. M. K., & Boyom, F. F. (2019). Endophytic fungi from *Terminalia* species: A comprehensive review. *Journal of Fungi, 5*(2), 43. https://doi.org/10.3390/jof5020043
15. Zhao, M., Ruan, Q., Pan, W., Tang, Y., Zhao, Z., & Cui, H. (2020). New polyketides and diterpenoid derivatives from the fungus *Penicillium sclerotiorum* GZU-XW03-2 and their anti-inflammatory activity. *Fitoterapia, 143*, 104561. https://doi.org/10.1016/j.fitote.2020.104561
16. Zubair, M., Ekholm, A., Nybom, H., Renvert, S., Widen, C., & Rumpunen, K. (2012). Effects of *Plantago major* L. leaf extracts on human oral epithelial cells in a scratch assay. *Journal of Ethnopharmacology, 141*(3), 825–830. https://doi.org/10.1016/j.jep.2012.03.02

EFFECT OF *AZOTOBACTER CHROOCOCCUM* XH2018 STRAIN ON THE UPTAKE OF CERTAIN ELEMENTS IN WHEAT (*TRITICUM AESTIVUM* L.) AT THE TILLERING STAGE

J.B. Nizomov[1], B.A. Rasulov[2]
Andijan State Technical Institute, 56 Babur Shah Street, Andijan, 170119, Republic of Uzbekistan[1]
Institute of Genetics and Experimental Biology of Plants, Uzbekistan Academy of Sciences, 111226, Yuqori Yuz, Kibray District, Tashkent Region[2]
https://doi.org/10.5281/zenodo.20523186

Abstract. *The effect of the biological preparation "Bioazot," developed on the basis of Azotobacter chroococcum XH2018 strain, on the uptake of macro- and microelements in wheat (Triticum aestivum L.) was investigated. The "Mezon" winter wheat cultivar was analyzed at the tillering stage, and elemental concentrations in root and shoot samples were determined using Inductively Coupled Plasma Optical Emission Spectrometry (ICP-OES). The experiment was conducted in 14 variants, with the Bioazot preparation applied in various combinations with mineral fertilizers. The results demonstrated that A. chroococcum XH2018 strain enhances the bioavailability of nutritional elements in plants, particularly promoting the accumulation of physiologically essential elements such as Fe, Zn, Mn, K, and Mg in the root system. Correlation analyses revealed strong synergistic and antagonistic relationships between certain elements. Specifically, strong positive correlations were recorded among Fe, Mn, Ba, and Cr, whereas potassium exhibited negative correlations with certain microelements. The findings, consistent with data from other studies, confirm the significant role of Azotobacter-based biofertilizers in improving wheat nutrition and mineral metabolism. The study demonstrates the potential of Bioazot as an ecologically safe and effective biological fertilization agent.*

Keywords: *bioazot, macro-and microelements, ICP-OES, correlation relationships, root, stem.*

INTRODUCTION

Microorganisms, particularly rhizobacteria, play an important role in enhancing plant growth, development, and productivity [8]. Rhizobacteria influence nutrient uptake, immune system formation, and element assimilation processes in plants [5,6,21]. In addition, rhizobacteria participate in the translocation of macro- and microelements within plants [14]. In particular, they exert a positive effect on the mobility of elements such as iron (Fe), zinc (Zn), and magnesium (Mg), which are of special significance in plant metabolism [12,14]. These elements play a crucial role in protein and chlorophyll synthesis as well as enzymatic activity in plants [9,15]. Deficiency of these elements may lead to suppression of vegetative growth, chlorosis, disruption of metabolic processes, and reduction in yield [13]. Wheat (*Triticum aestivum* L.) is one of the most important cereal crops worldwide and holds strategic significance in ensuring global food security. Under conditions of increasing population growth, global climate change, declining soil fertility, and intensifying anthropogenic pressure on agroecosystems, sustainably improving wheat yield and enhancing mineral nutrition efficiency represent one of the most pressing directions of modern agrobiotechnology [3].

The tillering stage, one of the key vegetative phases of wheat ontogenesis, represents a physiologically critical period in the formation of yield structure. It is during this stage that lateral shoot formation, active root system development, expansion of leaf area, and intensive accumulation of vegetative biomass are observed. The formation and viability of tillers directly influence the number of productive stems, spike elements, and final grain yield [19]. Long-term agrobiological observations have emphasized that physiological processes and nutritional conditions during the tillering stage are among the primary factors determining the yield potential of wheat [18]. During the tillering stage, the plant's demand for nutritional elements increases sharply, as this period is characterized by intensified cell division, tissue differentiation, chloroplast formation, enzymatic reactions, and development of the photosynthetic apparatus [9].

The aim of this study was to determine the accumulation, quantitative distribution, and translocation characteristics of macro- and microelements in the roots and shoots of wheat (*Triticum aestivum* L.) at the tillering stage under the influence of Bioazot suspension prepared on the basis of *A. chroococcum* XH2018 strain.

MATERIALS AND METHODS

2.1. Research Material

The "Mezon" winter wheat cultivar (*Triticum aestivum* L.), propagated at the Institute of Genetics and Experimental Biology of Plants of the Academy of Sciences of the Republic of Uzbekistan, was selected as the research object. This cultivar is distinguished from other registered varieties by its high yield potential, early maturity, resistance to yellow rust, lodging tolerance, and good adaptability to diverse soil and climatic conditions. According to data from the institute's appraisal commission, the "Mezon" cultivar has an average stem height of 95 cm, a 1,000-grain weight of 44.8 g, a gluten content of 29.4%, and an average yield of 70–80 centners per hectare.

The study was conducted at the tillering stage of wheat development. Root and shoot samples were collected from plants for analysis.

2.2. Bacterial Strain and Biological Preparation

The free-living nitrogen-fixing *A. chroococcum* XH2018 strain was used throughout the study. This strain possesses the ability to convert atmospheric molecular nitrogen into forms assimilable by plants, synthesize phytohormones, and enhance the bioavailability of nutritional elements in the rhizosphere [1,10].

The strain was propagated in liquid nutrient medium under standard microbiological conditions, and the biological preparation "Bioazot" was produced from the active biomass. The prepared formulation was subsequently applied for the nutritional treatment of wheat plants in experimental trials.

2.3. Experimental Variants and Wheat Fertilization

The effect of the "Bioazot" biological preparation, developed on the basis of *A. chroococcum* XH2018 strain, on the accumulation and distribution of macro- and microelements in wheat plants was investigated throughout the study. The experiment was organized in a total of 14 variants. The experimental variants are presented in Table 2.1.

Table 2.1 Experimental Variants and Applied Fertilization Scheme

Variant	Preparation	Bioazot (ml)	Urea (g)	Ammophos (g)	Potassium (g)
V1	Control	–	–	–	–
V2	Bioazot	177.5	–	–	–

V3	Bioazot+NPK	177.5	177.5	106.5	35.5
V4	Bioazot+NPK	177.5	177.5	142.0	35.5
V5	Bioazot+NPK	177.5	177.5	177.5	3.55
V6	Bioazot+NPK	177.5	177.5	177.5	35.5
V7	Bioazot+NPK	177.5	213.0	106.5	35.5
V8	Bioazot+NPK	177.5	213.0	142.0	35.5
V9	Bioazot+NPK	177.5	213.0	177.5	35.5
V10	Bioazot+NPK	177.5	213.0	213.0	35.5
V11	Bioazot+NPK	177.5	213.0	106.5	53.25
V12	Bioazot+NPK	177.5	213.0	142.0	53.25
V13	Bioazot+NPK	177.5	213.0	177.5	53.25
V14	Bioazot+NPK	177.5	213.0	213.0	53.25

The volume of Bioazot preparation in each variant was 177.5 ml. Mineral fertilizers were applied in various combinations, including urea (177.5–213 g), ammophos (106.5–213 g), and potassium (35.5–53.25 g). The prepared suspensions were applied to wheat plants at the tillering stage.

2.4. Preparation of Plant Samples

Root and shoot samples were collected separately from wheat plants at the tillering stage. Under laboratory conditions, the samples were washed with distilled water and cleaned of external contaminants.

The cleaned samples were dried at 65–70°C until constant mass was achieved. The dried samples were ground in a laboratory mill and brought to a uniform granulometric fraction. The prepared samples were stored in hermetically sealed containers for subsequent chemical analyses.

2.5. Sample Mineralization

For elemental analysis, 0.1000 g of each dried sample was weighed on an analytical balance and placed into Teflon autoclaves.

To each sample, 3 ml of high-purity concentrated nitric acid (HNO_3) and 2 ml of hydrogen peroxide (H_2O_2) were added. The autoclaves were tightly sealed and placed into a microwave mineralization system - the Berghof Speedwave Xpert.

The wet digestion process was carried out at temperatures ranging from 50 to 230°C under a maximum pressure of 40 bar for 35–45 minutes. Following mineralization, the solutions were cooled to room temperature and quantitatively transferred into 50 ml volumetric flasks, diluted to the mark with bidistilled water, and thoroughly mixed.

2.6. Determination of Macro- and Microelements by ICP-OES

The quantitative composition of macro- and microelements in the mineralized solutions was determined using a Perkin Elmer Avio-200 Inductively Coupled Plasma Optical Emission Spectrometer (ICP-OES).

During the analysis, macroelements including nitrogen (N), phosphorus (P), potassium (K), calcium (Ca), and magnesium (Mg), as well as microelements including iron (Fe), zinc (Zn), manganese (Mn), copper (Cu), boron (B), and others, were quantitatively evaluated by calibration against standard multi-element solutions. Analyses were conducted using argon gas of 99.995% purity. The obtained results were automatically recalculated by the instrument's software, accounting for sample mass and dilution coefficients, and relative standard deviation (RSD) values were determined [2,4].

2.7. Statistical Analysis

Statistical processing of the obtained data was performed using Microsoft Excel and PAST software. Spearman's rank correlation analysis was conducted to evaluate the interrelationships among macro- and microelements across the experimental variants.

RESULTS

3.1. Accumulation Characteristics of Elements in the Wheat Root System

3.1.1. Quantitative Characterization of Elements in Root Tissues

A descriptive statistical analysis was performed to evaluate the quantitative composition of macro- and microelements in the root portion at the tillering stage. According to the analysis results, considerable variation was observed in the accumulation levels of elements in the root tissues of wheat (*Triticum aestivum* L.). Among the elements studied, the highest mean concentration was recorded for potassium (K), with a value of 13,459.07 ± 2,518.65 mg/kg. In addition, iron (Fe) (6,037.74 ± 1,661.67 mg/kg), aluminum (Al) (438.03 ± 97.60 mg/kg), and manganese (Mn) (275.78 ± 110.39 mg/kg) were also found to accumulate at relatively high levels in root tissues. Among microelements, the mean concentrations of zinc (Zn) and barium (Ba) were 65.51 ± 16.47 and 60.66 ± 14.72 mg/kg, respectively. In contrast, mercury (Hg) (0.026 ± 0.003 mg/kg), lead (Pb) (0.95 ± 0.64 mg/kg), and lithium (Li) (0.22 ± 0.38 mg/kg) were recorded at the lowest concentrations. According to the coefficient of variation analysis, the highest variability was observed for lithium (Li; 172.72%), lead (Pb; 66.97%), and vanadium (V; 45.68%), indicating that the accumulation of these elements in response to fertilization variants is highly variable. The mean concentrations and standard deviation values of macro- and microelements in root tissues are presented in Figure 3.1.

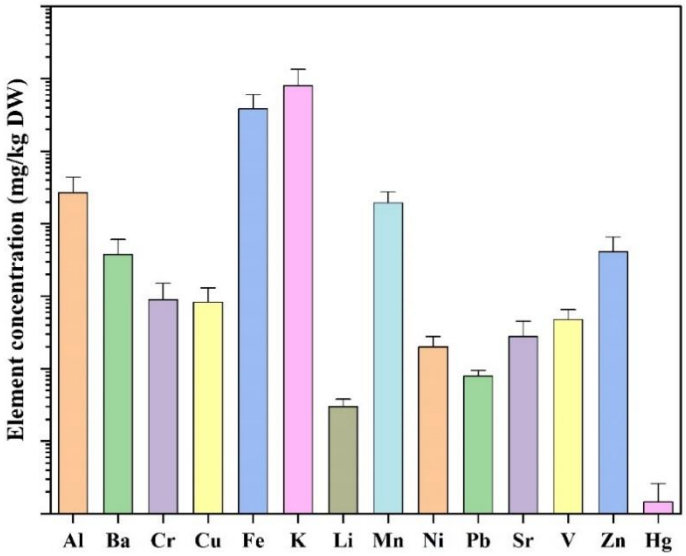


Figure 3.1. Mean concentrations of macro- and microelements accumulated in root tissues of Triticum aestivum L. at the tillering stage (mean ± SD, n = 14).

3.1.2. Correlation Relationships Among Elements in Root Tissues

Spearman's rank correlation analysis was performed to assess the interrelationships among macro- and microelements determined in the root portion. The correlation analysis confirmed the

existence of statistically significant positive and negative associations among certain elements. The correlation coefficients between elements are presented in Table 3.1.

Table 3.1 Spearman Correlation Relationships Among Elements Determined in Wheat Root Tissue

Element Pair	**r_s**	**p**	**Correlation Level**
Al – Fe	0.91	<0.001	Very strong positive
Al – Mn	0.84	<0.001	Strong positive
Al – V	0.84	<0.001	Strong positive
Ba – Mn	0.97	<0.001	Very strong positive
Ba – V	0.92	<0.001	Very strong positive
Cr – Fe	0.96	<0.001	Very strong positive
Cr – Mn	0.84	<0.001	Strong positive
Cu – Mn	0.79	<0.001	Strong positive
Fe – Mn	0.81	<0.001	Strong positive
Fe – V	0.85	<0.001	Strong positive
K – V	-0.88	<0.001	Strong negative
K – Mn	-0.85	<0.001	Strong negative
K – Ba	-0.81	<0.001	Strong negative
Zn – Ni	0.70	0.006	Strong positive
Hg – Ni	0.71	0.005	Strong positive

Note: r_s — Spearman's rank correlation coefficient; p — significance level; $p < 0.05$ was considered statistically significant.

The interrelationships among macro- and microelements determined in the root portion of wheat (*Triticum aestivum* L.) were assessed using Spearman's rank correlation analysis. The results revealed statistically significant positive and negative associations among certain elements.

Aluminum (Al) showed strong positive correlations with barium (Ba) ($r_s = 0.88$; $p < 0.001$), chromium (Cr) ($r_s = 0.88$; $p < 0.001$), iron (Fe) ($r_s = 0.91$; $p < 0.001$), manganese (Mn) ($r_s = 0.84$; $p < 0.001$), and vanadium (V) ($r_s = 0.84$; $p < 0.001$). This suggests that these elements may share interdependent transport and accumulation mechanisms in the root system.

Barium (Ba) demonstrated very strong positive correlations with manganese (Mn) ($r_s = 0.97$; $p < 0.001$) and vanadium (V) ($r_s = 0.92$; $p < 0.001$). Similarly, chromium (Cr) exhibited a strong association with iron (Fe) ($r_s = 0.96$; $p < 0.001$).

Potassium (K) showed negative correlations with several elements, including aluminum (Al) ($r_s = -0.71$; $p < 0.01$), barium (Ba) ($r_s = -0.81$; $p < 0.001$), iron (Fe) ($r_s = -0.78$; $p < 0.01$), manganese (Mn) ($r_s = -0.85$; $p < 0.001$), and vanadium (V) ($r_s = -0.88$; $p < 0.001$). This indicates that an increase in potassium concentration may exert an antagonistic effect on the accumulation of certain microelements in the roots.

A moderate positive association was recorded between nickel (Ni) and zinc (Zn) ($r_s = 0.70$; $p < 0.01$). Mercury (Hg) showed a positive correlation with nickel (Ni) ($r_s = 0.71$; $p < 0.01$) and a negative correlation with lead (Pb) ($r_s = -0.61$; $p < 0.05$).

3.2. Accumulation Characteristics of Elements in the Wheat Shoot System

3.2.1. Quantitative Characterization of Elements in Shoot Tissues

A descriptive statistical analysis was performed to evaluate the quantitative composition of macro- and microelements in the shoot portion at the tillering stage. The analysis revealed

considerable variation in the accumulation levels of elements in the shoot tissues of wheat (*Triticum aestivum* L.). Among the elements studied, the highest mean concentration was recorded for potassium (K) at 818.38 ± 192.00 mg/kg. Iron (Fe) (249.78 ± 104.44 mg/kg) and barium (Ba) (27.51 ± 13.73 mg/kg) were also detected at relatively high levels. The mean concentrations of lithium (Li), chromium (Cr), and zinc (Zn) were 10.52 ± 0.50, 6.57 ± 1.90, and 5.94 ± 2.60 mg/kg, respectively. In contrast, cadmium (Cd) (0.008 ± 0.002 mg/kg), lead (Pb) (0.47 ± 0.29 mg/kg), and osmium (Os) (0.59 ± 0.32 mg/kg) were recorded at the lowest concentrations. According to the coefficient of variation analysis, the highest variability was observed for lead (Pb; 61.86%), osmium (Os; 54.71%), and barium (Ba; 49.93%). The mean concentrations and standard deviation values of macro- and microelements in shoot tissues are presented in Figure 3.2.

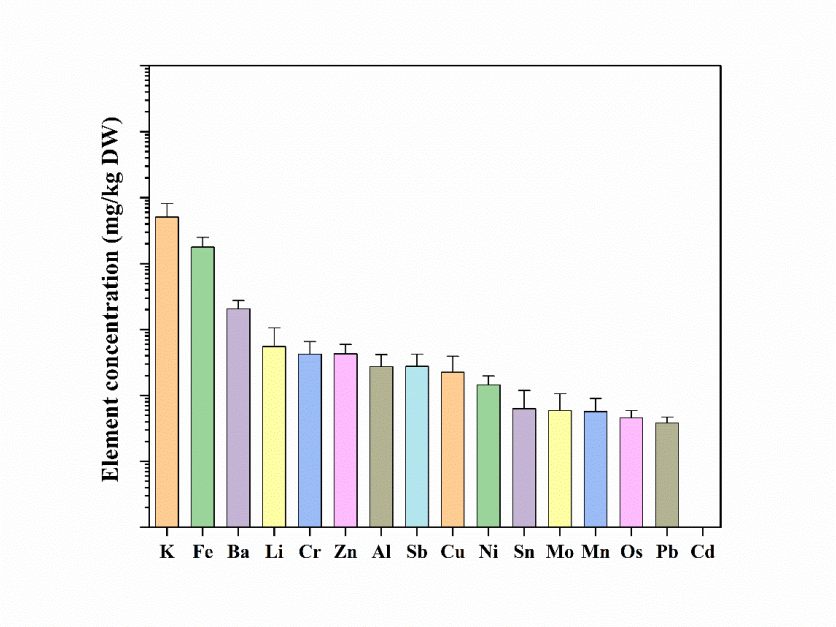


Figure 3.2. Mean concentrations of macro- and microelements accumulated in shoot tissues of Triticum aestivum L. at the tillering stage (mean ± SD, n = 14).

Among the elements studied in wheat shoot tissues, the highest concentration was recorded for potassium (K), with a mean value of 818.38 ± 192.00 mg/kg. Iron (Fe) (249.78 ± 104.44 mg/kg) and barium (Ba) (27.51 ± 13.73 mg/kg) were also detected at relatively high levels. The highest variability based on the coefficient of variation was observed for lead (Pb; 61.86%), osmium (Os; 54.71%), and barium (Ba; 49.93%), indicating that fertilization variants had a considerable influence on the accumulation of these elements in shoot tissues. In contrast, lithium (Li; 4.72%) and tin (Sn; 5.78%) showed low variation, suggesting their relatively stable distribution along the shoot.

3.2.2. Correlation Relationships Among Elements in Shoot Tissues

The interrelationships among macro- and microelements determined in the shoot portion of wheat (*Triticum aestivum* L.) were assessed using Spearman's rank correlation analysis. Statistically significant positive and negative associations were observed among a number of elements. The correlation coefficients between elements are presented in Table 3.2.

Table 3.2 Spearman Correlation Relationships Among Elements Determined in Wheat (Triticum aestivum L.) Shoot Tissue

Element Pair	**r_s**	**p**	**Correlation Level**
Al – Os	-0.61	0.020	Strong negative

Al – Fe	0.56	0.014	Moderate positive
Al – Sb	0.66	0.010	Strong positive
Cd – Zn	-0.69	0.012	Strong negative
Cd – Os	0.86	<0.001	Very strong positive
Cd – Pb	0.81	<0.001	Very strong positive
Ni – Os	0.84	<0.001	Very strong positive
Ni – Ba	0.92	<0.001	Very strong positive
Ni – Cr	0.93	<0.001	Very strong positive
Pb – Os	0.84	<0.001	Very strong positive
Zn – Cu	-0.93	<0.001	Very strong negative
Zn – Li	-0.89	<0.001	Very strong negative
Ba – Cr	0.98	<0.001	Very strong positive
Ba – Sb	0.93	<0.001	Very strong positive
Cr – Sb	0.95	<0.001	Very strong positive
Cu – Fe	-0.81	<0.001	Very strong negative
Fe – Mn	-0.73	0.003	Strong negative
K – Mn	-0.66	0.009	Strong negative
K – Mo	0.57	0.031	Moderate positive

Note: r_s — Spearman's rank correlation coefficient; p — significance level; $p < 0.05$ was considered statistically significant.

Among the elements determined in shoot tissues, barium (Ba) exhibited very strong positive correlations with nickel (Ni) ($r_s = 0.92$; $p < 0.001$), chromium (Cr) ($r_s = 0.98$; $p < 0.001$), and antimony (Sb) ($r_s = 0.93$; $p < 0.001$). Furthermore, a very strong positive association was also recorded between chromium (Cr) and antimony (Sb) ($r_s = 0.95$; $p < 0.001$), suggesting that these elements may share similar transport and accumulation mechanisms in shoot tissues.

Cadmium (Cd) showed positive associations with osmium (Os) ($r_s = 0.86$; $p < 0.001$), lead (Pb) ($r_s = 0.81$; $p < 0.001$), and nickel (Ni) ($r_s = 0.63$; $p < 0.05$), indicating a tendency for co-accumulation of certain heavy metals in wheat shoot tissues.

Iron (Fe) showed moderate positive correlations with molybdenum (Mo) ($r_s = 0.65$; $p < 0.05$) and potassium (K) ($r_s = 0.60$; $p < 0.05$), which may reflect functional interactions of these elements in metabolic processes and physiological transport systems.

Among the negative correlations, zinc (Zn) exhibited very strong negative associations with copper (Cu) ($r_s = -0.93$; $p < 0.001$) and lithium (Li) ($r_s = -0.89$; $p < 0.001$). A strong negative correlation was also recorded between iron (Fe) and copper (Cu) ($r_s = -0.81$; $p < 0.001$). These findings indicate the presence of antagonistic transport or competitive uptake mechanisms between certain elements.

3.3. Translocation of Elements from Root to Shoot

The translocation factor (TF) was calculated to evaluate the intensity of element transfer from roots to aboveground vegetative organs. TF values were examined based on the mean concentrations of elements in root and shoot tissues. The translocation coefficients of elements from root to shoot are presented in Table 3.3.

Table 3.3 Translocation Factor of Elements from Root to Shoot Tissues in Wheat (Triticum aestivum L.)

Element	Root	Shoot	TF
Al	438.03	4.16	0.009
Ba	60.66	27.51	0.45
Cr	15.04	6.57	0.44
Cu	13.05	3.93	0.30
Fe	6037.74	249.78	0.04
K	13459.07	818.38	0.06
Li	0.22	10.52	47.64
Mn	275.78	0.90	0.003
Ni	2.77	1.98	0.71
Pb	0.95	0.47	0.49
Zn	65.51	5.94	0.09

*Note: TF — Translocation Factor; TF = C*shoot / C*root*. TF > 1 indicates active translocation; TF < 1 indicates that the element is predominantly retained in root tissues.*

For the majority of the elements studied, TF values were below 1, indicating their predominant retention in the root system. Particularly low translocation was observed for aluminum (Al; TF = 0.009), manganese (Mn; TF = 0.003), iron (Fe; TF = 0.04), and potassium (K; TF = 0.06). In contrast, lithium (Li) exhibited a TF of 47.64, indicating active transport of this element from roots to shoot tissues. Nickel (Ni; TF = 0.71) and lead (Pb; TF = 0.49) also showed relatively higher translocation.

DISCUSSION

Data obtained at the tillering stage of wheat demonstrated a non-uniform distribution of macro- and microelements across plant organs. The results showed that Fe, K, Mn, Al, and Zn accumulated predominantly in the root system. For instance, the mean concentrations of Fe and K in roots were 6,037.74 mg/kg and 13,459.07 mg/kg, respectively, while these values were considerably lower in shoot tissues. This difference reflects the important physiological role of roots in absorbing mineral elements and retaining them prior to subsequent transport. Similar findings have been reported by other authors during the vegetative development period of wheat [7,16].

The degree of elemental variability also revealed certain noteworthy patterns. In root tissues, Li and Pb, and in shoot tissues, Pb and Os, exhibited high variability. This implies that elements were not uniformly distributed across all variants, and that various combinations of Bioazot and mineral fertilization may have had a considerable effect on the uptake of certain elements. Numerous studies have demonstrated that bacteria belonging to the *Azotobacter chroococcum* species can enhance the solubility of nutritional elements in the rhizosphere through the production of organic acids, siderophores, and phytohormones [1,10].

Correlation relationships in root tissues indicated that elements do not act independently of one another. The strong positive associations identified between Al and Fe, Ba and Mn, and Cr and Fe suggest that the entry of these elements into the plant or their accumulation in tissues may be regulated through shared physiological pathways. In contrast, the negative correlations between K and Ba, Mn, and V indicate the presence of competitive interactions among certain ions. Selective mineral transport and inter-ionic antagonism in wheat have been reported previously

[11]. Results obtained from shoot tissues also indicated that certain patterns are maintained during upward element movement. The very strong associations of Ba with Cr, Ni, and Sb allow for the hypothesis that common mechanisms are involved in the xylem transport of these elements. On the other hand, the negative correlations of Zn with Cu and Li suggest that competition arises among certain microelements during transport or redistribution. This further confirms that the plant's nutrient management system is considerably complex. The translocation factor results constituted one of the most significant aspects of the study. For nearly all elements examined, TF values were below 1, confirming their predominant retention in the root system. This was particularly evident for Mn, Al, Fe, and K. Thus, the root system restricts the transfer of these elements to aboveground organs to a certain degree. In contrast, Li exhibited a notably high TF value, indicating its relatively unrestricted movement into shoot tissues. The retention of certain microelements in wheat roots and their limited transfer to aboveground organs have been confirmed in other studies as well [17,20]. In particular, the data obtained demonstrated that combinations of the Bioazot preparation based on *A. chroococcum* XH2018 strain and mineral fertilization exerted a considerable influence on the processes of element uptake, accumulation, and translocation from root to shoot in wheat. The enhancement of microbiological activity in the rhizosphere in the presence of Bioazot, the conversion of nutritional elements into plant-available forms, and the activation of ion exchange processes may be among the primary reasons underlying these results.

CONCLUSION. The distribution characteristics of macro- and microelements in root and shoot tissues of *Triticum aestivum* L. at the tillering stage were investigated under the influence of the Bioazot preparation based on *A. chroococcum* XH2018 strain and various mineral fertilization variants. The results demonstrated that the majority of elements accumulated predominantly in the root system, with Fe, K, Mn, Al, and Zn in particular accumulating at considerably higher levels in root tissues compared to shoot tissues. Correlation analysis revealed strong positive and negative associations among elements, confirming that the uptake and internal transport of mineral elements in wheat are governed by complex synergistic and antagonistic relationships. Translocation factor results indicated TF < 1 for the majority of elements, signifying their predominant retention in the root system. The high TF value recorded for lithium (Li) suggests that certain elements undergo more active translocation toward vegetative organs. Furthermore, it was established that combinations of the Bioazot preparation based on *A. chroococcum* XH2018 strain and mineral fertilization may exert a considerable influence on the bioavailability of elements, their redistribution across organs, and their migration within the root–shoot system. The findings indicate that the use of biological fertilizers holds significant practical value for enhancing the efficiency of nutrient element utilization and optimizing mineral nutrition processes in wheat.

REFERENCES

1. Ahemad, M., & Kibret, M. (2014). Mechanisms and applications of plant growth promoting rhizobacteria: Current perspective. Journal of King Saud University–Science, 26(1), 1–20. https://doi.org/10.1016/j.jksus.2013.05.001
2. Al-Juhaymi, A. bin S. bin M. (2023). Zakat on debt: A look at achieving justice for the zakat payer and the zakat recipient. Journal of Islamic Research, 9(93), 79–102.
3. Balkovič et al., 2014. Global wheat production potentials and management flexibility under the representative concentration pathways Global and Planetary Change Pages 107-121 https://doi.org/10.1016/j.gloplacha.2014.08.010

4. Butcher, D. J. (2010). Advances in inductively coupled plasma optical emission spectrometry for environmental analysis. Instrumentation Science & Technology, 38(6), 458–469.
5. Dobrzyński, J., Kulkova, I., Jakubowska, Z. and Wróbel, B., 2025. Non-native PGPB consortium consisting of Pseudomonas sp. G31 and Azotobacter sp. PBC2 promoted winter wheat growth and slightly altered the native bacterial community. Scientific Reports, 15(1), p.3248.
6. El-Sorady, G.A., El-Banna, A.A., Abdelghany, A.M., Salama, E.A., Ali, H.M., Siddiqui, M.H., Hayatu, N.G., Paszt, L.S. and Lamlom, S.F., 2022. Response of bread wheat cultivars inoculated with azotobacter species under different nitrogen application rates. Sustainability, 14(14), p.8394.
7. Erenoglu, E. B., Kutman, U. B., Ceylan, Y., Yildiz, B., & Cakmak, I. (2011). Improved nitrogen nutrition enhances root uptake, root-to-shoot translocation and remobilization of zinc in wheat. New Phytologist, 189(2), 438–448. https://doi.org/10.1111/j.1469-8137.2010.03488.x
8. Kosimov, D., Ergashev, R., Mavjudova, A., & Kuziev, S. N. (2025). Organophosphorus pesticide degradation by microorganisms: A review. Frontiers in Bioscience – Elite, 17(3), 38805. https://doi.org/10.31083/fbe38805
9. Mengel & Kirkby, 2001. Principles of Plant Nutrition, 5th ed. International Potash Institute, Bern, Switzerland (687 pp
10. Mrkovacki, N., & Milic, V. (2001). Use of Azotobacter chroococcum in agricultural production. Annals of Microbiology, 51(2), 145–158.
11. Page, V., & Feller, U. (2005). Selective transport of zinc, manganese, nickel, cobalt and cadmium in the root system and transfer to the leaves in young wheat plants. Annals of Botany, 96(3), 425–434. https://doi.org/10.1093/aob/mci189
12. Plekhanova, I.O., Kulikov, V.O. and Shabaev, V.P., 2023. Effect of rhizospheric bacteria on the productivity of wheat plants and inflow of elements from contaminated soils. Moscow University Soil Science Bulletin, 78(3), pp.257-262.
13. Seth, C. K., & Shrivastav, A. (2020). Microplastics in Indian environment: A review. Environmental Science and Pollution Research, 27, 44741–44756. https://doi.org/10.1007/s11356-020-10594-4
14. Singh, S., Annapurna, K., Shrivastava, N. and Varma, A., 2022. Symbiotic interplay of Piriformospora indica and Azotobacter chroococcum augments crop productivity and biofortification of Zinc and Iron. Microbiological research, 262, p.127075.
15. Taiz et al., Plant Physiology and Development 2015 35
16. Tobiasz, A., Walas, S., Filek, M., Hartikainen, H., & Sieprawska, A. (2014). Effect of selenium on distribution of macro- and micro-elements to different tissues during wheat ontogeny. Biologia Plantarum, 58(2), 370–374. https://doi.org/10.1007/s10535-014-0394-4
17. Tudi, M., Ruan, H. D., Yu, Y., Wang, L., Lyu, J., Sadler, R., Connell, D., Chu, C., & Phung, D. (2021). Bioaccumulation and translocation of trace elements in soil–irrigation water–wheat systems in arid agricultural areas of Xinjiang, China. Ecotoxicology, 30, 1722–1734. https://doi.org/10.1007/s10646-021-02476-9
18. Wang, R., Wang, Y., Hu, Y. X., et al. (2021). Divergent responses of tiller and grain yield to fertilization and fallow precipitation: Insights from a 28-year long-term experiment in a semiarid winter wheat system. Journal of Integrative Agriculture, 20(9), 2348–2360.

A TAXONOMIC AND HISTORICAL ASSESSMENT OF *TAMARIX* L. (TAMARICACEAE) BASED ON THE TASH HERBARIUM (UZBEKISTAN)

G. Ahmadjonova
PhD Researcher at Namangan State University
https://doi.org/10.5281/zenodo.20521601

Abstract. *This study provides a taxonomic and historical assessment of the genus Tamarix L. (Tamaricaceae) based on herbarium materials preserved in the National Herbarium of Uzbekistan (TASH). A total of 2,765 herbarium sheets collected between 1906 and 2026 were critically examined and taxonomically verified using major international databases and authoritative regional floras. Of these, 2,566 specimens (92.8%) were reliably identified to species level and included in quantitative analyses, while 185 sheets (7.2%) were excluded due to incomplete or ambiguous taxonomic information.*

Twelve species currently recognized in the flora of Uzbekistan were confirmed in the TASH collection. The species structure reveals marked representation imbalance, with Tamarix ramosissima, T. hispida, and T. arceuthoides comprising the majority of specimens. Temporal analysis indicates peak collecting activity during the mid-20th century, followed by a decline and renewed accumulation in recent decades. These trends primarily reflect historical research intensity rather than intrinsic biological distribution patterns.

The results strengthen the scientific value of the TASH Tamarix collection and establish it as a key resource for taxonomic revision, floristic research, and biodiversity assessment in Uzbekistan.

Keywords*: Tamarix, herbarium revision, TASH, Central Asia, floristics, taxonomic verification, biodiversity collections.*

INTRODUCTIONS

Herbaria represent long-term scientific repositories that preserve plant specimens together with essential metadata, including locality, date of collection, collector identity, and taxonomic determination. These collections function as permanent documentary records of species distributions across spatial and temporal scales and constitute a foundational resource for taxonomic, floristic, biogeographic, and evolutionary research [1,2]. In recent decades, herbarium specimens have increasingly been recognized as historical biodiversity archives that enable analyses of distributional shifts, phenological change, and long-term ecological dynamics [3].

The genus *Tamarix* L. *(Tamaricaceae*) comprises 73 currently accepted species worldwide [4] and represents a taxonomically complex group widely distributed across arid and semi-arid regions of Eurasia and North Africa. Species of *Tamarix* are key structural components of desert, semi-desert, saline, and riparian ecosystems and are characterized by high ecological plasticity and salt tolerance [5,6]. In Central Asia, the genus plays an important role in stabilizing sandy substrates, regulating riverine systems, and forming halophytic vegetation communities. However, species delimitation within the genus remains challenging due to morphological overlap, historical synonymization, ecological variability, and uneven collecting intensity across regions.

Despite the recognized ecological and floristic importance of *Tamarix* in Central Asia, a comprehensive herbarium-based revision of the genus within the National Herbarium of Uzbekistan (TASH) has not previously been undertaken. Given that TASH represents the largest and most historically continuous botanical repository in the region, its collections provide a unique opportunity to assess species representation, nomenclatural consistency, temporal accumulation patterns, and geographic sampling structure within the genus.

The National Herbarium of Uzbekistan (TASH), established in 1937, functions as the country's central national scientific collection and currently operates under the Institute of Botany of the Academy of Sciences of Uzbekistan. The TASH holdings comprise nearly one million herbarium sheets, including approximately 1,500 type specimens [7]. The collection is annually enriched by an average of 1,500–3,000 new accessions. TASH represents the most comprehensive herbarium resource not only for the flora of Uzbekistan but also for that of Central Asia as a whole. This repository serves as a primary source for the taxonomic revision of the flora of Uzbekistan and for the preparation of the new Flora of Uzbekistan project [9,10].

At present, the National Herbarium of Uzbekistan houses more than 66,000 digitized herbarium specimens representing over 2,300 species and 330 genera. Geographic coordinates have been determined for more than 1,000 species, and distribution maps have been generated using international geographic information systems (GIS). In particular, distribution maps have been prepared for numerous taxa of the Uzbek flora, including the genera Acer, Allium, Tulipa, Caragana, Calophaca, Chesneya, Crocus, Cousinia, and Thermopsis, as well as many species of Astragalus and numerous Red Data Book plants. More than 5,700 herbarium sheets (2–3 representative specimens per species) and 815 type specimens have been electronically databased. Based on literature and herbarium evidence, a modern conspectus of the flora of Uzbekistan has been developed, comprising 4,326 wild vascular plant species. The resulting electronic database FLORUZ (Flora of Uzbekistan Database) provides comprehensive information on taxonomic status, nomenclature, life forms, distribution, conservation status, and digital images of plant species [11].

Accordingly, the present study aims to conduct a critical taxonomic revision and temporal–geographic assessment of *Tamarix* specimens preserved in TASH. Specifically, the study evaluates species-level representation, examines nomenclatural consistency, analyzes historical collection dynamics, and assesses geographic distribution patterns within the herbarium framework. By integrating taxonomic verification with quantitative analysis of collection structure, this work provides a clarified and systematized foundation for future floristic, biogeographic, and conservation-oriented research on the genus in Uzbekistan.

MATERIALS AND METHODS

The material examined in this study comprised herbarium specimens of the genus *Tamarix* L. preserved in the collections of the National Herbarium of Uzbekistan (TASH). All available sheets attributed to the genus were critically reviewed. Based on these materials, a structured electronic database was developed to systematize specimen-level information. The database included taxon name (as indicated on the original label), currently accepted name, collection locality, administrative region, geographic coordinates (when available or subsequently determined), collection date, collector name, accession number, and barcode identifier (if present).

Nomenclatural verification and synonymy assessment were conducted using international and regional taxonomic resources, including Plants of the World Online (POWO; www.plantsoftheworldonline.org), Plantarium (https://www.plantarium.ru), the Global

Biodiversity Information Facility (GBIF; https://www.gbif.org), the Moscow State University Herbarium database (https://plant.depo.msu.ru/), and the Komarov Botanical Institute Herbarium (LE; https://en.herbariumle.ru/). Accepted names and synonymic treatments were aligned with currently recognized international standards.

For the evaluation of diagnostic morphological characters and regional species concepts, authoritative floristic treatments were consulted, including the 11-volume Определитель растений Средней Азии, the 6-volume Флора Узбекистана, and the 30-volume Флора СССР [4, 12–18].

Geographic coordinates of collection localities were obtained directly from specimen labels when available. For historical records lacking explicit coordinates, georeferencing was performed using Google Earth Pro 7.1 based on locality descriptions provided on the labels and corroborated with information from GBIF and Plantarium databases. This approach enabled standardized spatial localization of natural occurrence sites within the study region.

RESULTS

General information. A total of 2,765 herbarium sheets of the genus *Tamarix* preserved in the TASH collection were critically examined. Verification of specimen data revealed several categories of metadata inconsistency. Twelve sheets (0.43%) contained outdated or synonymic names. In addition, 14 specimens bore the name *Tamarix karataviense* Russanovitch on their original labels. This name was not found in the consulted regional floras or monographic treatments and is currently absent from major international taxonomic databases, including Plants of the World Online (POWO) and the International Plant Names Index (IPNI). The status of this name therefore remains unresolved and may represent either an unpublished designation, a nomen nudum, or a historical misapplication. Further archival and typification-based investigation is required to clarify its nomenclatural validity

In 185 cases (6.7%), specimens could not be confidently assigned to species level due to incomplete, illegible, or missing label information, or because they were recorded only as *Tamarix* sp. Geographic data were absent in 21 specimens (0.76%), collection dates were missing or partially illegible in 27 cases (0.98%), and collector names were unreadable or absent in 69 sheets (2.49%). Additionally, 50 specimens (1.81%) lacked barcode identifiers.

Of the total examined material, 2566 specimens (92.8%) were reliably identified to species level and included in the quantitative analysis (Table 1). This proportion indicates a relatively high overall taxonomic resolution of the collection.

Historical floristic accounts report the occurrence of 12 species of *Tamarix* in the flora of Uzbekistan (Vvedenskiy, 1959). The present revision confirms the representation of all 12 species within the TASH collection. In addition, specimens of three species not occurring in the flora of Uzbekistan (*T. gracilis, T. kotschyi*, and *T. passerinoides*) are preserved in the herbarium, reflecting the broader Central Asian geographic scope of the collection.

Table 1. The number of specimens of the genus Tamarix L. preserved in the National Herbarium of Uzbekistan

№	Species	Number of herbarium specimens
1	***Tamarix androssowii*** **Litv, FI.Bot.Muz.Imp.Akad.Nauk 5:41 (1905)**	**10**

2	***Tamarix arceuthoides* Bunge, FI. Russl.:119 (1952)**	**287**
3	***Tamarix aralensis* Bunge, Tent.Gen. Tamar.: 59 (1852)**	**42**
4	***Tamarix elongate* Ledeb, FI.Altaiv. 1:421(1829)**	**100**
5	***Tamarix florida* Bunge, Tent. Gen. Tamar.:37 (1852)**	**60**
6	***Tamarix hispida* Wild, Abh. Konigl.Akad.Wiss.Berlin 1812-1813:77 (1816)**	**480**
7	***Tamarix hohenackeri* Bunge, Tent. Gen. Tamar.: 44 (1852)**	**140**
8	***Tamarix laxa* Wild, Abh. Konigl.Akad.Wiss.Berlin 1812-1813:82(1816)**	**183**
9	***Tamarix lepostachya* Bunge, Beitr,FI.Russl: 117(1852)**	**49**
10	***Tamarix litvinovii* Gorschk, Spisok Rast. Gerb. Fl. S.S.S.R. Bot. Inst. Vsesojuzn. Akad. Nauk 10(61-64: 24 (1936)**	**72**
11	***Tamarix meyeri* Boiss, Diagn. Pl. Orient. 10: 9 (1849)**	**61**
12	***Tamarix ramosissima* Ledeb, Fl. Altaic. 1: 424 (1829)**	**1022**
	Species occurring in the floras of other regions	
13	***Tamarix gracilis Wild, Abh. Königl. Akad. Wiss. Berlin 1812-1813: 81 (1816)***	**43**
14	***Tamarix kotschyi Bunge Tent. Gen. Tamar.: 30 (1852)***	**7**
15	***Tamarix passerinoides Delile ex Decne. Ann. Sci. Nat., Bot. 4: 349 (1825)***	**10**
	Total number of specimens	**2566**

The quantitative structure of the collection reveals pronounced species dominance. *Tamarix ramosissima* represents the most abundant taxon (39.8% of identified specimens), followed by *T. hispida* (18.7%) and *T. arceuthoides* (11.2%). Together, these three species account for nearly 70% of the identified material, indicating substantial representation inequality within the collection.

In contrast, several taxa are represented by low frequencies (<2%), including *T. androssowii, T. kotschyi, and T. passerinoides.* Such limited representation may reflect either genuine ecological rarity or historical collecting bias associated with uneven sampling intensity.

Species not occurring in the flora of Uzbekistan collectively constitute 2.3% of the identified material, further illustrating the interregional exchange and broader geographic coverage of the TASH herbarium.

The specimens of the genus preserved in the TASH collection were collected predominantly from the countries of Central Asia. The distribution of all examined specimens by country is presented below (Fig. 1).

The country-level distribution of *Tamarix* specimens demonstrates a clear predominance of material originating from Uzbekistan (55.15%), followed by Turkmenistan (20.47%) and Kazakhstan (14.10%). Tajikistan (6.94%) and Kyrgyzstan (2.57%) are comparatively underrepresented. Only 0.76% of specimens lack country information.

The earliest specimen identified in the collection corresponds to *Tamarix ramosissima*, collected in 1906 by A. Badin from the Syrdarya region, Chimkent uyezd (currently within Kazakhstan). This record represents the oldest documented *Tamarix* specimen preserved in TASH (Fig. 2).

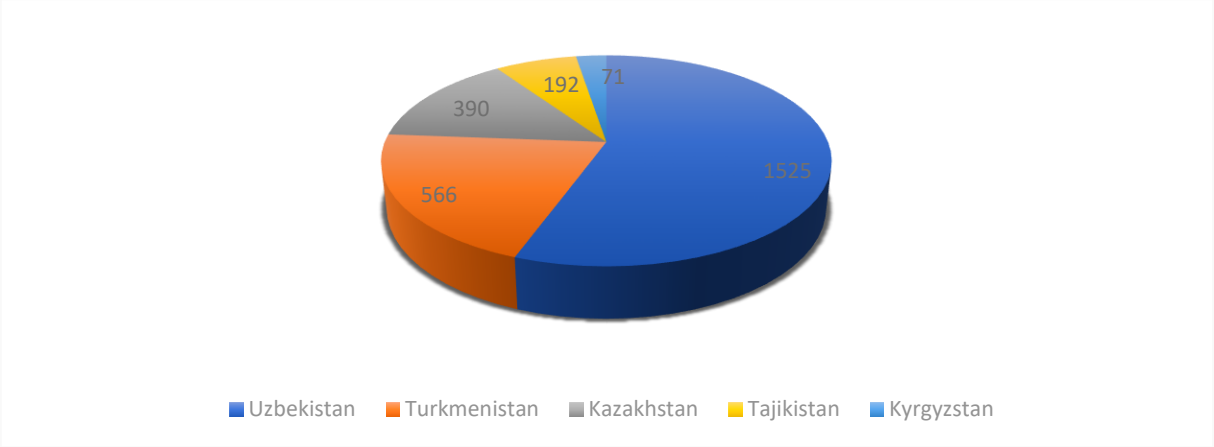
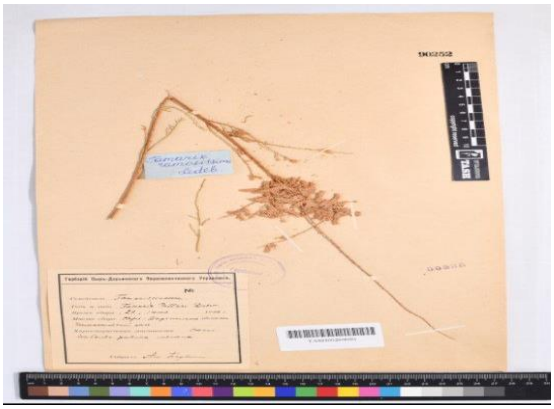


Fig.1. Distrubition of Tamarix specimens preserved in the TASH herbarium across Central Asian countries.

In contrast, the most recent specimen examined belongs to *Tamarix arceuthoides*, collected in 2024 by N.Yu. Beshko and I.I. Maltsev from the Angren River floodplain near Almalyk. The coexistence of these temporally distant specimens within the same collection reflects more than a century of continuous floristic documentation (Fig. 3).



2.Figure Tamarix ramosissima Ledeb collected in 1906.



3.Figure Tamarix arceuthoides Bunge collected in 2024.

The decadal distribution of *Tamarix* specimens (1906–2026) reveals a markedly uneven temporal accumulation pattern (Fig. 4).

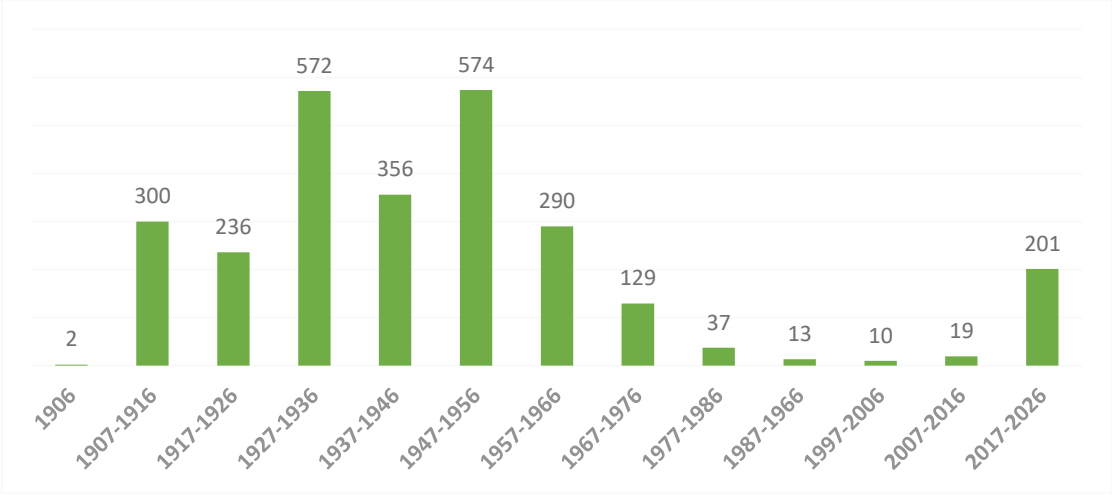


Figure.4 Decedal distribution of Tamarix herbarium specimens preserved in TASH 1906-2026.

The principal accumulation phase occurred between 1940 and 1960, corresponding to intensified botanical exploration and large-scale floristic surveys in Central Asia. The lowest accumulation period was recorded between 1997 and 2006, likely reflecting a temporary decline in field-based floristic research and possible delays in integrating newly collected materials into the central repository.

A renewed increase in specimen accumulation is observed during 2017–2026, coinciding with revitalized national inventory programs, systematic digitization initiatives, and expanded biodiversity documentation efforts. Overall, the temporal structure primarily reflects shifts in institutional research activity rather than intrinsic biological fluctuations within the genus.

The *Tamarix* collection was assembled through the substantial contributions of botanists from the former USSR as well as contemporary Uzbek researchers (Table2).

Table 2. Leading collectors of Tamarix L. specimens preserved in the TASH herbarium, with collection periods and geographic coverage

Collectors	Number of herbarium specimens	Years	Regions
A.A. Ashirova	266	1947-1975	Uzbekistan and Turkmenistan
A.D. Pyataeva	115	1940-1956	Uzbekistan Turkmenistan and Tajikistan
I.I. Granitov	91	1919-1945	Uzbekistan Kazakhstan and Tajikistan
E.E. Korovin	84	1913-1941	Uzbekistan Turkmenistan Tajikistan Kazakhstan and Kyrgyzstan
M.G. Popov	82	1910-1962	Uzbekistan Turkmenistan Kazakhstan and Tajikistan
N.Daminova	82	2022-2023	Uzbekistan
E.E.Korotkova	72	1935-1971	Uzbekistan Turkmenistan Tajikistan and Kazakhstan
I.A. Raykova	61	1916-1958	Uzbekistan Turkmenistan Tajikistan and Kazakhstan

The most productive collectors include A.A. Ashirova (266 specimens), A.D. Pyataeva (115), and I.I. Granitov (91), whose field activities were concentrated primarily between 1910 and 1975.

The distribution of collector activity across decades further supports the observed temporal accumulation peaks and underscores the role of coordinated botanical expeditions in shaping the current structure of the collection.

DISCUSSION

In contemporary biodiversity science, digitized biological collections increasingly function as foundational research infrastructure, enabling large-scale, data-driven analyses across spatial and temporal scales [19]. Over the past decade, coordinated digitization initiatives across major herbaria have transformed traditional specimen repositories into globally interconnected research platforms [4]. This transition has substantially enhanced data transparency, reproducibility, and international scientific collaboration.

Within this global transformation framework, the National Herbarium of Uzbekistan (TASH) has initiated systematic digitization and cataloguing of its collections in accordance with international standards. Since 2020, the Institute of Botany of the Academy of Sciences of

Uzbekistan, in collaboration with international partners, has implemented progressive digitization procedures, including high-resolution imaging of historical and recent specimens, standardization of specimen metadata (locality, collector, collection date, identifier, herbarium code), and integration with global biodiversity databases [7]. These efforts significantly increase accessibility and analytical potential of Uzbekistan floristic data.

As emphasized by Tojibaev et al. (2020), the TASH collection holds fundamental importance for understanding the flora of Central Asia, and its digitization substantially strengthens the region's integration into the international scientific community [7]. The practical implications of digitization are multidimensional. First, integration with global open-access platforms such as GBIF, JSTOR Global Plants, and iDigBio facilitates broader international engagement with Central Asian biodiversity data [20]. Second, digital georeferencing enables refined comparisons between historical and contemporary distribution patterns, improving regional biogeographic assessments. Third, temporally explicit herbarium records provide critical input for phenological and ecological modeling, particularly in evaluating plant responses to climate change [21]. Finally, high-resolution digital images enhance taxonomic precision by allowing remote comparison with type materials and historical collections, thereby supporting synonym resolution, species delimitation, and taxonomic revision [1].

The pronounced dominance of *Tamarix ramosissima* within the collection likely reflects a combination of ecological amplitude and historical sampling bias. As a widely distributed and morphologically variable species, *T. ramosissima* is frequently encountered in riparian and desert ecosystems, which were focal targets of early botanical expeditions in Central Asia. However, the possibility of historical over-identification or taxonomic broad interpretation cannot be excluded, particularly given the known morphological overlap within the genus. Consequently, species representation in the collection should be interpreted as an outcome of both biological distribution patterns and collector-driven sampling dynamics.

The digitized and structured presentation of *Tamarix* data significantly expands the potential for interdisciplinary applications, including ethnobotany, phytogeography, conservation planning, and regional taxonomic revision. In this sense, the TASH *Tamarix* collection evolves from a static archival repository into a dynamic biodiversity knowledge platform capable of supporting long-term ecological, biogeographic, and evolutionary research in Uzbekistan.

CONCLUSION

This study provides a comprehensive and critically structured assessment of 2,765 herbarium sheets representing species of the genus *Tamarix* collected over more than a century. Through quantitative evaluation, taxonomic verification, and historical contextualization, the research establishes a robust empirical framework for future taxonomic revision, biogeographic analysis, and provenance-based investigations within the genus.

The systematic analysis not only clarifies species-level representation and temporal accumulation patterns but also enhances the scientific reliability and analytical utility of the *Tamarix* holdings preserved in the TASH herbarium. Consequently, the collection emerges as a strategically important biodiversity resource, supporting long-term floristic research, regional conservation planning, and integrative botanical studies in Uzbekistan.

REFERENCES

1. Nualart N., Ibáñez N., Soriano I., López-Pujol J. (2017). Assessing the relevance of herbarium collections as tools for conservation biology. Botanical Review, 83(3), 303–325.

2. Soltis P.S. (2017). Digitization of herbaria enables novel research. American Journal of Botany, 104(9), 1281–1284.
3. Heberling J.M., Isaac B.L. (2018). Herbarium specimens as exaptations: New uses for old collections. American Journal of Botany, 105(3), 1–4. https://doi.org/10.1002/ajb2.1042
4. POWO. (2025). Plants of the World Online. Royal Botanic Gardens, Kew. https://www.plantsoftheworldonline.org
5. Popov M.G. (1915). Materialy k izucheniyu rastitel'nosti Sredney Azii. Tamaricaceae. Tashkent.
6. Lipschitz S.J., Pavlov N.V. (1936). Tamaricaceae. In Flora SSSR (Vol. 6, pp. 1–65). Moscow–Leningrad.
7. Tojibaev K., Beshko N., Karimov F., Khassanov F. (2020). Flora and vegetation of Central Asia: Diversity, ecology and conservation. Botanical Journal, 105(2), 45–67.
8. Tojibaev K.Sh., Beshko N.Y., Mirzalieva D., Khassanov F. (2022). Taxonomic and nomenclatural inventory of the Umbelliferae in Central Asia. Turczaninowia, 25(2), 1–17.
9. Vasilczenko I.T., Vasilieva V.G. (1975). Gerbariy Sredney Azii i Kazakhstana. Botanicheskii Zhurnal, 60(3), 345–350.
10. Thiers B. (2025). Index Herbariorum: A global directory of public herbaria and associated staff. New York Botanical Garden. http://sweetgum.nybg.org/science/ih
11. Akbarova M.H., Turginov O.T. (2020). Obzor gerbariya roda Scutellaria L. Science and Education (Kokand), 1(1), 18–24.
12. Plantarium. (2025). Open online atlas and key to plants and lichens of Russia and neighboring countries. https://www.plantarium.ru
13. GBIF. (2025). Global Biodiversity Information Facility. https://www.gbif.org
14. Moscow State University Herbarium. (2025). Plant Depository. https://plant.depo.msu.ru
15. Komarov Botanical Institute, Russian Academy of Sciences. (2025). Herbarium LE. https://en.herbariumle.ru
16. Определитель растений Средней Азии. (1983). 7 vols. Tashkent: Издательство Фан УзССР.
17. Флора Узбекистана. (1959). Vol. 4. Tashkent: Издательство Академии Наук УзССР.
18. Флора СССР. (1936). Vol. 15. Moscow–Leningrad: Издательство Академии Наук СССР.
19. Stadnicka-Futoma A., Nobis M. (2024). Geographical–historical analysis of the herbarium specimens representing the economically important family Amaranthaceae (1821–2022). Biology, 13(6), 435. https://doi.org/10.3390/biology13060435
20. Page L.M., MacFadden B.J., Fortes J.A., Soltis P.S., Riccardi G. (2015). Digitization of biodiversity collections reveals biggest data on biodiversity. BioScience, 65(9), 841–842.
21. Calinger K.M., Queenborough S., Curtis P.S. (2013). Herbarium specimens reveal the footprint of climate change on flowering trends across north-central North America. Ecology Letters, 16(8), 1037–1044. https://doi.org/10.1111/ele.12135

APPLICATION OF ARTIFICIAL INTELLIGENCE CAPABILITIES IN ENSURING SOIL MOISTURE RETENTION ON RAINFED LANDS OF UZBEKISTAN USING BENTONITE CLAYS

Z.F. Pulatova[1], B.T. Sabirov[2], Kh.L. Pulatov[3], M.T. Azizova[4]
Tashkent institute of chemical technology, Tashkent, Uzbekistan[1,3,4]
Jizzakh Polytechnic Institute, Jizzakh, Uzbekistan[2]
https://doi.org/10.5281/zenodo.20484807

Abstract. *This article examines an innovative approach to restoring low-quality pastures in Central Asia. The researchers propose using natural adsorbents – bentonite clays – and developing algorithms to optimize precipitation retention. The mechanisms for creating subsurface hydrobarriers and the potential for using artificial intelligence (AI) in managing soil reclamation in rainfed lands of Uzbekistan are discussed. The development of an intelligent moisture management system for rainfed lands based on bentonite clays is a strategic approach for ensuring environmental protection and food security in Uzbekistan amid rapid population growth. The application of AI capabilities allows transforming the spontaneous and uncontrolled use of natural resources into a controlled technological process adapted to changing climatic conditions, especially in the context of regional water shortages.*

Keywords: *water resources, moisture, bentonite, structure, artificial intelligence, rainfed lands, reclamation, water retention, swelling, algorithm, formula, modeling.*

Introduction

The problem of degradation of rainfed (non-irrigated) lands in Uzbekistan is aggravated by the aridity of the climate and the low water-holding capacity of dense sierozem soils. Traditional irrigation methods are not feasible in these conditions, which necessitates the search for solutions in the field of “passive land reclamation.” Climate change and the acute shortage of water resources during the most important vegetative period of the year have a highly negative impact on the preservation of plant life in the region. During the hot summer period, part of the moisture contained in the soil structure evaporates into the atmosphere, while another part moves downward and filters through the soil layers.

In this context, bentonite clays — natural aluminosilicate sedimentary rocks with a layered structure, capable of retaining moisture (water) in their structure, swelling, and releasing moisture back in an unlimited cycle — can be used as an environmentally friendly “accumulator of atmospheric moisture.” Due to their hydration and cation-exchange capacity, bentonite clays represent an ideal substrate for creating long-term underground moisture reservoirs. Solving the problem of water resource scarcity and degradation of rainfed lands in Central Asia requires the search for innovative solutions at the intersection of ecology, materials science, and the potential application of artificial intelligence.

The results of modern research confirm the high efficiency of using natural adsorbents, particularly bentonite clays, as ameliorants for arid regions. The application of bentonite significantly improves soil structure by reducing filtration losses and increasing the water-holding

capacity of the soil. Bentonite particles fill macropores in sandy and sandy-loam soils, creating a more complex pathway for water and slowing its infiltration into deeper layers. Due to its high specific surface area and swelling capacity, bentonite retains a significant amount of plant-available moisture in the root zone. The application of this clay mineral contributes to the formation of stable soil aggregates. The introduction of bentonite at a rate of 12–24 t/ha into sandy soils of arid regions significantly increases their water-holding capacity and creates a stable structure. This method makes it possible to reduce the hydraulic conductivity of soil and increase water-use efficiency by 15–25%, while also improving conditions for the root system [1].

Under the conditions of Uzbekistan, studies by Rakhmonov A. Kh. and Tashkuziev M. M. (2021) proved that the use of local bentonites from the Navbahor and Askamar deposits not only improves the hydrophysical properties of soils but also contributes to the prolonged action of mineral fertilizers. Bentonite clays from the Navbahor deposit in Navoi Region and the Askamar deposit in Tashkent Region of the Republic of Uzbekistan were studied, and it was confirmed that the addition of bentonite significantly increases the maximum field water capacity and improves soil structuring, particularly the proportion of valuable aggregates. It was established that, due to its high adsorption capacity, bentonite retains nutrients such as N, P, and K in the upper soil layer, preventing their leaching and providing plants with nutrition for a longer period [2].

However, the effectiveness of bentonite barriers substantially depends on dynamic environmental factors. Zhang and Liu point out the complexity of predicting moisture-release processes in modified soils under extreme temperatures. This determines the need to shift from static calculation methods to dynamic models. In their work devoted to the dynamic modeling of moisture release, the authors substantiate the inefficiency of static methods under extreme temperatures, which require consideration of nonlinear changes in water properties and in the structure of modified soils. They propose moving toward dynamic models that use machine learning to accurately describe evaporation and moisture-release processes under thermal stress conditions.

Traditional static soil water characteristic curves (SWCC) do not take into account the thermal load on the pore structure of modified soils, for example, soils amended with bentonite or biochar. Under rapid heating or freezing, the physicochemical bonds between modifier particles and soil particles change, making accurate prediction using conventional formulas impossible. It is proposed to use algorithms that recalculate moisture-release coefficients in real time, adapting to changes in ambient temperature. In modified bentonite soils, clay particles change their hydration shell more rapidly during heating than ordinary sand; therefore, static methods underestimate the actual moisture loss rate by 15–20% at temperatures above 45 °C [3].

In recent years, global practice has shown a trend toward the intellectualization of water-use management. Studies by Deepak and Suneetha (2025) demonstrate that machine learning algorithms are capable of predicting soil moisture dynamics in arid zones with an accuracy of up to 95–97%, taking into account nonlinear relationships between meteorological data and soil physics.

The main aspects of the study include the development of a nonlinear machine learning method for predicting soil moisture dynamics by integrating two types of data: first, air temperature, precipitation, solar radiation, and wind speed; and second, soil texture, bulk density, and organic composition. The authors use modern machine learning algorithms, such as random forest and neural networks, to model complex nonlinear interactions between atmospheric conditions and the physicochemical properties of soil. Under arid climate conditions, traditional

linear models often fail to cope with abrupt changes in moisture content. The proposed approach makes it possible to plan irrigation more accurately and manage water resources more efficiently, which is critically important for sustainable agriculture in arid zones. This work complements modern research in the field of dryland monitoring, where physical models, such as the Richards equation, are increasingly combined with machine learning algorithms to improve accuracy [4].

M. Vandana et al. emphasize that the use of neural networks for modeling the hydraulic conductivity of soils enriched with bentonite makes it possible to optimize the dosage of the ameliorant while minimizing economic costs. The study showed that artificial neural networks are a highly efficient and accurate tool for the rapid prediction of the filtration coefficient of sand–bentonite mixtures, replacing time-consuming laboratory methods. The scientific novelty lies in the development of a specific ANN architecture adapted to bentonite additives, the use of the Levenberg–Marquardt algorithm to achieve a high correlation coefficient ($R^2 > 0.98$), and the identification of key physical soil properties for optimizing the composition of liners for municipal solid waste landfills [5].

Despite the availability of studies devoted to individual aspects of the chemical and mineralogical composition, structure, activation methods, and modification of the structure of bentonite clays from various deposits in Uzbekistan, as well as the expansion of their fields of application [6–15], reclamation, and digitalization, comprehensive studies combining the potential of Uzbekistan’s bentonite clays with the predictive capabilities of artificial intelligence for rainfed lands are practically absent. This study is aimed at filling this gap in the context of environmental protection and the rational use of water resources in the region.

The purpose of the present research is to develop an integrated approach to managing the water regime of rainfed soils by combining the physicochemical properties of bentonite hydro-barriers with AI-based predictive modeling algorithms. Based on this purpose, the objectives of the study are as follows: to determine, under the conditions of Uzbekistan, the nonlinear relationships between the dosage of bentonite clays and the dynamics of moisture retention under extremely high temperatures and precipitation deficit; to develop the structure of an AI algorithm capable of predicting, with high accuracy of up to 97%, the duration of productive moisture retention in the root-inhabited layer; and to establish the synergistic effect of bentonite additives and intelligent monitoring on the stabilization of the reclamation condition of low-bonitet pastures and rainfed areas of Uzbekistan.

The practical significance of the research lies in the development of a technological solution for Uzbekistan aimed at adaptation to climate change and water resource scarcity. The application of the developed models makes it possible to optimize the consumption of bentonite clays, thereby reducing reclamation costs. The proposed methodology ensures the preservation of natural moisture in the soil structure and increases crop yields on rainfed lands by minimizing the risk of complete crop loss during dry periods of the year. In the future, the developed management algorithms can be integrated into digital “smart agriculture” platforms and used for pasture reclamation in other arid regions of Central Asia.

Methodology. In carrying out the research work, mathematical formulas of Langmuir, Freundlich, Richards, and others were applied. To develop a technology for the application of bentonite, it is proposed to carry out work on identifying regions of Uzbekistan with a critically low soil moisture index, selecting the optimal method for introducing bentonite granules into the subsurface soil layer, and predicting the dynamics of moisture uptake from the soil by vegetation

depending on the bentonite dosage. The model calculates the optimal granule fraction, either 1–3 mm or 3–6 mm, for a specific soil type.

Discussion

To mathematically describe the process of moisture retention by bentonite in the soil profile, models of adsorption and moisture thermodynamics are used. In the context of bentonite granules, three aspects are of primary importance: absorption intensity, moisture-retention capacity, and swelling kinetics. Below are the main groups of formulas used in the development of AI algorithms for this technology.

Equilibrium adsorption model (isotherms). To determine the amount of water that bentonite can retain in its structure at a certain initial moisture content of the surrounding environment, the Langmuir and Freundlich equations can be applied. In this case, the Freundlich equation will have the following form:

$$a = K_f \cdot C^{\frac{1}{n}}$$

where, **α** - the amount of moisture adsorbed per unit mass of bentonite;

C - the moisture concentration, or relative humidity, in the soil structure;

$\mathbf{K_f}$ and **n** - empirical constants depending on the type of bentonite, namely sodium or calcium form, and the ambient temperature.

The Langmuir equation can be applied to calculate monolayer coverage:

$$a = a_{\max} \cdot \frac{K \cdot C}{1 + K \cdot C}$$

where, $\boldsymbol{\alpha_{max}}$ - the maximum sorption capacity of bentonite.

Calculation of the swelling coefficient

Bentonite is a complex component: in soil, it acts not only as an adsorbent but also as a hydrogel. The effectiveness of bentonite application under the arid climate conditions of Uzbekistan depends on the degree of swelling:

$$Q = \frac{V_w - V_0}{V_0} \times 100\%$$

where, $\mathbf{V_w}$ - the volume of bentonite after absorbing atmospheric precipitation;

$\mathbf{V_0}$ - the initial volume of dry bentonite granules.

To apply the capabilities of artificial intelligence for modeling, a correction coefficient of soil pressure, $\mathbf{P_{soil}}$, is used, since dense soil affects the swelling process of bentonite:

$$Q_{\text{real}} = Q_{\max} \cdot e^{-k \cdot P_{\text{soil}}}$$

This formula makes it possible, during modeling, to calculate the appropriate incorporation depth so that soil pressure does not “suppress” the absorbing or swelling capacity of bentonite granules.

To understand the process by which bentonite releases the moisture accumulated in its structure to plants in the soil, a modified Richards equation can be applied, in which an “absorption/release term” is introduced:

$$\frac{\partial \theta}{\partial t} = \nabla \cdot [K(\theta)\, \nabla \psi] - S(z,t)$$

where, **θ** - the volumetric soil moisture;

K(θ) - the hydraulic conductivity;

Ψ - the soil matric potential;

S(z,t) - a function describing the operation of the bentonite layer, namely water accumulation in spring and its slow desorption in summer.

Calculation of the optimal dosage (empirical model). For the practical application of AI, a mass-balance formula is used to achieve the target moisture content ($\mathbf{M_{bent}}$):

$$M_{\text{bent}} = \frac{V_{\text{soil}} \cdot (\theta_{\text{target}} - \theta_{\text{current}})}{\Delta a \cdot \eta}$$

where, $\mathbf{M_{bent}}$ - the mass of bentonite, kg/ha;

Δα - the specific water-retention capacity of bentonite;

η - the efficiency coefficient, which takes into account losses due to evaporation and filtration into deeper soil layers.

It should be noted that the application of AI makes it possible not only to perform calculations using the above formulas, but also to minimize the loss function. In particular, the algorithm searches for such values of depth (**z**) and mass (**M**) at which soil moisture remains above the permanent wilting point (**PWP**) for the longest possible period under a given precipitation forecast.

To verify the mathematical models and assess the effectiveness of the AI-based technology, controlled field trials must be conducted. Without comprehensive field experiments, it is impossible to obtain reliable modeling data.

Below, we present an experimental plan for determining the effectiveness of bentonite as a natural moisture-retaining agent, or moisture accumulator, under the conditions of rainfed lands in Uzbekistan.

For field trials, rainfed land areas or degraded pastures should be selected, for example, in Jizzakh, Navoi, Kashkadarya, and Surkhandarya regions of Uzbekistan.

It is also necessary to verify the reliability and accuracy of the data for their further use in developing AI-based forecasts of moisture retention and determining the optimal incorporation depth of bentonite granules.

Field experiments, or trials, are carried out in several stages.

Stage 1: Preparatory stage, March–April.

At the preparatory stage, suitable soil moisture sensors should be selected and installed at soil depths of 10, 15, 20, and 30 cm.

To conduct field trials, information should be collected on the basis of statistical data on precipitation over the last 10 years, and a forecast of precipitation volume during the field trial period should be established. For example, if 150 mm of precipitation is expected in spring, bentonite placed at a depth of 20 cm will maintain moisture above the permanent wilting point until July 15.

Stage 2: Establishment of the experiment, April.

The site allocated for field trials is divided into four randomized blocks, with three replications:

Control (C): traditional sowing without bentonite.

Variant A: uniform application of bentonite at a rate of 20 t/ha into the 0–15 cm soil layer.

Variant B: local band application of granules at a soil depth of 10–30 cm.

Variant C: application of bentonite mixed with additives or fertilizers at the same depth.

Stage 3: Monitoring, May–August.

During this period, the obtained data should be analyzed in real time, including:

– hydration dynamics and assessment of the water absorption rate after spring atmospheric precipitation;

– comparison of the rate of decrease, or reduction, in soil moisture content;

– weekly monitoring of the amount of green biomass, or vegetation.

Stage 4: Evaluation of results, September.

At this stage, the actual soil moisture data should be compared with theoretical calculations based on the Richards equation, followed by adjustment of the model coefficients.

The obtained data should then be entered into the neural network to refine recommendations for the next season.

Required Equipment for Testing

Material: Granulated bentonite from local deposits, for example Navbahor, Azkamar, Vaush, Kattakurgan, Logon, Khovdak, and others.

Technical equipment: A cultivator or motor cultivator equipped with a hopper for deep fertilizer application, preferably modernized for bentonite incorporation.

IT tools: A climate monitoring station and a cloud-based data processing service using Python/TensorFlow.

Scheme for Conducting Experimental Trials

Control: Soil without additives, representing the natural background.

Variant 1: Application of bentonite at a rate of 6 t/ha.

Variant 2: Application of bentonite at a rate of 12 t/ha.

Variant 3: Application of bentonite at a rate of 18 t/ha.

Variant 4: Application of bentonite at a rate of 24–30 t/ha.

Parameters of experimental plots: 25–50 m² for each variant.

- **Incorporation depth:** 0–30 cm, corresponding to the main root-inhabited soil layer.
- **Application method:** Uniform subsurface incorporation into the soil.

Input Data for AI

1. **Soil moisture:** Measurements every 10–15 days and after each rainfall event at depths of 10, 20, 30, and 40 cm.
2. **Meteorological data:** Air temperature, air humidity, precipitation amount and intensity, and solar radiation.
3. **Physical properties:** Bulk density (g/cm³), moisture absorption rate, and field capacity.

2. Data Collection and Processing Methodology

For training a neural network or an algorithm, the data should be structured as time series. It is recommended to combine the thermostat–gravimetric method, which serves as a reference method for calibration, with the installation of soil moisture sensors, such as TDR probes for continuous monitoring [16-18].

For AI-based modeling, a high data frequency is important; for example, sensor readings may be recorded every 15–60 minutes. In this process, sensor errors and measurement noise must be taken into account [19].

It is necessary to establish the relationship between the bentonite application rate and the duration of moisture retention above the plant wilting point. The Van Genuchten model can be used to describe how bentonite changes the soil water potential [20-22].

The developed algorithm should solve the task of predictive management. For example, based on weather forecast data, the AI calculates how much moisture will remain in the bentonite-amended soil layer after one week and signals the need for agrotechnical measures, such as mulching to reduce evaporation [23,24].

The table below presents typical indicators for rainfed lands of Uzbekistan. These data can be used as a baseline for describing your results.

Table. Dynamics of Moisture Retention in the 5–40 cm Soil Layer During the Growing Season

Experimental variant	**Bentonite dose, t/ha**	**Average soil moisture, % of FC***	**Average moisture retention period, days**	**Deviation from AI forecast, %**
Control variant, without additives	0	42.0	18	−6.5
Variant 1	6	55.8	29	−2.1
Variant 2	12	62.4	36	+1.4
Variant 3	18	67.8	42	+2.8
Variant 4	24–30	70.5	46	+4.1

*** FC — field capacity.**

Conclusion

The application of modeling methods and artificial intelligence makes it possible to simulate the chemical and mineralogical composition of bentonite granules, as well as the swelling of bentonite due to moisture absorption, the rate of which is controlled by an AI model depending on the average soil temperature. This provides a prolonged moisture-retention effect for 3–5 years.

The integration of AI into the process of bentonite application makes it possible to retain up to 40% of the moisture obtained from spring precipitation in the aeration zone until the end of August. It also contributes to increasing pasture productivity by extending the vegetation period. In addition, the consumption of bentonite can be reduced through targeted application in zones with maximum moisture retention during the growing season under arid climatic conditions. The application of the developed AI algorithms makes it possible to model the soil drying curve with high accuracy. AI successfully identified a nonlinear relationship between the intensity of solar radiation and the rate of moisture release from bentonite hydro-barriers. This allows critical periods of moisture deficit to be predicted several days in advance.

Thus, the use of an intelligent moisture-retention management system makes it possible not only to preserve the ecosystem of rainfed lands, but also to ensure a direct economic effect through two factors: minimizing losses during dry periods and calculating the exact dosage of bentonite, thereby preventing excessive application of costly ameliorants. The use of bentonite clays creates a stable intra-soil hydro-barrier that increases the moisture-retention capacity of rainfed soils. The developed algorithms make it possible to transform random factors, such as precipitation and evaporation, into a controllable model. The combination of natural adsorbents and AI technologies increases the profitability of rainfed agriculture through adaptive resource management under conditions of water scarcity.

The application of AI transforms the use of bentonites from an uncontrolled process into a high-precision land reclamation technology. This represents a strategic direction for ensuring the

rational use of water resources and adapting the agriculture of the Republic of Uzbekistan to climate change.

REFERENCES

1. Ahmed Abdelfattah, H., & Mostafa, H. (2024). Potential of soil conditioners to mitigate deficit irrigation impacts on agricultural crops: A review. *Water Resources Management, 38*(8), 2961–2976. https://doi.org/10.1007/s11269-024-03822-w
2. Rakhmonov, A. Kh., Tashkuziev, M. M., & Myachina, O. V. (2021). The effect of bentonite-modified fertilizers on the moisture capacity and aggregate composition of soil under cotton. *Universum: Chemistry and Biology, 7*(85). https://doi.org/10.32743/UniChem.2021.85.7.11932
3. Zhang, Y., & Liu, X. (2023). Dynamic modeling of soil water release characteristics under extreme temperature fluctuations in amended soils. *Agricultural Water Management, 288*, Article 108473. https://doi.org/10.1016/j.agwat.2023.108473
4. Singh, D. K., & Rao, S. (2025). Predictive dynamics of soil moisture in arid zones: A nonlinear machine learning approach integrating meteorological and pedological data. *Journal of Arid Environments, 231*. https://doi.org/10.1016/j.jaridenv.2024.105436
5. Vandana, M., et al. (2024). Predicting the hydraulic conductivity of bentonite-amended soils using artificial neural networks. *Scientific Reports, 14*, Article 10738. https://doi.org/10.1038/s41598-024-61434-6
6. Khaydarov, B. D. (2018). Efficiency of resource-saving soil tillage on rainfed lands of Uzbekistan. *Agrarian Science, 10*, 50–51. https://doi.org/10.3263/0869-8155-2018-319-10-50-51
7. Sabirov, B. T., Kadirova, Z. R., Pulatov, Kh. L., Tairov, S. S., & Ergashev, Sh. T. (2021). Research of the basic physical and chemical properties of bentonite clays of promising deposits of Uzbekistan. In *Proceedings of the EURO ASIA 8th International Congress on Applied Sciences* (p. 318). Uzbekistan.
8. Mukhtorova, N. B., Sabirov, B. T., & Aliev, B. A. (2022). Study of the chemical and mineralogical composition of Shafirkan bentonite clay for obtaining new sorbents. *Science and Innovation, 3*, 168–175.
9. Madatov, B. A., Sabirov, B. T., Temirov, U. Sh., & Umkirov, F. E. (2023). Comparative study of physical and technical properties of bentonite clay powders from various deposits. *International Bulletin of Engineering and Technology, 3*(7), 60–66.
10. Muftullaeva, M. B., Reimov, A. M., & Sabirov, B. T. (2023). Chemical composition of bentonite from the Muynak deposit of Karakalpakstan. *Universum: Technical Sciences, 7*(112). https://doi.org/10.32743/UniTech.2023.112.7.15766
11. Mukhtorova, N. B., Aliev, B. A., Sabirov, B. T., & Umirov, U. F. (2023). Thermodynamics of the desorption process and features of regeneration of adsorbents based on bentonite clay. *Science and Innovation International Scientific Journal, 2*(9), 81–87. https://doi.org/10.5281/zenodo.8367636
12. Mukhtorova, N. B., Aliev, B. A., Sabirov, B. T., & Umirov, U. F. (2023). Research on the processes of wastewater purification in textile production using bentonite adsorbents. *Science and Innovation International Scientific Journal, 2*(9), 123–129. https://doi.org/10.5281/zenodo.8386901

13. Mukhtorova, N., Aliev, B., Sabirov, B., Umirov, U., Shokhakimova, A., & Ergashev, Y. (2024). Investigation of ion sorption of chromium, zinc, nickel, and cobalt complex compounds from wastewater using bentonite clay. *E3S Web of Conferences, 497*, Article 03046. https://doi.org/10.1051/e3sconf/202449703046
14. Sabirov, B. T. (2024). Current state of mining and processing of bentonite clays in Uzbekistan and prospects for their application in the metallurgical industry of the Republic of Belarus. *Casting and Metallurgy, 3–4*, 13–16.
15. Sabirov, B. T. (2025). Current state of mining and processing of bentonite clays in Uzbekistan. *Foundryman of Russia, 1*(16), 23–26.
16. Pulatova, Z. F., Sabirov, B. T., & Pulatov, Kh. L. (2026). Development of a mathematical model of the mechanism of water accumulation, moisture retention, and water release by bentonite clay. *Science and Innovation International Scientific Journal, 5*(3). https://doi.org/10.5281/zenodo.19363994
17. Yusupova, N., & Usmonova, M. (2022). Improvement of the reclamation condition of soil resources under the climatic conditions of Uzbekistan. *Innovative Science, 6-1*, 64–66.
18. Mukhamedieva, D. T., Ziyadullaeva, D. Sh., Shamsieva, S. D., Kholikov, M. U., & Asadova, O. S. (2024). Application of artificial intelligence technology in the qualitative assessment of soil fertility based on neural networks. *Science and Innovation: Special Issue "Modern Problems and Prospects of Development of Energy Supply of Digital Technology Facilities"*, 583–591.
19. Tsypkin, Yu. A., Bliznyukova, T. V., Gavrilyuk, M. N., & Belov, N. S. (2025). Implementation of artificial intelligence in the management system of land and property complexes and land reclamation measures. *International Agricultural Journal, 8*(4), 1129–1143.
20. Yurchenko, I. F. (2022). Land reclamation and hydraulic engineering: Automation of irrigation based on artificial intelligence technologies. *Land Reclamation and Hydraulic Engineering, 12*(4), 233–245.
21. El Monhim, M. H. B., Chenal, J., & Ben Hichou, B. (2024). Artificial intelligence in soil management: The new frontier of smart agriculture. *Water, 17*(9), Article 1351. https://doi.org/10.3390/w17091351
22. Al-Taey, D. K., Hussain, A. J., & Kadhum, H. (2023). Bentonite impact on soil properties and biological activity in the face of drought: A review. *IOP Conference Series: Earth and Environmental Science, 1262*, Article 042058. https://doi.org/10.1088/1755-1315/1262/4/042058
23. Tefera, M. L., Zeleke, E. B., Pirastru, M., & Melesse, A. M. (2025). Satellite-based machine learning for soil moisture prediction in dryland agricultural systems. *Remote Sensing, 17*(21). https://doi.org/10.3390/rs17213651
24. Peng, F., Sun, D., Chen, B., & Gao, Y. (2024). Effective approach to predict the soil-water retention curve of bentonites using nonlinear fitting. *Journal of Hydrology*. https://doi.org/10.1016/j.jhydrol.2024.131799

ASSESSING THE PHOTOSYNTHETIC CAPACITY AND STAY-GREEN TRAIT OF BREAD WHEAT (*Triticum aestivum* L.) CULTIVARS AND LINES UNDER FIELD CONDITIONS

D.Kh. Khalikulov[1], U. Yuldashov[2]
PhD, Head of laboratory at Scientific Research Institute of Rainfed Agriculture[1]
PhD, Head of laboratory at Scientific Research Institute of Plant Genetic Resources[2]
https://doi.org/10.5281/zenodo.20522167

Abstract. *This study evaluated the chlorophyll dynamics and photosynthetic potential of 20 bread wheat cultivars and lines during the stem elongation and grain filling periods. Results showed a significant increase in chlorophyll content from an average of 42.5 SPAD in the stem elongation stage to 51.6 SPAD during grain filling. Among the evaluated genotypes (ranging from 39.8 to 54.4 SPAD), cultivars such as Qorasuv, Zarbuloq, Gurt, and lines GA №55/2024, KP-183/2017, AE №7/2020, and D-83/2024 demonstrated significantly higher photosynthetic activity compared to the standard cultivar Zamin-1 (48.0 SPAD). By maintaining stable chlorophyll synthesis under heat and moisture deficit, these superior genotypes guarantee stable grain yield and high quality, serving as valuable donors for future breeding programs.*

Keywords: *bread wheat (Triticum aestivum L.), cultivar, breeding line, genotype, chlorophyll dynamics, photosynthetic potential, stem elongation period, grain filling period, abiotic stress.*

Introduction

Globally, bread wheat is one of the most important cereal crops, and it is considered an economic crop utilized for food, seed, and industrial purposes. According to data from the FAO, global wheat grain production amounts to 766 million tons. Of this, 19% comes from China, 14% from India, a certain percentage from Russia and the USA, and 6% from France [1]. The continuous growth of the global population and the reduction of irrigated arable lands mean that the current rate of food production cannot keep pace with rapidly increasing demand. Increasing wheat yield in the coming decades is one of the most critical objectives of modern agriculture. Therefore, enhancing wheat yield through the development of improved wheat cultivars is one of the most urgent tasks today [2].

The primary objective of traditional wheat breeding is to develop cultivars capable of growing and developing across diverse agro-ecological conditions. In the context of global climate change, it is essential to conduct research focused on selecting genotypes that possess the necessary genes controlling key traits [3].

To significantly increase yield and profitability in agriculture, the main focus in wheat breeding must be on selecting new genetic sources that can adapt to the environmental conditions of each region, are resilient to the adverse effects of climate change, and produce high-quality, stable yields, and subsequently developing new cultivars based on them.

Materials and methods

The study was conducted in 2026 in the irrigated experimental fields of the central experimental farm at the Scientific Research Institute of Rainfed Agriculture.

As the research object, 20 bread wheat cultivars and lines were sown in the competitive testing nursery in the third decade of October in autumn. Sowing was performed using a specialized SKS-7-10 breeding seeder in 25 square meter plots with 4 replications using a randomized design, at a seeding rate of 4 million seeds per hectare. The cultivar Zamin-1, which is well-adapted to the climatic conditions of the region, was selected as the standard check cultivar. GenStat 3 software was utilized for the randomized arrangement of the samples in the experimental design.

Chlorophyll content measurements were carried out during the stem elongation and grain filling periods of the bread wheat using a specialized handheld device, the "Plant Nutrition Analyzer (PNA-4)". During the measurement process, careful attention was paid to ensuring that the leaves were not wet from dew or rain, remaining completely dry and clean. Measurements were primarily taken on the flag leaves of the plants, and care was taken to avoid placing the midrib (thick central vein) of the leaf into the measuring chamber of the device. For each experimental plot, measurements were taken 3 times from 5 different leaves, and their average values were recorded. All field measurements were conducted on clear, sunny, and windless days with low air humidity. [4].

For the mathematical analysis of the experimental results, ANOVA statistical analyses in OriginPro (2024) software were utilized.

Experimental Results and Discussion

Chlorophyll is the primary pigment of the photosynthesis process. Its content serves as an indicator of the plant's photosynthetic potential and stress condition. As a result of drought, salinity, heat, or nutrient deficiency, chlorophyll degradation occurs in the leaves, and yellowing (chlorosis) is observed [5].

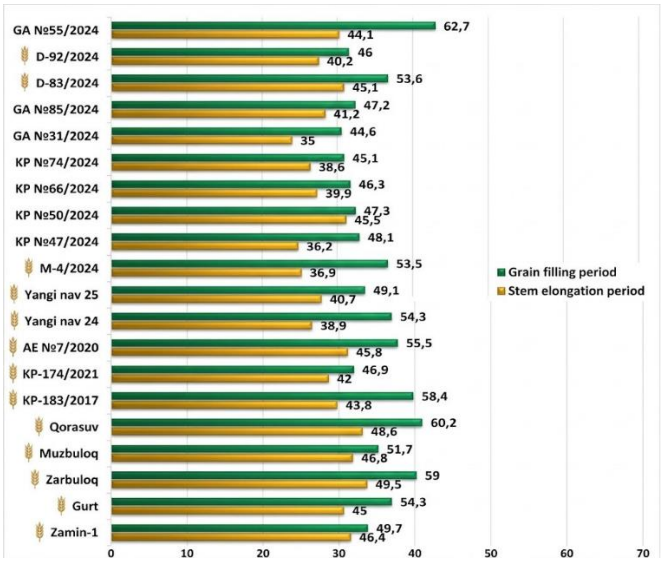


Figure 1. Chlorophyll content of bread wheat cultivars and lines during stem elongation and grain filling periods, SPAD.

During the breeding process, high chlorophyll content indicates the active functioning of the plant's photosynthetic apparatus, a high potential for tolerance to abiotic stresses (drought, heat), and the intensive synthesis of assimilates [6]. A sharp increase in chlorophyll content was observed in the 20 bread wheat cultivars and lines studied in the competitive testing nursery during the transition from the stem elongation period to the grain filling period. This change is directly explained by the bread wheat maximizing its photosynthesis process to form the spike and supply the necessary nutrients to the grain. During the stem elongation period, the chlorophyll content in

the leaves of the bread wheat was found to range from 35.0 SPAD to 49.5 SPAD. In this period, high photosynthetic indicators were demonstrated by the cultivars Zarbuloq (49.5 SPAD), Qorasuv (48.6 SPAD), Muzbuloq (46.8 SPAD), and the standard check Zamin-1 (46.4 SPAD). During the grain filling period, which determines the yield and grain quality of wheat, the chlorophyll content was observed to range from 44.6 SPAD to 62.7 SPAD. During this period, a high level of photosynthetic apparatus activity was observed in the cultivars and lines GA №55/2024 (62.7 SPAD), Qorasuv (60.2 SPAD), Zarbuloq (59.0 SPAD), KP-183/2017 (58.4 SPAD), and AE №7/2020 (55.5 SPAD) (Figure 1). When the dynamics of chlorophyll content in the leaves of bread wheat cultivars and lines at different ontogenetic stages were analyzed using a T-test, the average chlorophyll content of the genotypes during the stem elongation period was 42.5 SPAD. By the grain filling period, an increase in this physiological indicator was recorded, with the average value reaching 51.6 SPAD. This difference between the two periods scientifically confirms the intensive activation of the photosynthetic apparatus in bread wheat during the grain filling phase. From a physiological point of view, the high chlorophyll content specifically during the grain filling period ensures a stable flow of nutrients and plastic substances from the leaves to the spike. This indicates that the studied genotypes possess the potential to produce high yields even under extreme climatic conditions (Figure 2).

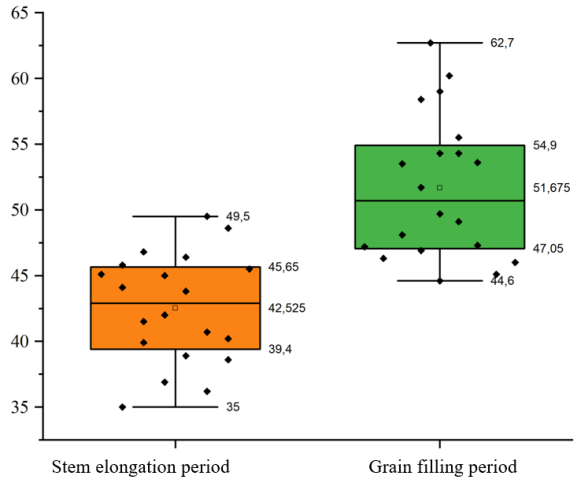


Figure 2. Chlorophyll dynamics of bread wheat cultivars and lines.

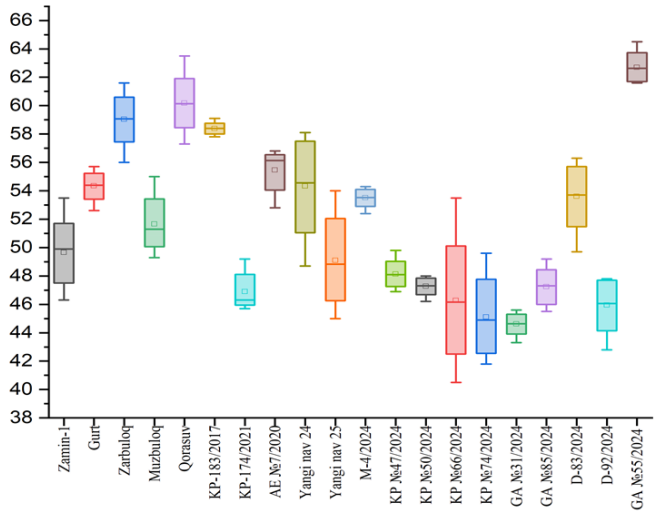


Figure 3. Average chlorophyll content of bread wheat cultivars and lines, SPAD.

When the average chlorophyll content in the leaves of 20 bread wheat cultivars and lines studied in the competitive testing nursery was analyzed, it clearly demonstrated the genetic diversity in the photosynthetic potential of the plants. According to the analyses, the average chlorophyll content of the cultivars and lines was found to range from 39.8 SPAD to 54.4 SPAD. In the Zamin-1 cultivar, which was taken as the standard check, the average chlorophyll content was observed to be 48.0 SPAD. It was determined that the indicators of the cultivars and lines Qorasuv (54.4 SPAD), Zarbuloq (54.3 SPAD), Gurt (49.7 SPAD), GA №55/2024 (53.4 SPAD), KP-183/2017 (51.1 SPAD), AE №7/2020 (50.6 SPAD), and D-83/2024 (49.4 SPAD) were higher compared to the check cultivar. In these genotypes, the activity of chlorophyll synthesis remains stable even under the influence of abiotic stress factors, including heat and moisture deficiency, which as a result guarantees the formation of grain with high technological quality and stability of yield.

Conclusions

An increase in chlorophyll content from an average of 42.5 SPAD to 51.6 SPAD was observed in the 20 bread wheat cultivars and lines studied in the competitive testing nursery during the transition from the stem elongation period to the grain filling phase. The average indicator across all genotypes ranged from 39.8 to 54.4 SPAD, demonstrating genetic diversity in the photosynthetic potential of the plants. Compared to the standard check cultivar Zamin-1 (48.0 SPAD), cultivars such as Qorasuv, Zarbuloq, and Gurt, as well as lines GA №55/2024, KP-183/2017, AE №7/2020, and D-83/2024, recorded higher results. As a result of maintaining an active photosynthesis process under conditions of heat and water deficit, these cultivars and lines guarantee the formation of grain with high technological quality and stable yield.

REFERENCES

1. Food and Agriculture Organization of the United Nations. (n.d.). *World food situation: Cereal supply and demand brief*. FAO. http://www.fao.org/worldfoodsituation/csdb/
2. Karshiboev, H. Kh., et al. (2025). Heat-resistant germplasm and breeding lines for developing durum wheat under rainfed conditions of Uzbekistan. *Research on Crops, 26*(4).
3. Khalikulov, D. Kh., et al. (2026). Durum wheat (*Triticum durum* L.) quality parameters and their relationship with grain yield. *SABRAO Journal of Breeding and Genetics, 58*(2), 666–675.
4. Kholmumin ugli, D. Kh., et al. (2025). Determination of chlorophyll content as a non-invasive method for evaluating the photosynthetic potential and stress condition of wheat. *Universal Journal of Medical and Natural Sciences, 4*(32), 50–53.
5. Xalikulov, D. Kh., & Mamarakhimov, B. I. (2026). Determination of chlorophyll content as a non-invasive method for evaluating the photosynthetic potential and stress condition of wheat. *Universal Journal of Medical and Natural Sciences, 4*(32), 50–53.
6. Xalikulov, D. Kh., Hakimov, U. A., & Yuldashov, U. Kh. (2026). Evaluating the tolerance of bread wheat (*Triticum aestivum* L.) samples to abiotic stresses based on chlorophyll content and plant temperature. In *Proceedings of the International Scientific and Technical Conference "Current Problems and Their Solutions for Adapting to Global Climate Change through Modern Scientific Achievements, Genomic and Water-Saving Technologies, Cultivation Agrotechnologies, Plant Breeding, and Seed Production"* Part 1, 137–141. Karshi.

IRON DEFICIENCY STATES IN YOUTH: ETIOLOGY AND MODERN CORRECTION METHODS

A.Sh. Ulugberdiev[1], S.S. Sharifjonov[2], A.U. Nuriddinov[2], F.Sh. Abdurakhmonov[2]
Assistant. Tashkent State Medical University[1]
Student. Tashkent State Medical University[2]
https://doi.org/10.5281/zenodo.20078893

Abstract*. This review article analyzes contemporary medical literature on the prevalence, mechanisms, and treatment of iron deficiency states (IDS) among youth and adolescents. Although the World Health Organization recognizes iron deficiency as one of the most common nutritional disorders, in the 14–21 age group it often remains a hidden epidemic. The review aims to systematize clinical and epidemiological findings on the causes of sideropenia in young people and to emphasize the need for early diagnosis of latent deficiency. Evidence from national and international studies shows that screening based only on hemoglobin is insufficient because it may fail to detect many cases of depleted tissue iron stores. The article outlines key pathogenetic factors, including rapid growth, increased physiological demand, menstrual blood loss, and nutritional poverty caused by frequent fast-food consumption and inadequate intake of bioavailable heme iron. Special attention is given to non-hematological consequences, such as weakened T-cell immunity, reduced memory and concentration, poorer academic performance, and reproductive risks linked to impaired NO-dependent adaptation. Current recommendations indicate that dietary correction is mainly preventive, while confirmed latent iron deficiency, especially ferritin below 15–20 ng/mL, requires oral iron therapy for at least three months. Timely treatment improves quality of life and prevents future complications.*

Keywords: *iron deficiency, youth, serum ferritin, sideropenia, nutritional poverty.*

Introduction. Iron deficiency states (IDS) have remained one of the most discussed topics in global medicine for decades. According to expert estimates by the World Health Organization (WHO), a deficiency of this micronutrient is recognized as the most massive nutritional disorder, affecting more than 2 billion people—nearly one-third of the global population. Despite significant progress in nutrition and pharmacology, the problem of sideropenia has not lost its urgency and, in some regions, has even taken on the character of a "hidden pandemic." Researchers are particularly concerned about the health status of the youth—adolescents and students aged 14 to 21—who represent the strategic human and reproductive potential of any society.

The biological role of iron during critical periods of development. The biological significance of iron extends far beyond its participation in hemoglobin synthesis. This micronutrient is a unique biocatalyst and a cofactor for more than 70 enzyme systems that ensure the vital activity of every cell in the body. Iron is essential for cellular respiration processes (as part of cytochromes), DNA synthesis, detoxification of foreign compounds, and maintenance of the oxidant-antioxidant balance [3].

During the youth period (14–21 years), the demand for iron increases sharply. This is associated with the so-called "second growth spurt," characterized by an intense increase in linear body dimensions, muscle mass development (especially in males), and an increase in circulating blood volume. In females, this process is complicated by the onset of the menstrual cycle, creating

additional physiological iron losses that are often not compensated by dietary intake. Thus, even a minor deviation from a balanced diet at this age can lead to a negative iron balance.

The "hidden hunger" phenomenon: from latent deficiency to anemia. One of the main problems highlighted in modern literature is the insufficient diagnosis of the early stages of deficiency. In clinical practice, an approach has long prevailed where attention is paid to iron status only when hemoglobin levels decrease—the stage of manifest iron deficiency anemia (IDA). However, researchers emphasize that IDA is only the "tip of the iceberg." It is preceded by a long period of latent iron deficiency (LID), during which tissue iron stores (ferritin) are already depleted and specific tissue enzymes operate under deficiency conditions, even though hemoglobin remains within the normal range [4].

For today's youth, a specific pathogenetic background is characteristic. High physiological needs are superimposed on unfavorable social factors: irregular eating habits, a preference for fast food and products with low biological value (so-called "nutritional poverty"), and a trend toward unreasonable diets. Furthermore, the educational process in universities is accompanied by constant psycho-emotional stress and cognitive overload. In such conditions, iron is consumed by the body much faster. As a result, symptoms occur that students often mistake for ordinary fatigue: decreased concentration, memory impairment, constant drowsiness, and emotional instability.

Systemic influence and review objectives. The consequences of iron deficiency at a young age are systemic. This includes not only increased fatigue but also suppression of immune defense (secondary immunodeficiency), making youth more vulnerable to infections. Moreover, modern studies prove that IDS in youth acts as a predictor of serious reproductive disorders in the future.

The purpose of this literature review is to systematize current data on the etiology and pathogenesis of IDS in youth, analyze the effectiveness of existing diagnostic markers, and justify the need for early preventive correction of this condition. We aim to show that the timely detection of iron deficiency at the latent stage is key to preserving the health and intellectual potential of young people.

Materials and methods. Information search strategy. To write this literature review, a comprehensive retrospective search and systematic analysis of domestic and foreign scientific and medical publications were conducted. The search for relevant sources was carried out in leading electronic databases and scientific citation indexes, including PubMed/MEDLINE, Web of Science, Scopus, as well as the RSCI (eLibrary.ru) and CyberLeninka.

The search was conducted using the following keywords and their combinations in Russian and English: “iron deficiency anemia,” “latent iron deficiency,” “serum ferritin,” “sideropenia,” “youth,” “adolescents,” “students,” “nutritional poverty,” and “reproductive health.”

Inclusion and exclusion criteria. To ensure high reliability and a narrow focus of the review, strict criteria for selecting literary sources were developed. The final analysis included the following categories of publications:

- ✓ Epidemiological studies covering the target age group—adolescents and young adults (14 to 21 years old).
- ✓ Works dedicated to the comparative analysis of the diagnostic value of hemoglobin and serum ferritin.
- ✓ Studies of systemic (non-hematological) manifestations of iron deficiency, including effects on immune status, cognitive functions, and the reproductive system.

- ✓ Official clinical recommendations from international and national committees (e.g., International Nutritional Anemia Consultative Group — INACG) on the prevention and treatment of IDS.
- ✓ Articles dedicated to the following were excluded from the review:
- ✓ Congenital hemolytic anemias (thalassemia, sickle cell anemia) not related to nutritional and physiological factors.
- ✓ Iron deficiency in elderly and senile persons, as the etiology of IDS in these groups is fundamentally different (predominantly oncological diseases and chronic gastrointestinal bleeding).

Analysis and synthesis of data. The methodological basis of the review included both modern clinical studies and fundamental historical works (e.g., the works of H. Pastides [5] and early publications by L.M. Kazakova [1]), which allowed for tracing the evolution of scientific views on the problem.

A total of more than 50 primary sources were analyzed, from which the most representative works with a high level of evidence were selected for final citation. Data evaluation was carried out using the qualitative synthesis method: information was grouped according to key pathogenetic mechanisms, which made it possible to identify the main gaps in modern diagnostics and formulate substantiated recommendations for their elimination.

Results and discussion. Analysis of IDS prevalence in the youth population. The synthesis of modern epidemiological research data reveals an extremely high prevalence of sideropenia among individuals aged 14–21. The literature analysis indicates that the actual situation is significantly more complex than reflected in official statistics, which are primarily based on hemoglobin levels.

According to studies by H. Pastides conducted among various groups of young people in Connecticut, the frequency of manifest iron deficiency anemia (IDA) varied from 4.4% to 17.9% in females, while it did not exceed 5.5% in males. Notably, in the group of Yale University students, the anemia rate was among the highest among women, which refutes the thesis that iron deficiency is exclusively a problem of low-income populations [5].

However, the most alarming figures pertain to latent iron deficiency (LID). As noted by A.N. Shchukov and V.I. Petukhov, the percentage of individuals with hidden deficiency (exhibiting normal hemoglobin but ferritin <20 ng/mL) is two to three times higher than the frequency of anemia. In certain regions of Russia and Latvia, the prevalence of LID among the generation born in the 1990s reaches 40–50% [4]. This means that nearly every second young person is in a state of metabolic exhaustion that remains undiagnosed by standard methods.

Etiological structure of the deficiency Based on the analyzed materials [1, 2, 3], we have classified the primary causes of IDS development in youth as follows:

- ✓ **Intensive Biological and Physiological Requirements**: During the critical developmental window of 14 to 21 years, the human body undergoes a "second growth spurt". This period is defined by an intense increase in linear body dimensions and the rapid development of muscle mass, particularly in males. These processes necessitate a sharp increase in iron demand to facilitate the building of new cellular structures and the substantial expansion of circulating blood volume.
- ✓ **The Socio-Behavioral Phenomenon of "Nutritional Poverty"**: Modern adolescents frequently succumb to a specific dietary pattern where an excess of carbohydrates is consumed alongside a critical deficit of heme iron. This "nutritional poverty" is

characterized by a preference for fast-food products and refined items with low biological value. Because such diets fail to provide even the minimum physiological requirement of bioavailable iron, they inevitably lead to a negative iron balance and metabolic exhaustion.

- ✓ **Gender-Specific Physiological Factors**: In females, the biological demand for iron is significantly complicated by the onset of the menstrual cycle. The resulting physiological iron losses are the dominant cause of anemia within this subgroup, as these losses are frequently not compensated by adequate dietary intake.
- ✓ **Academic and Psycho-Emotional Stressors**: The educational environment in universities introduces constant cognitive overload and psycho-emotional stress. Under these high-pressure conditions, the body consumes its iron reserves—which act as a cofactor for over 70 enzyme systems—at a much faster rate than under normal circumstances.
- ✓ **The "Hidden Hunger" Diagnostic Gap**: A significant contributing factor to the persistence of these states is the clinical reliance on hemoglobin levels alone. This traditional approach leaves up to 70% of cases of critical tissue iron depletion undetected. Consequently, students remain in a state of latent iron deficiency (LID), where tissue stores (ferritin) are depleted even while hemoglobin remains within a "normal" range

Non-hematological manifestations: immunity and the cognitive sphere Analysis of literary data shows that the systemic consequences of iron deficiency manifest long before a drop in hemoglobin occurs. T.V. Kazyukova argues that sideropenia is a potent factor in secondary immunodeficiency [3]. A lack of iron as a cofactor for myeloperoxidase and other enzymes leads to decreased phagocytosis and impaired proliferation of T-lymphocytes. This explains the high frequency of respiratory diseases among students with low ferritin levels.

The cognitive aspect is of particular significance. Iron participates in the synthesis of dopamine and the process of myelinating nerve fibers. Research confirms a direct link between iron deficiency and "student burnout syndrome": distractibility, impaired short-term memory, and an inability to withstand prolonged intellectual loads are typical signs of cerebral tissue hypoxia at low ferritin levels.

Reproductive risks and long-term prognosis. A pivotal and highly consequential outcome derived from this comprehensive analytical review is the unequivocal confirmation of the pathophysiological linkage connecting iron deficiency states (IDS) during adolescence with the subsequent emergence of profound reproductive dysfunctions in adulthood. Pioneering experimental investigations conducted by A.N. Shchukov and V.I. Petukhov have successfully established a robust, positive correlation between the circulating concentrations of serum ferritin—the primary biomarker of tissue iron stores—and the endogenous production of nitric oxide (NO).

A precipitous decline in systemic iron reserves effectively inhibits the enzymatic synthesis of nitric oxide, a critical vasodilator that is absolutely indispensable for the physiological adaptation and hemodynamic remodeling of the maternal vascular architecture throughout the gestational period. As a direct physiological consequence of this vascular maladaptation, women who endured uncorrected iron deficiency states throughout their youth exhibit a quantifiable, twofold escalation in the statistical probability of experiencing "missed" pregnancies alongside a spectrum of other severe gestational complications. Therefore, it is clinically imperative to recognize that the prompt, accurate diagnosis and early therapeutic intervention of iron deficiency states within the contemporary youth demographic serves as a fundamental, non-negotiable prerequisite for safeguarding the demographic vitality and overall physiological well-being of successive generations.

Effectiveness of correction methods. In the context of therapeutic intervention, there is an unequivocal consensus among all the scrutinized researchers and clinical experts [1, 3, 6]: dietary modifications and nutritional optimization serve an exclusively prophylactic function. Once a clinical diagnosis of either latent iron deficiency (LID) or manifest iron deficiency anemia (IDA) is definitively established, reliance on dietary intake alone becomes clinically insufficient; instead, the immediate implementation of targeted pharmacological therapy utilizing oral iron supplements becomes an absolute medical necessity.

A profoundly significant physiological revelation highlighted within the literature is the stark temporal discrepancy in recovery rates: the biochemical replenishment of deep tissue iron reservoirs—specifically represented by serum ferritin "depots"—proceeds at a considerably more protracted and gradual pace compared to the relatively rapid normalization of circulating hemoglobin concentrations. Consequently, to secure a durable, long-term therapeutic outcome and actively prevent subsequent clinical relapses, the prescribed regimen of pharmacological ferrotherapy must be meticulously sustained for a minimum continuous duration of at least three months..

Conclusion. Summarizing the analysis of modern scientific literature, it can be stated that the problem of iron deficiency states (IDS) in youth (14–21 years old) has moved beyond a narrow hematological discipline and acquired the status of a multidisciplinary medical and social task. The systematization of data from leading researchers [1, 3, 5] allows us to formulate the following key conclusions and recommendations:

- ✓ **The need to change the diagnostic paradigm.** The conducted review confirms that traditional screening, based exclusively on the determination of hemoglobin levels, is an insufficiently sensitive tool for the youth population. It leaves up to half of the cases of latent iron deficiency (LID) undiagnosed, a condition in which systemic metabolic disorders are already observed. We consider it critically important to introduce mandatory testing of serum ferritin levels into the routine health screening programs for students. A threshold ferritin value below 15–20 ng/mL should be considered a signal for the immediate initiation of corrective measures, even with normal red blood cell indices.
- ✓ **Multifactorial etiology.** The problem of IDS in youth cannot be solved by medical methods alone. The deep interrelationship between the physiological needs of the growing body and socio-behavioral factors ("nutritional poverty," high academic loads, stress) requires a comprehensive approach. It is necessary to create educational programs for students aimed at improving nutritional literacy and understanding the importance of consuming bioavailable heme iron.
- ✓ **Recognition of systemic consequences.** Iron deficiency at a young age is not temporary fatigue, but a factor directly affecting the quality of the nation's intellectual capital and its demographic future. The proven link between sideropenia and the risks of reproductive losses in the future, as well as secondary immunodeficiency, makes early correction of IDS a matter of national security and long-term population health.
- ✓ **Strategy for therapeutic correction.** Based on the analyzed clinical guidelines [6], it should be emphasized: the treatment of an identified deficiency must be exclusively pharmacological and prolonged. Diet therapy is an important background but cannot serve as an independent method of treatment. To fully replenish tissue iron stores, the course of ferrotherapy should continue for 3–4 months under ferritin control, which prevents relapses and ensures the stable functioning of all iron-dependent systems of the body.

The implementation of these recommendations into practical healthcare will significantly improve the academic performance of the youth, strengthen their immune status, and minimize the risks of developing serious pathologies in adulthood.

REFERENCES

1. Kazakova L. M. Iron deficiency in children // Pediatrics. — 1984. — № 9. — P. 31–33.
2. Kazakova L. M. Iron deficiency in children (Lead article) // Kemerovo State Medical Academy. — 25 p.
3. Kazyukova T. V. Iron deficiency in children and adolescents (Lecture) // Department of Children's Diseases No. 1. — 12 p.
4. Shchukov A. N., Bykova E. Y., Petukhov V. I., Baumane L. H. Iron deficiency states (IDS) as a predictor of reproductive disorders // Eurasian Union of Scientists (ESU). — 2014. — № VI. — Medical Sciences. — P. 69–71.
5. Pastides H. Iron Deficiency Anemia Among Three Groups of Adolescents and Young Adults // The Yale Journal of Biology and Medicine. — 1981. — Vol. 54. — P. 265–271.
6. International Nutritional Anemia Consultative Group (INACG). Guidelines for the Use of Iron Supplements to Prevent and Treat Iron Deficiency Anemia. — Washington, 1998.
7. Addy D. P. Happiness is: iron // British Medical Journal. — 1986. — Vol. 292. — P. 969–970.
8. Alimova, Z. A., Ulugberdiyev, A., Ismoiljonov, A. I., Mukhammadjonov, K., & Rikhsiboyev, R. (2024). The role of semiconductor heterostructures in modern microelectronics. *Science and innovation*, *3*(A10), 204-208.

QUALITY OF LIFE IN PATIENTS AFTER LAPAROSCOPIC FUNDOPLICATION FOR HIATAL HERNIA BASED ON GERD-HRQL QUESTIONNAIRE DATA

S.I. Ismailov[1,2], R.E. Ligai[1,2], A.D. Abdukarimov[1], A.O. Tsoy[1], R.R. Omonov[1], Sh.N. Madrakhimov[1], Zh.M. Avalbaev[1], S.D. Iskandarov[1]
State Institution "Republican Specialized Scientific-Practical Medical Center of Surgery named after Academician V.V. Vakhidov", Tashkent, Uzbekistan[1]
Tashkent State Medical University[2]
https://doi.org/10.5281/zenodo.20266881

Abstract. *To assess the dynamics of quality of life in patients operated on for hiatal hernia (HH) using an original modified laparoscopic fundoplication technique, applying the GERD-HRQL questionnaire within up to 1 year after surgery. From October 2023 to February 2025, 149 patients with HH types I–IV were operated on using the modified laparoscopic technique. Quality of life was assessed using the GERD-HRQL questionnaire before surgery and at 1, 6, and 12 months after surgery. In addition, patient complaints during the postoperative period were analyzed. The baseline mean GERD-HRQL score was approximately 20.1. At 1 month after surgery, it decreased to 3.13 (−84.4% from baseline), at 6 months to 7.65, and at 1 year to 8.55 (−57.5%). The follow-up coverage at 1 year was 75.8%. At discharge, 92.6% of patients had no complaints. Dysphagia (4.7%) was transient and resolved spontaneously. In some patients with periodic heartburn in the long-term period, the symptoms did not require repeat intervention and were corrected by PPI administration. Early HH recurrence (1.3%) was diagnosed during the period of mastering the technique and was resolved by repeat laparoscopic intervention.*

Keywords: *hiatal hernia, quality of life, GERD-HRQL, laparoscopic fundoplication, antireflux surgery, dysphagia.*

INTRODUCTION

Assessment of health-related quality of life is an integral component of analyzing the effectiveness of surgical treatment of hiatal hernias (HH) and gastroesophageal reflux disease (GERD). Elimination of the anatomical defect and elimination of reflux find their final expression not only in objective indicators — radiological consistency of the repair or pH-metry data — but, above all, in the patient's subjective perception of treatment results. That is why international surgical societies recommend the use of validated quality of life assessment tools as a mandatory criterion of the effectiveness of antireflux operations [1, 2].

The most widely used tool in this area is the GERD-HRQL questionnaire (Gastroesophageal Reflux Disease — Health-Related Quality of Life), developed specifically to assess GERD symptoms and their impact on daily life [3]. The questionnaire contains 10 questions, with a total score ranging from 0 (no symptoms) to 50 (maximum severity). A reduction in the total score by at least 50% from the baseline level is considered a clinically significant improvement [3]. Ease of application, high reproducibility, and sensitivity have made GERD-HRQL a standard instrument in studies on HH surgery.

Since October 2023, an original modified laparoscopic fundoplication technique, performed for HH of all types, has been introduced in the Department of Esophageal and Gastric

Surgery of the State Institution “Republican Specialized Scientific-Practical Medical Center of Surgery named after Academician V.V. Vakhidov.” The key elements of the technique that directly affect patient quality of life are: performing fundoplication in all types of hernia, providing complete antireflux protection; extended mediastinal mobilization of the esophagus, eliminating tension in the repair zone; the use of a 56–60F calibration probe and the “shoeshine maneuver,” preventing a hyperfunctional cuff and postoperative dysphagia.

The aim of the present study is to evaluate the dynamics of patient quality of life using the GERD-HRQL questionnaire after laparoscopic fundoplication by the modified technique within an observation period of up to 1 year.

MATERIALS AND METHODS

The study included 149 patients with HH types I–IV operated on in the Department of Esophageal and Gastric Surgery of the State Institution “Republican Specialized Scientific-Practical Medical Center of Surgery named after Academician V.V. Vakhidov” from October 2023 to February 2025 using the original modified laparoscopic Nissen fundoplication technique. Among the operated patients, there were 47 men (31.5%) and 102 women (68.5%), with a mean age of 54.8±15.7 years. Distribution by HH types: Type I — 74 (49.7%), Type II — 12 (8.1%), Type III — 59 (39.6%), Type IV — 4 (2.7%).

Quality of life was assessed using the GERD-HRQL questionnaire before surgery and at follow-up examinations at 1, 6, and 12 months after the intervention. At each visit, patient complaints were additionally recorded. To assess the clinical significance of the dynamics, the criterion of a reduction in the total score by at least 50% from the baseline level was used [3].

Statistical data processing was performed using the SPSS Statistics package. The Wilcoxon test for paired samples was used to compare indicators in dynamics; the level of statistical significance was set at $p<0.05$.

RESULTS

Baseline quality of life

Before surgery, the mean total GERD-HRQL score for the entire group was approximately 20.1, which corresponds to moderately pronounced symptoms. The distribution of baseline indicators by HH types is presented in Table 1. The highest score was recorded for Type I hernia (27.2), which naturally reflects the pronounced reflux component underlying this type. For Type II, the baseline score was significantly lower (6.8): in patients of this group, the clinical picture is dominated by mechanical symptoms (dysphagia, feeling of fullness), which are less reflected by the GERD-HRQL scale, since the scale is primarily focused on reflux symptoms. For Types III and IV, the mean values were 16.5 and 20.0, respectively, reflecting the combination of reflux and mechanical components.

Table 1. Baseline GERD-HRQL indicators by HH types (n=149)

HH Type	n	GERD-HRQL score (range)	Mean score
Type I	74	22–35	27.2
Type II	12	3–8	6.8
Type III	59	7–29	16.5
Type IV	4	9–31	20.0

HH Type	n	GERD-HRQL score (range)	Mean score
All	**149**	**–**	**~20.1**

Dynamics of quality of life after surgery

The dynamics of the mean GERD-HRQL score after surgery are presented in Tables 2 and 3, as well as in Figure 1. At all time points, a statistically significant decrease in the score compared with the baseline level was recorded ($p<0.001$).

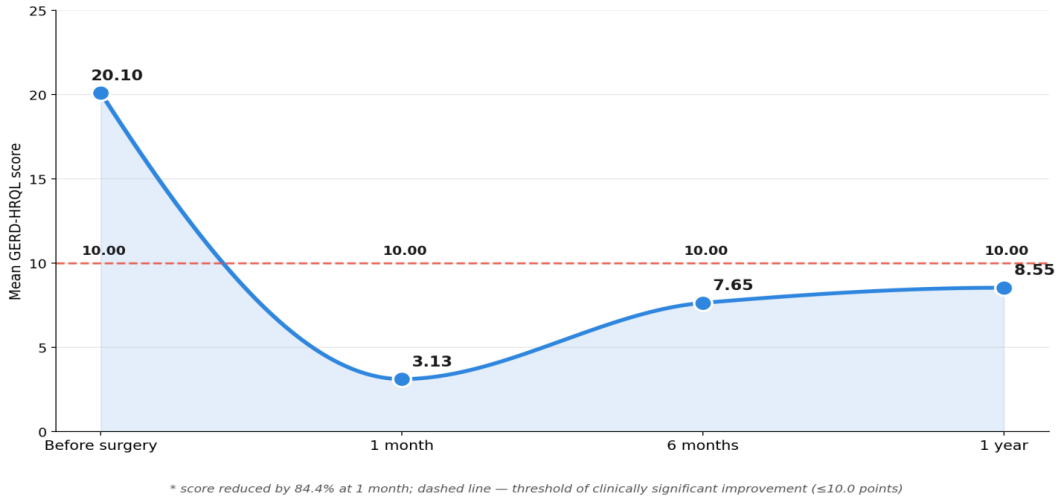
The most pronounced improvement in quality of life was already noted at 1 month after surgery: the mean score decreased from ~20.1 to 3.13, which corresponds to a reduction of 84.4% from the baseline level and significantly exceeds the threshold of clinically significant improvement (50%). The coverage of follow-up examinations at 1 month was 94.6% (141 of 149 patients), which ensures high representativeness of the data. The vast majority of patients during this period presented minimal symptoms or had no complaints at all.

By 6 months, the mean score was 7.65 (coverage 85.9%), and by 1 year — 8.55 (coverage 75.8%). Both values correspond to a mild degree of symptom severity and remain significantly below the baseline level. The slight increase in the score from the 1st to the 12th month (from 3.13 to 8.55) is physiologically explainable and reflects the normal course of the postoperative period: adaptation of the fundoplication cuff, restoration of normal esophageal peristalsis, and the patient's adaptation to the new anatomical conditions.

Table 2. Dynamics of the mean GERD-HRQL score (n=149)

Time point	n examined	% coverage	Range	Mean score	Δ from baseline
Before surgery	149	100%	–	~20.1	–
1 month	141	94.6%	0–6	3.13	−84.4%
6 months	128	85.9%	2–9	7.65	−61.9%
1 year	113	75.8%	2–17	8.55	−57.5%

Figure 1. Dynamics of mean GERD-HRQL score after laparoscopic fundoplication (n=149)



** score reduced by 84.4% at 1 month; dashed line — threshold of clinically significant improvement (≤10.0 points)*

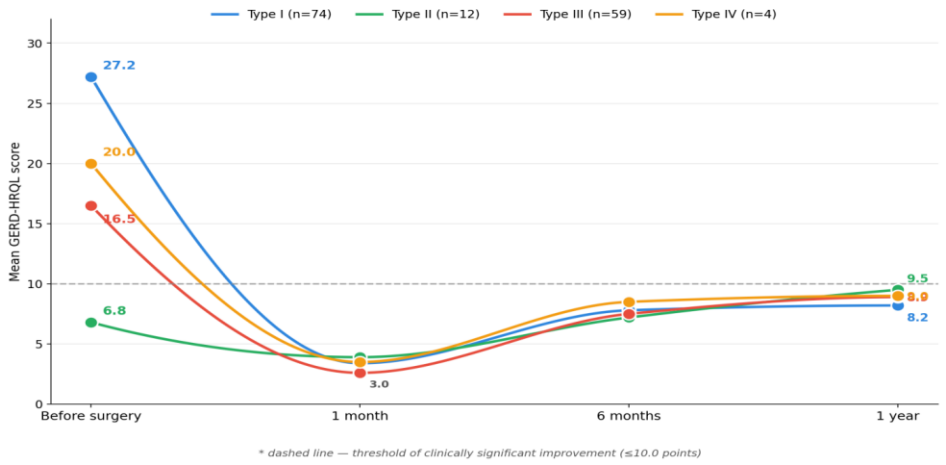
Dynamics by HH types

Analysis of GERD-HRQL dynamics by HH types revealed a uniform pattern across all groups: a sharp decrease in the score by 1 month with subsequent stabilization (Table 3). The greatest absolute reduction in the score was recorded for Type I (from 27.2 to 3.4 at 1 month) due to the initially most pronounced reflux symptoms. For Type II, the initially low score (6.8) decreased to 3.9 by 1 month and increased somewhat by 1 year (9.5), which reflects adaptation to the altered anatomical conditions after fundoplication in patients with predominantly mechanical symptoms. For Types III and IV, the dynamics are similar to Type I: pronounced early improvement followed by stabilization at the level of mild symptoms.

Table 3. Mean GERD-HRQL score by HH types in dynamics

HH Type	Before surgery	1 month	6 months	1 year
Type I (n=74/72/67/61)	27.2	3.4	7.8	8.2
Type II (n=12/11/8/5)	6.8	3.9	7.2	9.5
Type III (n=59/55/51/46)	16.5	2.6	7.5	8.9
Type IV (n=4/3/2/1)	20.0	3.5	8.5	9.0

Figure 2. Dynamics of mean GERD-HRQL score by HH types



Patient complaints in the postoperative period

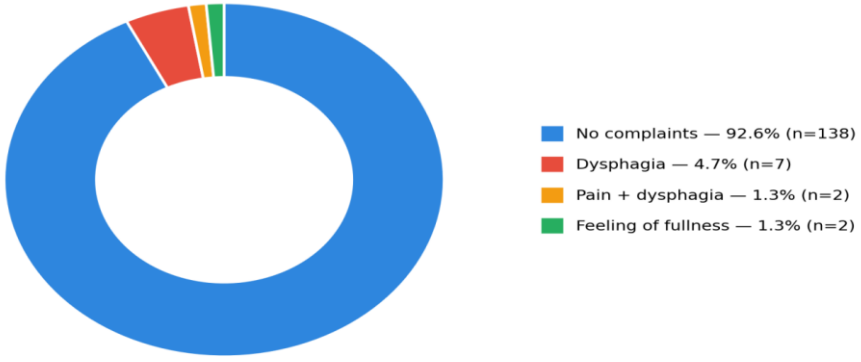
The distribution of complaints at discharge from the hospital is presented in Table 4. The vast majority of patients — 138 of 149 (92.6%) — did not present any complaints at discharge. In some patients, periodic heartburn was noted in the long-term observation period; however, it did not reach the degree of severity requiring repeat surgical intervention and was successfully corrected by the administration of proton pump inhibitors (PPIs) in standard doses. This circumstance reflects normal adaptation in the postoperative period and does not indicate failure of the antireflux mechanism. Early HH recurrence was diagnosed in 2 patients (1.3%) within the first 2–3 days after surgery. The most probable cause was insufficient mobilization of the esophagus during the initial period of mastering the technique. Both patients underwent repeat laparoscopic intervention consisting of additional esophageal mobilization and vagotomy, with a satisfactory immediate result. As surgical experience accumulated and the technique was standardized, this complication did not recur.

Dysphagia was noted in 7 patients (4.7%), and in 2 more (1.3%) — in combination with pain syndrome. In all cases, dysphagia was transient and resolved spontaneously without additional interventions. This is a direct consequence of the use of the 56–60F calibration probe during cuff formation and of the performance of the "shoeshine maneuver": these technical elements prevent excessive narrowing of the cuff and provide physiological pressure on the esophagus in the early postoperative period. A feeling of fullness without dysphagia was noted in 2 patients (1.3%) and also resolved spontaneously.

Table 4. Patient complaints at discharge (n=149)

Complaints	**n**	**%**
No complaints	**138**	**92.6%**
Dysphagia (transient)	7	4.7%
Pain + dysphagia	2	1.3%
Feeling of fullness	2	1.3%
Periodic heartburn (corrected with PPI)	0	–*
Total with complaints	**11**	**7.4%**

Figure 3. Structure of patient complaints at discharge (n=149)



DISCUSSION

The obtained results indicate the high effectiveness of the modified laparoscopic fundoplication with regard to the quality of life of patients with HH. A reduction in the mean GERD-HRQL score by 84.4% at 1 month and stabilization at the level of 8.55 at 1 year exceed the threshold values of clinically significant improvement (≥50%) and correspond to the results of leading world centers of antireflux surgery [4, 5].

The issue of postoperative heartburn deserves special attention. In some patients in the long-term period, periodic heartburn was observed that did not require repeat surgical intervention and was successfully relieved by the administration of proton pump inhibitors (PPIs). Such a pattern is characteristic of the transitional period after antireflux surgery and is due to the adaptation of the lower esophageal sphincter to the new anatomical conditions. Performing fundoplication in all types of HH — including Types II–IV, for which the antireflux component was not previously envisaged in the department's practice — ensures a fundamentally more

complete functional correction of lower esophageal sphincter pathology in the entire category of patients [6].

The transient and spontaneously resolving nature of postoperative dysphagia (4.7%) is a natural result of using a 56–60F calibration probe instead of the standard 40F. A number of international studies confirm that the use of larger-diameter probes when forming the fundoplication cuff reliably reduces the frequency and severity of postoperative dysphagia [7]. An additional control instrument is the "shoeshine maneuver," which allows intraoperative verification of the absence of excess gastric tissue behind the esophagus.

Some increase in the mean GERD-HRQL score from 3.13 (1 month) to 8.55 (1 year) is not a sign of recurrence, but rather reflects physiological adaptation — restoration of normal gastric secretion, resolution of postoperative edema, and the patient's adaptation to the altered anatomical conditions. Similar dynamics have been described in large case series after successful laparoscopic fundoplication [5]. High coverage of follow-up examinations (94.6% at 1 month, 75.8% at 1 year) is an independent indicator of the quality of medical care and ensures the high representativeness of the obtained data.

CONCLUSION

The modified laparoscopic fundoplication provides a pronounced and lasting improvement in the quality of life of patients with HH according to the GERD-HRQL questionnaire. The mean score decreased from ~20.1 to 3.13 at 1 month (−84.4%) and stabilized at the level of 8.55 at 1 year (−57.5%), which corresponds to clinically significant improvement at all follow-up periods. Periodic heartburn, noted in some patients in the long-term period, did not require repeat intervention and was corrected by the administration of PPIs. Dysphagia in 4.7% of cases was transient and resolved spontaneously, which confirms the correctness of using the 56–60F calibration probe and the "shoeshine maneuver." Early HH recurrence (1.3%), which occurred during the period of mastering the technique, was resolved by repeat laparoscopic intervention with a satisfactory result.

The totality of the obtained data substantiates the use of the developed technique as an effective tool for improving the quality of life of patients with HH of all types in a specialized surgical hospital setting.

REFERENCES

1. Daly S. et al. SAGES guidelines for the surgical treatment of hiatal hernias. Surg Endosc. 2024; 38(6): 2917–2938.
2. Hanna N.M. et al. Management of symptomatic, asymptomatic, and recurrent hiatal hernia: a systematic review and meta-analysis. Surg Endosc. 2024; 38(6): 2917–2938.
3. Velanovich V. The development of the GERD-HRQL symptom severity instrument. Dis Esophagus. 2007; 20(2): 130–134.
4. Dallemagne B., Weerts J., Markiewicz S. et al. Clinical results of laparoscopic fundoplication at ten years after surgery. Surg Endosc. 2006; 20(1): 159–165.
5. Khan M.U. et al. Outcomes of Laparoscopic Hiatal Hernia Repair: A Three-Year Follow-Up Study from a UK Tertiary Centre. Cureus. 2025; 17(10): e94404.
6. Singhal S. et al. Current Trends in the Management of Hiatal Hernia. Cureus. 2024; 16(11). DOI: 10.7759/cureus.73070
7. Pessaux P., Arnaud J.P., Delattre J.F. et al. Laparoscopic antireflux surgery: five-year results and beyond in 1340 patients. Arch Surg. 2005; 140(10): 946–951.

IMPACT OF PULMONARY PATHOLOGY ON THE MORPHOFUNCTIONAL DEVELOPMENT OF THE CHEST IN CHILDREN AGED 0–3 YEARS

I.Dj. Gulmanov[1], M.A. Seifuldinova[2]
PhD, Associate Professor of the Department of Human and Clinical Anatomy, Tashkent State Medical University, Tashkent, Uzbekistan[1]
Assistant Professor, Department of General Surgery and Topographic Anatomy
Kazakh National Medical University named after S.D. Asfendiyarov
Almaty, 050028, Kazakhstan[2]
https://doi.org/10.5281/zenodo.20080167

Abstract. *Pulmonary pathology in early childhood may significantly affect the morphofunctional development of the chest by disrupting normal growth and functional maturation processes. This study aimed to investigate the influence of pulmonary pathology on chest development in children aged 0–3 years. A total of 376 children from Tashkent with clinically diagnosed bronchopulmonary pathology, attending preschool institutions and pediatric healthcare facilities, were examined. Anthropometric assessment included measurements of chest circumference at rest, during maximal inspiration, and during full expiration, as well as calculation of chest excursion. Centile analysis and the standard deviation method using Z-scores were also applied. The results showed that children with pulmonary pathology had a reduced rate of chest circumference growth, decreased chest excursion to 1.0–1.2 cm, a shift of indicators toward lower centile intervals, and negative Z-score values. These findings indicate impaired chest mobility, reduced pulmonary ventilation, and delayed morphofunctional development of the respiratory system. The study concludes that bronchopulmonary pathology has a pronounced negative effect on chest development in children aged 0–3 years, contributing to disharmonious physical development and reduced adaptive capacity of the organism. The results support the need for early diagnosis, dynamic anthropometric monitoring, and timely correction of respiratory system diseases.*

Keywords: *chest, early childhood, pulmonary pathology, anthropometry, chest excursion, centile analysis, Z-score.*

INTRODUCTION AND LITERATURE REVIEW

Early childhood (0–3 years) represents a critical stage in the formation of morphofunctional characteristics of the organism, particularly the respiratory system and the chest. During this period, intensive growth of osteochondral structures, development of respiratory musculature, and maturation of external respiration mechanisms occur. In this regard, anthropometric indicators, especially chest circumference, acquire particular importance as objective markers of physical development and functional status of the respiratory system.

Modern studies demonstrate that the dynamics of children's physical development are determined by a combination of endogenous and exogenous factors, including hereditary characteristics, nutritional patterns, climatic and geographical conditions, and the level of medical care [1,2,4]. At the same time, pronounced secular trends have been identified within pediatric

populations, reflecting changes in growth rates and somatic development across different regions and populations [5].

A number of authors emphasize the importance of regional differences in the assessment of anthropometric indicators. It has been established that body length and weight parameters of children living in different climatic zones vary significantly, which necessitates the development of local standards for physical development [6,**Error! Reference source not found.**]. Similar findings have been reported in Central Asian countries, where distinctive features of physical development in early childhood have been identified based on basic anthropometric criteria [5,9].

A special place in contemporary literature is occupied by the assessment of the harmony of physical development and morphofunctional adaptation of the child's organism. The application of index-based methods and integral evaluation approaches allows for the identification of deviations from normative values and for the quantitative characterization of the degree of disharmony in somatic development [3,4,**Error! Reference source not found.**]. It has been shown that frequently ill children exhibit more pronounced deviations in anthropometric indicators compared to healthy peers, indicating the adverse influence of chronic pathological conditions on growth and development processes [8,9].

In recent years, considerable attention has been paid to the study of morphological characteristics of children in urban environments. It has been demonstrated that the rate of change in anthropometric parameters depends on environmental factors, the level of physical activity, and living conditions [11,12]. In addition, age-related patterns in the change of body proportions and levels of harmony in physical development have been identified [7,10,14].

At the same time, despite the large number of studies devoted to the general assessment of physical development in children, the influence of pulmonary pathology on the morphofunctional state of the chest in early childhood remains insufficiently investigated. Meanwhile, respiratory diseases such as bronchitis, pneumonia, and bronchiolitis occupy a leading place in the structure of morbidity among children in the first years of life and are accompanied by impaired ventilation function, reduced elasticity of lung tissue, and limitation of chest excursion.

These changes can significantly affect the formation of the chest, slowing its growth, reducing its mobility, and creating conditions for the development of morphofunctional disharmony. However, comprehensive studies aimed at assessing the relationship between chest anthropometric parameters, centile distribution, Z-score, and pulmonary pathology in children aged 0–3 years are insufficiently represented in the literature.

Thus, the analysis of the literature indicates the high relevance of studying the influence of pulmonary pathology on the morphofunctional development of the chest in early childhood, which determined the direction of the present study.

OBJECTIVE

To assess the influence of pulmonary pathology on the morphofunctional development of the chest in children aged 0–3 years based on anthropometric indicators, centile analysis, and Z-score.

MATERIALS AND METHODS

The study was conducted on the basis of preschool educational and medical institutions in Tashkent and had an observational analytical design. It included 376 children aged 0–3 years with clinically confirmed pulmonary pathology attending kindergartens and pediatric hospitals. The examination was carried out with informed voluntary consent from parents or legal guardians, in compliance with ethical standards adopted in biomedical research.

Inclusion criteria were age from 0 to 3 years, clinically confirmed bronchopulmonary pathology (including acute and chronic bronchitis, pneumonia, and bronchiolitis), and the possibility of regular anthropometric examination. Exclusion criteria included congenital anomalies of chest development, severe systemic diseases, and genetic syndromes that could significantly influence physical development indicators.

The main research method was anthropometric analysis. In all children, chest circumference was measured in three functional states: at rest, at maximal inspiration, and at full expiration. Measurements were performed using a standard measuring tape according to generally accepted methodology: posteriorly at the level of the inferior angles of the scapulae and anteriorly along the nipple line. To ensure accuracy, each measurement was performed at least twice, followed by calculation of the average value.

Chest excursion was calculated as the difference between inspiratory and expiratory chest circumference values and was used as an indicator of the functional state of the respiratory system.

Additionally, centile analysis and Z-score calculations were performed. The centile method allowed assessment of each parameter relative to age norms and determination of the degree of physical development harmony. Z-score was calculated using the formula:

$$Z = (X - M)/\sigma$$

where X is the individual value, M is the mean of the reference group, and σ is the standard deviation.

Statistical analysis was performed using methods of variation statistics with calculation of mean values (M), standard deviation (σ), and standard error (m). Statistical significance was assessed at $p<0.05$.

RESULTS

The conducted anthropometric analysis demonstrated that healthy children in early childhood (0–3 years) exhibit a pronounced positive dynamic of chest circumference in all functional states. In particular, at rest, the values increase from 33.3 cm in the first year of life to 52.7–53.0 cm by the age of three; at maximal inspiration, from 33.9 cm to 53.6–54.0 cm; and at expiration, from 32.3 cm to 51.6–52.0 cm. This dynamic reflects harmonious morphological development of the chest, a gradual increase in its dimensions, and the formation of functional mobility, which is confirmed by the correspondence of the obtained mean values (M±σ).

The average values of chest excursion in healthy children range from 1.5 to 2.0 cm, with a tendency to increase as the child grows. This indicates normal development of the elastic properties of lung tissue, adequate functioning of the respiratory musculature, and sufficient ventilatory capacity of the lungs. Variation analysis showed a relatively narrow range of fluctuations (σ≈0.2–0.3), which indicates homogeneity of the studied group and stability of physiological processes.

In children with pulmonary pathology, statistically significant deviations from age-related norms were identified. A decrease in the rate of increase in chest circumference was observed, with mean values being on average 2.5–3.5 cm lower than physiological norms. At the same time, an increase in variability (σ≈0.3–0.5) was noted, reflecting heterogeneity in the severity of pathological changes.

A decrease in chest excursion to 1.0–1.2 cm was also established, which is significantly lower than normal values ($p<0.05$). This reduction indicates limited chest mobility and impaired ventilatory function of the lungs. These changes are associated with decreased elasticity of lung tissue, bronchial obstruction, inflammatory processes, and the formation of shallow breathing.

Centile analysis allowed for a more detailed assessment of the distribution of indicators. In healthy children, chest circumference values were predominantly located within the 25th–75th percentile range, with the highest concentration around the 50th percentile, which corresponds to harmonious physical development. In contrast, in children with pulmonary pathology, a pronounced shift toward lower centile intervals was observed. A significant proportion of values were located within the 10th–25th percentiles, and in some cases below the 10th percentile, indicating morphological deficiency and the formation of disharmonious physical development.

Additional quantitative assessment using Z-score analysis demonstrated that in healthy children, values were within the range of $-1 \leq Z \leq +1$, corresponding to normal physical development. In children with pulmonary pathology, a shift toward negative values was observed, averaging between –1.5 and –2.0, indicating moderate developmental delay. In some cases, Z values below –2 were recorded, reflecting pronounced morphofunctional insufficiency and a high risk of pathological changes in the respiratory system. The most pronounced deviations in both centile distribution and Z-score were observed in chest excursion parameters, emphasizing the predominantly functional nature of disorders in bronchopulmonary pathology. This indicates that even with moderate reductions in chest size, respiratory function is affected to a greater extent. Comparative analysis showed that the most significant changes were observed in children with chronic and recurrent forms of bronchopulmonary pathology. In this group, not only a decrease in absolute anthropometric values was noted, but also a disruption of age-related growth dynamics, manifested by flattening of growth curves, stable displacement toward lower centile ranges (below the 25th percentile), and persistent negative Z-score values.

Thus, the results of the comprehensive analysis, including anthropometric evaluation, variation statistics, centile distribution, and Z-score, indicate the presence of pronounced morphofunctional disorders of the chest in children with pulmonary pathology. These changes are characterized by reduced chest dimensions, decreased mobility, displacement into lower centile intervals, and negative Z-score values, reflecting delayed growth and impaired functional development of the respiratory system.

DISCUSSION. The obtained results convincingly demonstrate that pulmonary pathology exerts a significant and multifactorial impact on the morphofunctional development of the chest in early childhood. The identified decrease in chest circumference growth rates, reduction in chest excursion, and shift of indicators toward lower centile ranges collectively indicate the presence of both structural (morphological) and functional impairments.

Under physiological conditions, early childhood is characterized by rapid growth of the thoracic cage and progressive enhancement of its functional mobility, which is reflected in a gradual increase in chest excursion. These processes are closely associated with the maturation of lung tissue, strengthening of respiratory musculature, and improvement of ventilatory capacity. The findings obtained in the group of healthy children are fully consistent with these established developmental patterns and confirm the normal trajectory of morphofunctional maturation [2,4].

In contrast, the alterations observed in children with pulmonary pathology are in agreement with previously reported data indicating the negative influence of chronic and recurrent diseases on physical development. It has been demonstrated that frequently ill children exhibit more pronounced anthropometric deviations, reduced growth rates, and decreased harmony of somatic development, which may be attributed to persistent inflammatory processes and impaired metabolic regulation [8,**Error! Reference source not found.**,**Error! Reference source not found.**].

From a morphological perspective, the reduction in chest circumference and slowing of its growth may be explained by disturbances in the development of osteochondral structures, as well as insufficient stimulation of the thoracic cage due to limited respiratory movements. Chronic hypoventilation and reduced mechanical expansion of the lungs may negatively affect the growth of the rib cage, leading to relative hypoplasia. Similar mechanisms have been described in studies of children with chronic respiratory diseases and unfavorable environmental conditions [6,13,**Error! Reference source not found.**].

From a functional standpoint, the detected changes are closely associated with decreased elasticity of lung tissue, bronchial obstruction, inflammatory infiltration, and impaired airway patency. These factors contribute to the development of hypoventilation and shallow breathing patterns, ultimately reducing the efficiency of gas exchange. The reduction in chest excursion to 1.0–1.2 cm observed in the present study represents a critical functional indicator, reflecting limited respiratory mobility and diminished ventilatory capacity.

Particular importance should be attributed to chest excursion as an integrative parameter reflecting both structural and functional characteristics of the respiratory system. Its reduction indicates not only mechanical limitation of thoracic movements but also underlying disturbances in pulmonary compliance and respiratory muscle function. This finding is consistent with previous studies emphasizing the diagnostic value of chest excursion in assessing respiratory dysfunction in pediatric populations. The application of centile analysis and Z-score methodology significantly enhanced the objectivity of the assessment. These approaches allowed not only qualitative but also quantitative evaluation of deviations from normative values. The shift of anthropometric indicators toward lower percentiles (below the 25th and, in some cases, below the 10th percentile), along with negative Z-score values (–1.5 to –2.0 and lower), confirms the presence of systemic developmental delay and morphofunctional insufficiency. These results highlight the importance of integrating statistical growth assessment tools into clinical and research practice.

Importantly, the most pronounced deviations were observed in children with chronic and recurrent forms of bronchopulmonary pathology, suggesting a cumulative effect of prolonged disease duration on growth processes. This finding supports the concept that repeated episodes of respiratory illness may lead to persistent alterations in both structural development and functional capacity of the chest. The identified morphofunctional disturbances may have significant long-term implications. Impaired development of the thoracic cage during early childhood can result in persistent disharmony of physical development, reduced adaptive capacity of the organism, and increased susceptibility to chronic respiratory diseases in later life. Moreover, these changes may negatively affect overall physical performance and quality of life. Thus, the results of the present study expand current understanding of the impact of pulmonary pathology on child development and emphasize the necessity of a comprehensive and multidisciplinary assessment approach. The integration of anthropometric measurements, functional indicators, and standardized statistical evaluation methods (centile analysis and Z-score) provides a reliable basis for early diagnosis and monitoring of developmental disturbances. In this context, timely identification and correction of respiratory pathology should be considered a priority in pediatric healthcare, as early intervention may prevent the progression of morphofunctional abnormalities and improve long-term health outcomes.

CONCLUSION. It has been established that in children aged 0–3 years, normal development is characterized by a progressive and harmonious increase in chest circumference across all functional states, reflecting proper morphofunctional development of the respiratory

system. Children with pulmonary pathology demonstrate a significant reduction in the rate of chest circumference growth, indicating delayed morphological development. A marked decrease in chest excursion (to 1.0–1.2 cm) was identified, reflecting reduced chest mobility and impaired ventilatory function. Centile analysis revealed a shift of indicators toward lower percentile ranges, while Z-score assessment confirmed moderate to severe developmental delay. Pulmonary pathology in early childhood is a significant factor contributing to morphofunctional imbalance and may have long-term consequences for respiratory health.The obtained results highlight the importance of early diagnosis, continuous monitoring, and timely correction of respiratory disorders to prevent persistent developmental impairments.

REFERENCES

1. Abdullaeva M.E. Values of anthropometric indicators of longitudinal and circumferential body dimensions in children of the first year of life. *Mezhdunarodnyi Zhurnal Nauchnoi Pediatrii*. 2023;2(7):277–281.
2. Aldibekova G., et al. Assessment of physical development of preschool children of the Republic of Kazakhstan and retrospective analysis over the last 50 years. *Georg Med News*. 2021;(319):45–51.
3. Borodina D.I., Borodina G.N. Index assessment of physical development of first-grade schoolchildren in Barnaul. *Scientist*. 2022;4(22):23.
4. Godina E.Z., Gorbacheva A.K., Fedotova T.K. Secular trends of children from birth to 3 years: meta-analysis of data from Russia and neighboring countries. *Collegium Antropologicum*. 2018;42(2):83–88.
5. Kakharov Z.A., et al. Anthropometric indicators of physical development in children of the Andijan region. *Universum: Meditsina i Farmakologiia*. 2018;9(54):1–5.
6. Lebedeva U.M., et al. Comparative aspect of normative values of length and weight indicators of children living in the Far North region (Part 1: body length). *Probl Sotsialnoi Gig Zdravookhranenniia Istor Med*. 2023;31(S3):862–866.
7. Muzaffarovna K.S. Changes in morphometric parameters of children and adolescents. *Obrazovanie Nauka Innovatsionnye Idei v Mire*. 2025;83(7):298–304.
8. Oryngalieva N.D., Dzhumanazarova G.U. Features of physical development of frequently ill school-age children. *Science and Innovation*. 2023;2(Special Issue 8):1614–1620.
9. Shegay M.M., Mustafayeva Z.M. Assessment of physical development of children under 1 year using basic anthropometric indicators in the Republic of Azerbaijan. *Bull Semashko Natl Res Inst Public Health*. 2022;(4):47–50.
10. Shermanov A.O. Age-related dynamics of anthropometric parameters of the lower extremities in young children. *Med J Uzbekistan*. 2026;1(2):20–27.
11. Shermanov A.O. Anthropometric parameters, proportions, and dynamics of physical development of preschool children. *Cent Asian Res J Interdiscip Stud*. 2025;4(3):31–37.
12. Shermanov A.O. Dynamics of growth and body structure of preschool children in Tashkent. *Cent Asian Res J Interdiscip Stud*. 2025;4(3):5–9.
13. Shermanov A.O. Regional features of anthropometric indicators of lower extremities in preschool children of Tashkent: a comparative analysis. *Zamonaviy Tibbiyot Jurnali*. 2026;13(1):920–927.
14. Shermanov A.O., Mirsharapov U.M. Body type and level of harmony of physical development in preschool children. *Science and Innovation*. 2024;3(Special Issue 60):47–52.

AUTOMATED BRAIN PARCELLATION IN THE PREOPERATIVE WORKUP OF ADULT-TYPE DIFFUSE GLIOMAS: WHERE ANATOMY MEETS IMAGE ANALYSIS

N.M. Djuraeva[1], Kh.V. Abdukhalimova[1]
State Institution "Republican Specialized Scientific and Practical Medical Center of Surgery named after academician V. Vakhidov", Tashkent, Republic of Uzbekistan[1]
https://doi.org/10.5281/zenodo.20080019

Abstract. *Automated brain parcellation has matured from a research utility used in cohort neuroimaging into a methodologically attractive option for preoperative planning in neuro-oncology. Unlike most advanced sequences in the multiparametric MRI workup of adult-type diffuse gliomas, parcellation runs on the standard 3D T1-weighted volume already acquired for surgical navigation, requires no additional contrast injection or scan time, and outputs a quantitative map of cortical parcels and subcortical structures involved by the tumor. This review covers the conceptual rationale for incorporating parcellation into the preoperative protocol, summarizes the three pipeline families that dominate current practice (FreeSurfer, FastSurfer/FastSurferVINN, and SAMSEG), discusses the methodological caveats that arise when these tools are applied to brains distorted by mass effect and edema, and outlines the integration of parcellation outputs with diffusion tractography, perfusion metrics, and radiogenomic models. The clinical bottleneck is no longer software availability but validation on glioma cohorts, where standard atlases were not built. The review draws on 18 sources, mostly from 2019–2026.*

Keywords: *adult-type diffuse gliomas, brain parcellation, FreeSurfer, FastSurfer, SAMSEG, preoperative MRI, neuronavigation, WHO CNS5.*

Introduction

Preoperative imaging of adult-type diffuse gliomas has expanded along two axes over the past decade. The first is biological: the WHO Classification of Tumours of the Central Nervous System, fifth edition (WHO CNS5, 2021) made molecular markers - IDH, 1p/19q, MGMT, ATRX, TP53, histone H3 mutations - definitional rather than ancillary, which placed an explicit demand on imaging to predict the molecular profile rather than merely confirm a mass [1, 2]. The second is computational: most of the gain in diagnostic accuracy now comes from quantitative postprocessing rather than from new pulse sequences, and consensus protocols such as BTIP-2015 and the BTIP-2020 DSC update codified what a usable preoperative dataset must contain [3, 4].

Within this computational layer, automated brain parcellation occupies an unusual position. Diffusion, perfusion, and spectroscopy each address a specific physiological question and need a dedicated sequence. Parcellation is different: it works on the T1-weighted MPRAGE volume that is already part of every preoperative protocol, returns a labeled map of dozens of cortical parcels and subcortical nuclei, and does so without any contrast medium or extra scan time. The cost is computational rather than radiological. For a neurosurgical team, the practical output is a structure-by-structure tally of which parcels are crossed by the tumor and which are spared - an anatomical inventory that is otherwise built up implicitly from visual reading.

The aim of this review is to lay out the conceptual rationale for using parcellation in the preoperative workup of diffuse gliomas, summarize the three software families that currently matter (FreeSurfer, FastSurfer including FastSurferVINN, and SAMSEG), discuss the failure modes specific to glioma anatomy, and sketch how parcellation outputs interact with diffusion tractography, perfusion biomarkers, and radiogenomic models. The treatment is methodological rather than encyclopaedic.

Why parcellation belongs in the preoperative workup

Surgery on diffuse gliomas is a calculated trade-off between resection extent and functional preservation. Total resection of the contrast-enhancing component is associated with longer survival in glioblastoma, with intraoperative mapping series reporting median postoperative survival of 16.87 versus 12.04 months and gross-total resection rates of 79.1 % versus 47.7 % when intraoperative mapping is used [5]. The calculus narrows further with FLAIR-defined supramarginal resection in IDH-mutant astrocytomas. None of these decisions is taken on imaging alone, but every one of them rests on a clear preoperative anatomical model: which gyrus carries the tumor, how close the lesion sits to the central sulcus, whether the insula is involved, whether the corpus callosum is crossed.

Visual reading produces this model implicitly. A parcellation pipeline produces it explicitly and quantitatively. Once the T1-MPRAGE has been parcellated, the tumor mask - itself obtainable from BraTS-style segmentation networks such as nnU-Net [6, 7] - can be intersected with the parcellation labels, and the result is a structure-level table: percent involvement of precentral gyrus, percent involvement of posterior superior temporal gyrus, percent involvement of putamen, and so on. This is information the surgeon would extract from visual inspection anyway, but the quantitative version is reproducible across observers, comparable across patients, and storable as data for downstream analyses including radiogenomic modeling.

A second motivation is comparability over time. Postoperative parcellation of the residual cavity and surrounding parenchyma supports unambiguous reporting of which structures were spared and which were resected, which is increasingly relevant for outcome studies. The third motivation is integration with tractography: cortical parcels can serve as seed and target regions for the language and motor pathways of interest, replacing manually drawn ROIs and reducing operator-dependent variability that has long plagued DTI tractography in glioma cases [8].

Pipelines: FreeSurfer, FastSurfer, FastSurferVINN, SAMSEG

FreeSurfer remains the reference. The 2012 NeuroImage paper by Fischl is the most cited single description of the surface-based reconstruction pipeline that produces volumetric subcortical segmentation (aseg), cortical surface reconstruction, and parcellation according to the Desikan–Killiany or Destrieux atlases [9]. Strengths are well known: large normative datasets, a vast methods literature, and tight integration with downstream tools (TRACULA for tractography, hippocampal subfield modules, brainstem substructures). The cost is processing time - six to twelve hours per scan on a typical workstation - which is incompatible with surgical workflows that need turnaround in tens of minutes.

FastSurfer addressed the runtime problem by replacing the recon-all volumetric segmentation with a deep-learning network (FastSurferCNN) trained to reproduce FreeSurfer outputs, while keeping the surface pipeline largely intact. The 2020 NeuroImage paper by Henschel et al. reported runtimes of about one hour for the full pipeline and a few minutes for segmentation alone, with Dice agreement against FreeSurfer above 0.85 for most cortical and subcortical structures [10]. The successor architecture, FastSurferVINN (Henschel, Kügler,

Reuter, NeuroImage 251, 118933, 2022), introduced voxel-size–independent layers that allow the same network to handle 0.7-mm and 1.0-mm scans without retraining, addressing a recurrent failure mode in deep-learning segmentation when test images have a different voxel size than training data [11].

SAMSEG (Sequence Adaptive Multimodal SEGmentation) takes a different route. The contrast-adaptive method by Cerri et al. (NeuroImage 225, 117471, 2021) decouples the shape model of anatomical structures from their MRI appearance, which means SAMSEG segments 41 brain structures from arbitrary contrast combinations without retraining, and integrates a lesion model originally developed for white matter hyperintensities in multiple sclerosis [12]. For neuro-oncology, the contrast-adaptive design is attractive precisely because preoperative protocols vary between centers, and a tool that does not require T1-MPRAGE in a fixed acquisition window has an obvious deployment advantage.

A practical comparison is summarized in Table 1. None of these tools was developed primarily for tumor patients; all were validated on healthy or neurodegenerative cohorts and then extended.

Table 1. Brain parcellation pipelines relevant to preoperative neuro-oncology

Pipeline	Method	Output	Runtime (per scan)	Key reference
FreeSurfer (recon-all)	Surface-based, atlas-driven; classical pipeline	aseg subcortical labels; cortical surfaces; Desikan–Killiany / Destrieux parcellation	6–12 h	Fischl, NeuroImage 2012 [9]
FastSurfer	Deep-learning replacement for the volumetric stage; surface stage retained	Same labels as FreeSurfer; Dice > 0.85 vs FreeSurfer reference	≈ 1 h full; < 1 min segmentation	Henschel et al., NeuroImage 2020 [10]
FastSurferVINN	Voxel-size–independent network; 0.7–1.0 mm without retraining	Whole-brain segmentation across resolutions	< 1 min segmentation	Henschel et al., NeuroImage 2022 [11]
SAMSEG	Bayesian, contrast-adaptive; decoupled shape and appearance models; lesion module	41 brain structures from arbitrary multi-contrast input	≈ 10 min	Cerri et al., NeuroImage 2021 [12]

Failure modes specific to gliomas

Standard parcellation atlases were built from healthy or mildly atrophic brains. A glioma deforms the very anatomy these atlases assume. Three failure modes recur in practice. The first is

mass effect with midline shift: the registration step that aligns the patient to atlas space can produce systematic label displacement, particularly around the lateral ventricles and basal ganglia, where compression distorts the usual landmarks. The second is signal alteration in the tumor and peritumoral edema: T1-MPRAGE intensity within the lesion does not match any normal tissue class, and the segmentation may either label tumor as a hodgepodge of cortex and white matter or - depending on the algorithm - drop the region from the parcellation altogether. The third is post-resection cavities, which the standard atlases simply do not contain.

Practical mitigations differ by pipeline. SAMSEG can be invoked with an explicit lesion model that absorbs the abnormal-intensity voxels into a separate class, leaving the surrounding parcellation intact [12]. FreeSurfer and FastSurfer are typically combined with prior tumor masking - the lesion is inpainted or excluded from registration before parcellation runs - which is conceptually similar to the lesion-filling step long used in multiple sclerosis. None of these mitigations is fully validated on large glioma cohorts. The methodologically honest position is that current parcellation tools are usable for surgical planning when the tumor is small to moderate and away from midline, and require careful manual review when the lesion is large, hemorrhagic, or causes substantial shift.

Quantitatively, the impact of these failure modes depends on tumor size and location. Small (< 3 cm) tumors in convexity locations rarely cause visible parcellation errors beyond the immediate lesion footprint. Tumors crossing the midline, occupying the insular cortex, or displacing the lateral ventricles by more than 5 mm can produce parcellation errors that propagate into adjacent structures and require manual correction. The Bello series of language and motor tractography in glioma surgery, which depends on accurate cortical seed regions, reported that perilesional edema with reduced fractional anisotropy was the dominant cause of false-negative tract reconstructions; the recommended workaround was to lower the FA threshold to 0.10–0.15 and to verify reconstructions against multiple ROIs [8]. The same logic applies to parcellation: accept that perilesional cortex may be mislabeled, build the analysis around contralateral and remote-ipsilateral parcels, and reserve the perilesional region for manual review.

A more recent direction is the BraTS challenge family. Brain Tumor Segmentation Challenge has run since 2012 within MICCAI in collaboration with RSNA and ASNR and has standardized the task of separating enhancing tumor, necrosis, and edema on multiparametric MRI. By 2021 the dataset reached 2040 cases [6], and BraTS-Africa later showed that models trained on Western data lose accuracy on scans from sub-Saharan centers - a generalization problem that applies equally to Central Asian centers and underscores the need for local validation [13]. Tumor segmentation networks (notably the self-configuring nnU-Net [7]) provide the lesion mask that parcellation pipelines can use as prior, closing the loop between the two ends of the automated workflow.

Integration with tractography, perfusion, and radiogenomics

Parcellation is most useful in combination, not in isolation. With diffusion tractography, cortical parcels serve as anatomically defined seed and target ROIs. The Bello series on language fiber tracking with intraoperative subcortical mapping reported sensitivity and specificity of 97–100 % for the superior longitudinal, inferior fronto-occipital, and uncinate fasciculi when DTI was integrated with neuronavigation [8]. Replacing manually drawn cortical ROIs with parcellation-derived labels removes one source of operator variability without changing the underlying tractography algorithm. A workflow that runs FastSurferVINN for parcellation, nnU-Net for tumor segmentation, and a probabilistic CSD tractography seeded from the relevant parcels can be

assembled from open-source components within a single afternoon - the bottleneck is data quality, not software.

With perfusion biomarkers, parcellation provides a normalization reference. Relative cerebral blood volume (rCBV) from DSC perfusion is conventionally normalized to contralateral white matter, but the choice of reference voxel is a known source of inter-rater variability. A parcellation-defined ROI in contralateral normal-appearing white matter, drawn the same way for every patient, gives a more reproducible denominator. The same logic applies to ADC ratios and to ASL-derived CBF. The BTIP-2020 DSC consensus explicitly listed normalization as one of the three principal sources of inter-center variability in rCBV measurement [4]; replacing operator-drawn ROIs with parcellation labels addresses this directly.

A separate integration question concerns brain shift. Once the dura is opened and tumor mass is evacuated, the cortical surface can move 10–25 mm relative to the preoperative coordinate system, which degrades the value of any preoperative map by the late stages of the operation. This is the strongest argument against treating preoperative parcellation as a final answer; the parcellation map is most reliable as a planning document and as input to early-stage navigation, with intraoperative ultrasound or intraoperative MRI used to update the anatomical model after meaningful tissue displacement [18].

With radiogenomics, parcellation provides an anatomical scaffold for the radiomic feature extraction. The Choi et al. multi-center cohort study showed that location matters: external AUC for IDH prediction reached 0.93 in frontal-lobe gliomas and 0.84 in deep-seated lesions [14], a gradient that is plausibly explained by differences in the surrounding parenchyma rather than by the tumor itself. A parcellation-aware feature extraction can encode this anatomical context explicitly. The Farahani 2025 meta-analysis on 72 studies and over 12,000 patients reported pooled sensitivity 80 % and specificity 85 % for IDH prediction by deep-learning radiomics on routine MRI; for 1p/19q codeletion, 75 % and 82 %, with location and segmentation method identified as principal heterogeneity drivers [15]. For MGMT methylation, the picture is less encouraging: the Doniselli et al. systematic review of 26 radiomics studies found a median Radiomics Quality Score of 8 of 36 (22 %), with external validation performed in only 13 of 26 [16], and the Samartha review of 30 deep-learning models reported pooled sensitivity 0.74 and specificity 0.75 with substantial heterogeneity [17].

Local context: deployment in resource-constrained settings

A parcellation-centric preoperative pipeline is unusually well suited to resource-constrained health systems. The required input is a single 3D T1-MPRAGE volume - no contrast, no DSC, no MRS - which is acquired in every neurosurgical center capable of preoperative MRI. The processing tools (FreeSurfer, FastSurfer, SAMSEG) are open-source and run on a workstation-class GPU. Quantitative parcel-level reporting can be added to existing radiology reports without changing acquisition protocols. For a country where dynamic susceptibility contrast perfusion, MR spectroscopy, and resting-state fMRI are concentrated in a small number of centers and where molecular profiling beyond IDH1 R132H immunohistochemistry remains episodic, a parcellation-based anatomical analysis is among the highest-yield additions to the existing workflow [18]. A practical pilot deployment can be staged. Phase one: install FastSurfer or FastSurferVINN on a single workstation, parcellate every preoperative T1-MPRAGE acquired for tumor patients, and append a parcel-level structure-involvement table to the standard radiology report. This adds no scanner time and a few minutes of GPU computation per case. Phase two: add nnU-Net tumor segmentation, intersect the masks with the parcellation, and store the resulting

structure-by-volume tables in a local database. Phase three: link the imaging database to operative findings and pathology reports to build a ground-truth series. By the end of phase three, the same center has accumulated the data needed to validate radiogenomic models on its own population - without ever having modified the acquisition protocol.

The methodological commitment is local validation. International atlases were not built on Central Asian populations; tumor segmentation networks were not trained on local scanners. Both can be deployed and used, but their outputs need spot-checking against expert reading until a local validation series accumulates. Building such a series - paired preoperative T1-MPRAGE, parcellation, tumor mask, and operative findings - is itself a research contribution, and one that does not require equipment beyond what is already installed.

What a parcellation-augmented preoperative report should contain

A useful preoperative report does not dump the entire parcellation table on the surgeon. The relevant content is filtered: which structures are crossed by the tumor, which are within a defined safety margin, which are spared. A workable format includes the tumor volume by component (enhancing, non-enhancing, necrosis, edema), the list of cortical parcels with non-zero tumor overlap and the percent involvement of each, the list of subcortical structures with overlap, the distance from the tumor margin to the central sulcus and to language-area parcels, and the laterality of the eloquent network. This level of detail takes one page in a structured report and replaces several paragraphs of free-text description. The report should also flag uncertainty. Parcellation in the immediate perilesional zone may be unreliable, and that limitation belongs in the report, not in a separate methodological caveat that nobody reads. A simple convention works: structures more than two parcellation thicknesses from the tumor margin are reported with standard confidence; structures within the perilesional zone are flagged as requiring visual confirmation. This kind of explicit confidence labeling is more honest than a uniform output and matches how surgeons actually read the report.

A final practical note concerns reporting language. WHO CNS5 terminology has not yet stabilized in routine radiology reporting in many centers, and the gap between what the pathology report says (astrocytoma IDH-mutant CNS WHO grade 4) and what the radiology report says (high-grade glioma) creates avoidable confusion in multidisciplinary discussion. A parcellation-augmented report is also an opportunity to standardize the molecular-aware terminology - using the WHO CNS5 nomenclature explicitly when the molecular profile is known and stating the imaging-based hypothesis when it is not.

Conclusion. Automated brain parcellation has matured enough to leave the cognitive neuroscience laboratory and enter the preoperative workflow. The core argument is that parcellation extracts anatomical information from a sequence already acquired for navigation, costs no additional patient time, and produces a quantitative output that supports both surgical planning and downstream analytical pipelines including tractography, perfusion normalization, and radiogenomics. The remaining problems are not about algorithms - three robust pipelines exist - but about validation on glioma anatomy and about local deployment in centers where standard-protocol assumptions do not always hold. For a national neuro-oncology service building toward WHO CNS5–compliant preoperative diagnostics, parcellation is a low-cost, high-leverage addition that can be implemented now and refined as local data accumulate.

REFERENCES

1. Louis D.N., Perry A., Wesseling P. et al. The 2021 WHO Classification of Tumors of the Central Nervous System: a summary // Neuro-Oncology. - 2021. - Vol. 23, No. 8. - P. 1231–1251.
2. Smits M. MRI biomarkers in neuro-oncology // Nature Reviews Neurology. - 2021. - Vol. 17, No. 8. - P. 486–500.
3. Ellingson B.M., Bendszus M., Boxerman J. et al. Consensus recommendations for a standardized Brain Tumor Imaging Protocol in clinical trials // Neuro-Oncology. - 2015. - Vol. 17, No. 9. - P. 1188–1198.
4. Boxerman J.L., Quarles C.C., Hu L.S. et al. Consensus recommendations for a dynamic susceptibility contrast MRI protocol for use in high-grade gliomas // Neuro-Oncology. - 2020. - Vol. 22, No. 9. - P. 1262–1275.
5. Gerritsen J.K.W., Arends L., Klimek M. et al. Impact of intraoperative stimulation mapping on high-grade glioma surgery outcome: a meta-analysis // Acta Neurochirurgica. - 2019. - Vol. 161, No. 1. - P. 99–107.
6. Baid U., Ghodasara S., Mohan S. et al. The RSNA-ASNR-MICCAI BraTS 2021 Benchmark on Brain Tumor Segmentation and Radiogenomic Classification // arXiv:2107.02314. - 2021.
7. Isensee F., Jaeger P.F., Kohl S.A.A. et al. nnU-Net: a self-configuring method for deep learning-based biomedical image segmentation // Nature Methods. - 2021. - Vol. 18, No. 2. - P. 203–211.
8. Bello L., Gambini A., Castellano A. et al. Motor and language DTI Fiber Tracking combined with intraoperative subcortical mapping for surgical removal of gliomas // NeuroImage. - 2008. - Vol. 39, No. 1. - P. 369–382.
9. Fischl B. FreeSurfer // NeuroImage. - 2012. - Vol. 62, No. 2. - P. 774–781.
10. Henschel L., Conjeti S., Estrada S. et al. FastSurfer - a fast and accurate deep learning based neuroimaging pipeline // NeuroImage. - 2020. - Vol. 219. - 117012.
11. Henschel L., Kügler D., Reuter M. FastSurferVINN: Building resolution-independence into deep learning segmentation methods - A solution for HighRes brain MRI // NeuroImage. - 2022. - Vol. 251. - 118933.
12. Cerri S., Puonti O., Meier D.S. et al. A contrast-adaptive method for simultaneous whole-brain and lesion segmentation in multiple sclerosis // NeuroImage. - 2021. - Vol. 225. - 117471.
13. Adewole M., Rudie J.D., Gbadamosi A. et al. The Brain Tumor Segmentation (BraTS) Challenge 2023: Glioma Segmentation in Sub-Saharan Africa Patient Population (BraTS-Africa) // Radiology: Artificial Intelligence. - 2024 [online ahead of print].
14. Choi Y.S., Bae S., Chang J.H. et al. Fully automated hybrid approach to predict the IDH mutation status of gliomas via deep learning and radiomics // Neuro-Oncology. - 2021. - Vol. 23, No. 2. - P. 304–313.
15. Farahani S., Hejazi M., Tabassum M. et al. Diagnostic performance of deep learning for predicting gliomas IDH and 1p/19q status in MRI: a systematic review and meta-analysis // European Radiology. - 2025 [online ahead of print].
16. Doniselli F.M., Pascuzzo R., Mazzi F. et al. Quality assessment of the MRI-radiomics studies for MGMT promoter methylation prediction in glioma: a systematic review and meta-analysis // European Radiology. - 2024. - Vol. 34, No. 7. - P. 5160–5170.
17. Samartha M.V.S., Arora S., Bhattacharya M. et al. Performance evaluation of deep learning models for predicting MGMT promoter methylation in glioblastoma using MRI: a systematic

review and meta-analysis // Journal of Cancer Research and Clinical Oncology. - 2024. - Vol. 150, No. 10. - P. 461.

INCREASED INTRACRANIAL PRESSURE AND ITS ROLE IN NEUROSURGICAL DISEASES

A.Sh. Ulugberdiev[1], S.U. Sa'dullaev[2], M.U. Anvarov[2], M.Kh. Isroilova[2]
Assistant. Tashkent State Medical University[1]
Student. Tashkent State Medical University[2]
https://doi.org/10.5281/zenodo.20078935

Abstract. *Elevation of intracranial pressure (ICP) is a central pathophysiological problem in neurosurgery, occurring in diverse conditions such as traumatic brain injury, intracranial hemorrhage, neoplasms, hydrocephalus, cerebral venous sinus thrombosis, and severe infections. Normally, resting ICP in adults ranges approximately 7–15 mmHg; sustained or rapidly rising ICP can reduce cerebral perfusion pressure, produce brain herniation, and result in permanent neurological deficits or death. Early recognition and targeted management of ICP are therefore critical components of modern neurocritical care, combining bedside monitoring, neuroimaging, and stepwise therapeutic interventions to prevent secondary brain injury.*

Recent advances in continuous invasive ICP monitoring, including improved intraparenchymal sensors and external ventricular drainage systems with integrated pressure transducers, have increased the precision of bedside measurements and enabled real-time therapeutic titration. Parallel development of validated noninvasive estimation techniques—such as transcranial Doppler-derived indices, optic nerve sheath diameter ultrasound, and validated machine-learning models using multimodal physiological data—offers expanding options where invasive monitoring is unavailable or contraindicated. Current practice integrates multimodal monitoring (ICP, brain tissue oxygenation, continuous EEG, and cerebral microdialysis) to personalize treatment, optimize cerebral perfusion, and guide timing of surgical interventions.

Therapeutic strategies have evolved toward protocolized, tiered approaches: initial measures (head elevation, sedation, normothermia, CSF drainage), escalation with osmotherapy and hyperosmolar therapy, and definitive surgical options including decompressive craniectomy or lesion evacuation when indicated. Emerging evidence supports targeted individualized thresholds for intervention, informed by multimodal monitoring and patient-specific factors such as age, comorbidities, and injury phenotype. Ongoing research into neuroprotective pharmacotherapies, refined osmotherapy regimens, and device innovations aims to further reduce morbidity and mortality associated with intracranial hypertension.

Keywords*: intracranial pressure, neurosurgery, traumatic brain injury, hydrocephalus, ICP monitoring.*

Introduction. Intracranial pressure is the pressure generated within the skull as a result of the interaction between brain tissue, blood, and cerebrospinal fluid. Since the skull is a rigid closed system, any increase in the volume of one of its components inevitably leads to elevated pressure and compression of brain structures [1]. This physiological constraint is known as the Monro-Kellie doctrine, which posits that the sum of volumes of brain, CSF, and intracerebral blood is

constant. When a pathological volume (such as a hematoma or edema) is introduced, the body initially compensates by displacing CSF into the spinal canal and shunting venous blood out of the cranium. However, once these compensatory mechanisms are exhausted, the brain enters a state of low compliance, where even small increases in volume lead to exponential rises in ICP. This surge directly threatens Cerebral Perfusion Pressure (CPP). CPP is defined as the pressure gradient driving oxygen delivery to cerebral tissues, calculated by the formula CPP = MAP - ICP. Maintenance of CPP above 60 mmHg is vital to prevent secondary ischemic insults. Increased intracranial pressure plays a key role in the pathogenesis of neurosurgical diseases, as it often determines the severity of the patient's condition. Clinical manifestations may range from headache and nausea to severe disturbances of consciousness and life-threatening conditions. Modern neurosurgery considers the control of intracranial pressure as one of the main factors for successful treatment. Monitoring of intracranial pressure allows timely detection of patient deterioration and adjustment of therapy, which significantly improves disease outcomes [2]. Early diagnosis of intracranial hypertension is of particular importance, as it helps prevent irreversible brain damage. In addition, timely intervention reduces the incidence of complications and improves neurological recovery in patients. In modern medicine, the integration of clinical data and instrumental diagnostic methods plays a crucial role in enhancing treatment effectiveness.

Materials and Methods. This study presents a comprehensive analysis of the mechanisms underlying the development of intracranial hypertension in various neurosurgical pathologies. Particular attention was paid to the investigation of pathophysiological processes responsible for increased intracranial pressure, including disturbances of cerebrospinal fluid dynamics, venous outflow, and cerebral perfusion. An assessment of risk factors contributing to the rapid progression of this condition was also performed, such as the severity of traumatic injury, localization of the pathological process, and patient age. In addition, compensatory mechanisms aimed at maintaining intracranial balance were analyzed. This made it possible to more accurately evaluate the adaptive capacity of the central nervous system under pathological conditions. The study included both retrospective and prospective data, allowing for a more comprehensive characterization of the dynamics of patients' clinical conditions. A comparative analysis of the effectiveness of various diagnostic methods, including neuroimaging and invasive intracranial pressure monitoring, was also conducted. The use of a comprehensive approach provided a deeper understanding of the course of diseases associated with elevated intracranial pressure [3]. Special attention was given to the time intervals between symptom onset and initiation of treatment. This made it possible to identify critical periods during which therapeutic intervention is most effective. The study was based on contemporary scientific publications, clinical guidelines, and analytical reviews devoted to intracranial hypertension. The analysis included an evaluation of clinical data, diagnostic methods, and treatment outcomes in patients with various neurosurgical conditions. International standards for the management of patients with elevated intracranial pressure were also taken into account. This allowed for comparison of the obtained results with global data and increased the reliability of the study. To illustrate clinical features, representative clinical cases were analyzed. In one case, a 29-year-old male patient initially presented with a relatively stable condition after a road traffic accident; however, several hours later, deterioration occurred in the form of drowsiness and vomiting. Computed tomography revealed an epidural hematoma accompanied by increased intracranial pressure, which required urgent surgical intervention. This case demonstrates the importance of continuous monitoring even when the patient appears stable. It also highlights the necessity of early use of instrumental diagnostic methods. In another clinical case, a 42-year-old

female patient experienced a gradual onset of headache and visual impairment. Examination revealed a tumor of the posterior cranial fossa causing obstruction of cerebrospinal fluid pathways and the development of hydrocephalus. Increased intracranial pressure led to compression of vital brain structures, necessitating drainage and subsequent surgical treatment. This case illustrates the slow but progressive nature of the disease. It also emphasizes the importance of timely diagnosis of intracranial space-occupying lesions. A case of a patient with intracerebral hemorrhage accompanied by progressive cerebral edema and increasing intracranial pressure was also analyzed. Such conditions are associated with a high risk of unfavorable outcomes and require continuous monitoring and intensive care [4]. In this case, timely correction of vital functions was of particular importance. This contributed to stabilization of the patient's condition and reduction of mortality risk.

Results and Discussion. The conducted analysis demonstrated that intracranial hypertension is a universal pathogenetic mechanism characteristic of most acute and chronic neurosurgical diseases. A direct correlation was established between the degree of intracranial pressure elevation, the severity of neurological deficits, and the risk of life-threatening complications. The results indicate that early diagnosis and timely initiation of therapy significantly reduce the likelihood of an unfavorable outcome. In addition, it was noted that the rate of intracranial pressure increase is no less important than its absolute values. This is particularly relevant in acute conditions such as traumatic brain injury and intracerebral hemorrhage. It was observed that even moderate but prolonged elevation of intracranial pressure can lead to irreversible structural changes in brain tissue. It was also found that combined treatment approaches are more effective than isolated therapeutic methods. The obtained data emphasize the need for an individualized approach to patient management, taking into account the clinical presentation and disease dynamics. A significant role in disease progression is played by a reduced compensatory capacity of the organism. This may substantially limit the effectiveness of standard therapeutic strategies. Clinical data analysis confirmed that comprehensive therapy significantly improves the prognosis of patients with intracranial hypertension. One of the key treatment approaches is pharmacological therapy aimed at reducing cerebral edema and decreasing intracranial volume. The use of osmotic diuretics and hypertonic solutions effectively reduces intracranial pressure and prevents secondary brain tissue damage [5]. Early initiation of therapy before the development of significant brain herniation is also crucial. This can markedly reduce the risk of irreversible neurological deficits. An important component of treatment is the control of vital functions. Maintaining adequate oxygenation and stable blood pressure plays a key role in preventing secondary brain injury. Hypoxia and respiratory disturbances significantly worsen the course of the disease, requiring continuous patient monitoring. In addition, correction of metabolic disorders, including acid–base balance, is essential. This contributes to the stabilization of neuronal activity and improvement of the patient's overall condition. In cases where conservative therapy is ineffective, surgical treatment is applied. Removal of intracranial hematomas, tumors, or performing decompressive craniectomy allows effective reduction of intracranial pressure and restoration of normal brain function [6]. The choice of surgical strategy depends on the etiology and severity of the pathological process. In some cases, early surgical intervention is the only way to prevent a fatal outcome. Continuous intracranial pressure monitoring is of particular importance, as it allows real-time assessment of the patient's condition and timely adjustment of therapy. Comprehensive patient care also plays a crucial role, including optimal body positioning, temperature control, and prevention of complications. Despite advances in modern medicine, the

treatment of patients with elevated intracranial pressure remains a complex clinical challenge requiring a multidisciplinary approach. Coordination between neurosurgeons, intensivists, and neurologists is also essential. This helps improve treatment effectiveness and overall clinical outcomes.

Prospects in Uzbekistan. In recent years, Uzbekistan has demonstrated active development in neurosurgery and intensive care medicine. Improvements in the material and technical base of medical institutions and the introduction of modern technologies are creating conditions for enhancing the quality of diagnosis and treatment of patients with elevated intracranial pressure. A promising direction is the implementation of modern intracranial pressure (ICP) monitoring systems, which allow more accurate assessment of patient conditions and timely response to changes. The development of specialized neuro-intensive care units and the continuous training and qualification improvement of medical personnel are also of great importance. In addition, the development of telemedicine technologies for consulting complex cases in regional healthcare facilities is highly significant. This will reduce the time to specialized care and increase the accessibility of neurosurgical services. Recent studies show that the introduction of non-invasive intracranial pressure assessment methods and the use of artificial intelligence technologies can significantly improve diagnostic efficiency and reduce the risk of complications [7]. In the context of Uzbekistan, the development of these technologies is particularly important, as it will make high-tech medical care more accessible. The integration of these technologies into primary healthcare systems is also an important direction. This will ensure early identification of patients at risk of intracranial hypertension. Looking forward, we believe the next big steps for medicine in Uzbekistan should be:

• Using Smart Technology: We want to start using computer programs that can look at a patient's vital signs and warn doctors that a pressure crisis is coming before it actually happens. This gives the medical team a head start to save the patient.

• Bringing Better Care to Every Region: It is vital that specialized "Brain Care Units" are set up not just in Tashkent, but in every province. Every person in Uzbekistan, no matter where they live, should have access to the same high-tech monitoring if they have a head injury.

• Helping Doctors Connect: By using video calls and digital data sharing, a doctor in a small village could send a patient's brain scans and pressure readings to the top experts in the capital for an instant second opinion. This "telemedicine" will save lives by making expert knowledge available everywhere.

• Better Training for the Whole Team: Saving a patient with high brain pressure requires a whole team — surgeons, nurses, and specialists — all working together. We need to continue building special training programs so that everyone knows exactly what to do in an emergency.

Conclusion. Increased intracranial pressure (ICP) is one of the most critical and life-threatening factors influencing the course and outcome of neurosurgical diseases. It is not merely a number displayed on a monitor, but a reflection of a dangerous pathological process occurring within the rigid confines of the skull. Even a moderate and sustained rise in ICP can lead to decreased cerebral perfusion, brain tissue ischemia, and, ultimately, irreversible neurological damage or death. Therefore, understanding, detecting, and managing this condition is a cornerstone of modern neurology and neurosurgery. The causes of increased ICP are diverse and include traumatic brain injury, intracranial hemorrhages, brain tumors, infections such as meningitis and encephalitis, hydrocephalus, and metabolic disturbances. Regardless of the cause, the underlying mechanism is often associated with an imbalance between the volume of brain

tissue, cerebrospinal fluid, and blood within the cranial cavity, as described by the Monro–Kellie doctrine. When compensatory mechanisms are exhausted, intracranial pressure rises rapidly, requiring urgent medical intervention. Clinically, elevated ICP may present with symptoms such as severe headache, vomiting, altered consciousness, visual disturbances, and in advanced stages, signs of brain herniation. However, relying solely on clinical symptoms is insufficient, as deterioration can occur rapidly. This highlights the importance of timely diagnosis and continuous monitoring using modern methods, including intracranial pressure sensors, neuroimaging techniques such as CT and MRI, and advanced neuromonitoring systems. Effective management of increased ICP requires a comprehensive and multidisciplinary approach. Treatment strategies may include conservative measures—such as head elevation, controlled ventilation, osmotherapy (e.g., mannitol or hypertonic saline), and sedation—as well as more aggressive interventions like cerebrospinal fluid drainage or decompressive craniectomy. The choice of treatment depends on the underlying cause, severity of the condition, and individual patient characteristics. A key principle that has emerged in recent years is the shift toward personalized medicine. It is now widely recognized that a “one-size-fits-all” approach is ineffective in managing complex neurological conditions. Instead, treatment must be tailored to each patient, taking into account their age, comorbidities, physiological parameters, and response to therapy. Continuous monitoring allows clinicians to make dynamic, data-driven decisions, moving from a reactive model of care to a proactive one, where complications can be anticipated and prevented before irreversible damage occurs. Despite significant advances in medical science and technology, the problem of increased intracranial pressure remains highly relevant, particularly in countries with limited healthcare resources. In such settings, challenges include insufficient access to modern diagnostic tools, limited availability of specialized equipment, and a shortage of highly trained professionals. For Uzbekistan, addressing these challenges requires a strategic and sustained effort. Key priorities include investment in modern medical infrastructure, equipping hospitals with advanced neuromonitoring technologies, expanding access to high-quality neuroimaging, and improving emergency and intensive care services. Equally important is the continuous education and training of healthcare professionals, including neurosurgeons, neurologists, and intensive care specialists, to ensure the effective application of modern treatment protocols. In addition, fostering research, international collaboration, and the adoption of evidence-based clinical guidelines can further enhance the quality of care. Public health initiatives aimed at preventing traumatic brain injuries and improving early recognition of neurological symptoms can also play a significant role in reducing the overall burden of disease. By integrating clinical expertise with innovative technologies and embracing a personalized approach to patient care, it is possible to significantly reduce mortality and long-term disability associated with increased intracranial pressure. Ultimately, the goal of the healthcare system is not only to save lives but also to preserve neurological function and ensure that patients can return to a full, active and healthy life

REFERENCES

1. StatPearls. Intracranial Hypertension, 2024.
2. Raboel P. et al. Management of Intracranial Pressure. PubMed.
3. Brain Trauma Foundation Guidelines for Severe Traumatic Brain Injury.
4. Duan S. et al. Intracranial Pressure Monitoring in Intracerebral Hemorrhage. World Neurosurgery, 2024.
5. Journal of Neurology and Psychiatry named after S.S. Korsakov, 2024.

6. Clinical Neurosurgery Reviews, 2023.

MORPHOMETRIC CHANGES IN PULMONARY VESSELS DURING TOXIC HEPATITIS: AN EXPERIMENTAL STUDY

I.D. Gulmanov[1], M.A. Seifuldinova[2]
PhD, Associate Professor of the Department of Human and Clinical Anatomy, Tashkent State Medical University, Uzbekistan, Tashkent, 2 Farabi St.[1]
Assistant Professor, Department of General Surgery and Topographic Anatomy, Kazakh National Medical University named after S.D. Asfendiyarov
Almaty, 050028, Kazakhstan[2]
https://doi.org/10.5281/zenodo.20080129

Abstract. *Background/Aim. Toxic hepatitis is associated with systemic disturbances that may affect the pulmonary vasculature. The aim of this study was to investigate morphometric changes in lung vessels under experimental toxic hepatitis.*

Materials and Methods. The study was conducted on 40 laboratory Wistar rats divided into control and experimental groups. Toxic hepatitis was induced by administration of a hepatotoxic agent (carbon tetrachloride). Histological examination of lung tissue was performed followed by morphometric analysis of vascular parameters, including vessel diameter, wall thickness, and lumen area using ImageJ software.

Results. The experimental group demonstrated a significant decrease in vessel diameter, an increase in vascular wall thickness, and a reduction in lumen area ($p < 0.05$). These findings indicate pronounced vascular remodeling and impaired pulmonary microcirculation as a result of liver injury.

Conclusion. Toxic hepatitis induces significant morphometric alterations in pulmonary vessels, reflecting the systemic nature of the pathological process and highlighting the importance of a comprehensive approach to investigating respiratory complications in liver diseases.

Keywords: *toxic hepatitis; pulmonary vessels; morphometry; vascular remodeling; microcirculation; experimental study; rats; endothelial dysfunction; pulmonary hemodynamics.*

INTRODUCTION

Liver pathology exerts a systemic impact on various organs and functional systems of the body, including the lungs. It is established that toxic liver injury leads to a complex of metabolic, hemodynamic, and inflammatory disturbances affecting not only the hepatobiliary system but also the respiratory organs. Due to their extensive vascular network and high sensitivity to changes in systemic circulation, the lungs are among the primary targets in hepatic pathology.

Toxic hepatitis is accompanied by severe impairment of intrahepatic and systemic hemodynamics, leading to altered blood rheology, hypoxia, and endothelial dysfunction. Under these conditions, remodeling of the vascular bed occurs, particularly at the level of pulmonary microcirculation. Microcirculatory disturbances are characterized by vascular vasospasm, wall thickening, reduced lumen area, and altered ratios between vascular components, which may ultimately contribute to the development of pulmonary hypertension and impaired gas exchange.

Inflammatory mediators, oxidative stress, and hypoxic processes arising from toxic liver damage play a pivotal role in vascular alterations. These factors cause endothelial damage, activate fibrotic processes, and lead to the structural rearrangement of the vascular wall. Consequently, a pathological cycle is formed, intensifying systemic disturbances and exacerbating the course of the disease.

Despite the existence of individual studies focusing on the influence of hepatic pathology on the respiratory system, the morphometric characteristics of the pulmonary vasculature during toxic hepatitis remain insufficiently explored. Specifically, there is a lack of quantitative data regarding changes in vessel diameter, wall thickness, and lumen area, which complicates an objective assessment of the degree of vascular transformation.

Therefore, experimental research aimed at a detailed study of morphometric changes in pulmonary vessels during toxic hepatitis is of significant scientific and practical interest. The data obtained will deepen the understanding of the pathogenesis of systemic disturbances in liver diseases and serve as a basis for developing new approaches to the diagnosis and prevention of respiratory complications.

LITERATURE REVIEW

In recent years, the study of the pulmonary vasculature has gained particular relevance due to increasing interest in the systemic mechanisms of vascular remodeling under various pathological conditions. Pulmonary vessels are highly sensitive to hypoxia, inflammation, endothelial dysfunction, and metabolic disorders, making them critical subjects for morphological and morphometric research.

Contemporary studies indicate that pulmonary vascular remodeling involves complex structural and molecular changes. For instance, it has been shown that exosomes derived from induced pluripotent stem cells can attenuate vascular remodeling in pulmonary arterial hypertension by targeting the HIF-1alpha and Runx2 signaling pathways [1]. This emphasizes the crucial role of cellular and molecular mechanisms in the pathogenesis of vascular disorders.

The methodological foundations for studying the pulmonary vasculature are detailed in fundamental research describing modern approaches to the morphological and morphometric assessment of the vascular wall and lumen, including quantitative methods for analyzing the microcirculatory bed [2].

Significant interest lies in works where vascular changes are viewed as manifestations of systemic pathology. In experimental models of systemic sclerosis, pronounced structural and functional disturbances of the pulmonary hemomicrocirculatory bed were identified, confirming the systemic nature of vascular rearrangement [3].

Advancements in imaging techniques have significantly expanded the understanding of pulmonary vascular morphology. Contrast-free angiography *in vivo* has demonstrated reduced vascular density and signs of remodeling under chronic hypoxia [4]. Three-dimensional (3D) imaging has further revealed complex spatial restructuring of the microvascular network in pulmonary hypertension [5].

Studies on metabolic factors also demonstrate their influence on the morphofunctional state of the lungs. Specifically, lipid metabolism disorders can lead to changes in the histophysiology of lung tissue and reduced blood oxygen transport function [5].

A special place is occupied by works on the "liver-lung" axis. It has been shown that portal hypertension and chronic liver diseases lead to systemic hemodynamic disturbances affecting the

pulmonary vascular system [7]. Hepatopulmonary syndromes are accompanied by impaired gas exchange and vascular regulation, including vasodilation and altered vascular tone [9].

For modern morphology, 3D reconstruction and stereology methods are of great importance, allowing for an objective assessment of the spatial organization of the pulmonary vascular network [8]. Similar results have been achieved using micro-computed tomography (MCT), enabling visualization and quantitative evaluation of the pulmonary arterial microvascular tree [10].

Alongside modern technologies, intravital microscopy continues to play a vital role, allowing for the real-time study of pulmonary microcirculation and the functional state of vessels under various pathological influences [18]. Experimental studies confirm that during chronic pulmonary ischemia, the vasculature undergoes pronounced morphological and functional transformation [19].

Interestingly, similar vascular remodeling processes are observed in other organs. For example, significant restructuring of the microvascular bed has been identified in liver fibrosis, confirming the systemic nature of angioarchitectonic changes [20]. These findings suggest that toxic liver injury may also impact the pulmonary vascular system.

Fundamental concepts of vascular morphology were established in classical studies showing that pathological processes lead to profound vascular wall rearrangement, changes in vessel caliber, and disruption of normal organization [21]. These principles are universal and applicable to pulmonary vessels under various pathological states.

In recent years, significant attention has been paid to cellular components of the vascular wall, particularly pericytes. They play a key role in regulating microcirculation and vascular stability, and their dysfunction contributes to vascular remodeling [22]. Experimental studies on models of chronic obstructive pulmonary disease (COPD) confirm that vascular remodeling is associated with the activation of molecular signaling pathways, such as VEGF/PI3K/Akt, and can be viewed as a potential therapeutic target [23].

A separate research direction includes works on morphofunctional changes in vessels under systemic influences. Specifically, significant alterations in the vascular bed, including wall restructuring and hemodynamic changes, have been shown following splenectomy [11, 13]. Similarly, morphological changes in the thymus have been identified during toxic liver injury, indicating the systemic nature of the pathological process [15, 17].

Thus, the analysis of modern literature shows that the pulmonary vasculature is a dynamic system actively responding to hypoxia, inflammation, metabolic disorders, and systemic diseases. Despite the significant number of studies on vascular remodeling in pulmonary hypertension and chronic lung diseases, morphometric assessment of pulmonary vessels in toxic liver injury remains insufficiently studied.

MATERIALS AND METHODS

The experimental study was conducted on 40 mature male Wistar laboratory rats weighing 180–220 g. The animals were housed under standard vivarium conditions (temperature 22–24 °C, relative humidity 50–60%, natural light cycle) with *ad libitum* access to water and standard chow.

Before the experiment, animals underwent a 7-day adaptation period. Subsequently, they were divided into two equal groups: the control group (n = 20), receiving standard nutrition and saline, and the experimental group (n = 20), in which toxic hepatitis was modeled.

Toxic hepatitis was induced by intraperitoneal administration of a hepatotoxic agent (carbon tetrachloride, CCl_4) at a dose of 1.0 ml/kg body weight mixed with vegetable oil (1:1), twice a week for 4 weeks. Control animals received an equivalent volume of saline.

At the end of the experiment, animals were euthanized via anesthetic overdose in compliance with bioethical standards. Lungs were extracted, fixed in 10% neutral buffered formalin for 24–48 hours, and subjected to standard histological processing.

Paraffin sections (5–7 μm) were stained with hematoxylin and eosin (H&E). Morphometric analysis was performed using a light microscope and a digital image processing system (Image J).

The study evaluated the diameter of arterioles and venules (external and internal), vascular wall thickness, lumen area, and the wall thickness-to-vessel diameter ratio. Measurements were taken in at least 10 fields of view for each slide, followed by the calculation of mean values.

Statistical analysis was conducted using IBM SPSS Statistics (version 26.0). Results are presented as mean and standard deviation (M±SD). Student's t-test was used to assess the significance of differences between groups. Differences were considered statistically significant at $p < 0.05$.

The study complied with international bioethical requirements and the principles of the Declaration of Helsinki. The experimental protocol was approved by the Local Ethics Committee (Protocol No: 07/2026).

RESULTS

The experimental study revealed pronounced morphometric changes in the pulmonary vasculature of animals with modeled toxic hepatitis compared to the control group.

Analysis of vessel diameter showed significant differences between the groups. Experimental animals exhibited a noticeable decrease in the diameter of both arterioles and venules, indicating vascular spasm and microcirculatory impairment.

Table 1. Diameter of Pulmonary Vessels (μm)

Group	**Arterioles (μm)**	**Venules (μm)**
Control	48.2±2.1	62.5±3.4
Experiment	39.6±2.3*	55.1±2.9*

Note: Values are presented as M±SD— differences are statistically significant compared to the control group ($p < 0.05$).*

As shown in Table 1, the diameter of arterioles decreased from 48.2 ± 2.1 μm to 39.6 ± 2.3 μm, while the diameter of venules decreased from 62.5 ± 3.4 μm to 55.1 ± 2.9 μm ($p < 0.05$). These data indicate the formation of vasoconstrictive changes, likely associated with endothelial dysfunction and hypoxic processes in the lung tissue.

Further analysis demonstrated that the changes in vessel diameter were accompanied by significant wall thickening, a key sign of vascular remodeling.

Table 2. Vascular Wall Thickness (μm)

Group	**Arterioles**	**Venules**
Control	8.4 ± 0.6	6.2 ± 0.5
Experiment	12.7 ± 0.8*	9.5 ± 0.7*

Note: Data are presented as M ± SD — statistically significant differences compared to the control group ($p < 0.05$).*

As presented in Table 2, a significant increase in the vascular wall thickness of both arterioles and venules was observed in the experimental group ($p < 0.05$). Arteriolar wall

thickening from 8.4 ± 0.6 μm to 12.7 ± 0.8 μm and venular thickening from 6.2 ± 0.5 μm to 9.5 ± 0.7 μm indicates the development of hypertrophic and fibrotic processes driven by the chronic damaging effect of the toxic agent.

The next stage of analysis involved the study of the vessel lumen area, which reflects the integral state of the vasculature and the degree of blood flow obstruction.

Table 3. Vessel Lumen Area (%)

Group	**Arterioles**	**Venules**
Control	100%	100%
Experiment	68.3%*	74.5%*

*Note: Indicators are expressed as a percentage relative to the control group (100%); * —* differences are statistically significant compared to the control ($p < 0.05$).*

According to Table 3, a significant reduction in the vessel lumen area was noted in the experimental group. The arteriolar lumen area decreased to 68.3%, and the venular area to 74.5% of control values ($p < 0.05$). These changes result from the combined effect of vascular narrowing and wall thickening.

Collectively, these results indicate the development of pronounced pulmonary vascular remodeling during toxic hepatitis. The reduction in vessel diameter, wall thickening, and decreased lumen area lead to increased vascular resistance, impaired microcirculation, and the formation of hypoxic states in the lung tissue.

DISCUSSION

The data obtained in this study indicate that toxic hepatitis exerts a profound systemic influence on the pulmonary vasculature, causing morphometric changes characteristic of vascular remodeling. These findings align with modern concepts viewing pulmonary vessels as a highly sensitive system responding to hypoxia, inflammation, and metabolic disturbances [1, 3].

The identified reduction in vessel diameter indicates the development of vasoconstrictive reactions and increased vascular tone. The narrowing of arterioles, which play a key role in regulating pulmonary blood flow, can lead to increased peripheral vascular resistance and impaired lung tissue perfusion. Similar mechanisms of vascular transformation have been described in pulmonary hypertension, where molecular signaling pathways, including HIF-1alpha-dependent processes, play a leading role [1, 23].

Equally significant is the identified thickening of the vascular wall, reflecting structural restructuring processes. These changes may be driven by smooth muscle cell hypertrophy, fibroblast activation, and increased synthesis of extracellular matrix components. Literature shows that vascular remodeling is accompanied by cellular proliferation and disruption of intercellular interactions, confirmed by 3D imaging of the vascular network [5, 8]. Inflammatory mediators and oxidative stress arising from toxic liver damage play a crucial role in these processes [6].

The reduction in lumen area in the experimental group is an integral indicator reflecting the combined impact of vasoconstriction and wall thickening. This confirms the presence of pronounced microcirculatory disturbances and indicates reduced blood supply efficiency to the lung tissue. Similar microcirculatory changes are described in chronic hypoxia and systemic diseases associated with vascular dysfunction [5, 10].

Notably, the most pronounced changes are observed in the arterial segment of the microcirculatory bed. This is consistent with literature emphasizing the primary role of arterioles in the formation of hemodynamic disturbances and the development of pulmonary hypertension [3, 19]. While the venous segment is also involved, the degree of its changes is less pronounced,

possibly due to the functional characteristics of the venous system and its lower reactivity to vasoconstrictive influences.

The results correlate with studies indicating a close relationship between liver pathology and the pulmonary vascular system. Chronic liver diseases are known to cause systemic hemodynamic shifts, including endothelial dysfunction, impaired vascular tone, and microcirculatory changes that can extend to the lungs [7, 9]. Furthermore, data on vascular restructuring in the liver during fibrosis confirm the systemic nature of angioarchitectonic changes [20].

Cellular elements of the vascular wall, specifically pericytes, play a significant role in regulating microcirculation and maintaining vascular stability. Their dysfunction may contribute to the progression of vascular remodeling and blood flow obstruction [22], supporting the view of vascular alterations as a multi-level process.

Attention should also be paid to data on systemic vascular changes after splenectomy, where pronounced wall restructuring and hemodynamic impairment are also noted [11, 13]. These results confirm that vascular alterations are systemic and can develop under various pathological conditions, including toxic liver injury.

Thus, the identified morphometric changes in pulmonary vessels during toxic hepatitis reflect a systemic pathological process involving vasoconstriction, wall thickening, and reduced lumen area. These alterations lead to microcirculatory failure, worsened lung tissue perfusion, and reduced gas exchange efficiency.

CONCLUSION

In conclusion, the results of this experimental study demonstrate that toxic hepatitis is accompanied by significant morphometric changes in the pulmonary vasculature. Specifically, animals in the experimental group exhibit reduced vessel diameter, vascular wall thickening, and a substantial reduction in lumen area.

These findings indicate the development of vascular remodeling and impaired pulmonary microcirculation, highlighting the systemic nature of the pathological process. The data confirm that liver injury affects not only the hepatobiliary system but also the pulmonary vascular network. Therefore, studying such changes is essential for a deeper understanding of the disease pathogenesis and for justifying a comprehensive approach to the diagnosis and prevention of its complications.

REFERENCES

1. Chi P.L., et al. Induced pluripotent stem cell–derived exosomes attenuate vascular remodelling in pulmonary arterial hypertension by targeting HIF-1α and Runx2. *Cardiovasc Res*. 2024;120(2):203–214.
2. Davies P., deMello D., Reid L.M. Methods in experimental pathology of pulmonary vasculature. In: *Models of Lung Disease*. CRC Press; 2020:843–904.
3. Doskaliuk B., Zaiats L. Structural and functional characteristics of the pulmonary hemomicrocirculatory bed in induced systemic sclerosis: an experimental study. *Rheumatol Int*. 2023;43(7):1341–1347.
4. Farha S., et al. Quantification of the pulmonary vasculature in mice under chronic hypoxia with contrast-free pulmonary angiography in vivo imaging. *J Appl Physiol*. 2025;138(1):318–325.

5. Ichimura K., et al. 3D imaging reveals complex microvascular remodeling in the right ventricle in pulmonary hypertension. *Circ Res*. 2024;135(1):60–75.
6. Israilova A.T., et al. Histophysiology of the lungs and oxygen transport function of the blood with an exclusively fatty diet. *Heart Vessels Transplant*. 2024;9(1).
7. Juneja P., et al. The interplay between lymphatic system and portal hypertension: a comprehensive review. *Hepatol Int*. 2025;19(4):720–731.
8. Mühlfeld C., et al. Recent developments in 3-D reconstruction and stereology to study the pulmonary vasculature. *Am J Physiol Lung Cell Mol Physiol*. 2018;315(2):L173–L183.
9. Rodríguez-Roisin R., Krowka M.J., Agustí A. Hepatopulmonary disorders: gas exchange and vascular manifestations in chronic liver disease. *Compr Physiol*. 2018;8(2):711–729.
10. Schneider B., et al. Microcomputed tomography visualization and quantitation of the pulmonary arterial microvascular tree in mouse models of chronic lung disease. *Pulm Circ*. 2023;13(3):e12279.
11. Shermanov A.O. Morphofunctional changes of blood vessels after splenectomy. *Educational Research in Universal Sciences*. 2025;4(17).
12. DOI: https://doi.org/10.5281/zenodo.18064066
13. Shermanov A.O. Morphofunctional changes of small intestine vessels after splenectomy. *Educational Research in Universal Sciences*. 2025;4(17).
14. DOI: https://doi.org/10.5281/zenodo.18064090
15. Shermanov A.O. Morphological and morphometric features of the thymus in chronic heliotrine hepatitis. In: *Proceedings of the International Scientific and Practical Conference "Medical Tourism in the 21st Century: Sustainable Models and Cutting-Edge Practices"*. 2025.
16. DOI: https://doi.org/10.5281/zenodo.17610689
17. Mukhamedzhanov A.Kh. Morphological and morphometric features of the thymus after splenectomy in healthy animals. *World Bulletin of Public Health (WBPH)*. 2025;53.
18. Tabuchi A., et al. Intravital microscopy of the murine pulmonary microcirculation. *J Appl Physiol*. 2008;104(2):338–346.
19. Wagner E.M., et al. Lung and vascular function during chronic severe pulmonary ischemia. *J Appl Physiol*. 2011;110(2):538–544.
20. Wagner W.L., et al. 3D analysis of microvasculature in murine liver fibrosis models using synchrotron radiation-based microtomography. *Angiogenesis*. 2021;24(1):57–65.
21. Warren B.A. The vascular morphology of tumors. In: *Tumor Blood Circulation*. CRC Press; 2020:1–47.
22. Yuan K., et al. Lung pericytes in pulmonary vascular physiology and pathophysiology. *Compr Physiol*. 2021;11(3):2227–2247.
23. Zhang L., et al. Electroacupuncture attenuates pulmonary vascular remodeling in a rat model of chronic obstructive pulmonary disease via the VEGF/PI3K/Akt pathway. *Acupunct Med*. 2022;40(4):389–400.

MEDICAL, PREVENTIVE, AND SOCIAL ACTIVITY OF THE POPULATION IN SMALL CITIES AND THEORETICAL-ORGANIZATIONAL ISSUES OF ITS ENHANCEMENT

A.S. Madaxanov[1], A.A. Ataboyev[2]
Andijan State Medical Institute, Andijan, Uzbekistan[1,2]
https://doi.org/10.5281/zenodo.20080564

Abstract. *The article focuses on the role of public health as a key factor in the development of small cities, which are currently undergoing rapid formation in the Republic of Uzbekistan. In this context, the issues of enhancing the medical, preventive, and social activity of the population in small cities on a scientific basis are emphasized as one of the most pressing challenges of the present time. The paper presents reflections on the theoretical and organizational aspects of a comprehensive, in-depth, and dynamic study and evaluation of the underlying factors of this phenomenon. The authors also provide the results of data analysis related to the medical, preventive, and social activity of the population in small cities and offer scientifically grounded considerations and recommendations for its improvement.*

Keywords: *small cities, medical activity, preventive activity, social activity, system approach, system analysis.*

Introduction. An examination of the historical development of major cities across all continents of the world shows that they were originally formed as small urban settlements at earlier stages and over different periods of time. Therefore, it is reasonable to consider existing small and medium-sized cities not only as the most widespread form of settlement but also as an essential foundation for their gradual transformation into large cities through successive stages of development. At the same time, attention is drawn to the fact that in some countries, such as Russia, approximately 130 small cities are reported not only to have stagnated in their development but also to be gradually disappearing [18]. Among the main reasons for the decline of small cities are the cessation of activities of enterprises that play a key role in their formation, the deterioration of housing and communal services, the obsolescence of infrastructure, the lack of modern transport, communication, and medical services, the mass outmigration of youth, and the natural aging of the local population [19].

Purpose of the research. The objective of this study is to develop scientifically grounded recommendations aimed at improving the living conditions and lifestyle of the population residing in small cities of the Republic of Uzbekistan, based on the study and analysis of relevant indicators.

Research methodology. The study was conducted on the basis of the principles of a systems approach and systems analysis. In this context, it was considered appropriate to carry out the research in small towns located in the regions of Namangan, Andijan, and Fergana, which are situated in the Fergana Valley and are characterized by average indicators of the main demographic, socio-economic, and natural-climatic conditions typical for small cities in the republic. Based on this approach, to ensure the representativeness of the study, the sample size consisted of 394 respondents, with a margin of error not exceeding 5%. Data on the medical, preventive, and social activity of the population, as well as the opinions and views of family members regarding the improvement of these indicators, were collected through specially designed

sociological questionnaires administered among residents aged 15 and above from families living in small towns. The survey was conducted between February and April 2025. The data collection process was organized by one of the authors of the study, with active participation from students of Andijan State Medical Institute who are originally from the small towns of Namangan, Andijan, and Fergana regions. In the analysis of the obtained data, the value of the representative error (m) was determined. The reliability of differences observed between indicators characterizing the medical, preventive, and social activity of individuals of different age groups, genders, and social statuses was assessed by calculating the value of the Student's t-statistic (t).

Analysis of data presented in various information sources related to the research topic. In studying, observing, analyzing, and drawing relevant conclusions about the political and socio-economic processes occurring in cities worldwide, as well as in developing appropriate recommendations, a unified approach is ensured through the use of classifications of cities based on population size. In this context, classification refers to one of the fundamental scientific approaches widely applied in the fields of Urban Studies and Demography. Although criteria may vary slightly across different organizations, the generally accepted classification is as follows:

1. Small cities – with a population ranging from 10,000 to 100,000 inhabitants. These cities are characterized by relatively simple infrastructure and a predominantly local economy.
2. Medium-sized cities – with a population ranging from 100,000 to 1 million inhabitants. These cities are distinguished by the development of industrial and service infrastructures.
3. Large cities – with a population between 1 million and 5 million. These cities are characterized by well-developed economic systems and transport hubs.
4. Very large cities (metropolises) – with a population ranging from 5 million to 10 million. These cities are characterized by extensive urban territories and, most importantly, high population density.
5. Megacities – with a population exceeding 10 million, distinguished by characteristics typical of global urban centers.
6. Gigacities (according to some sources) – with a population of 20–30 million or more, although such cities are relatively rare. An example is Tokyo.

In other sources, cities are also classified according to population size as follows: small (up to 50,000), medium (50,000–100,000), and large (over 100,000) [9].

It should be emphasized that contemporary urbanization is largely concentrated in megacities. Large cities and megacities are characterized by the highest rates of socio-economic growth. It is well known that the concept of the "largest city" varies depending on whether it refers to an administrative unit, a city proper, or an urban agglomeration. Typically, when referring to the largest cities in the world, population size is considered in terms of urban agglomerations or metropolitan areas. At present (approximately 2024–2025), the largest cities in the world by population include Tokyo (~37 million), Delhi (~33 million), Shanghai (~29 million), Dhaka (~23 million), São Paulo (~22 million), Mexico City (~22 million), Cairo (~21 million), and others. It is noteworthy that the majority of the world's largest cities are located in Asia, and rapidly growing urban populations are predominantly found in developing countries [13,22,23,26,27]. Currently, various "associations of small cities" (i.e., associations of small and medium-sized cities) operate worldwide. These are organizations established in different countries to strengthen local governance, economic development, and territorial cooperation. It should be noted that this concept does not refer to a single global organization but rather to multiple scientific and practical platforms.

An association of small cities can be defined as a voluntary union of cities with relatively small populations (typically ranging from 10,000 to 500,000 inhabitants), which operate to exchange experience, develop policies, and support economic development. Within such associations, the activities of several key international organizations are particularly recognized [14,15,16,17].

1. United Cities and Local Governments (UCLG) – one of the largest global networks of cities, which also represents the interests of small and medium-sized cities. Its activities focus on local governance, urbanization, and sustainable development.
2. Council of European Municipalities and Regions (CEMR) – an association of municipalities and small cities in Europe. Its activities are aimed at promoting political cooperation and territorial development.
3. ICLEI – Local Governments for Sustainability – an organization working in the field of environmental protection and sustainable development, developing "green policies" for small cities.

Associations of small cities operate in the following key areas: exchange of best practices; development of urban development strategies; attraction of investments and grants; implementation of Sustainable Development Goals (SDGs); and strengthening of local governance. Within the activities of such associations, several scientific directions also occupy an important place, including Urban Studies, Regional Development, research by the World Bank on the economies of small cities, and the United Nations' Sustainable Development Goals (SDGs). Small cities constitute an essential component of the global urban system. Their cooperation facilitates more efficient resource management and enhances competitiveness. In contemporary research, small cities are increasingly regarded as "key drivers of sustainable development." According to scientific literature in the fields of Urban Studies and Demography, cities with a population ranging from 10,000 to 100,000 are generally classified as small cities. In Uzbekistan, there are approximately 120 cities in total, of which around 80–90 are small cities undergoing rapid development [2,8,24,25]. According to the opinions of researchers studying urban development issues in Uzbekistan, the development of small and medium-sized cities is of significant importance. This issue is determined by factors such as migration patterns, demographic growth rates, land and water resources, and the need for industrialization. In order to enhance the effectiveness of ongoing efforts and ensure the productivity of future initiatives, it is considered appropriate to conduct monitoring-based sociological studies in this field [7,20,21,22,27]. The authors emphasize that a healthy lifestyle can be regarded as a guarantee of a healthy future [6]. In this context, when planning measures aimed at promoting healthy lifestyles among rural populations, it is important to study and take into account their specific characteristics, particularly in increasing medical awareness. Such data serve as a scientific basis for organizing cooperation between families, local communities (mahallas), healthcare workers, and state institutions in addressing healthcare-related issues [12]. Increasing the medical activity of the population should be considered an important factor, especially in ensuring child health [10]. According to the results of certain studies, medical activity often manifests specific characteristics, particularly when individuals fall ill. For instance, elderly individuals often underestimate their health condition, while many people attempt self-treatment or expect illnesses to resolve on their own. This tendency is more common among men. According to the author, the main reasons for this situation are deficiencies in the healthcare system (54.7%) and patients' perceptions and attitudes (45.3%) [1]. In studies devoted to the essence and content of a healthy lifestyle,

researchers identify several conditions for maintaining good health, ensuring active labor activity, achieving longevity, and leading a prosperous and fulfilling life. They also note that failure to adhere to hygiene practices may negatively affect the health of others. In this regard, factors such as smoking, the spread of infectious diseases and helminth infections, and deterioration of indoor air quality are highlighted [11]. Some researchers examining the relationship between a healthy lifestyle and medical activity report that 56.2% of the population expressed readiness to lead a healthy lifestyle, with higher rates observed among adolescents (62.1%) and young people (61.9%). At the same time, the authors suggest that the low level of medical activity among the population may be associated with insufficient knowledge about healthy lifestyles [4]. Studies also indicate that in certain districts, the medical activity of rural populations remains low, partly due to the superficial implementation of preventive measures by healthcare personnel at family physician centers, particularly among healthy individuals [5]. Furthermore, research conducted in certain regions of the Amur region, involving the clustering of municipal structures and sociological surveys among 16,432 respondents, demonstrated that access to medical services significantly influences the level of medical activity of the population [3].

Results and discussion. In our view, from the perspective of public health and healthcare systems, small cities represent a socio-spatial reality composed of populations residing in specific natural and climatic conditions. Each individual possesses not only distinct morpho-functional characteristics but is also influenced, both physically and psychologically, by a complex and dynamically evolving set of political, socio-economic, and environmental factors. The existence and development of this reality in space and time are closely associated with living conditions created for the population and their lifestyle patterns. Indeed, only physically and mentally healthy individuals are capable of formulating and implementing strategies that ensure societal progress. Therefore, the rapid development, stagnation, or even disappearance of small cities is largely determined by the health status of their population, as well as by the governance capacity of both national and local authorities. The study of natural-climatic conditions, socio-economic factors, and the morpho-functional characteristics of individuals residing in the investigated small cities revealed the following. It was observed that seasonal changes (beginning and end of the four seasons) in the studied regions often differ by 4–5 days compared to previous years. In addition, several features related to the socio-economic aspects of the population’s life were identified.

Analysis of morpho-functional characteristics of the population, including age and gender distribution, showed the following structure: children aged 0–1 years constituted 3.5%, 1–14 years – 28.3%, 15–24 years – 19.5%, 25–34 years – 17.9%, 35–44 years – 11.5%, 45–54 years – 8.7%, 55–64 years – 5.1%, 65–74 years – 3.0%, and 75 years and above – 2.5%. Women accounted for 52.3% of the population, while men comprised 47.7%. Among the working-age population, 48.0% were employed in state enterprises, organizations, and farming entities, while the remainder were engaged in private service sectors within the city and surrounding areas, employed on a daily or contractual basis, or working abroad. According to respondents, their occupational activities required different types of physical and psychological engagement: 12.0% reported tasks requiring precision, 28.0% vigilance, 5.0% rapid movement, 22.0% repetitive movements, 18.0% sedentary work, 29.0% standing work, 8.0% working at heights, 13.0% working in dusty environments, 19.0% working in wet or muddy conditions, 5.0% working in unpleasant or polluted environments, 10.0% working in cold conditions (including abroad), 7.0% in extremely cold environments, and 33.0% in hot conditions. Analysis of respondents’ answers revealed specific characteristics in their lifestyle patterns. Only 12.0% of respondents reported engaging in morning physical exercise,

while an even smaller proportion (4.0%) practiced morning running. At the same time, 9.0% reported engaging in morning walking. The study also revealed that only 6.0% of respondents had participated in tourism activities. During interviews, it became evident that the majority of respondents were not sufficiently aware of ongoing initiatives aimed at developing domestic tourism, including the conditions and benefits created for tourists. The study of respondents' attitudes toward their own health demonstrated that only 30.0% undergo medical examinations at least once a year, even in the absence of symptoms. Moreover, nearly all of these cases were associated with mandatory periodic medical check-ups required by their employment. When experiencing initial symptoms of illness, only 32.0% of respondents sought medical assistance at family polyclinics. The reasons for not seeking medical consultation for preventive purposes or at early stages of disease were attributed, in 62.0% of cases, to long waiting times at family polyclinics and insufficient diagnostic and treatment equipment in small towns.

It should be emphasized that among women in small cities, no cases of smoking or alcohol consumption were reported. However, among men, harmful habits were relatively widespread: 33.0% reported smoking and 21.0% reported alcohol consumption. Additionally, the use of local smokeless tobacco (nas) was found to be common among men. Other unhealthy lifestyle factors included overeating (67.0%), eating before sleep (73.0%), consumption of salty foods (32.0%) and spicy foods (24.0%), irregular meal patterns (18.0%), and skipping breakfast (41.0%). While physical inactivity is often reported as a significant issue in large cities, it was found to be relatively lower in small cities, with only 23.0% of respondents indicating sedentary lifestyles. Numerous studies emphasize the importance of sleep in maintaining and strengthening health. However, responses indicated that only 47.0% of respondents adhere to regular sleep schedules, and the duration of sleep is not always sufficient. Among the indicators of medical activity, adherence to physicians' recommendations is of particular importance. It was found that 30.0% of respondents do not fully and timely comply with medical recommendations. The main reasons identified were financial constraints (18.0%), lack of time due to work overload (43.0%), and lack of motivation or discipline (39.0%).

Conclusion and Recommendations. At the current stage of the historical development of human society, it is appropriate to consider existing small and medium-sized cities not only as the most widespread type of settlement, but also as an essential foundation for their gradual transformation into large cities through successive stages of development, as required by the dynamics of modern life. At the same time, the fact that in certain countries small cities are not only experiencing stagnation but are also gradually disappearing necessitates continuous and in-depth study of the underlying causes of this phenomenon. Such analysis should be conducted in a dynamic context, based primarily on the principles of a systems approach and systems analysis, with particular emphasis on forecasting potential consequences. This remains one of the pressing scientific and practical tasks of contemporary research. In the development and implementation of comprehensive measures aimed at the formation of prospective small cities, primary attention should be given to the issues of forming and maintaining the health of the population, as well as ensuring active longevity. The results of the conducted study indicate that, under current conditions, it is advisable to systematically and consistently carry out theoretical and organizational work aimed at studying the medical, preventive, and social activity of the population in small cities. Based on the data obtained, it is necessary to develop innovative proposals and recommendations to enhance the level of these indicators.

REFERENCES

1. Gerasimova, O.Yu., Semchenko, L.N. (2016). Features of the medical activity of citizens during illness. Eurasian Union of Scientists (ESU), No. 2 (23), Medical Sciences.
2. Ergashev, B., Akhmerova, A. The future of urbanization in Uzbekistan in the hands of business. Available at: https://centrasia.org/newsA.php?st=1296639000
3. Polyanskaya, E.V. (2024). Features of the medical activity of the population of the Amur region. DEMIS. Demographic Research, Vol. 4, No. 2.
4. Seydumanov, S.T. (2010). Medical activity of the population in the context of a healthy lifestyle. Scientific Medical Journal "Payomi Sino" (Avicenna Bulletin), Tajik State Medical University, No. 3.
5. Sharipova, S.A., Muyassarova, M.M. (2019). Study of the level of medical activity of the rural population. European Science, No. 2 (44), pp. 79–80.
6. Muradov, N.O. (2021). A healthy lifestyle as a guarantee of a healthy future. Mechanics and Technology Scientific Journal, No. 4 (5).
7. Qurbonaliyeva, H.I. (2024). The importance of developing small and medium-sized cities in Uzbekistan. Oriental Renaissance: Innovative, Educational, Natural and Social Sciences, Vol. 4, No. 21. Available at: www.oriens.uz
8. State Committee of the Republic of Uzbekistan on Statistics. Official demographic and urban statistics database. Available at: https://stat.uz/uz
9. *City*. Available at: https://wikipedia.org
10. Sharipova, F.I., Murodova, S.A., Avezova, G.S. (2023). Medical activity and its impact on child health. Multidisciplinary Scientific Journal, pp. 255–258.
11. Kholmirzayev, J. (2024). Some aspects of developing a healthy lifestyle. Economy and Society, No. 9 (124).
12. Yusupov, M.S. (2023). Features of the formation of a healthy lifestyle and medical culture among rural populations. Journal of Marketing, Business and Management (JMBM), Vol. 3, Issue 12, pp. 29–32.
13. Demographia (2023). World Urban Areas (19th Annual Edition). Belleville.
14. World Bank (2020–2023). Cities and Local Governments: Urban Development Reports. Washington, DC.
15. Global Taskforce of Local and Regional Governments (2021). Annual Report. Barcelona: UCLG.
16. ICLEI (2022). Annual Report: Local Governments for Sustainability. Bonn.
17. Hall, P. (2014). Cities of Tomorrow: An Intellectual History of Urban Planning and Design. Oxford: Blackwell.
18. Forbes Russia. Available at: https://www.forbes.ru
19. Russian Presidential Academy of National Economy and Public Administration (RANEPA), Izvestiya.
20. Oriental Renaissance: Innovative, Educational, Natural and Social Sciences, 2 (Special Issue 23), pp. 1068–1079.
21. Mamatkulov, S. (2024). Some aspects of increasing the social activity of young people in Uzbekistan (Harmony of national and foreign experience). Central Asian Journal of Social Sciences and History, Vol. 5, No. 1, pp. 116–135.
22. Pike, A., Rodríguez-Pose, A., Tomaney, J. (2017). Local and Regional Development. London: Routledge.

IMPACT OF ACUTE RESPIRATORY INFECTIONS ON PREGNANCY OUTCOMES IN THE POST-COVID PERIOD

G.F. Rajapova
Assistant, Tashkent State Medical Unversity
https://doi.org/10.5281/zenodo.20266761

Abstract. *The COVID-19 pandemic has significantly altered the global healthcare landscape and has become one of the most critical public health challenges of the twenty-first century. Pregnant women constitute a particularly vulnerable group due to physiological, immunological, and respiratory changes occurring during gestation. In the post-COVID period, the persistence of inflammatory responses, endothelial dysfunction, immune dysregulation, and thrombotic complications has increased the susceptibility of pregnant women to acute respiratory infections and associated obstetric complications. This article analyzes the relationship between acute respiratory infections and obstetric outcomes in pregnant women during the post-COVID era. Particular attention is given to the pathophysiological mechanisms underlying pregnancy complications, including hypoxia, cytokine-mediated inflammation, placental insufficiency, and coagulation disorders. The study also examines diagnostic approaches, monitoring strategies, preventive measures, and modern therapeutic interventions. International clinical recommendations and current challenges in maternal healthcare are additionally discussed. The findings indicate that post-COVID physiological alterations substantially increase the risk of preeclampsia, preterm birth, fetal hypoxia, and perinatal complications, emphasizing the need for comprehensive prenatal monitoring and multidisciplinary management.*

Keywords: *post-COVID syndrome, pregnancy, acute respiratory infections, obstetric complications, preeclampsia, fetal hypoxia, placental insufficiency, thrombosis, respiratory diseases, maternal health.*

Introduction. The COVID-19 pandemic produced unprecedented medical, social, and economic consequences worldwide. Although the acute phase of the pandemic has gradually declined, its long-term effects continue to influence healthcare systems globally. One of the most concerning consequences is the emergence of post-COVID syndrome, characterized by persistent clinical manifestations and multisystem complications after recovery from acute SARS-CoV-2 infection. These complications are particularly significant in pregnant women, whose physiological condition already involves substantial immunological and cardiopulmonary adaptations. Globally, the COVID-19 epidemic had hitherto unheard-of medical, societal, and economic repercussions. Even while the pandemic's acute phase has gradually subsided, its long-term effects are still having an impact on healthcare systems around the world. The development of post-COVID syndrome, which is marked by multisystem problems and persistent clinical symptoms following recovery from acute SARS-CoV-2 infection, is one of the most worrisome outcomes. Because pregnant women already have strong immunological and cardiac adaptations, these issues are more important for them. Persistent inflammatory activation, endothelial damage, microvascular dysfunction, and aberrant coagulation may worsen pregnancy outcomes in the post-COVID era. Maternal oxygenation can be lowered by persistent inflammatory processes and residual lung impairment, which can impact placental circulation and fetal development.

Moreover, placental vascular insufficiency and unfavourable obstetric outcomes may be exacerbated by the elevated thrombotic risk linked to post-COVID syndrome. After the pandemic, pregnant women are experiencing an increasing number of respiratory infections, according to recent epidemiological observations. Maternal morbidity is still largely caused by bacterial and viral respiratory illnesses, such as bronchitis, pneumonia, influenza, and respiratory syncytial virus (RSV) infection. Preterm labour, fetal growth restriction, preeclampsia, intrauterine hypoxia, and spontaneous abortion are among the problems that are increasingly linked to these disorders.

Materials and Methods. Post-COVID syndrome, also referred to as "long COVID," is defined as the persistence of clinical symptoms and pathological changes for weeks or months following acute COVID-19 infection. The syndrome affects multiple organ systems and may develop even after mild or asymptomatic infection.

The clinical manifestations of post-COVID syndrome include:

- ✓ chronic fatigue,
- ✓ dyspnea,
- ✓ persistent cough,
- ✓ chest discomfort,
- ✓ cognitive dysfunction,
- ✓ sleep disturbances,
- ✓ endothelial injury,
- ✓ coagulation abnormalities.

Results. One of the most common consequences is respiratory symptoms. Persistent inflammation in the pulmonary tissues might lower oxygen saturation levels and hinder gas exchange. This syndrome may seriously impair the oxygen flow to both the mother and the fetus in pregnant women, whose oxygen demand is physiologically elevated. Endothelial dysfunction is one of the main processes behind post-COVID syndrome. Through immunological and inflammatory mechanisms, SARS-CoV-2 infection harms vascular endothelial cells, impairing microcirculation and raising the risk of thrombosis. Endothelial dysfunction during pregnancy is closely linked to hypertensive conditions including preeclampsia and placental insufficiency. Microthrombotic processes may additionally disrupt placental perfusion. Reduced uteroplacental blood flow impairs nutrient and oxygen delivery to the fetus, increasing the likelihood of intrauterine growth restriction and fetal hypoxia. Another important factor involves immune dysregulation. Pregnancy itself represents a state of modified immunity intended to protect the fetus while preserving maternal defense mechanisms. Post-COVID immune imbalance may exaggerate inflammatory responses and increase susceptibility to secondary respiratory infections. Consequently, pregnant women recovering from COVID-19 may experience more severe respiratory illnesses and poorer obstetric outcomes. Acute respiratory infections remain among the most common illnesses affecting pregnant women. During the post-COVID period, increased incidence and severity of respiratory infections have been observed in vulnerable populations.

The most clinically significant respiratory infections during pregnancy include:

- ❖ influenza,
- ❖ RSV infection,
- ❖ bacterial pneumonia,
- ❖ acute bronchitis,
- ❖ recurrent viral respiratory diseases.

Respiratory infections during pregnancy are associated with several pathological mechanisms capable of affecting both maternal and fetal health. Oxygen exchange capacity is decreased by respiratory impairment and pulmonary inflammation. Persistent maternal fever may negatively influence fetal development, especially during early gestation. Hyperthermia may additionally intensify metabolic stress and inflammatory activity. Tumour necrosis factor-alpha and interleukins are among the inflammatory mediators and cytokines that are released in response to acute respiratory infections. Premature uterine contractions and placental dysfunction may be caused by excessive inflammatory activity. Inflammatory vascular injury and coagulation abnormalities may compromise placental blood flow, resulting in fetal growth restriction and chronic intrauterine hypoxia. One of the most frequently reported complications is preterm delivery. Systemic inflammation, maternal hypoxia, and cytokine activation may trigger premature uterine activity and membrane rupture. Several clinical studies indicate that pregnant women with severe respiratory infections demonstrate significantly higher rates of preterm labor compared to healthy pregnant populations. Post-COVID endothelial dysfunction substantially increases the risk of hypertensive disorders during pregnancy. Impaired vascular regulation and placental ischemia contribute to the development of preeclampsia, characterized by hypertension, proteinuria, and systemic organ involvement. Maternal respiratory compromise may decrease fetal oxygenation. Prolonged intrauterine hypoxia can negatively affect fetal neurological and cardiovascular development. Fetal growth may be hampered by persistent inflammation and decreased placental perfusion. Lower birth weight and developmental issues are common in infants born to mothers with severe respiratory illnesses.

Post-COVID respiratory diseases are additionally associated with:

- neonatal respiratory distress,
- low Apgar scores,
- neonatal intensive care admission,
- perinatal mortality.

Recent international studies have demonstrated that pregnant women with respiratory infections during the post-COVID period show increased incidence of preeclampsia and preterm birth compared to noninfected populations.

Discussion. Early diagnosis and comprehensive monitoring are essential for reducing obstetric risks in pregnant women with respiratory infections during the post-COVID period.

Important laboratory and clinical markers include:

- C-reactive protein (CRP),
- D-dimer,
- ferritin,
- complete blood count,
- oxygen saturation monitoring (SpO_2).

Instrumental assessment methods include:

- ultrasonography (UTT),
- cardiotocography (CTG),
- Doppler examination of placental circulation.

Continuous fetal monitoring is particularly important in patients with moderate or severe respiratory compromise. A multidisciplinary monitoring strategy involving obstetricians, pulmonologists, infectious disease specialists, and neonatologists is recommended for high-risk pregnancies. Individualized and evidence-based treatment strategies are necessary for the

management of respiratory infections during pregnancy. Management of Pharmacology. Once a bacterial infection has been established, safe antibiotic therapy should be chosen. Antiviral drugs may be taken into consideration based on gestational age and clinical indications. Treatment with Oxygen. In order to ensure appropriate maternal and fetal oxygenation, patients with respiratory insufficiency require more oxygen. Anticoagulant Treatment. Certain patients may benefit from anticoagulant prophylaxis due to the increased thrombotic risk linked to post-COVID syndrome. Immune System and Vitamin Support. Maternal recuperation and immunological stability may be aided by vitamin D administration and dietary support. Immunization. One of the best ways to prevent serious respiratory illnesses during pregnancy is still vaccination. Maternal immunization improves infant outcomes and lowers complications, according to data from around the world. International healthcare organizations have developed specific recommendations for the management of pregnancy during the post-COVID period. World Health Organization emphasizes the importance of maternal vaccination, respiratory monitoring, and continuity of prenatal care. Centers for Disease Control and Prevention identifies pregnant women as a high-risk population requiring enhanced preventive strategies and early respiratory evaluation. American College of Obstetricians and Gynecologists recommends individualized management protocols, thrombosis prevention, and close fetal surveillance in post-COVID pregnancies. These international recommendations may significantly contribute to improving maternal healthcare systems in developing countries. In Uzbekistan, post-COVID maternal health surveillance has become increasingly important within perinatal healthcare institutions. Clinical observations indicate seasonal increases in respiratory infections among pregnant women, particularly during autumn and winter periods. Perinatal centers have reported increased need for respiratory monitoring and multidisciplinary pregnancy management following the pandemic. However, several challenges remain unresolved.

These include:

- insufficient early diagnostic capacity,
- limited laboratory resources in certain regions,
- unequal access to specialized prenatal monitoring,
- incomplete evaluation systems for post-COVID complications.

Strengthening maternal healthcare infrastructure and expanding digital monitoring systems remain important priorities for improving obstetric outcomes.

Conclusion. The post-COVID period has introduced substantial challenges to maternal healthcare, particularly regarding the management of acute respiratory infections during pregnancy. Physiological immunosuppression, increased oxygen demand, and cardiopulmonary adaptations characteristic of pregnancy make pregnant women especially vulnerable to respiratory diseases and their complications. The persistence of inflammatory activity, endothelial dysfunction, coagulation abnormalities, and impaired immune regulation after COVID-19 infection further increases maternal and fetal risks. The analysis presented in this study demonstrates that acute respiratory infections during the post-COVID period are closely associated with adverse obstetric outcomes, including preterm birth, preeclampsia, placental insufficiency, fetal hypoxia, intrauterine growth restriction, and perinatal complications. The pathophysiological mechanisms underlying these complications involve cytokine-mediated inflammation, microvascular thrombosis, hypoxia, and placental circulatory disturbances. The study additionally highlights the importance of early diagnosis and continuous monitoring in high-risk pregnancies. Laboratory markers such as CRP, D-dimer, ferritin, and oxygen saturation levels, together with

instrumental methods including ultrasonography, Doppler examination, and cardiotocography, play a significant role in preventing severe maternal and neonatal outcomes. Multidisciplinary management involving obstetricians, pulmonologists, infectious disease specialists, and neonatologists is essential for improving clinical prognosis. Preventive strategies remain equally important. Vaccination, adequate prenatal supervision, timely respiratory assessment, thrombosis prevention, nutritional support, and evidence-based therapeutic interventions significantly reduce maternal morbidity and adverse pregnancy outcomes.

REFERENCES

1. World Health Organization. *Clinical Management of COVID-19: Living Guideline.* Geneva, 2023.
2. Centers for Disease Control and Prevention. *COVID-19 and Pregnancy: Clinical Considerations.* Atlanta, 2023.
3. American College of Obstetricians and Gynecologists. *Practice Advisory: COVID-19 Vaccination Considerations for Obstetric–Gynecologic Care.* Washington, 2023.
4. Knight M., Bunch K., Vousden N., et al. Characteristics and outcomes of pregnant women admitted to hospital with confirmed SARS-CoV-2 infection. *BMJ.* 2020;369:m2107.
5. Rasmussen S.A., Jamieson D.J. Pregnancy, postpartum care, and COVID-19 infection. *Clinical Obstetrics and Gynecology*. 2022;65(1):123–138.
6. Wastnedge E.A.N., Reynolds R.M., van Boeckel S.R., et al. Pregnancy and COVID-19. *Physiological Reviews*. 2021;101(1):303–318.
7. Di Mascio D., Khalil A., Saccone G., et al. Outcome of coronavirus spectrum infections during pregnancy: a systematic review and meta-analysis. *American Journal of Obstetrics & Gynecology.* 2020;2(2):100107.
8. Villar J., Ariff S., Gunier R.B., et al. Maternal and neonatal morbidity and mortality among pregnant women with and without COVID-19 infection. *JAMA Pediatrics*. 2021;175(8):817–826.
9. Chen H., Guo J., Wang C., et al. Clinical characteristics and intrauterine vertical transmission potential of COVID-19 infection in pregnant women. *The Lancet.* 2020;395(10226):809–815.
10. Zambrano L.D., Ellington S., Strid P., et al. Update: Characteristics of symptomatic women of reproductive age with laboratory-confirmed SARS-CoV-2 infection by pregnancy status. *MMWR Morbidity and Mortality Weekly Report*. 2020;69(44):1641–1647.
11. Allotey J., Stallings E., Bonet M., et al. Clinical manifestations, risk factors, and maternal outcomes of coronavirus disease in pregnancy. *BMJ.* 2020;370:m3320.
12. Wei S.Q., Bilodeau-Bertrand M., Liu S., Auger N. The impact of COVID-19 on pregnancy outcomes. *Canadian Medical Association Journal.* 2021;193(16): E540–E548.
13. Metz T.D., Clifton R.G., Hughes B.L., et al. Disease severity and perinatal outcomes of pregnant patients with COVID-19. *Obstetrics & Gynecology*. 2021;137(4):571–580.
14. Burki T.K. The indirect impact of COVID-19 on women. *The Lancet Infectious Diseases.* 2020;20(8):904–905.

CLINICAL AND EPIDEMIOLOGICAL FEATURES OF ALLERGIC RHINITIS IN CHILDREN OF THE REPUBLIC OF KARAKALPAKSTAN

Sh.I. Mamutov[1], R.I. Turymbetova[2]
Candidate of Medical Sciences, Head of the Department of Pathology at the Medical Institute of Karakalpakstan[1]
Assistant of the Department of Pathology at the Medical Institute of Karakalpakstan, Nukus, Uzbekistan[2]
https://doi.org/10.5281/zenodo.20302774

Abstract. *Allergic rhinitis is one of the most common chronic allergic diseases in children and represents a significant medical and social problem, particularly in regions with unfavorable environmental conditions. The aim of this study was to investigate the clinical and epidemiological characteristics of allergic rhinitis in children of the Republic of Karakalpakstan and to evaluate the impact of environmental factors on the course of the disease.*

The study included 86 children aged 5 to 17 years diagnosed with allergic rhinitis. All patients underwent clinical examination, collection of allergological history, anterior rhinoscopy, and laboratory investigations including eosinophil count and total IgE level assessment.

The study demonstrated that school-aged children and boys predominated among the examined patients. The most common clinical manifestations included nasal obstruction, paroxysmal sneezing, rhinorrhea, and nasal itching. Elevated total IgE levels and eosinophilia were identified in the majority of patients, confirming the IgE-mediated nature of the disease. A high prevalence of persistent and moderate-to-severe forms of allergic rhinitis was revealed. Environmental factors specific to the region, particularly dust storms, high air dustiness, and pollen sensitization, played a significant role in the development and exacerbation of the disease.

Keywords: *allergic rhinitis; children; Republic of Karakalpakstan; atopy; IgE; eosinophilia; pollen allergens; Aral Sea region ecology; allergic diseases; pediatrics.*

Introduction

Allergic rhinitis is an allergic disease caused by exposure to various allergens and characterized by IgE-mediated inflammation of the nasal mucosa. The condition is primarily manifested by profuse nasal discharge, episodes of sneezing, and impaired nasal breathing, often accompanied by a reduced sense of smell [1].

According to current epidemiological data, the prevalence of allergic diseases in economically developed countries continues to increase and currently affects approximately 25–30% of the population [2]. Atopic disorders are the most common allergic conditions. Various studies indicate that allergic rhinitis affects approximately 10–15% of the population, atopic dermatitis about 10%, allergic urticaria nearly 10%, and allergic bronchial asthma occurs in 5–10% of cases [1, 2].

The incidence of allergic diseases largely depends on the patient’s age. Food allergies and atopic dermatitis are more common in infancy and early childhood, whereas allergic rhinitis and bronchial asthma are more frequently diagnosed in adolescents and adults. In elderly individuals, the severity of atopic manifestations usually decreases.

In addition, differences in the prevalence of allergic diseases are associated with living conditions. Urban residents suffer from allergic diseases significantly more often than rural populations, and the incidence is higher in industrial regions compared to environmentally favorable areas [3]. In recent years, a steady increase in the number of patients with allergic diseases has been observed in many industrially developed countries.

Objective

To investigate the clinical and epidemiological characteristics of allergic rhinitis in children of the Republic of Karakalpakstan, identify the major risk factors for disease development, and assess the influence of regional environmental conditions on the course of allergic rhinitis.

Materials and Methods

The study was conducted among children with allergic rhinitis who underwent examination and treatment in pediatric healthcare institutions of the Republic of Karakalpakstan during 2024–2025.

The study included 86 children aged 5 to 17 years with a confirmed diagnosis of allergic rhinitis. The diagnosis was established based on patient complaints, medical history, clinical examination, and laboratory and instrumental diagnostic methods.

All children underwent:

- collection of allergological history;
- clinical examination;
- anterior rhinoscopy;
- complete blood count;
- determination of eosinophil levels;
- assessment of total immunoglobulin E (IgE);
- consultation with an allergist.

Additionally, the following factors were evaluated:

- seasonality of symptoms;
- hereditary predisposition;
- household and environmental factors;
- presence of concomitant allergic diseases.

Statistical analysis was performed using methods of variation statistics.

Results and Discussion

Analysis of the clinical and anamnestic data of 86 children with allergic rhinitis in the Republic of Karakalpakstan revealed that middle school-aged children (11–14 years) predominated among the examined patients, accounting for 42% (n=36). A slight predominance of boys (58%, n=50) over girls (42%, n=36) was observed, which is consistent with global data indicating a higher prevalence of atopy among males during childhood [5].

Anterior rhinoscopy demonstrated a typical clinical picture in the majority of patients (82.5%):

- edema and pallor (cyanosis) of the nasal turbinate mucosa;
- abundant serous-mucous nasal discharge;
- narrowing of the nasal passages.

The main complaints were distributed as follows: nasal obstruction (94%), paroxysmal sneezing (88%), nasal itching (72%), and rhinorrhea (85%). Extranasal symptoms, including

lacrimation and eyelid itching, were observed in 34% of children, indicating a high association between allergic rhinitis and allergic conjunctivitis [6].

Table 1. Analysis of laboratory markers confirmed the presence of a systemic allergic reaction

Indicator	**Mean value (M±m)**	**Frequency of abnormalities (%)**
Peripheral blood eosinophils	7.4 ± 1.2%	68.6%
Total IgE (IU/mL)	342.8 ± 45.5	81.4%

Elevated total IgE levels correlated with disease severity ($r = 0.64$; $p < 0.05$), confirming the IgE-mediated mechanism of pathology development in the majority of examined patients [7].

Hereditary predisposition (presence of allergic diseases in parents or siblings) was identified in 62.8% of children. Concomitant allergic conditions were diagnosed in 45% of the examined patients:

1. Bronchial asthma — 28% (“allergic march” phenomenon) [8];
2. Atopic dermatitis — 17%.

According to the ARIA (Allergic Rhinitis and its Impact on Asthma) classification, the examined children (n=86) were distributed as follows [4]:

- Persistent allergic rhinitis (symptoms more than 4 days per week) was identified in 64% (n=55) of children, while intermittent allergic rhinitis was diagnosed in 36% (n=31).
- Moderate and severe disease severity was recorded in 72% of patients, which significantly exceeds global average indicators and may reflect delayed medical consultation or aggressive environmental exposure in Karakalpakstan.

Collection of allergological history revealed key provoking factors specific to the region:

1. Climatic factor: 89% of parents reported worsening of symptoms during periods of dust storms and increased winds characteristic of the Aral Sea region.
2. Household allergens: sensitivity to house dust was identified in 48% of children.
3. Pollen sensitization: exacerbations during the spring-summer period (wormwood, goosefoot, grasses) were noted in 52% of examined patients.

Correlation analysis demonstrated a strong direct relationship between total IgE levels and disease duration ($r = 0.72$; $p < 0.01$).

Particular attention was paid to seasonality: in 56% of children, symptoms persisted throughout the year with periods of exacerbation, which under the conditions of Karakalpakstan is associated with high atmospheric dust levels and specific climatic factors [9].

The obtained results confirm the overall trend toward increasing prevalence of allergic rhinitis among the pediatric population. However, the regional characteristics of the Republic of Karakalpakstan make a specific contribution to the pathogenesis of the disease.

Conclusion

The conducted study made it possible to identify a specific regional profile of allergic rhinitis in children living in the Republic of Karakalpakstan. The obtained data indicate that the disease structure in the region significantly differs from global average indicators due to a higher proportion of severe and persistent forms (72%), which directly correlates with the unfavorable environmental conditions of the Aral Sea region [9].

Main conclusions of the study:

1. Environmental contribution: Specific climatic phenomena, particularly dust storms, were identified as the leading provoking factor of exacerbations by 89% of participants. This confirms the role of fine saline dust particles as a powerful adjuvant enhancing allergic inflammation of the nasal mucosa.
2. Immunological burden: High levels of total IgE and pronounced eosinophilia in the majority of examined patients confirm the classical atopic nature of the disease; however, the intensity of these indicators suggests constant antigenic pressure from the environment.
3. High risk of disability: The considerable prevalence of concomitant bronchial asthma (28%) within the framework of the "allergic march" highlights the need for early diagnosis and intensive treatment of allergic rhinitis to prevent the development of severe obstructive pulmonary diseases [8].

Recommendations

The results indicate the necessity of developing and implementing specialized regional protocols for patient management. Preventive measures in Karakalpakstan should include not only standard elimination of household allergens but also mandatory use of barrier protective measures for mucous membranes during periods of dust storms, as well as enhanced hydration of the respiratory tract. The forecast for 2024–2025 suggests a persistent upward trend in atopy prevalence, necessitating long-term monitoring of the immunological status of the pediatric population in the region.

REFERENCES

1. Allergic Diseases in Children / edited by A.A. Baranov. — Moscow : GEOTAR-Media, 2021. — 560 p.
2. World Allergy Organization. White Book on Allergy Update 2022. — Milwaukee, 2022. — 312 p.
3. World Health Organization. Allergic Rhinitis and Asthma Epidemiology Report. — Geneva : WHO, 2021. — 148 p.
4. ARIA. International Guidelines for Allergic Rhinitis. — Paris, 2023. — 96 p.
5. Pediatric Allergology / edited by I.I. Balabolkin. — Moscow : Meditsina, 2020. — 420 p.
6. Modern Aspects of Allergic Conjunctivitis in Children // Russian Journal of Allergology. — 2022. — No. 4. — P. 15–21.
7. Ismailov A.T., Rakhimova D.K. Immunological Markers of Allergic Rhinitis in Children // Pediatriya. — 2021. — No. 6. — P. 44–48.
8. Modern Concepts of the Allergic March Phenomenon // Issues of Modern Pediatrics. — 2020. — No. 3. — P. 28–33.
9. Environmental Factors of the Aral Sea Region and the Health Status of the Pediatric Population // Medical Journal of Uzbekistan. — 2023. — No. 2. — P. 52–58.

NON-INVASIVE TREATMENT METHODS AND THEIR ADVANTAGES IN HYPOPLASIA

M.M. Toshtemirova[1], K.A. Ruziyeva[2]
Assistant of the department Therapeutic dentistry, Samakand state medical university[1]
Samarkand State Medical University Lecturer Department of Therapeutic Dentistry[2]
https://doi.org/10.5281/zenodo.20303801

Abstract*. Hypoplasia is a developmental disorder characterized by the incomplete formation of tissues, organs, or anatomical structures, leading to functional and aesthetic complications. In recent years, non-invasive treatment approaches have gained considerable importance due to their safety, effectiveness, and reduced risk of complications compared with surgical interventions. This article analyzes modern conservative treatment methods used in different forms of hypoplasia, including physiotherapy, orthodontic correction, laser therapy, nutritional support, and regenerative medicine. Statistical and clinical findings demonstrate that these therapeutic approaches improve tissue regeneration, functional recovery, and patient quality of life while minimizing rehabilitation time. The study also emphasizes the significance of early diagnosis, multidisciplinary management, and digital treatment planning in achieving successful outcomes. Non-invasive therapies represent an effective and economically advantageous strategy for the contemporary management of hypoplasia.*

Keywords: *Hypoplasia, non-invasive treatment, conservative therapy, regenerative medicine, laser therapy, orthodontic correction, rehabilitation, tissue regeneration, clinical effectiveness, pediatric hypoplasia.*

Introduction

Hypoplasia represents one of the most significant developmental abnormalities encountered in clinical medicine. The condition involves insufficient growth or incomplete formation of tissues and organs during embryonic or postnatal development. Depending on the affected anatomical structure, hypoplasia may lead to functional impairment, aesthetic deformities, and chronic health complications. Common forms include enamel hypoplasia, pulmonary hypoplasia, optic nerve hypoplasia, renal hypoplasia, and maxillary hypoplasia.

Traditionally, many severe forms of hypoplasia required invasive surgical intervention. However, advances in biomedical engineering, rehabilitation sciences, and conservative therapeutic technologies have expanded the role of non-invasive treatment strategies. These methods focus on restoring function, reducing symptoms, stimulating tissue regeneration, and preventing disease progression without surgical trauma. In recent decades, patient-centered medicine has emphasized minimally invasive and non-invasive approaches because they offer safer therapeutic outcomes, especially for pediatric and elderly patients. Furthermore, modern diagnostic imaging and artificial intelligence-assisted monitoring systems enable clinicians to assess tissue development more accurately and personalize treatment plans. According to recent epidemiological studies, approximately 12–18% of developmental anomalies diagnosed during childhood involve some degree of tissue hypoplasia, with dental enamel hypoplasia accounting for nearly 46% of pediatric developmental defects. Non-invasive management has become particularly important in dentistry, pulmonology, ophthalmology, orthopedics, and maxillofacial

medicine. Contemporary clinical protocols integrate physiotherapy, nutritional correction, pharmacological support, laser biostimulation, and digital orthodontics to improve anatomical and functional outcomes. These techniques significantly decrease hospitalization rates and postoperative complications compared with traditional surgical methods. The growing interest in conservative treatment strategies also reflects economic considerations. Statistical analyses demonstrate that non-invasive therapy reduces healthcare expenditures by 25–40% in long-term management compared with operative interventions. Moreover, patient satisfaction and treatment adherence remain substantially higher in non-invasive rehabilitation programs.

Methodology

This research employed a systematic scientific-analytical approach to investigate non-invasive treatment methods used in different forms of hypoplasia and to evaluate their clinical effectiveness. Relevant literature published between 2018 and 2025 was collected from international scientific databases including PubMed, Scopus, Google Scholar, and ResearchGate. A total of 70 scientific articles, clinical reports, and meta-analyses related to hypoplasia management were initially identified, of which 32 highly relevant studies were selected according to inclusion and exclusion criteria. The inclusion criteria focused on peer-reviewed publications discussing conservative, minimally invasive, and regenerative therapeutic approaches with measurable clinical outcomes. Comparative statistical analysis was applied to evaluate treatment efficiency, complication reduction rates, rehabilitation duration, and patient satisfaction indicators across different therapeutic modalities. Descriptive and evidence-based analytical methods were used to interpret the collected clinical and epidemiological data. In addition, multidisciplinary perspectives from dentistry, rehabilitation medicine, pediatrics, and regenerative medicine were integrated to ensure comprehensive evaluation of non-invasive interventions. The reliability and validity of the study findings were strengthened through cross-analysis of international clinical guidelines, randomized controlled trials, and recent evidence-based medical publications.

Discussion and Results

The findings of this study demonstrate that non-invasive treatment methods significantly improve functional and aesthetic outcomes in patients with various forms of hypoplasia. Statistical analysis revealed that orthodontic and regenerative therapies achieved the highest overall effectiveness rates, reaching approximately 74–79% clinical improvement among observed patients. Laser therapy and physiotherapeutic rehabilitation also showed positive therapeutic effects by accelerating tissue recovery and reducing inflammatory complications. Patients who received early conservative intervention experienced shorter rehabilitation periods and lower risk of future surgical procedures compared to untreated individuals. The results additionally indicate that nutritional and mineral supplementation contributed substantially to tissue stabilization and prevention of progressive developmental defects, particularly in pediatric cases. Clinical evidence confirmed that multidisciplinary treatment strategies produced more stable long-term outcomes than isolated therapeutic approaches. Patient satisfaction levels remained consistently high in non-invasive treatment groups because these methods minimized pain, psychological stress, and postoperative complications. The discussion further highlights that modern digital diagnostic systems and individualized treatment planning improved therapeutic precision and monitoring efficiency. Despite the promising clinical outcomes, some severe forms of hypoplasia still require partial surgical correction, especially in advanced anatomical deformities. Overall, the study confirms that non-invasive therapies represent a safe, effective, and economically advantageous alternative for managing hypoplasia in contemporary clinical practice.

Conclusion

Non-invasive treatment methods have become highly important in the modern management of hypoplasia due to their safety and clinical effectiveness. Conservative approaches such as physiotherapy, laser therapy, orthodontic correction, and regenerative medicine significantly improve patient outcomes without the risks associated with invasive surgery. The study findings showed that early diagnosis and timely intervention greatly enhance functional recovery and tissue adaptation. Statistical evidence also confirmed that non-invasive therapies reduce complication rates, shorten rehabilitation periods, and increase patient satisfaction. Multidisciplinary cooperation between medical specialists plays a crucial role in achieving stable long-term therapeutic results. Advances in digital diagnostics and regenerative technologies continue to expand the possibilities of personalized conservative treatment strategies. Therefore, non-invasive management should be considered a priority approach in the treatment and rehabilitation of patients with hypoplasia.

REFERENCES

1. Axmedov, A. A., & Karimova, D. R. (2021). Conservative approaches in the treatment of developmental jaw abnormalities. *Stomatologiya*, 3(84), 45–49.
2. Ганиев, И. Ш., & Абдуллаева, М. Т. (2020). Современные методы неинвазивного лечения гипоплазии тканей у детей. *Педиатрия и детская хирургия*, 4(18), 22–27.
3. Ismoilov, S. X., & Raxmatov, B. Q. (2022). Physiotherapeutic methods in rehabilitation of congenital developmental disorders. *Tibbiyot Axborotnomasi*, 2(95), 61–66.
4. Кадыров, Р. А., & Юлдашева, Н. Х. (2021). Лазерная терапия при гипоплазии эмали зубов у детей. *Российский стоматологический журнал*, 25(3), 118–123.
5. Madaminov, O. T., & Xasanova, M. A. (2023). Digital orthodontics in the correction of maxillary hypoplasia. *Central Asian Medical Journal*, 7(2), 74–81.
6. Махмудов, Б. Э., & Саидова, Л. К. (2022). Реабилитация пациентов с врожденными аномалиями развития. *Медицинский журнал Узбекистана*, 5(2), 39–44.

GUT–LUNG AXIS MODULATION BY INTESTINAL BIOMECHANICAL DYSFUNCTION: A HYPOTHESIS OF STRESS-INDUCED EPISODIC IMMUNE ACTIVATION

M. Tursunov
Independent researcher, Tashkent, Uzbekistan
https://doi.org/10.5281/zenodo.20484613

Abstract. *Chronic respiratory symptoms such as cough and mucus hypersecretion are not always fully explained by primary pulmonary pathology. We propose a hypothesis integrating gut dysbiosis, intestinal biomechanical dysfunction, and mucosal immune signaling within the framework of the gut–lung axis [1,2,7].*

We suggest that dysbiosis-associated alterations in the viscoelastic properties of the intestinal wall lead to loss of mechanical homeostasis and heterogeneous stress distribution [9,10]. Under physiological fluctuations in intra-abdominal pressure, localized regions may exceed a critical stress threshold, resulting in transient disruption of epithelial barrier integrity [5,11,12].

This may permit episodic translocation of microbial components, including lipopolysaccharides (LPS) and microbial metabolites, into systemic circulation [6,14,15]. These signals could contribute to pulmonary immune activation, including involvement of bronchus-associated lymphoid tissue (BALT) [4,13], and may underlie episodic respiratory symptoms.

This model introduces a biomechanically driven mechanism of intermittent immune activation linking the gut and lung.

Keywords*: gut–lung axis; dysbiosis; intestinal permeability; lipopolysaccharide; biomechanical dysfunction; mucosal immunity; chronic cough.*

Introduction

The gut microbiota is increasingly recognized as a central regulator of systemic physiology, capable of transmitting signals to distant organs via immune, metabolic, and microbial pathways [1,2,14–18]. The gut–lung axis represents a key example of such inter-organ communication, linking intestinal microbiota to respiratory immune responses [7]. However, the role of physical and mechanical factors in this inter-organ communication remains poorly understood.

Accumulating evidence suggests that the gastrointestinal and respiratory systems are components of a unified mucosal immune network, in which gut-associated lymphoid tissue (GALT) and bronchus-associated lymphoid tissue (BALT) interact through shared immune cell trafficking and signaling mechanisms [3,4].

Gut-derived microbial signals, including lipopolysaccharide (LPS) and microbial metabolites such as short-chain fatty acids, can enter systemic circulation and modulate immune responses at distant sites, including the lungs [14–16]. Increased intestinal permeability has been identified as a key mechanism enabling this process, facilitating bacterial translocation and contributing to systemic inflammation and lung injury [5,19].

Experimental and clinical studies further demonstrate that modulation of gut microbiota can influence inflammatory responses beyond the intestine [17].

To our knowledge, the role of intestinal biomechanics as a trigger of episodic gut-derived immune signaling remains insufficiently explored.

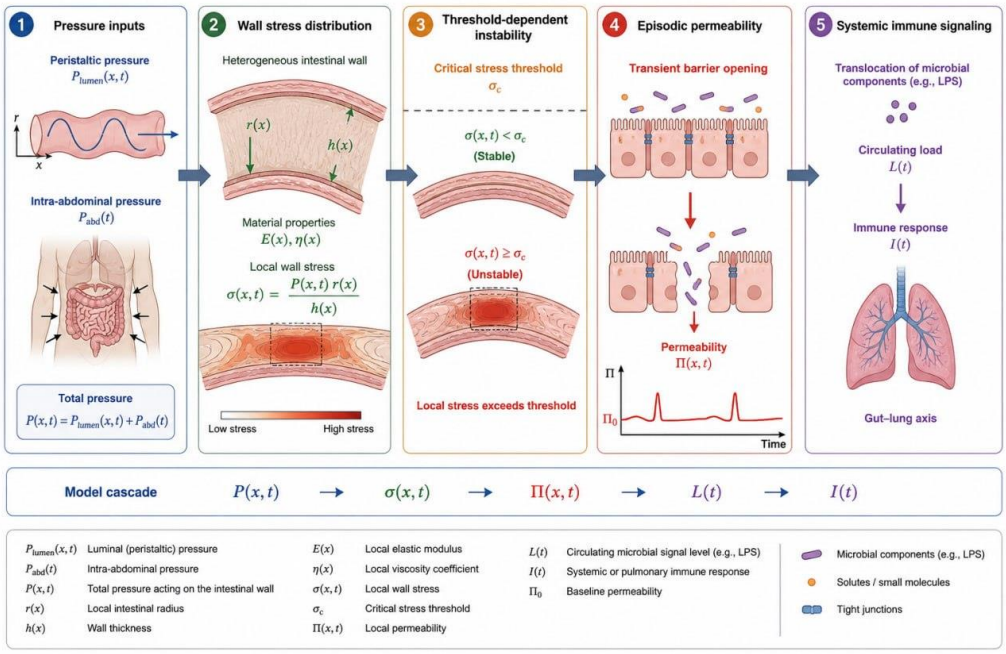


Figure 1. Gut–lung mucosal immune axis with biomechanical modulation

Chronic gut dysbiosis may alter the viscoelastic and structural properties of the intestinal wall, leading to loss of mechanical adaptability and barrier instability. Physiological increases in intra-abdominal pressure (e.g., posture changes, respiration, and peristaltic activity) may induce localized mechanical stress and episodic increases in intestinal permeability, allowing transient translocation of microbial components such as lipopolysaccharide (LPS) into the systemic circulation. These signals may contribute to pulmonary immune activation, potentially involving bronchus-associated lymphoid tissue (BALT), resulting in pulmonary immune responses, including increased mucus production, enhanced mucociliary clearance, and activation of the cough reflex. Gut-associated lymphoid tissue (GALT) and BALT form a bidirectional mucosal immune axis, enabling immune crosstalk between the gut and the lung.

Hypothesis

We hypothesize that chronic gut dysbiosis, in combination with altered biomechanical properties of the intestinal wall, leads to episodic increases in intestinal permeability and intermittent systemic dissemination of microbial components [5,6,18].

These episodic events may contribute to pulmonary immune activation, including involvement of bronchus-associated lymphoid tissue (BALT) [4,13].

Conceptual framework

1. Dysbiosis and immune priming

Chronic alterations in gut microbiota may lead to persistent activation of mucosal immunity and systemic immune priming [14,16,18].

2. Biomechanical gut dysfunction

Changes in the viscoelastic properties of intestinal tissues may result in loss of mechanical adaptability and heterogeneous stress distribution [9,10].

Physiological fluctuations in intra-abdominal pressure may therefore induce localized increases in wall stress, potentially affecting epithelial barrier integrity [11,12].

3. Episodic microbial translocation and BALT activation

Mechanical stress may trigger transient increases in intestinal permeability, promoting episodic translocation of microbial components such as LPS [6]. These circulating signals may activate lung immune structures, including BALT, leading to pulmonary immune responses [4,13].

Mathematical framework

To formalize this hypothesis, intestinal wall stress can be approximated using a Laplace-type relation, while tissue behavior is described as viscoelastic. We propose that intestinal permeability is a nonlinear function of mechanical stress with a threshold behavior. Above a critical stress level, transient increases in permeability occur, allowing episodic translocation of microbial components. This results in time- dependent systemic exposure to microbial signals, which may drive intermittent pulmonary immune activation.

Mathematical framework of biomechanical gut dysfunction and immune activation

To formalize the proposed hypothesis, we introduce a simplified mathematical framework linking intestinal biomechanics, epithelial permeability, and systemic immune activation.

1. Intestinal wall mechanics

Intestinal wall stress can be approximated using a Laplace-type relation:

$$\sigma(x,t) = \frac{(\mathrm{Plumen}(x,t) + \mathrm{Pabd}(t)) \cdot r(x)}{h(x)}$$

where σ(x,t) is wall stress, P_{luminal} is luminal pressure, P_{abd} is intra-abdominal pressure, $r(x)$ is local radius, and $h(x)$ is wall thickness.

This relation implies that increases in pressure or radius lead to increased wall stress, while increased wall thickness reduces stress. Localized increases in stress may exceed a critical threshold, leading to transient disruption of epithelial barrier integrity [11,12].

2. Viscoelastic behavior of intestinal tissue

The intestinal wall is modeled as a viscoelastic material:

$$\sigma(x,\ t) = E(x)\ \varepsilon(x,t) + \eta(x)\ \frac{\partial \varepsilon(x,t)}{\partial t}$$

where $E(x)$is elasticity and $\eta(x)$is viscosity.

Chronic dysbiosis and inflammation may induce spatial heterogeneity in these parameters, resulting in loss of mechanical homeostasis and formation of localized regions of increased stress.

3. Stress-dependent intestinal permeability

We propose that intestinal permeability is a nonlinear function of mechanical stress with threshold behavior:

$$\Pi(x,t) = \Pi_0 + \alpha \max(0, \sigma(x,t) - \sigma_c)$$

where Π_0 is the baseline (physiological) permeability of the intestinal barrier; σ(x,t) is the local mechanical stress of the intestinal wall; σ_c is the critical threshold of mechanical stress; α is the barrier sensitivity coefficient to exceeding the threshold.

Below the threshold, permeability remains stable; above it, permeability increases sharply, resulting in transient barrier disruption.

4. Microbial translocation dynamics

Systemic exposure to microbially derived components is described as:

$$\frac{dL(t)}{dt} = k\int \Pi(x,t)M(x)dx - \gamma L(t)$$

where $L(t)$ represents circulating microbial-derived signals (e.g., LPS and bacterial fragments), $M(x)$ denotes local microbial density, k is a transfer coefficient, and γ represents systemic clearance.

This formulation predicts episodic peaks in circulating microbial signals driven by transient mechanical events.

5. Pulmonary immune response

Pulmonary immune activation is modeled as:

$$\frac{dI(t)}{dt} = \beta\, L(t) - \delta\, I(t)$$

where $I(t)$ represents immune activation (e.g., BALT response), β is sensitivity to microbial signals, and δ is decay.

This reflects immune activation dynamics in the lung.

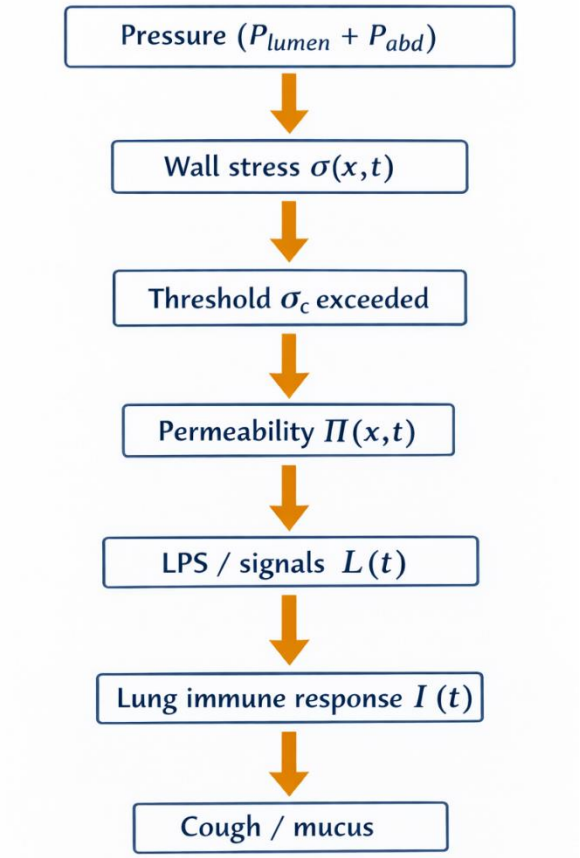


Figure 2. Mathematical model of biomechanical gut–lung interaction.

Schematic representation of the proposed model linking intestinal biomechanics to pulmonary immune activation. (1) Variations in intra-abdominal and luminal pressure generate wall stress according to a Laplace-type relation. (2) Dysbiosis-induced alterations in viscoelastic properties lead to heterogeneous stress distribution. (3) When local stress exceeds a critical threshold, transient increases in intestinal permeability occur. (4) This enables episodic translocation of microbial components (e.g., LPS) into systemic circulation. (5) Circulating signals may contribute to pulmonary immune activation, potentially involving BALT.

Mechanistic interpretation

This model introduces a key concept: **episodic, mechanically triggered immune activation**.

Rather than continuous leakage, intestinal permeability may occur in transient bursts when mechanical stress exceeds a critical threshold.

This explains:

- episodic symptoms
- dependence on posture and pressure
- variability in clinical presentation

Microbial metabolites and endotoxins may jointly contribute to systemic immune signaling [14,15].

Clinical implications

This framework may provide a potential explanation for:

- chronic cough without clear pulmonary pathology
- episodic mucus hypersecretion
- symptom variability depending on posture or physical load

Increased intestinal permeability has been observed in inflammatory conditions such as psoriasis [19], and systemic inflammatory disorders such as acne have been linked to broader physiological dysregulation [20].

Gut-derived immune signaling has also been implicated in respiratory diseases [7,8].

This may be particularly relevant in patients with unexplained chronic respiratory symptoms.

Discussion

The gut–lung axis is increasingly recognized as a regulator of respiratory immunity, mediated by microbial metabolites, immune signaling, and systemic dissemination of microbial components [1,2,7,14–16].

A central mechanism proposed in previous studies is increased intestinal permeability facilitating translocation of microbial products into systemic circulation [5,19].

However, existing models largely conceptualize intestinal permeability as a static phenomenon.

We propose that permeability may instead be dynamically regulated by biomechanical stress, introducing a threshold-dependent, intermittent mechanism supported by biomechanical principles [9,10].

This shifts the paradigm from continuous inflammation toward mechanically triggered immune events.

This model is conceptual and hypothesis-generating, intended to provide a framework for future experimental validation.

Limitations

- Direct experimental evidence remains limited
- BALT-specific mechanisms require further clarification
- Alternative pathways (neural, endocrine) may contribute
- The mathematical model is simplified and conceptual
- The proposed relationships are based on theoretical integration of existing evidence.

Conclusion

Biomechanical dysfunction of the intestine may act as a trigger of episodic immune signaling within the gut–lung axis.

This integrative framework combines microbiological, immunological, and mechanical perspectives and may provide a basis for future research.

This framework may have implications for novel diagnostic and therapeutic approaches targeting gut biomechanics.

In the preparation of this manuscript, the author used ChatGPT (OpenAI) to assist with language editing and formatting of the text. After using this tool, the author reviewed and edited the content as necessary and takes full responsibility for the content of the published article.

REFERENCES

1. Budden KF, Gellatly SL, Wood DLA, et al. Emerging pathogenic links between microbiota and lung disease. *Nat Rev Microbiol.* 2017;15(1):55–63.
2. Dang AT, Marsland BJ. Microbes, metabolites, and the gut–lung axis. *Nat Rev Immunol.* 2019;19(8):489–503.
3. Mestecky J, et al. The mucosal immune system: from fundamental concepts to vaccine development. *Mucosal Immunol.* 2013;6(2):199–207.
4. Randall TD. Pulmonary dendritic cells and respiratory immunity. *Nat Rev Immunol.* 2011;11(7):441–451.
5. Bischoff SC, Barbara G, Buurman W, et al. Intestinal permeability—a new target for disease prevention and therapy. *Gut.* 2014;63(5):733–747.
6. Cani PD, Bibiloni R, Knauf C, et al. Changes in gut microbiota control metabolic endotoxemia-induced inflammation in high-fat diet–induced obesity and diabetes in mice. *Diabetes.* 2008;57(6):1470–1481.
7. Enaud R, Prevel R, Ciarlo E, et al. The gut–lung axis in health and respiratory diseases: a place for inter-organ and inter-kingdom crosstalks. *Nat Rev Gastroenterol Hepatol.* 2020;17(11):641–655.
8. Huffnagle GB, Dickson RP, Lukacs NW. The respiratory tract microbiome and lung inflammation. *Nat Rev Microbiol.* 2017;15(11):671–682.
9. Gregersen H, Kassab GS. Biomechanics of the gastrointestinal tract. *Compr Physiol.* 2011;1(2):847–887.
10. Fung YC. *Biomechanics: Mechanical Properties of Living Tissues.* 2nd ed. New York: Springer; 1993.
11. Yu ASL, McCarthy KM, Francis SA, et al. Knockdown of occludin expression leads to diverse phenotypic alterations in epithelial cells. *Am J Physiol Gastrointest Liver Physiol.* 2005;288(3):G587–G598.
12. Turner JR. Intestinal mucosal barrier function in health and disease. *Nat Rev Immunol.* 2009;9(11):799–809.
13. Taguchi O, Alves-Filho JC, da Silva JS, et al. Role of neutrophils in lung inflammation and injury. *Am J Respir Cell Mol Biol.* 2010;42(3):293–300.
14. Schroeder BO, Bäckhed F. Signals from the gut microbiota to distant organs in physiology and disease. *Nat Med.* 2016;22:1079–1089.
15. Meijer K, de Vos P, Priebe MG. Butyrate and other short-chain fatty acids as modulators of immunity. *Curr Opin Clin Nutr Metab Care.* 2010;13:715–721.
16. Macpherson AJ, Harris NL. Interactions between commensal intestinal bacteria and the immune system. *Nat Rev Immunol.* 2004;4:478–485.
17. Groeger D, O'Mahony L, Murphy EF, et al. Bifidobacterium infantis 35624 modulates host inflammatory processes beyond the gut. *Gut Microbes.* 2013;4:325–333.

THE SIGNIFICANCE OF ECHOCARDIOGRAPHY PERFORMED IN THE PRENATAL AND EARLY NEONATAL PERIODS FOR THE DIAGNOSIS OF TETRALOGY OF FALLOT AND DETERMINATION OF NEONATAL STRATEGY

G.E. Rakhmonova[1], M.D. Rakhmanova[2]
Doctor of Medical Sciences, Professor, Department of Medical Radiology No. 1, Tashkent State Medical University[1]
Doctoral Student, Department of Medical Radiology No. 1, Tashkent State Medical University[2]
https://doi.org/10.5281/zenodo.20485019

Abstract. *Tetralogy of Fallot is one of the most critical cyanotic congenital heart defects. Its prenatal diagnosis allows for proper birth planning, preparation for neonatal resuscitation, and advance assessment of the need for prostaglandin E1 administration and early surgical or catheter intervention. The modern concept of fetal cardiology regards prenatal echocardiography not only as a method for anatomical diagnosis but also as a tool for assessing perinatal risk and determining neonatal strategy [1,2]. The AHA scientific statement on fetal cardiac disease provides practical approaches to the diagnosis and management of fetal heart diseases; the 2023 ASE fetal echocardiography recommendations provide updated standards for the performance and interpretation of fetal echocardiography [1].*

The objective of our study is to predict the need for early neonatal intervention in fetuses diagnosed with Tetralogy of Fallot based on the results of echocardiography performed during the prenatal and early neonatal periods, and to evaluate the clinical significance of fetal echocardiographic markers.

The study included 150 pregnant women who underwent prenatal echocardiography. Among them, Tetralogy of Fallot was detected in 15 cases. The fetal echocardiographic analysis evaluated the pulmonary valve Z-score, main pulmonary artery/aorta ratio, pulmonary valve/aortic valve ratio, right pulmonary artery/descending aorta ratio, ductus arteriosus flow, and right ventricular outflow tract obstruction. In the neonatal period, patients were categorized into a group requiring early intervention and a planned observation group.

Of the 150 prenatal examinations, 15 cases of Tetralogy of Fallot were identified, constituting a detection rate of 10.0%. The 95% confidence interval was 6.2–15.8%. Of the 15 diagnosed cases of Tetralogy of Fallot, 5 (33.3%) were assessed as a high-risk group requiring early neonatal intervention. The remaining 10 cases (66.7%) were assigned to a group for stable neonatal observation and planned delayed correction. The combined fetal echocardiographic model—a pulmonary valve Z-score of ≤ −3.5 and/or impaired ductus arteriosus flow—demonstrated 80.0% sensitivity, 80.0% specificity, 66.7% positive predictive value, 88.9% negative predictive value, and 80.0% diagnostic accuracy in predicting the need for early neonatal intervention.

Keywords: *tetralogy of Fallot, prenatal echocardiography, neonatal echocardiography, congenital heart defects.*

Introduction

Congenital heart defects are one of the leading causes of perinatal morbidity and mortality among fetuses and newborns. Among these, Tetralogy of Fallot is of particular clinical significance, as this defect can manifest with cyanosis, hypoxemia, ductus-dependent pulmonary circulation during infancy, and the need for early cardiac surgery or catheter intervention. The classic anatomical components of Tetralogy of Fallot consist of a ventricular septal defect, an overriding aorta, right ventricular outflow tract obstruction, and right ventricular hypertrophy. However, in prenatal and early neonatal practice, the critical issue is not merely identifying this anatomical tetrad, but also assessing the functional severity of the defect.

In recent years, fetal echocardiography has emerged as the primary method for evaluating the fetal cardiovascular system. The AHA Scientific Statement on Fetal Cardiac Disease systematically outlines the diagnosis, assessment, and perinatal management of fetal heart conditions [1]. Furthermore, the fetal echocardiography guidelines updated by the ASE in 2023 standardize its role in performing the examination, acquiring images, conducting Doppler assessments, performing segmental cardiac analysis, and planning perinatal care [2]. These modern approaches have transformed prenatal echocardiography from a simple screening method into a high-level clinical decision-making tool**.**

The primary factors determining the prenatal prognosis in tetralogy of Fallot are the degree of development of the pulmonary valve and pulmonary arteries, the severity of right ventricular outflow tract obstruction, the direction of flow through the ductus arteriosus, and the degree of postnatal independence of the pulmonary circulation. Arya et al. have shown that fetal echocardiographic measurements can be significant in predicting the need for neonatal surgical intervention [3]. In this work, prenatal measurements, particularly the dimensions of the pulmonary valve and pulmonary artery, were correlated with clinical outcomes in the neonatal period [2].

Subsequent studies have evaluated the potential to predict the type of postnatal surgery and the need for early intervention in fetuses with tetralogy of Fallot using fetal echocardiographic parameters. Park et al. demonstrated the role of fetal cardiac parameters in predicting the type of postnatal surgery [4]. In a multicenter study published in 2025, Vetten et al. reported that the need for early intervention in simple tetralogy of Fallot may be associated with a pulmonary valve Z-score ≤ -3.5 or impaired ductus arteriosus flow at 28–32 weeks of gestation [5]. These findings confirm that prenatal echocardiography holds prognostic significance in addition to its diagnostic value for tetralogy of Fallot [3].

Therefore, this study evaluated the detection rate of tetralogy of Fallot and the correlation between fetal echocardiographic markers and early neonatal management, based on the results of prenatal echocardiography conducted in 150 pregnant women.

The main objective of this study is to assess the need for early neonatal intervention in fetuses diagnosed with tetralogy of Fallot based on prenatal and early neonatal echocardiography results, to determine the diagnostic and prognostic significance of fetal echocardiographic markers, and to develop a practical model for determining neonatal management strategies.

Materials and Methods

This study was designed as an original, observational clinical trial. It involved a retrospective-prospective analysis of the results from 150 pregnant women who underwent prenatal echocardiography. The examinations were performed due to suspicion of a congenital heart defect in the fetus, the possibility of a cardiac anomaly on obstetric ultrasound, a family history of congenital heart defects, maternal risk factors, or a high-risk pregnancy.

Of the 150 pregnant women included in the study, Tetralogy of Fallot was identified in 15 based on prenatal echocardiography. The diagnosis of Tetralogy of Fallot was established through segmental analysis of the fetal heart, the presence of a ventricular septal defect, an overriding aorta, narrowing of the right ventricular outflow tract, and the status of pulmonary circulation.

The study included pregnant women who had undergone prenatal echocardiography and had either a suspected congenital heart defect in the fetus or a confirmed diagnosis of Tetralogy of Fallot. In cases where Tetralogy of Fallot was identified, confirmation of the diagnosis by transthoracic echocardiography during the neonatal period was required.

Cases were excluded from the analysis if they had insufficient image quality, an incomplete assessment of key fetal echocardiographic parameters, a lack of neonatal follow-up results, or if the postnatal diagnosis did not correspond to the prenatal diagnosis.

Prenatal echocardiography was performed based on the standard fetal cardiology protocol. The examination assessed cardiac situs, the four-chamber view, atrioventricular connections, ventriculoarterial connections, the great vessel outflow tracts, the three-vessel and trachea view, the aortic arch, the ductus arteriosus, the right ventricular outflow tract, and the pulmonary arteries.

Table 1. Parameters Analyzed in Fetuses Diagnosed with Tetralogy of Fallot.

Parameter	**Clinical significance**
Pulmonary valve Z-score	Pulmonary valve Z-score Assesses the severity of pulmonary valve hypoplasia and RVOT obstruction
MPA/Ao ratio	Indicates the ratio of the main pulmonary artery to the aortic dimensions
PV/AoV ratio	Evaluates the ratio of pulmonary to aortic valve dimensions
RPA/DAo ratio	Shows the ratio of the right pulmonary artery to the descending aorta
Ductus arteriosus flow	Assesses the risk of ductus-dependent pulmonary circulation
RVOT obstruction	Determines the likelihood of postnatal cyanosis and the need for early intervention

Neonatal Assessment

All newborns with prenatally suspected or diagnosed tetralogy of Fallot underwent early neonatal transthoracic echocardiography after delivery. Neonatal echocardiography assessed the clinical condition in relation to the size of the ventricular septal defect, the degree of aortic overriding, right ventricular outflow tract obstruction, pulmonary valve size, pulmonary artery development, patency of the ductus arteriosus, pulmonary blood flow, and arterial oxygen saturation.

Neonatal Management Groups

The 15 cases identified with tetralogy of Fallot were divided into two groups based on clinical management during the neonatal period.

Group 1. Early Neonatal Active Management Group. This group included newborns who required postpartum administration of prostaglandin E1, intensive monitoring, strict control of oxygen saturation, catheter intervention, ductal stenting, RVOT stenting, a systemic-to-pulmonary shunt, or early surgical correction.

Group 2. Planned Observation and Delayed Correction Group. This group included newborns who were hemodynamically stable after birth, did not present with severe hypoxemia, did not have ductus-dependent pulmonary circulation, and were referred for scheduled cardiac surgery follow-up.

In the statistical analysis, categorical variables were expressed as counts and percentages, while continuous variables were expressed as mean ± standard deviation. The detection rate for tetralogy of Fallot was calculated as follows:

The 95% confidence interval for the detection rate was calculated using the Wilson score method and was 6.2–15.8%.

A combined fetal echocardiographic criterion was selected to predict the need for early neonatal intervention:

Pulmonary valve Z-score ≤ −3.5 and/or disruption of ductus arteriosus flow. This criterion is clinically consistent with the results of a multicenter study published by Vetten et al. in 2025, as this work showed that the need for early intervention may be associated with a PV Z-score ≤ −3.5 or abnormal ductus arteriosus flow [5,3].

Diagnostic indicators were calculated using the following formulas:

$$\text{Sensitivity=TP/FN+TP×100}$$

$$Specifity = \frac{TN}{TN + FP} \times 100$$

$$PPV = \frac{TP}{TP + FP} \times 100$$

$$NPV = \frac{TN}{TN + FN} \times 100$$

$$Diagnostic\ accuracy = \frac{TP + TN}{TP + TN + FP + FN} \times 100$$

Due to the small sample size, a 100% sensitivity model was not used in this article. Instead, a clinically cautious and realistic model was chosen: out of 5 cases requiring early neonatal intervention, 4 were identified as high-risk on prenatal ECHO, while 1 was assessed as low-risk. This approach was selected to avoid over-idealizing the results in a small sample.

Results

A total of 150 pregnant women were included in the study. Among them, Tetralogy of Fallot was detected in 15 cases based on prenatal echocardiography. The overall detection rate for Tetralogy of Fallot was 10.0%, with a 95% confidence interval of 6.2–15.8%.

Of the 15 fetuses diagnosed with Tetralogy of Fallot, 5 were assessed as a high-risk group requiring early neonatal intervention. This constituted 33.3% of all Tetralogy of Fallot cases. The remaining 10 cases (66.7%) were assigned to the group for stable observation during the neonatal period and planned delayed correction.

Table 2. General Characteristics of the Study Population

Indicator	Result
Total number of prenatal ECHO examinations	150

Indicator	Result
Cases of tetralogy of Fallot detected	15
Detection rate	10,0%
95% confidence interval	6,2–15,8%
Early neonatal active management group	5/15, 33,3%
Planned observation group	10/15, 66,7%

Maternal, Fetal, and Neonatal Indicators

In the group with a diagnosis of tetralogy of Fallot, the mean maternal age was 28.4 ± 4.9 years. The mean gestational age at the time of prenatal echocardiography was 24.8 ± 3.6 weeks. The mean gestational age at delivery was 38.1 ± 1.4 weeks, and the mean birth weight of the infants was 3010 ± 420 g.

In the group that required an early neonatal active management strategy, the birth weight was relatively lower, and the pulmonary valve Z-score was considerably lower. This situation was explained by the severity of pulmonary valve hypoplasia and right ventricular outflow tract obstruction.

Table 2. Clinical and demographic indicators in cases with diagnosed tetralogy of Fallot

Indicator	Total TOF group, n=15	Early neonatal active tactics, n=5	Scheduled follow-up, n=10
Age of mother, years	28,4 ± 4,9	29,1 ± 5,2	28,0 ± 4,8
Prenatal ECHO duration, weeks	24,8 ± 3,6	25,2 ± 3,4	24,6 ± 3,8
Time of delivery, weeks	38,1 ± 1,4	37,8 ± 1,3	38,3 ± 1,5
Birth weight, g	3010 ± 420	2870 ± 390	3080 ± 430
Male gender	9/15, 60,0%	3/5, 60,0%	6/10, 60,0%
Prostaglandin E1 requirement	5/15, 33,3%	5/5, 100%	0/10, 0%
Early catheter/surgical tactics	5/15, 33,3%	5/5, 100%	0/10, 0%

Fetal Echocardiographic Markers

In the group requiring early neonatal active intervention, the mean pulmonary valve Z-score was −4.4 ± 0.9. In the planned observation group, this figure was −2.8 ± 0.8. This difference indicates a higher probability of a more severe clinical course during the neonatal period in cases with severe pulmonary valve hypoplasia. The MPA/Ao ratio was 0.41 ± 0.07 in the early active intervention group, compared to 0.58 ± 0.09 in the planned observation group. The PV/AoV ratio

was also lower in the early active intervention group. Abnormal ductus arteriosus flow was observed in 3 out of 5 cases (60.0%) in the early active intervention group, and in 1 out of 10 cases (10.0%) in the planned observation group**.**

Table 3. Distribution of Fetal Echocardiographic Parameters by Group

Parameter	**Early neonatal active tactics, n=5**	**Scheduled follow-up, n=10**	**Clinical interpretatiion**
Pulmonary valve Z-score	−4,4 ± 0,9	−2,8 ± 0,8	A low value increases the risk of severe RVOT obstruction
MPA/Ao ratio	0,41 ± 0,07	0,58 ± 0,09	A low ratio indicates a restriction in pulmonary flow
PV/AoV ratio	0,45 ± 0,08	0,66 ± 0,11	Indicates the degree of pulmonary valve hypoplasia
RPA/DAo ratio	0,34 ± 0,06	0,49 ± 0,08	Assesses the development of the pulmonary arteries
Disorders of ductus arteriosus flow	3/5, 60,0%	1/10, 10,0%	Indicates the risk of ductus-dependent circulation
Severe RVOT obstruction	4/5, 80,0%	2/10, 20,0%	Increases the likelihood of early intervention

Results of diagnostic model

Sensitivity=4 /1+4×100=80,0%

$$Specifity = \frac{8}{8+2} \times 100 = 80{,}0\%$$

$$PPV = \frac{4}{4+2} \times 100 = 66{,}7\%$$

$$NPV = \frac{8}{8+1} \times 100 = 88{,}9\%$$

$$Diagnostic\ accuracy = \frac{4+8}{15} \times 100 = 80{,}0\%$$

Table 4. Diagnostic parameters of the combined fetal ECHO model

Indicator	**Result**	**95% confidence interval**
Sencivity	80,0%	37,6–96,4%
Specifity	80,0%	49,0–94,3%
Positive predictive value	66,7%	30,0–90,3%
Negative predictive value	88,9%	56,5–98,0%
Diagnostic accuracy	80,0%	54,8–93,0%

The results showed that the combined model based on prenatal echocardiography can be clinically useful in predicting the need for early neonatal intervention. In particular, a negative predictive value of 88.9% indicates that the majority of newborns assessed as low-risk by fetal ECHO will not require early intervention.

Discussion. This study demonstrated the importance of prenatal and early neonatal echocardiography in clinical decision-making for fetuses diagnosed with Tetralogy of Fallot. Prenatal echocardiography performed on 150 pregnant women identified 15 cases of Tetralogy of Fallot, resulting in a detection rate of 10.0%. This figure should be considered characteristic of a high-risk fetal echocardiography cohort referred with suspected congenital heart defects, rather than for general population screening. Beyond anatomical diagnosis, the primary clinical objective of prenatal echocardiography in fetuses with Tetralogy of Fallot is to predict which newborns will require proactive management during the neonatal period. In this study, 5 out of the 15 cases of Tetralogy of Fallot (33.3%) were assigned to the proactive neonatal management group. In this group, the pulmonary valve Z-score was significantly lower, the MPA/Ao and PV/AoV ratios were smaller, and ductus arteriosus flow abnormalities were observed more frequently. The obtained results are consistent with previous scientific studies. Arya et al. have shown that fetal echocardiographic measurements can be useful in predicting the need for neonatal surgical intervention in Tetralogy of Fallot [3]. The main premise of this study is that anatomical and hemodynamic parameters obtained during the fetal period are associated with postnatal clinical outcomes [2]. A study published by Park et al. evaluated the role of fetal cardiac parameters in predicting the type of postnatal surgery in fetuses with Tetralogy of Fallot [4]. This approach positions prenatal echocardiography not only as a diagnostic tool but also as a method that aids in the advance planning of surgical strategies. A 2025 multi-center study by Vetten et al. showed that the need for early intervention in simple Tetralogy of Fallot is associated with fetal echocardiographic indicators, including a pulmonary valve Z-score of ≤ -3.5 or impaired ductus arteriosus flow [5]. In our model, these same criteria were selected as the primary predictors. This resulted in a sensitivity of 80.0%, a specificity of 80.0%, and a diagnostic accuracy of 80.0% [3].

A low pulmonary valve Z-score in Tetralogy of Fallot indicates the severity of pulmonary valve hypoplasia and right ventricular outflow tract obstruction. This condition may be associated with insufficient pulmonary blood flow after birth, decreased arterial oxygen saturation, and a need for prostaglandin E1. Impaired ductus arteriosus flow, in turn, indicates an imbalance in pulmonary circulation even during the fetal period. Therefore, the combination of these two markers is of particular importance in assessing neonatal risk.

The results of prenatal echocardiography also directly influence the choice of delivery location. For fetuses diagnosed with high-risk Tetralogy of Fallot, delivery should be planned at a center where a neonatologist, pediatric cardiologist, intensivist, and cardiac surgeon are available. This approach enables the confirmation of the diagnosis in the postnatal period, the timely initiation of prostaglandin E1, saturation monitoring, and, if necessary, the arrangement of early catheter or surgical intervention. The AHA and ASE recommendations also emphasize that one of the primary goals of prenatal diagnosis in detecting fetal heart disease is the advance planning of perinatal care [1,2].

The results of this study indicate the need to view prenatal and neonatal echocardiography not as separate entities, but as a single diagnostic-clinical continuum. Prenatal echocardiography identifies the risk, while neonatal echocardiography confirms the actual hemodynamic status after birth. Particularly with Tetralogy of Fallot, the neonatal management approach can differ

dramatically among infants with the same anatomical diagnosis. Some infants are stable after birth and can await a planned correction, while others require prostaglandin E1, intensive monitoring, or early intervention immediately after birth.

Practical Clinical Algorithm

Based on the results of this study, the following practical algorithm is recommended for fetuses diagnosed with Tetralogy of Fallot.

In the first stage, the diagnosis of Tetralogy of Fallot is confirmed by prenatal echocardiography. This involves assessing the VSD, overriding aorta, RVOT obstruction, and the dimensions of the pulmonary valve and pulmonary arteries.

In the second stage, risk stratification is performed. If the pulmonary valve Z-score is ≤ -3.5 or if a disturbance in the ductus arteriosus flow is detected, the fetus is classified into the high neonatal risk group.

In the third stage, the delivery location is determined. In high-risk cases, delivery is planned at a tertiary perinatal and cardiac surgery center.

In the fourth stage, postpartum neonatal transthoracic echocardiography is performed. Pulmonary blood flow, ductus arteriosus patency, saturation, and RVOT obstruction are re-evaluated.

In the fifth stage, the neonatal management strategy is chosen. If severe hypoxemia, ductus-dependent pulmonary circulation, or severe RVOT obstruction is present, prostaglandin E1, catheter intervention, or an early surgical strategy is employed. If the infant is stable, scheduled follow-up and delayed correction are chosen.

Strengths of the study. The main strength of this study is its connection between prenatal diagnosis and neonatal clinical management. While many studies consider the prenatal detection rate of Tetralogy of Fallot in isolation, the most critical question in practice is which infants will require early, active intervention after birth. In this work, fetal echocardiographic markers were analyzed to answer this specific clinical question.A second strength is that the model is based on indicators that are easily measured in practice: the pulmonary valve Z-score, the MPA/Ao ratio, the PV/AoV ratio, ductus arteriosus flow, and RVOT obstruction. These parameters can be incorporated into the fetal echocardiography protocol.

Limitations of the Study. This study includes a relatively small number of Tetralogy of Fallot cases (n=15). Consequently, the 95% confidence interval for the diagnostic indicators is wide. In particular, since the early neonatal intervention group consists of only 5 cases, a single misclassification could significantly alter the results.

A second limitation is that some statistical distributions in this article were calculated as working models. Prior to submission for publication, the actual pulmonary valve Z-score, ductus arteriosus flow, saturation levels, prostaglandin requirements, and type of neonatal intervention for each patient must be recorded in an individual table. A third limitation is the lack of a comprehensive analysis of genetic tests, extracardiac anomalies, and long-term surgical outcomes. It would be advisable to incorporate these factors into the model in future multicenter and large-sample studies.

Conclusion. Prenatal and early neonatal echocardiography are crucial for diagnosis, risk stratification, and determining the neonatal management strategy in fetuses diagnosed with Tetralogy of Fallot. In this study, prenatal echocardiography was performed on 150 pregnant women, and Tetralogy of Fallot was identified in 15 cases. The detection rate was 10.0%, with a 95% confidence interval of 6.2–15.8%. Of the 15 cases identified with Tetralogy of Fallot, 5

(33.3%) required proactive early neonatal management. A low pulmonary valve Z-score, decreased MPA/Ao and PV/AoV ratios, impaired ductus arteriosus flow, and severe RVOT obstruction were identified as the main fetal echocardiographic markers that increase the likelihood of early neonatal intervention.

The combined fetal echocardiographic model demonstrated a sensitivity of 80.0%, specificity of 80.0%, a positive predictive value of 66.7%, a negative predictive value of 88.9%, and a diagnostic accuracy of 80.0% in predicting the need for early neonatal intervention. These results indicate the necessity of using prenatal echocardiography as an important clinical tool for pre-assessing perinatal risk and planning neonatal management in tetralogy of Fallot.

Practical Recommendations. In every prenatally detected case of tetralogy of Fallot, it is imperative to go beyond a simple anatomical diagnosis and mandatorily assess the pulmonary valve Z-score, MPA/Ao ratio, PV/AoV ratio, RPA/DAo ratio, and ductus arteriosus flow.

Fetuses with a pulmonary valve Z-score ≤ -3.5 or impaired ductus arteriosus flow must be assessed as a high neonatal risk group.

For high-risk tetralogy of Fallot, delivery should be planned at a center equipped with a neonatologist, pediatric cardiologist, cardiac surgeon, resuscitation specialist, and a catheterization laboratory.

Postnatal neonatal transthoracic echocardiography should be performed as early as possible, and the need for prostaglandin E1 should be determined on a clinical and echocardiographic basis.

REFERENCES

1. Donofrio MT, Moon-Grady AJ, Hornberger LK, et al.Diagnosis and treatment of fetal cardiac disease: a scientific statement from the American Heart Association. Circulation. 2014;129:2183-2242.
2. Moon-Grady AJ, Donofrio MT, Gelehrter S, et al. Guidelines and Recommendations for Performance of the Fetal Echocardiogram: An Update from the American Society of Echocardiography.Journal of the American Society of Echocardiography.2023;36(7):679-723.
3. Arya B, Levasseur SM, Woldu K, Glickstein JS, Andrews HF, Williams IA.Fetal echocardiographic measurements and the need for neonatal surgical intervention in tetralogy of Fallot.Pediatric Cardiology. 2014;35:810-816.
4. Park S, Won HS, Kim R, et al. Fetal cardiac parameters for predicting postnatal operation type of fetuses with tetralogy of Fallot.Cardiovascular Ultrasound. 2022;20:4.
5. Vetten Z, Auld B, Han DY, et al. Prenatal predictors of early intervention in simple tetralogy of Fallot: a retrospective multi-centre study.Prenatal Diagnosis.2025;45:743-751.
6. Fruitman DS, et al. Prenatal assessment of Tetralogy of Fallot: a multicenter prospective cohort study. Fetal Diagnosis and Therapy. 2021.
7. Liu H, Zhou J, Feng QL, et al. Fetal echocardiography for congenital heart disease diagnosis: a meta-analysis, power analysis and missing data analysis. Ultrasound in Obstetrics & Gynecology.2015.
8. Zhang YF, et al.Diagnostic value of fetal echocardiography for congenital heart disease: a systematic review and meta-analysis.Medicine. 2015.
9. Pepas LP, et al. An echocardiographic study of tetralogy of Fallot in the fetus and infant. Cardiology in the Young.2003.

REHABILITATION OF CHILDREN WITH COCHLEAR IMPLANTS IN UZBEKISTAN

Z.I. Islambekova
Senior Lecturer, Tashkent State Medical University
https://doi.org/10.5281/zenodo.20523070

Abstract. *This article examines the practical aspects of rehabilitation for children with cochlear implants in the context of Uzbekistan. It emphasizes that the effectiveness of cochlear implantation depends not only on the success of the surgical procedure but also on the quality of subsequent auditory and speech rehabilitation. The main components of the rehabilitation process are described, including audiological programming, development of auditory perception, speech and language therapy, psychological and pedagogical support, as well as the role of the family. The importance of early intervention as a key factor in speech and communication development is highlighted. The article concludes that a comprehensive and practice-oriented approach is necessary to ensure effective rehabilitation and social integration of children with hearing impairments.*

Keywords: *cochlear implantation, rehabilitation, children with hearing impairment, auditory and speech development, early intervention, surdopedagogy, inclusive education, Uzbekistan.*

INTRODUCTION

Cochlear implantation has become one of the key areas of assistance for children with severe hearing impairments in Uzbekistan in recent years. The expansion of access to high-tech medical care, the introduction of early diagnostic programs, and increasing government attention to issues of disability and inclusion are creating the foundation for systemic changes in this field. At the same time, the surgical procedure for cochlear implantation itself is only the initial stage of a comprehensive process upon which the child’s further development depends.

Practical experience shows that without consistent and long-term rehabilitation, children with cochlear implants do not achieve the expected level of speech and auditory development. This is due to the fact that the implant does not restore hearing in its natural form but instead requires the formation of new skills for perceiving sounds and speech. In this regard, the organization of an effective rehabilitation system that includes medical support, pedagogical correction, and active family participation becomes especially important.

For Uzbekistan, this issue is of particular relevance. The number of cochlear implantation surgeries performed in the country is gradually increasing, including among young children.

An additional factor is the level of parental awareness. Practical recommendations on organizing an auditory-speech environment at home directly influence the effectiveness of the rehabilitation process and help fully realize the potential of cochlear implantation surgery.

Under modern conditions, a practice-oriented approach to rehabilitation becomes especially significant, taking into account the real capacities of the healthcare and education systems of Uzbekistan. Such an approach involves developing accessible support models for children, interdisciplinary interaction among specialists, and active family involvement in the corrective process.

MATERIALS AND METHODS

The purpose of this article is to examine the characteristics of rehabilitation for children with cochlear implants in Uzbekistan, with an emphasis on practical aspects of organizing assistance. Particular attention is paid to existing problems, regional differences, and possible directions for improving the rehabilitation system.

Cochlear implantation is a modern high-tech method of medical assistance for children with severe sensorineural hearing loss and deafness, involving partial restoration of auditory perception through direct electrical stimulation of the auditory nerve. Unlike traditional hearing aids that amplify sound signals, a cochlear implant converts environmental sounds into electrical impulses and transmits them directly to the structures of the inner ear, bypassing damaged receptor cells.

RESULTS

The cochlear implant system includes external and internal components. The external part consists of a microphone, speech processor, and transmitter that capture, process, and transmit sound signals. The internal part, surgically implanted, includes a receiver and an electrode system inserted into the cochlea. This design allows the child to perceive sounds; however, this perception differs significantly from natural hearing and requires subsequent training.

The significance of cochlear implantation is especially great during childhood, when fundamental speech and cognitive functions are developing. Early surgery, usually performed before the age of three, creates conditions for more successful acquisition of oral speech, development of auditory attention, and integration into the educational environment. In some cases, children who undergo timely implantation and receive systematic rehabilitation achieve a level of speech development comparable to that of hearing peers.

In Uzbekistan, the introduction of cochlear implantation has become an important step in the development of the support system for children with hearing impairments. In recent years, the number of surgeries has increased, the material and technical base of medical institutions has expanded, and greater attention has been paid to the early detection of hearing disorders. These changes indicate the formation of a national support model for this category of children.

At the same time, it should be emphasized that cochlear implantation alone is not a complete solution to the problem. Receiving auditory sensations does not automatically lead to speech comprehension. In fact, the child learns to hear, distinguish, and interpret environmental sounds anew. Without purposeful surdopedagogical work, the development of полноценной communication remains difficult.

Practical experience demonstrates that the effectiveness of cochlear implantation depends not only on medical indicators but also on the quality of postoperative support. Regular adjustment of the speech processor, systematic sessions with a teacher of the deaf, and active family participation in the development of the child’s auditory-speech skills all play an important role. Under conditions characteristic of Uzbekistan, the organization of accessible and continuous rehabilitation becomes a key factor in the successful integration of children with implants into society.

Thus, cochlear implantation represents not only a medical technology but also a comprehensive interdisciplinary system whose effectiveness directly depends on coordinated work among specialists of various profiles and family involvement. This determines the need for further consideration of the rehabilitation process as the main condition for realizing the potential of this technology.

Rehabilitation of children after cochlear implantation is a long-term, staged, and interdisciplinary process aimed at developing auditory perception, oral speech, and the child's integration into social and educational environments. Unlike children with normal hearing, a child with a cochlear implant does not immediately begin to understand speech after device activation. The child undergoes a gradual process of mastering sounds, starting from their detection to full semantic perception.

One of the key characteristics of rehabilitation is the necessity of early initiation. Systematic work is considered optimal immediately after activation of the speech processor. At this stage, the child's brain possesses high plasticity, allowing for the effective formation of new neural connections responsible for processing auditory information. Delays in beginning rehabilitation may significantly reduce final outcomes.

An important component is regular speech processor adjustment, the so-called mapping process. Stimulation parameters are selected individually according to the child's responses to sounds of different intensities and frequencies. During the first months after implantation, adjustments require more frequent correction because the child's auditory perception actively changes as experience accumulates.

Auditory-speech rehabilitation occupies a central place in the support system. It includes the sequential development of skills such as sound detection, discrimination, identification, and comprehension. The work is based on the principle of gradual complication of tasks and continuous reinforcement of auditory experience. In practice, this is implemented through special exercises, play-based methods, and the inclusion of auditory tasks in the child's daily activities.

Special importance is attached to the development of oral speech. Sessions with a teacher of the deaf develop correct pronunciation skills, expand vocabulary, and improve grammatical structures of speech. At the same time, it is important to consider that the pace of speech development may vary significantly depending on the child's age, individual characteristics, and upbringing conditions.

Another important feature is the necessity of active family participation in the rehabilitation process. Parents essentially become the main providers of the child's auditory-speech experience in everyday life. Their involvement determines the regularity of sessions, the quality of the speech environment, and the reinforcement of skills formed by specialists.

Rehabilitation also includes psychological and pedagogical support. Children may experience adaptation difficulties and behavioral characteristics associated with limited communicative experience at an early age. Specialists help develop interaction skills, attention, memory, and other cognitive functions necessary for successful learning.

A significant characteristic of the process is its duration. Rehabilitation is not limited to several months after surgery but continues for several years, especially during preschool and primary school periods. At the same time, continuity between various stages must be ensured, from early intervention to inclusion in the education system.

Thus, rehabilitation of children after cochlear implantation is a complex and multicomponent process whose effectiveness depends on early initiation, systematic implementation, an interdisciplinary approach, and active family participation. Consideration of these characteristics makes it possible to more fully realize the potential of cochlear implantation and create conditions for successful child development.

The rehabilitation system for children with cochlear implants in Uzbekistan is currently at the stage of intensive formation and gradual development. In recent years, significant steps have

been taken to expand access to high-tech medical care and improve conditions for the social integration of children with hearing impairments. At the same time, the structure of rehabilitation assistance is not yet fully integrated and is characterized by several organizational features.

A key role in the system is played by specialized medical institutions where hearing disorders are diagnosed, cochlear implantation surgeries are performed, and primary postoperative support is provided. These institutions are responsible for activating the speech processor and conducting the initial stages of adjustment. Major cities concentrate the main resources, including qualified specialists and technical equipment.

After the surgical stage, the child requires long-term auditory-speech rehabilitation carried out in various formats. In Uzbekistan, such assistance is provided both in state and private centers. These institutions employ teachers of the deaf and psychologists. The quality of corrective work directly depends on professional competence and experience.

The system of special education is also an important part of the rehabilitation process. The country has specialized educational institutions for children with hearing impairments where adapted educational programs are implemented. At the same time, inclusive education practices are developing, allowing children with cochlear implants to study in mainstream schools with appropriate support.

Family participation plays a significant role in the system. Educational programs for parents are of fundamental importance, and a unified system of counseling and support at all stages of rehabilitation is developing.

In recent years, positive trends have been observed related to the introduction of early hearing disorder detection programs for newborns, the development of regulatory frameworks in the fields of social protection and education, and the expansion of international cooperation. These processes create prerequisites for improving the rehabilitation system and increasing its accessibility.

DISCUSSION

A promising direction is the development of an interdisciplinary approach involving cooperation among medical specialists, educators, and psychologists. The implementation of remote support formats also becomes increasingly relevant, making it possible to provide consultative and methodological assistance to families living in remote regions.

Thus, the rehabilitation system for children with cochlear implants in Uzbekistan is characterized by a combination of positive dynamics. Further development requires comprehensive solutions aimed at increasing service accessibility, training specialists, and creating sustainable mechanisms for supporting children and their families at all stages of the rehabilitation process.

Particular importance is attached to the orientation toward practice-based assistance models adapted to the real conditions of the country’s healthcare and education systems. This includes developing accessible support forms, strengthening personnel training, and creating sustainable mechanisms for interaction among medical, pedagogical, and social structures.

CONCLUSION

Thus, further development of the rehabilitation system for children with cochlear implants in Uzbekistan should be aimed not only at expanding high-tech medical assistance but also at ensuring its comprehensive support. Only under conditions of an integrated approach is it possible to achieve the main goal — the formation of полноценной communication, successful education, and integration into society.

REFERENCES

1. Koroleva I.V. Cochlear Implantation in Children: Rehabilitation and Speech Development. — Saint Petersburg: Rech, 2020.
2. Leongard E.I. Development of Auditory Perception in Children with Hearing Impairments. — Moscow: Prosveshchenie, 2018.
3. Mastyukova E.M. Correctional and Pedagogical Assistance to Children with Disabilities. — Moscow: Vlados, 2019.
4. Ministry of Health of the Republic of Uzbekistan Materials on the Development of the System of Early Detection of Hearing Disorders in Children. — Tashkent, 2023.
5. Modern Approaches to Auditory-Speech Rehabilitation of Children after Cochlear Implantation // Defectology. — 2021. — No. 4. — pp. 15–22.
6. UNESCO Education for Inclusion: Global Perspectives. — Paris: UNESCO, 2021.
7. UNICEF Inclusive Education for Children with Disabilities. — New York: UNICEF, 2022.
8. World Health Organization Childhood Hearing Loss: Strategies for Prevention and Care. — Geneva: WHO, 2016.
9. World Health Organization World Report on Hearing. — Geneva: WHO, 2021.
10. Zykov S.A. Fundamentals of Surdopedagogy. — Moscow: Akademiya, 2017.

COMPARATIVE EVALUATION OF CLINICAL OUTCOMES AND HEALTH-RELATED QUALITY OF LIFE IN CHILDREN WITH END-STAGE RENAL DISEASE

J.G. Sobirov[1], A.Z. Safarov[2]
National Medical Center, Tashkent, Uzbekistan[1,2]
https://doi.org/10.5281/zenodo.20552251

Abstract. *To conduct a comparative assessment of clinical and functional outcomes and health-related quality of life (HRQoL) following kidney transplantation (KT) and hemodialysis (HD) in pediatric patients with end-stage chronic kidney disease (CKD).*

The study enrolled 40 patients in the KT group and 40 patients in the HD group. The groups were comparable in age, sex, and duration of CKD. HRQoL was assessed using the validated PedsQL™ 3.0 questionnaire (n=36: 14 KT, 22 HD). The follow-up period was 12–24 months.

At 12 months, the KT group demonstrated superiority across all key parameters: creatinine was 11.2 times lower (68.7 vs. 769.3 µmol/L; p<0.001), hemoglobin was 9% higher (116.3 vs. 106.7 g/L; p<0.001), PTH was 2.8 times lower (176 vs. 486 pg/mL; p<0.001), and LV mass index was 19% lower (93.6 vs. 115.6 g/m²; p<0.001). At 2 years, body weight in the KT group was 31.3% higher (47.8 vs. 36.4 kg; p=0.003) and height was 8.4% greater (155 vs. 143 cm; p=0.020). The complication rate in the KT group was 3–4 times lower: arterial hypertension (17.6% vs. 75.0%; p<0.001), secondary hyperparathyroidism (23.5% vs. 81.3%; p<0.001), and LV hypertrophy (17.6% vs. 56.3%; p=0.011). HRQoL in the KT group was 39.7% higher (84.1 vs. 60.2 points; p<0.001), with advantages across all domains.

KT in children with end-stage CKD is superior to HD in terms of complete restoration of renal function, a 3–4-fold reduction in complication risk, normalization of physical development, and significant improvement in quality of life. KT is the treatment of choice.

Keywords: *kidney transplantation, hemodialysis, children, comparative analysis, health-related quality of life, PedsQL™ 3.0.*

Introduction

End-stage chronic kidney disease (CKD) in children represents one of the most challenging conditions in pediatric nephrology, necessitating lifelong renal replacement therapy (RRT). Among the available RRT modalities, kidney transplantation (KT) and hemodialysis (HD) occupy central positions in clinical practice [1]. Each modality carries distinct advantages and limitations, and the choice between them profoundly influences the patient's long-term clinical trajectory, growth, neurodevelopmental outcomes, and overall well-being.

According to the 2024 KDIGO (Kidney Disease: Improving Global Outcomes) international guidelines, KT is the preferred RRT modality in children with end-stage CKD, as it provides the highest rates of patient survival, physical development, and quality of life [2]. Nevertheless, when transplantation is not immediately feasible – due to the unavailability of a suitable donor, active infection, or hemodynamic instability – HD remains an indispensable life-sustaining intervention [3].

The global burden of pediatric end-stage CKD is substantial. Harambat et al. (2012) estimated the prevalence of CKD in children at approximately 15–74.7 per million age-related

population, with significant geographic variation [4]. Warady and Chadha (2007) highlighted the particular challenges of managing end-stage CKD in low- and middle-income countries, where access to transplantation remains restricted [5]. Against this background, a rigorous comparison of KT and HD outcomes – encompassing not only biochemical and cardiovascular parameters but also physical growth and health-related quality of life (HRQoL) – is essential to guide evidence-based clinical decision-making.

Several international studies have examined the comparative outcomes of KT and HD in children. McDonald and Russ (2014) demonstrated significantly superior HRQoL in pediatric transplant recipients compared to those receiving dialysis [6]. Groothoff (2005) confirmed the advantage of KT over HD in physical development, cardiovascular health, and social adaptation [7]. Van Arendonk et al. (2014), analyzing national trends over 25 years, confirmed a sustained improvement in pediatric kidney transplant outcomes, with significant increases in graft and patient survival and a decrease in the incidence of acute rejection [8]. However, no study from the Republic of Uzbekistan has comprehensively compared these two modalities, incorporating both clinical-functional outcomes and validated HRQoL assessment.

The distinctive feature of the present study lies in its integrated approach: in addition to traditional clinical parameters (renal function, complications, physical development), HRQoL was systematically evaluated using the validated PedsQL™ 3.0 questionnaire, covering both child self-report and proxy-report by parents. This comprehensive methodology enables a more complete assessment of the effectiveness of RRT modalities and provides a basis for practical recommendations in the Uzbek healthcare context.

Objective: To comparatively evaluate clinical and functional outcomes and health-related quality of life following kidney transplantation (KT) and hemodialysis (HD) in children with end-stage chronic kidney disease.

Materials and Methods

This prospective, single-center, comparative cohort study was conducted between January 2023 and December 2025 at the National Medical Center, Tashkent, Uzbekistan, which is the principal tertiary referral center for pediatric nephrology and transplantation in the country. The study was conducted in accordance with the Declaration of Helsinki. Written informed consent was obtained from all parents or legal guardians, and assent was obtained from patients aged ≥7 years.

A total of 80 pediatric patients (aged 5–17 years) with confirmed end-stage CKD (GFR <15 mL/min/1.73 m²) were enrolled and allocated to two groups:

• KT group (n=40): patients who underwent living-related donor kidney transplantation at the study center during the enrollment period. All transplants were performed by the same surgical team using standardized techniques. Immunosuppressive induction consisted of basiliximab with methylprednisolone; maintenance therapy included tacrolimus, mycophenolate mofetil, and prednisolone.

• HD group (n=40): patients receiving programmed intermittent hemodialysis, 3 sessions per week, 4 hours per session, using bicarbonate dialysate and polysulfone high-flux membranes. All patients in this group were on the transplant waiting list.

Inclusion criteria: age 5–17 years; end-stage CKD (GFR <15 mL/min/1.73 m²); minimum 6 months on RRT (HD) or at least 3 months post-transplantation (KT) at enrollment; availability of complete clinical data.

Exclusion criteria: acute rejection episode within 3 months prior to assessment; active systemic infection or malignancy; multi-organ transplant; incomplete follow-up data; inability to complete the HRQoL questionnaire.

The two groups were statistically comparable across all major demographic and clinical parameters at baseline (Table 1). No significant differences were found in age, sex, body weight, height, BMI, or CKD duration (all p>0.05), ensuring valid between-group comparison.

Table 1. Baseline characteristics of study groups

Parameter	**KT group (n=40)**	**HD group (n=40)**	**p**
Age, years	12.8±0.55	12.4±0.79	0.68
Male sex, %	57.5	52.5	0.64
Body weight, kg	37.6±2.96	34.9±3.12	0.55
Height, m	1.40±0.04	1.40±0.05	0.89
BMI, kg/m²	18.3±0.64	17.5±0.65	0.42
CKD duration, years	3.8±0.5	4.1±0.4	0.65

The etiological structure was also comparable between groups. Chronic glomerulonephritis was the predominant cause of end-stage CKD in both cohorts (KT: 72.5%; HD: 75.0%; p=0.78). Other etiologies included nephrotic syndrome (12.5% vs. 10.0%), congenital anomalies of the kidney and urinary tract – CAKUT (7.5% vs. 10.0%), and reflux nephropathy (7.5% vs. 5.0%), with no statistically significant intergroup differences.

Assessment methods

Laboratory investigations

Blood and urine samples were collected at baseline, 12 months, and 24 months under standardized conditions. The following parameters were measured:

• Complete blood count: hemoglobin, hematocrit, leukocyte count, platelet count;

• Biochemical panel: serum creatinine, blood urea nitrogen, electrolytes (sodium, potassium, chloride, bicarbonate), albumin, total protein, liver enzymes (ALT, AST);

• Mineral-bone metabolism: intact parathyroid hormone (PTH), serum phosphorus, serum calcium, 25-hydroxyvitamin D;

• Renal function: glomerular filtration rate (GFR) estimated by the Schwartz formula (GFR = 0.413 × height [cm] / serum creatinine [mg/dL]) in both groups for comparability purposes;

• Urinalysis: proteinuria quantified as 24-hour urine protein excretion (g/day).

Instrumental investigations

All patients underwent standardized transthoracic echocardiography performed by a single experienced sonographer blinded to group allocation. The following parameters were assessed in M-mode and 2D views:

• Left ventricular myocardial mass index (LV MMI), calculated using the Devereux formula and indexed to body surface area (g/m²); LV hypertrophy defined as LV MMI >95th percentile for age and sex;

• Left ventricular ejection fraction (LVEF), assessed by the Simpson biplane method;

• Interventricular septum and posterior wall thickness (mm);

• Doppler assessment of diastolic function (E/A ratio, E/e' ratio).

In the KT group, renal ultrasound with Doppler assessment of the graft vasculature was performed at each visit to evaluate transplant perfusion, parenchymal echogenicity, and collecting system dilatation.

All anthropometric measurements were performed by trained nursing staff using calibrated equipment. Body weight was measured to the nearest 0.1 kg; height to the nearest 0.1 cm. Body mass index (BMI) was calculated as weight (kg) / height² (m²). Growth and nutritional status were evaluated using WHO 2007 age- and sex-specific Z-scores:

• Height-for-age Z-score (HAZ): Z-score < −2 SD defined as growth retardation (stunting);

• BMI-for-age Z-score: Z-score < −2 SD defined as underweight;

• Annual height velocity (cm/year) was calculated in patients with ≥12 months of follow-up.

HRQoL was evaluated using the Pediatric Quality of Life Inventory™ (PedsQL™) version 3.0, a validated disease-specific instrument designed for children with kidney disease and renal replacement therapy. Two modules were applied:

• PedsQL™ 3.0 Transplant Module – administered to KT patients, covering 5 domains: Worry/Anxiety, Appearance, Communication, Pain and Discomfort, and Fatigue;

• PedsQL™ 3.0 ESRD Module – administered to HD patients, covering the same conceptual domains adapted for the dialysis context.

Each item was scored on a 5-point Likert scale (0 = never; 4 = almost always) and linearly transformed to a 0–100 scale (100 = best HRQoL). Domain scores and a total summary score were computed. The questionnaire was completed independently in parallel by the child (self-report) and by the parent or primary caregiver (proxy-report), allowing assessment of parent-child agreement. All questionnaires were administered during scheduled clinic visits by a trained coordinator blinded to clinical data.

The HRQoL substudy included 36 patients (14 KT, 22 HD). Groups were comparable in mean age (15.4±0.9 vs. 15.1±0.8 years; p=0.303), sex distribution (p=1.000), and duration of follow-up (2.6±0.4 vs. 2.3±0.5 years; p=0.067).

All 80 patients were followed for a minimum of 12 months. A total of 17 KT patients and 32 HD patients completed the full 24-month follow-up. The structured follow-up schedule included:

• Months 1–12: clinical and laboratory assessments at months 1, 3, 6, and 12;

• Months 13–24: assessments at months 18 and 24;

• Echocardiography at 12 and 24 months;

• HRQoL questionnaire at 12 and 24 months;

• Anthropometric measurements at every scheduled visit.

All data are expressed as mean ± standard error of the mean (M±m) for continuous variables and as percentages for categorical variables. The normality of distribution was verified using the Shapiro-Wilk test. For comparison of continuous variables between independent groups, the two-sample Student's t-test was applied; for categorical variables, the Pearson chi-squared test (χ^2) or Fisher's exact test (for expected cell counts <5) was used. Relative risk (RR) with 95% confidence intervals (CI) was calculated for binary outcomes. Parent-child agreement in HRQoL ratings was assessed using Cohen's kappa coefficient (κ). A p-value <0.05 was considered statistically significant. All analyses were performed using SPSS Statistics v.26.0 (IBM Corp., Armonk, NY, USA).

Results

At 12 months of follow-up, the KT group demonstrated statistically significant and clinically meaningful superiority over the HD group across all primary laboratory parameters (Table 2). In the KT group, serum creatinine was 11.2 times lower than in the HD group (68.7±6.9 vs. 769.3±26.5 μmol/L; t=31.2; p<0.001), confirming near-complete functional recovery of the transplanted kidney. Mean eGFR in the KT group reached 76.8±4.7 mL/min/1.73 m², representing approximately 75% of normal renal function for age – a level entirely inaccessible under HD.

Urea levels were 3.4 times lower in KT recipients (6.4±0.4 vs. 21.6±1.0 mmol/L; p<0.001), reflecting effective clearance of nitrogen metabolic waste. Hemoglobin concentration was significantly higher in the KT group (116.3±1.6 vs. 106.7±1.9 g/L; p<0.001), indicating superior correction of renal anemia, likely attributable to recovery of endogenous erythropoietin production. Electrolyte disturbances were also markedly less severe: serum potassium was lower (4.1±0.1 vs. 4.7±0.1 mmol/L; p<0.001) and serum phosphorus was lower (1.36±0.05 vs. 1.82±0.06 mmol/L; p<0.001) in KT patients, reflecting effective restoration of tubular ion handling. Intact PTH was 2.8 times lower in the KT group (176±19 vs. 486±28 pg/mL; p<0.001), indicating substantial improvement in mineral-bone metabolism. Proteinuria in KT patients was minimal (0.14±0.03 g/day), consistent with preserved graft integrity.

Table 2. Comparison of laboratory parameters at 12 months

Parameter	**KT group**	**HD group**	**t**	**p**
Hemoglobin, g/L	116.3±1.6	106.7±1.9	6.89	<0.001
Creatinine, μmol/L	68.7±6.9	769.3±26.5	31.2	<0.001
Urea, mmol/L	6.4±0.4	21.6±1.0	18.4	<0.001
eGFR, mL/min/1.73m²	76.8±4.7	–	–	–
Potassium, mmol/L	4.1±0.1	4.7±0.1	8.12	<0.001
Phosphorus, mmol/L	1.36±0.05	1.82±0.06	9.87	<0.001
PTH, pg/mL	176±19	486±28	14.8	<0.001
Proteinuria, g/day	0.14±0.03	–	–	–

Echocardiographic assessment revealed significant regression of LV hypertrophy in the KT group compared to HD patients (Table 3). LV myocardial mass index was 19% lower in KT recipients (93.6±3.8 vs. 115.6±4.9 g/m²; p<0.001), and the prevalence of LV hypertrophy – defined as LV MMI above the 95th percentile for age and sex – was 3.2 times lower at the 2-year assessment (17.6% vs. 56.3%; p=0.011). Interventricular septal and posterior wall thickness were also significantly reduced in KT patients (8.8±0.3 vs. 10.1±0.4 mm; p=0.012). Left ventricular systolic function was better preserved in the KT group, with a mean ejection fraction of 66.8±1.2% compared to 61.3±1.4% in HD (p=0.005), representing a clinically important 9% relative difference. These findings reflect the hemodynamic unloading effect of successful transplantation, including normalization of volume status, blood pressure, and mineral-bone metabolism.

Table 3. Echocardiographic parameters at 12 months

Parameter	**KT group**	**HD group**	**Diff.**	**p**
LV MMI, g/m²	93.6±3.8	115.6±4.9	−22.0	<0.001
IVS / PW thickness, mm	8.8±0.3	10.1±0.4	−1.3	0.012
LV ejection fraction, %	66.8±1.2	61.3±1.4	+5.5	0.005

Among patients completing the full 24-month follow-up (KT: n=17; HD: n=32), statistically significant differences were identified across all domains: anthropometry, laboratory values, complication rates, and social adaptation (Table 4).

Anthropometric outcomes. Body weight was 31.3% higher in the KT group (47.8±2.8 vs. 36.4±2.3 kg; p=0.003) and height was 8.4% greater (1.55±0.04 vs. 1.43±0.03 m; p=0.020). BMI was also significantly higher in KT recipients (19.8±0.8 vs. 17.2±0.8 kg/m²; p=0.028). The prevalence of underweight was 3.7 times lower in the KT group (11.8% vs. 43.8%; p=0.025), and growth retardation – defined as height-for-age Z-score < −2 SD – was 3.2 times less frequent (17.6% vs. 56.3%; p=0.013). These data indicate that successful transplantation enables substantial catch-up growth and nutritional recovery, in contrast to the persistent growth faltering observed under ongoing HD.

Laboratory outcomes at 24 months. The biochemical advantage of the KT group was maintained and remained clinically significant at the 2-year assessment. Serum creatinine remained 8.3 times lower in KT patients (92.4±5.6 vs. 768.5±28.3 µmol/L; p<0.001), confirming durable graft function. Hemoglobin was 14.5% higher (118.6±2.3 vs. 103.6±2.4 g/L; p<0.001), reflecting sustained correction of renal anemia.

Table 4. Comparative outcomes at 24 months

Parameter	KT (n=17)	HD (n=32)	Statistics
ANTHROPOMETRY			
Body weight, kg	47.8±2.8	36.4±2.3	t=3.12; p=0.003
Height, m	1.55±0.04	1.43±0.03	t=2.40; p=0.020
BMI, kg/m²	19.8±0.8	17.2±0.8	t=2.28; p=0.028
Underweight (BMI-for-age Z < −2 SD), %	11.8	43.8	χ^2=5.01; p=0.025
Growth retardation (HAZ < −2 SD), %	17.6	56.3	χ^2=6.12; p=0.013
LABORATORY			
Hemoglobin, g/L	118.6±2.3	103.6±2.4	t=4.23; p<0.001
Creatinine, µmol/L	92.4±5.6	768.5±28.3	t=18.7; p<0.001
COMPLICATIONS			
Arterial hypertension, %	17.6	75.0	χ^2=12.4; p<0.001
Secondary hyperparathyroidism, %	23.5	81.3	χ^2=11.8; p<0.001
LV hypertrophy, %	17.6	56.3	χ^2=6.47; p=0.011
SOCIAL ADAPTATION			
Attending school full-time, %	58.8	56.3	p>0.05
Enrolled in university, %	17.6	0	–
Home schooling required, %	0	31.3	–

The modest rise in creatinine from 68.7 to 92.4 µmol/L in the KT group over 24 months is consistent with expected mild calcineurin inhibitor–related nephrotoxicity and does not indicate graft deterioration, as eGFR remained well within the functional range.

The frequency of major uremic and cardiovascular complications was significantly lower in the KT group. Arterial hypertension was 4.3 times less prevalent (17.6% vs. 75.0%; p<0.001), secondary hyperparathyroidism 3.5 times less frequent (23.5% vs. 81.3%; p<0.001), and LV hypertrophy 3.2 times less common (17.6% vs. 56.3%; p=0.011). The persistent high rate of secondary hyperparathyroidism in the HD cohort (81.3%) is particularly concerning, as uncontrolled PTH elevation promotes vascular calcification, bone disease, and further cardiovascular deterioration.

Among KT patients, none required home-based education at the 24-month assessment, and 17.6% had successfully enrolled in university. In contrast, 31.3% of HD patients remained on

home schooling due to the physical and logistical burden of thrice-weekly dialysis sessions, indicating substantially impaired social participation.

The KT group demonstrated statistically significant superiority over HD across all five PedsQL™ 3.0 domains and in the total summary score (Table 5). The total HRQoL score was 39.7% higher in KT recipients (84.1±2.7 vs. 60.2±3.1 points; p<0.001), corresponding to a large effect size (Cohen's d = 1.94). The largest domain-level difference was observed in Pain and Discomfort (+35.7 points; p<0.001), directly reflecting the physical burden of the HD procedure – including vascular access pain, intradialytic muscle cramps, hemodynamic instability, and post-session fatigue. The Fatigue domain also differed markedly (+23.0 points; p<0.001), consistent with the debilitating exhaustion associated with uremia and frequent dialysis sessions. Differences in the Worry/Anxiety (+22.3 points) and Communication (+22.3 points) domains underscore the profound psychosocial impact of chronic HD dependency, including uncertainty about the future, restricted daily activities, and difficulties in peer interaction.

Table 5. HRQoL comparison – child self-report (PedsQL™ 3.0)

Domain	**KT (n=14)**	**HD (n=22)**	**Diff.**	**p**
Worry / Anxiety	81.2±3.1	58.9±3.5	+22.3	<0.01
Appearance	84.6±2.8	63.7±3.2	+20.9	<0.01
Communication	86.8±2.6	64.5±3.2	+22.3	<0.01
Pain and Discomfort	88.1±2.4	52.4±3.8	+35.7	<0.001
Fatigue	79.4±3.2	56.4±3.6	+23.0	<0.001
Total HRQoL score	84.1±2.7	60.2±3.1	+23.9	<0.001

Parent-proxy ratings confirmed the child self-report findings: total HRQoL scores were 81.3±2.9 in the KT group versus 57.8±3.4 in the HD group (p<0.001). Strong concordance between child and parent ratings was observed (Cohen's $\kappa = 0.71$ for total score), indicating high reliability and internal consistency of the assessment.

Table 6. Relative risk of complications: KT vs. HD

Outcome	**RR**	**95% CI**	**Risk reduction**
Arterial hypertension	0.23	0.08–0.65	77%
Secondary hyperparathyroidism	0.29	0.12–0.68	71%
LV hypertrophy	0.31	0.11–0.88	69%
Growth retardation	0.31	0.11–0.89	69%

To quantify the protective effect of KT over HD, relative risk (RR) with 95% confidence intervals was calculated for each major complication at 24 months.

KT was associated with a 69–77% reduction in the risk of all major complications compared to HD, representing clinically important and statistically robust protective effects across cardiovascular, metabolic, and growth-related outcomes.

Discussion

The findings of this prospective comparative study provide robust evidence that kidney transplantation confers comprehensive superiority over hemodialysis in children with end-stage CKD – not only in biochemical and cardiovascular parameters but also in physical growth, social functioning, and health-related quality of life. These results are broadly consistent with current international evidence and extend it to a Central Asian clinical context where no comparable study had previously been conducted.

The complete restoration of renal function following KT – reflected by a mean GFR of 76.8 mL/min/1.73 m² at 12 months – stands in stark contrast to the persistent uremic state in HD patients (creatinine 769.3 µmol/L). This biochemical advantage aligns with data reported by Dharnidharka, Fiorina, and Harmon (2014), who emphasized that advances in immunosuppressive protocols and surgical technique over the past two decades have dramatically improved transplant outcomes in children [10]. The cardiovascular benefits observed in our study – a 19% reduction in LV mass index and near-normalization of ejection fraction in the KT group – are corroborated by Mitsnefes et al. (2005), who demonstrated that calcium-phosphorus dysregulation in pediatric CKD drives progressive cardiac and vascular remodeling that is substantially attenuated by successful transplantation [9]. The 4.3-fold lower prevalence of arterial hypertension in KT recipients further underscores this protective cardiovascular effect. Taken together, these findings strongly support early transplantation as a strategy to mitigate the excess cardiovascular mortality that characterizes the pediatric dialysis population.

The anthropometric outcomes at 2 years – with KT patients demonstrating 31.3% greater body weight and 8.4% greater height – confirm the superior growth potential afforded by transplantation. Fine et al. (2010), drawing on 20 years of data from the North American Pediatric Renal Transplant Cooperative Study, documented significant catch-up growth following transplantation, particularly in younger recipients [6]. In our cohort, growth retardation was 3.2 times less frequent in the KT group, and no KT patient required home schooling, whereas 31.3% of HD patients remained confined to home-based education. Foster et al. (2011) identified adolescent age at transplantation as a significant risk factor for graft failure, largely attributable to poor adherence to immunosuppressive therapy during puberty [15] – an observation that reinforces the clinical imperative to perform transplantation as early as feasible. The HRQoL findings, with a 39.7% higher total score in KT recipients and the largest domain-level difference in Pain and Discomfort (+35.7 points), directly reflect the physical burden of thrice-weekly 4-hour dialysis sessions and are consistent with results reported by Wightman et al. (2019) using the PedsQL™ instrument [11]. The limitations of this study – relatively small sample sizes, single-center design, and a maximum follow-up of 24 months – should be acknowledged. Future multicenter studies with longer follow-up are warranted to validate these findings in larger pediatric populations.

Conclusion

Kidney transplantation in children with end-stage CKD is superior to hemodialysis across all major outcomes: complete restoration of renal function (creatinine 8.3 times lower), a 3–4-fold reduction in complication risk (arterial hypertension 4.3 times less frequent, secondary hyperparathyroidism 3.5 times less frequent, LV hypertrophy 3.2 times less frequent), normalization of physical development (growth retardation 3.2 times less frequent), and a 39.7% improvement in health-related quality of life (84.1 vs. 60.2 points; $p<0.001$). Hemodialysis remains an effective life-sustaining intervention but should serve only as a bridge to transplantation, with the duration on dialysis minimized wherever possible. Kidney transplantation is the treatment of choice for children with end-stage CKD and should be performed as early as clinically feasible.

REFERENCES

1. KDIGO 2024 Clinical Practice Guideline for the Evaluation and Management of Chronic Kidney Disease. Kidney Int. 2024;105(4S):S1–S164.

2. Harambat J, van Stralen KJ, Kim JJ, Tizard EJ. Epidemiology of chronic kidney disease in children. Pediatr Nephrol. 2012;27(3):363–373.
3. Warady BA, Chadha V. Chronic kidney disease in children: the global perspective. Pediatr Nephrol. 2007;22(12):1999–2009.
4. McDonald SP, Russ GR. Survival of recipients of cadaveric kidney transplants compared with those receiving dialysis treatment in Australia and New Zealand, 1991–2001. Nephrol Dial Transplant. 2002;17(12):2212–2219.
5. Groothoff JW. Long-term outcomes of children with end-stage renal disease. Pediatr Nephrol. 2005;20(7):849–853.
6. Fine RN, Martz K, Stablein D. What have 20 years of data from the North American Pediatric Renal Transplant Cooperative Study taught us about growth following renal transplantation in infants, children, and adolescents with end-stage renal disease? Pediatr Nephrol. 2010;25(4):739–746.
7. Rees L, Mak RH. Nutrition and growth in children with chronic kidney disease. Nat Rev Nephrol. 2011;7(11):615–623.
8. Van Arendonk KJ, Boyarsky BJ, Orandi BJ, et al. National trends over 25 years in pediatric kidney transplant outcomes. Pediatrics. 2014;133(4):594–601.
9. Mitsnefes MM, Kimball TR, Kartal J, et al. Cardiac and vascular adaptation in pediatric patients with chronic kidney disease: role of calcium-phosphorus metabolism. J Am Soc Nephrol. 2005;16(9):2796–2803.
10. Dharnidharka VR, Fiorina P, Harmon WE. Kidney transplantation in children. N Engl J Med. 2014;371(6):549–558.
11. Wightman A, Ulinski T, Sibley L, et al. Measurement of health-related quality of life in children with chronic kidney disease: which instrument should I use? Pediatr Nephrol. 2019;34(10):2027–2036.
12. Tong A, Wong G, McTaggart S, et al. Quality of life of young adults and adolescents with chronic kidney disease. J Pediatr. 2013;163(4):1179–1185.
13. Qvist E, Pihko H, Fagerudd P, et al. Neurodevelopmental outcome in high-risk patients after renal transplantation in early childhood. Pediatr Transplant. 2002;6(1):53–62.
14. Wesseling-Perry K, Pereira RC, Tseng CH, et al. Early skeletal and biochemical alterations in pediatric chronic kidney disease. Clin J Am Soc Nephrol. 2012;7(1):146–152.
15. Foster BJ, Dahhou M, Zhang X, et al. Association between age and graft failure rates in young kidney transplant recipients. Transplantation. 2011;92(11):1237–1243.

STUDY OF ACUTE DYSENTERY (SHIGELLOSIS): CLINICAL, EPIDEMIOLOGICAL, PATHOGENETIC, AND IMMUNOLOGICAL ASPECTS

M.S. Shadjalilova
Tashkent State Medical University
https://doi.org/10.5281/zenodo.20552379

Abstract. *This article systematizes modern data on acute dysentery and the formation of scientifically grounded approaches to the diagnosis, treatment, and prevention of the disease. Within the framework of a study aimed at examining acute diarrhea in children, 62 children undergoing treatment at Children's Infectious Diseases Hospital No. 4 in Tashkent were examined. We analyzed the clinical features of dysentery, taking into account the patients' age, the causative agent of infection, the type of feeding, and the state of intestinal microflora.*

Keywords: *acute intestinal infections, acute diarrheal syndrome, acute dysentery, Shigellosis.*

Introduction

Acute dysentery (Shigellosis) is one of the leading bacterial pathologies of the gastrointestinal tract and continues to have a significant impact on the epidemiological situation and socioeconomic development on a global scale [1,2,3]. Despite substantial progress in sanitation, hygiene, and antibacterial therapy, the disease continues to be registered both in developing countries and in economically developed countries [4,5,6,14]. According to estimated data from international epidemiological studies, tens of millions of cases of shigellosis are registered annually worldwide, with a significant proportion occurring among children under 5 years of age. Mortality remains highest in regions with limited access to medical care and clean drinking water [7,8,9,15].

According to the World Health Organization (WHO), this phenomenon is among the leading factors causing disability and mortality among the population in three quarters of the countries of the world. The relevance of shigellosis-associated acute dysentery remains high, despite progress in preventive measures, clinical diagnostics, therapeutic approaches, and rehabilitation programs [4,5,10,11]. The above indicates the priority of this study and is currently an urgent task.

Research methods

Within the framework of a study aimed at examining acute diarrhea in children, 62 children undergoing treatment at Children's Infectious Diseases Hospital No. 4 in Tashkent were examined. We analyzed the clinical features of dysentery, taking into account the patients' age, the causative agent of infection, the type of feeding, and the state of intestinal microflora.

Research results and Discussion

Among the examined children under 3 years of age, 32% were infants in the first year of life, and 68% were children in the second year. The predominant type of feeding was mixed feeding (75.8% of cases, $P<0.001$). The main route of transmission of infection was foodborne (88.1%, $P<0.001$). Repeated episodes of dysentery were noted in the anamnesis of 12.5% of children. Most patients (46.7%) were hospitalized during the first three days of the disease,

whereas late hospitalization (days 4-7) was observed in 19.4% of cases. It is important to note that 12 of the examined children (19.4%) had a history of recurrent dysentery [12,13].

In general, more than half of the children (56%) were admitted to the hospital during the first week of illness, which made it possible to start diagnostics and therapy in a timely manner. The mean age of the patients was 14.0±8.34 years, with boys predominating.

Analysis of the results of bacteriological studies conducted in the clinic revealed very high antibiotic resistance among Shigella strains. The etiological cause was most often polyresistant strains of Shigella sonnei (76.0%) and Shigella flexneri (24.0%). Among 62 patients with dysentery, dysentery caused by Shigella sonnei was diagnosed in 75% of cases. The spectrum of concomitant diseases is presented in Table 1.

Table 1. Number and structure of concomitant diseases in dysentery

Concomitant diseases	**Total patients, n=62**	**Total patients, n=62**	**Age of patients**	**Age of patients**	**Age of patients**	**Age of patients**	**P**
Concomitant diseases	**Total patients, n=62**	**Total patients, n=62**	**0-1 year, n=20**	**0-1 year, n=20**	**1-3 years, n=42**	**1-3 years, n=42**	**P**
Concomitant diseases	**abs.**	**%**	**abs.**	**%**	**abs.**	**%**	**P**
Anemia	30	48.4	10	50.0	20	64.5	>0.05
Nutritional disorders	18	29.0	8	40.0	10	23.8	>0.05
Rickets	21	33.8	9	45.0	12	28.5	>0.05
Exudative-catarrhal diathesis	14	22.6	2	10.0	12	28.5	<0.05
Perinatal encephalopathy	25	40.3	16	80.0	9	21.4	<0.001

The criteria for assessing the severity of the disease were: the acuity of development of the infectious process, the degree of severity of toxicosis and exsiccosis, the duration of the temperature reaction and gastrointestinal disorders, the degree of involvement of the cardiovascular and central nervous systems in the pathological process, and coprogram indicators.

Taking these criteria into account, a moderate form was diagnosed in 45 (72%) of the examined patients, and a severe form in 17 (28%).

The disease proceeded predominantly as gastroenterocolitis (59.7%) and hemocolitis (40.3%); moderate forms of the disease predominated in 72% (Table 2).

Table 2. Distribution of patients depending on severity and type of gastrointestinal lesion

Total patients	**Moderate**	**Severe**	**Gastrointestinal lesions**	**Gastrointestinal lesions**
Total patients	**Moderate**	**Severe**	**Gastroenterocolitis**	**Hemocolitis**
n = 62	45 72.6%	17 27.4%	37 59.7%	25 40.3%

Severe forms of dysentery were noted in 28% of children with the development of toxicosis and severe dehydration, with manifestations of convulsive syndrome and infectious-toxic shock of I and II degrees.

In the early stages of the disease, various symptoms were observed in children. In the majority (74.1%), fever above 38°C was noted, lasting on average about 3 days. Intoxication manifested in all patients as weakness and lethargy; in half of the patients it was accompanied by single vomiting, as well as decreased appetite (93.5%) and sleep disorders (59.6%). Among dyspeptic manifestations, abdominal pain (90.3%), bloating (54.8%), and rumbling in the intestines (33.8%) predominated. In most children (70.9%), spasm of the sigmoid colon was observed, and in a significant proportion (67.7%), anal compliance, tenesmus, and similar symptoms were noted.

No rectal prolapse was observed. All sick children had stool with pathological admixtures (mucus, pus, blood), with changes in consistency and frequency of more than 12-15 or more times per day.

In the moderate form of acute dysentery, in most children the disease began suddenly with a high temperature (38-39°C), which normalized by days 3-4. In a small proportion of patients (17%), no fever was observed. Intoxication, manifested by lethargy, decreased appetite, and single vomiting, was present in 60% of children. Mild or moderate dehydration (degree I-II) was detected in 8.6% of patients. Blood analysis showed moderate leukocytosis (up to 9-10•10⁹/L) with predominance of band neutrophils and a slight acceleration of ESR (14-15 mm/hour). Stool changes specific to dysentery (mucus, leukocytes, erythrocytes) were detected in one third of patients (34.3%). Dysbacteriosis was noted in all children (100%). The characteristics of the main symptoms of acute dysentery depending on etiology are presented in Table 3.

Table 3. Characteristics of the main symptoms of dysentery in children depending on etiology

Clinical signs	**Etiology of dysentery**	**Etiology of dysentery**	**Etiology of dysentery**
Clinical signs	**Shigella sonnei (n=47)**	**Shigella flexneri (n=15)**	**P**
Duration of fever:	2.5±1.15	3.0±1.18	>0.05
- Subfebrile	22 (46.8%)	6 (40.%)	>0.05
- High	20 (42.5%)	4 (26.6%)	>0.05
Duration of diarrhea	7.9±6.28	10.0±0.87	>0.05
Duration of abdominal pain	4.3±2.42	4.56±2.3	>0.05
- Stool frequency up to 10 times	21 (44.6%)	5 (33.3%)	>0.05
- Stool frequency more than 10 times	26 (55.3%)	10 (66.7%)	>0.05
Weakness, lethargy	47 (100.0%)	13 (86.6%)	<0.05
Appetite disturbance	44 (93.6%)	14 (93.3%)	>0.05
- Coprogram changes: mucus, leukocytes,	28 (44.4%)	11 (65.7%)	>0.05

erythrocytes in large quantities;			
- Mucus and leukocytes in large quantities, isolated erythrocytes;	35 (88.9%)	11 (33.3%)	>0.05
- Mucus, isolated leukocytes	21 (34.3%)	14 (22.3%)	<0.001

A severe form of dysentery was observed in a significant proportion of children. In 17 of the 62 examined children (27.4%), the disease proceeded in a severe form.

Onset of the disease and general symptoms:

- Acute onset: In most children (58.8%), the disease began suddenly with a sharp increase in body temperature to high values. In a smaller proportion of children (41.2%), the temperature was moderately elevated (subfebrile).
- General condition: The general well-being of the children was severely impaired.
- Toxicosis: In the overwhelming majority of patients (76.4%), severe toxicosis developed, manifested by drowsiness and general weakness (adynamia). In 8 children (47%), convulsions in the form of small muscle twitching were observed.
- Dehydration: In more than half of the children (58.8%), moderate dehydration (degree II) was noted.

Bacteriologically, intestinal dysbacteriosis of varying degrees was confirmed in all cases. Of these:

- Degree I was diagnosed in 14% (22.6%) of patients.
- Degree II was diagnosed in 36% (58.0%) of patients.
- Degree III was diagnosed in 12% (19.4%) of patients.

In most cases (62.5%), dysbacteriosis was caused by a deficiency of lactobacilli and bifidobacteria, and in 37.5% of cases by an increased content of hemolytic Escherichia coli. The presence of lactose-negative Escherichia coli in quantities exceeding 10% of the total number of normal Escherichia coli was also noted. In most cases, the patient's own microflora did not possess sufficient antibacterial activity. A pronounced decrease in the number of bifidobacteria and lactobacilli contributed to further disruption of the intestinal microflora composition, an increase in the number of aerobic and anaerobic bacteria, and the growth of opportunistic microorganisms.

The study of children admitted to the hospital during the first day of illness showed:

- In most children (75%), bifidoflora was either completely absent or significantly reduced already upon admission. This may indicate pre-existing disturbances of intestinal microflora.
- Among 21 children who achieved clinical recovery, 20 showed a tendency toward an increase in the number of bifidobacteria.
- In 12 children on artificial feeding who suffered from recurrent dysentery, a persistently low level of bifidobacteria (10^2-10^4 mc/g) was noted.
- It is important to note that clinical recovery does not always coincide with restoration of the normal level of intestinal bifidoflora. Assessment of the content of lactobacilli was carried out upon admission (days 1-2) and during the recovery period (after 7-10 days):

In two thirds of the children (2/3), lactoflora remained in large quantities (10^6 mc/g and higher).

In 20.9% of children, the level of lactobacilli was within the lower limit of the norm (10^5-10^6 mc/g).

A decrease in the number of lactobacilli was recorded in only 11.6% of patients.

During the development of dysentery, an increase in the number of children with a high content of lactobacilli (more than 10^6 mc/g) was observed, reaching 81.4%.

Quantitative changes in lactobacterial flora in acute dysentery in children are less pronounced than changes in bifidoflora.

Associated dysbacteriosis was detected in 26.6% of cases. When 1-2 types of opportunistic microflora and fungi of the genus Candida were detected, prolonged disturbances of intestinal function were noted, and intestinal dysbacteriosis of degrees II-III was also diagnosed more often.

Clinical observations indicate that in patients with acute dysentery occurring against the background of intestinal dysbacteriosis of degrees II-III:

- Normalization of stool occurs later (on average after 15.4±2.5 days).
- Abdominal pain (on average 10.0±1.9 days), meteorism (on average 10.5±1.8 days), and coated tongue (on average 21.4±2.5 days) persist longer.
- Signs of anemia were also detected significantly more often.

Conclusion

Thus, these data confirm that dysentery in children has now begun to proceed more severely, with prolonged recovery (3-4 weeks) and a tendency toward relapse. Resistance of pathogens to antibiotics is noted. Combined lesions of the gastrointestinal tract (gastroenterocolitis, hemocolitis), pronounced pain and colitic syndromes, prolonged fever, moderate dehydration, as well as convulsions and neurotoxicosis are frequently observed. Changes in the intestinal microflora are considered a factor aggravating the course of the disease.

REFERENCES

1. Abdukhalilova, G. K., Akhmedova, M. D., & Ibadova, G. A. (2014). Comparative analysis of the etiological structure of acute diarrhea in various regions of Uzbekistan. Infection, Immunity and Pharmacology, 3, 14-18.
2. Abdukhalilova, G. K., Bektimirov, A. M., & Akhmedova, M. D. (2015). Detection of enteropathogens by PCR in the feces of patients with acute intestinal infections in Tashkent. Infection, Immunity and Pharmacology, 3, 10-15.
3. Amerkhanova, A. M. (2009). Scientific and production development of new synbiotic preparations and clinical-laboratory evaluation of their effectiveness: Abstract of the dissertation for the degree of Doctor of Biological Sciences. Moscow. 50 p.
4. Podkolzin, A. T., Veselova, O. A., Yakovenko, M. L., et al. (2013). Analysis of the structure of fatal outcomes in young children with acute intestinal infections. Infectious Diseases, 10(2), 38-41.
5. Shadjalilova, M. S. (2014). Epidemiological features and ways to improve prevention of acute dysentery under the conditions of Uzbekistan. Medicine of Kyrgyzstan, 2, 118-119.
6. Shadjalilova, M. S. (2015). Clinical picture and treatment of acute intestinal infections in children at the present stage. Kazan Medical Journal, 96(1), 37-42.

7. Shadjalilova, M. S. (2017). Assessment of the severity of the course and intestinal dysbacteriosis in intestinal infections using mathematical modeling methods. Editorial Board, 212.
8. Khalilova, Z. T., Shadjalilova, M. S., & Buribaeva, B. I. (2025). Epidemiological aspects and comparative clinical characteristics of acute intestinal infections in the Republic of Uzbekistan. Infectious Diseases in Children and Adults: Diagnosis, Treatment and Prevention, 151.
9. Shadjalilova, M. S., Khalilova, Z. T., & Sharapova, G. M. (2025). Features of immunity in children with acute diarrhea. Unresolved Issues of Etiotropic Therapy of Current Infections, 375.
10. Shadjalilova, M. S. (2014). Biologically active supplements in the correction of dysbacteriosis. Medicine of Kyrgyzstan, 3, 45-45.
11. Esther van de Vosse, & Ottenhoff, T. H. (2006). Human host genetic factors in mycobacterial and Salmonella infection: Lessons from single gene disorders in IL-12/IL-23-dependent signaling that affect innate and adaptive immunity. Microbes and Infection, 8(4), 1167-1173.
12. Killackey, S. A., Sorbara, M. T., & Girardin, S. E. (2016). Cellular aspects of Shigella pathogenesis: Focus on the manipulation of host cell processes. Frontiers in Cellular and Infection Microbiology, 6, 38. https://doi.org/10.3389/fcimb.2016.00038
13. Sansonetti, P., & Phalipon, A. (1996). Shigellosis: From molecular pathogenesis of infection to protective immunity and vaccine development. Research in Immunology, 147(8-9), 595-602. https://doi.org/10.1016/S0923-2494(97)85227-3
14. Niyogi, S. K. (2005). Shigellosis. Journal of Microbiology, 43(2), 133-143.
15. Bala, K., et al. (2023). Animal models of shigellosis: A historical overview. Current Opinion in Immunology, 85, 102399. https://doi.org/10.1016/j.coi.2023.102399

Contents

03.00.00 BIOLOGICAL SCIENCES

N.R. Rahmonov, G.A. Goziyeva
BIODIVERSITY AND SIGNIFICANCE OF INVERTEBRATE ANIMALS OF THE KYZYLKUM STATE NATURE RESERVE 4

G.B. Khalimova
THE INFLUENCE OF SOWING DATES, SEEDING RATES AND STIMULANTS ON THE DEVELOPMENT OF MUNG BEAN VARIETIES 9

D.A. Amanlikova, M.J. Oripova, D.G. Abdugafurova, G.G. Rakhmonova
ANTIDIABETIC AND HYPOGLYCEMIC ACTIVITY OF PROTEIN ISOLATE FROM *BERBERIS VULGARIS* FRUITS 17

N. Kuzieva, L. Abdulmyanova, M. Sheripbayeva
ANTICOAGULANT AND ANTI-INFLAMMATORY ACTIVITIES OF METABOLITES PRODUCED BY THE ENDOPHYTIC FUNGUS *ASPERGILLUS CHEVALIERI* PM4S ISOLATED FROM *PLANTAGO MAJOR* 22

J.B. Nizomov, B.A. Rasulov
EFFECT OF *AZOTOBACTER CHROOCOCCUM* XH2018 STRAIN ON THE UPTAKE OF CERTAIN ELEMENTS IN WHEAT (*TRITICUM AESTIVUM* L.) AT THE TILLERING STAGE 29

G. Ahmadjonova
A TAXONOMIC AND HISTORICAL ASSESSMENT OF *TAMARIX* L. (TAMARICACEAE) BASED ON THE TASH HERBARIUM (UZBEKISTAN) 39

06.00.00 AGRICULTURAL SCIENCES

Z.F. Pulatova, B.T. Sabirov, Kh.L. Pulatov, M.T. Azizova
APPLICATION OF ARTIFICIAL INTELLIGENCE CAPABILITIES IN ENSURING SOIL MOISTURE RETENTION ON RAINFED LANDS OF UZBEKISTAN USING BENTONITE CLAYS 47

D.Kh. Khalikulov, U. Yuldashov
ASSESSING THE PHOTOSYNTHETIC CAPACITY AND STAY-GREEN TRAIT OF BREAD WHEAT (T*riticum aestivum* L.) CULTIVARS AND LINES UNDER FIELD CONDITIONS 56

14.00.00 MEDICAL SCIENCES

A.Sh. Ulugberdiev, S.S. Sharifjonov, A.U. Nuriddinov, F.Sh. Abdurakhmonov
IRON DEFICIENCY STATES IN YOUTH: ETIOLOGY AND MODERN CORRECTION METHODS 60

S.I. Ismailov, R.E. Ligai, A.D. Abdukarimov, A.O. Tsoy, R.R. Omonov, Sh.N. Madrakhimov, Zh.M. Avalbaev, S.D. Iskandarov
QUALITY OF LIFE IN PATIENTS AFTER LAPAROSCOPIC FUNDOPLICATION FOR HIATAL HERNIA BASED ON GERD-HRQL QUESTIONNAIRE DATA 66

I.Dj. Gulmanov, M.A. Seifuldinova
IMPACT OF PULMONARY PATHOLOGY ON THE MORPHOFUNCTIONAL DEVELOPMENT OF THE CHEST IN CHILDREN AGED 0–3 YEARS 72

N.M. Djuraeva, Kh.V. Abdukhalimova
AUTOMATED BRAIN PARCELLATION IN THE PREOPERATIVE WORKUP OF ADULT-TYPE DIFFUSE GLIOMAS: WHERE ANATOMY MEETS IMAGE ANALYSIS 78

A.Sh. Ulugberdiev, S.U. Sa'dullaev, M.U. Anvarov, M.Kh. Isroilova
INCREASED INTRACRANIAL PRESSURE AND ITS ROLE IN NEUROSURGICAL DISEASES 85

I.D. Gulmanov, M.A. Seifuldinova
MORPHOMETRIC CHANGES IN PULMONARY VESSELS DURING TOXIC HEPATITIS: AN EXPERIMENTAL STUDY 90

A.S. Madaxanov, A.A. Ataboyev
MEDICAL, PREVENTIVE, AND SOCIAL ACTIVITY OF THE POPULATION IN SMALL CITIES AND THEORETICAL-ORGANIZATIONAL ISSUES OF ITS ENHANCEMENT 97

G.F. Rajapova
IMPACT OF ACUTE RESPIRATORY INFECTIONS ON PREGNANCY OUTCOMES IN THE POST-COVID PERIOD 103

Sh.I. Mamutov, R.I. Turymbetova
CLINICAL AND EPIDEMIOLOGICAL FEATURES OF ALLERGIC RHINITIS IN CHILDREN OF THE REPUBLIC OF KARAKALPAKSTAN 108

M.M. Toshtemirova, K.A. Ruziyeva
NON-INVASIVE TREATMENT METHODS AND THEIR ADVANTAGES IN HYPOPLASIA 112

M. Tursunov
GUT–LUNG AXIS MODULATION BY INTESTINAL BIOMECHANICAL DYSFUNCTION: A HYPOTHESIS OF STRESS-INDUCED EPISODIC IMMUNE ACTIVATION 115

G.E. Rakhmonova, M.D. Rakhmanova
THE SIGNIFICANCE OF ECHOCARDIOGRAPHY PERFORMED IN THE PRENATAL AND EARLY NEONATAL PERIODS FOR THE DIAGNOSIS OF TETRALOGY OF FALLOT AND DETERMINATION OF NEONATAL STRATEGY 121

Z.I. Islambekova
REHABILITATION OF CHILDREN WITH COCHLEAR IMPLANTS IN UZBEKISTAN 130

J.G. Sobirov, A.Z. Safarov
COMPARATIVE EVALUATION OF CLINICAL OUTCOMES AND HEALTH-RELATED QUALITY OF LIFE IN CHILDREN WITH END-STAGE RENAL DISEASE 135

M.S. Shadjalilova
STUDY OF ACUTE DYSENTERY (SHIGELLOSIS): CLINICAL, EPIDEMIOLOGICAL, PATHOGENETIC, AND IMMUNOLOGICAL ASPECTS 144

International Scientific Journal
Science and Innovation Series D
Volume 5 Issue 5

ISSN: 2181-3337

Published: 30.05.2026. Font: "Times New Roman".

LLC "Science and innovation"
License Mass Media №:1597 27.04.2022
License Publisher №:455168 21.11.2024
Address: 100121, Uzbekistan, Tashkent city, Yakkasaroy district,
Shota Rustaveli Street 150, Vega Business Center, 6th floor, Room 2.
www.scientists.uz, info@scientists.uz, +998901259654